Arsenic Removal from Aqueous Solutions using a Binary Mixed Oxide

ADINA NEGREA[1]*, LAVINIA LUPA[1], MIHAELA CIOPEC[1], CORNELIA MUNTEAN[1], RADU LAZĂU[1], MARILENA MOTOC[2]

[1]"Politehnica" University of Timişoara, Faculty of Industrial Chemistry and Environmental Engineering, 2 Piaţa Victoriei, 300006 Timişoara, Romania

[2]University of Medicine and Pharmacy Timişoara, Faculty of Medicine "Victor Babeş", 2 Piaţa Eftimie Murgu, 300041, Timişoara, Romania

In the most cases the drinking water has been identified as one of the major sources of arsenic exposure by the general population. A variety of treatment processes has been studied for arsenic removal from water. One of the most used methods is the adsorption. The most efficient adsorbent materials are those with iron content considering the affinity of arsenic species towards iron compounds. In the present paper the As (III) adsorption performance of a binary mixed oxide Fe_2O_3-SiO_2 was investigated. The sorption process is best described by the pseudo-second-order kinetics. The theoretically predicted equilibrium adsorption capacity was close to the experimentally determined value (80.6 μg/g). Modeling of the equilibrium data with Freundlich and Langmuir isotherms lead to a better correlation coefficient in the case of Langmuir model. The value of the calculated maximum adsorption capacity is close to the experimental value (340 μg/g). The dimensional separation factor used to predict the essential characteristics of Langmuir isotherm indicates favorable adsorption in the studied concentration range (100-700 μg As(III) / L). The studied binary mixed oxide develops promising adsorbent properties concerning the arsenic (III) removal from aqueous medium.

Keywords: arsenic removal, binary mixed oxide, sorption kinetics, sorption equilibrium

Depending on the sources the drinking water contains many trace contaminants, both cationic and anionic [1]. Among common inorganic pollutants, arsenic species has been largely studied because of its potential harmfulness to human health [2]. The symptoms of chronic poisoning on human beings are numerous: skin cancer, liver, lung, kidney, and bladder cancer as well as conjunctivitis, hyperkeratosis, and in severe cases gangrene in the limbs and malignant neoplasm [3-5]. Therefore the arsenic species maximum permissible limit in drinking water according to World Health Organization (WHO) is 10 μg/L [6-9]. In conclusion there is a real need for development of removal methods for inorganic arsenic from drinking water and under ground water [6, 10, 11].

Varoius methods are proposed to reduce arsenic level in natural waters, including redox processes, precipitation, co-precipitation, adsorption, electrolysis, cementation, solvent extraction, ion-exchange, flotation, and biological processing [12-15]. According to the literature data [1-5] the adsorption is one of the most used methods for arsenic removal from water. Various types of adsorbents have been developed by researchers for the removal of arsenic from water, such as: coconut husk carbon, MnO_2 coated sand, basic yttrium carbonate, several iron compounds or iron containing wastes, activated alumina, carbon from fly ash, granular titanium dioxide and hybrid polymeric sorbents [5-10]. Among all these sorbents the iron salts based sorbents were found to be the most efficient in arsenic removal from drinking water, due to its strong affinity for dissolved arsenic. Arsenic species give interactions with iron compounds at each sorption site of the solids and so they are effectively removed from solution [2-6, 13-17].

The purpose of the present paper was to evaluate a binary mixed oxide Fe_2O_3-SiO_2 as potential As (III) adsorbent. We focused on this mixture because iron oxide is responsible for arsenic removal and the presence of silicon oxide leads to a higher surface area, so we expect to obtain a high adsorption capacity.

Experimental part

Obtaining of binary mixed oxide

The sorbent from a binary mixed oxide was obtained from a mixture of iron oxalate and SiO_2 which was introduced as Ultrasil VN3 (Degussa). SiO_2 has been wet homogenized with iron oxalate = 1:1 in a porcelain dish and dried at 110°C. The resulting mixture has been grinded and then annealed in an electric oven at 550°C in an porcelain crucible for the decomposition of iron oxalate to Fe_2O_3 [18]. The components dosage for the mixture has been made in such a way to have a sorbent Fe_2O_3 / SiO_2 1 :1. The BET surface area of the obtained sample has been determined by nitrogen adsorption-desorption using a MICROMERITICS ASAP 2020 INSTRUMENT and the surface area has been compared with those of the simple oxides.

Sorption performance

The influence of different physico-chemical parameters (contact time and initial concentration of arsenic species in liquid phase) upon the arsenic species adsorption onto binary mixed oxide was investigated. In order to establish the adsorption performance the experiments were carried out with 0.1 g of binary mixed oxide in 100 mL solution having the concentration of 100 μg/L in $AsCl_3$. In the first instance the effect of contact time was studied. The samples were stirred using a glass rod (stirring speed 200 rpm) at different contact times (15, 30, 45, 60, 90, 120 and 150 min). Similar batch experiments were performed to study the influence of the initial As (III) concentration (100, 200, 300, 400, 500, 600 and 700 μg/L). After stirring, the samples were centrifuged at 1200 rpm for 30 min using a ROTINA 420 centrifuge. The arsenic residual concentration in the resulting solutions was determined through atomic absorption spectrometry with hydride generation, using a spectrophotometer VARIAN SpectrAA 110 VGA 77, at 193.7 nm. As (III) species was selectively reduced to arsenic hydride H_3As with natrium boronhydride $NaBH_4$ (0.6% w/v) solution in NaOH buffer (0.5% w/v).

* *email: adina.negrea@chim.upt.ro, Tel.: +40 256 404192*

The adsorption performance expressed as the amount of As (III) adsorbed per gram of sorbent q_e (μg/g), is calculated from experimental data using the following equation [3, 7, 16, 17, 19]:

$$q_e = (C_o - C_e)\frac{v}{m} \quad (1)$$

where:

C_o - initial concentration of arsenic in solution, μg/L;

C_e - equilibrium concentration of arsenic in solution, μg/L;

v - volume of solution, L;

m - amount of adsorbent, g.

During adsorption experiments the initial *p*H of the solutions was kept between 6.7 and 7, which is the most common pH value found in the natural waters. The *p*H of the solutions was measured using a multi parameter instrument WTW Multi 197i. The experiments were performed at the ambient temperature (20 ± 1°C).

Results and discussion

Sorbent properties

The BET specific surface area of the binary mixed oxide is 78.01 m^2/g, which is higher than the surface area of Fe_2O_3 (14.57 m^2/g) and smaller than the surface area of SiO_2 (144.04 m^2/g). One may notice that the addition of Ultrasil powders to Fe_2O_3 sample leads to the increase of the Fe_2O_3 surface area. This was the reasons for the choice of this mixture as potential arsenic adsorbent [18].

Effect of contact time and kinetic studies

In order to determine the time necessary to reach the equilibrium it was studied the effect of stirring time on the adsorption capacity of the binary mixed oxide in the process of As (III) species removal from water. The results presented in figure 1 show that the equilibrium was reached after 90 min, when more than 90% of arsenic was adsorbed.

In order to express the kinetics of arsenic adsorption onto binary mixed oxide the results were analyzed using the below presented models.

The pseudo-first-order kinetic model based on the solid capacity, proposed by Lagergren can be used to determine the rate constant for the adsorption process. Its integrated form [3, 7, 16, 17, 20] is expressed by equation (2):

$$\ln(q_e - q_t) = \ln q_e - k_1 t \quad (2)$$

where:

q_t and q_e represent the amounts of the arsenic adsorbed on the binary mixed oxide at time t and at equilibrium time, respectively, μg/g;

k_1 - the specific adsorption rate constant, min^{-1}.

The pseudo-first-order rate constant (k_1) and the equilibrium adsorption capacity (q_e) are determined from the linear plot of $\ln(q_e - q_t)$ versus t (fig. 2).

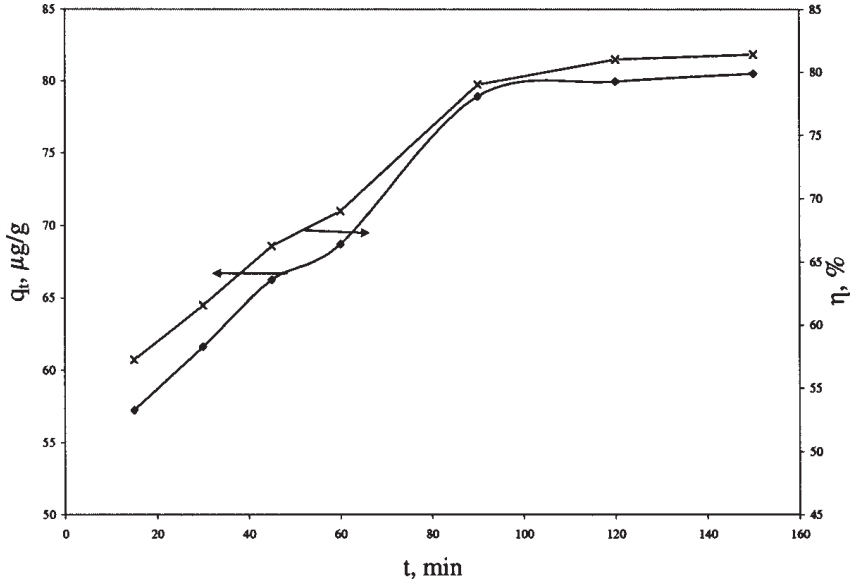

Fig. 1. Effect of stirring time on arsenic adsorption capacity of Fe_2O_3-SiO_2

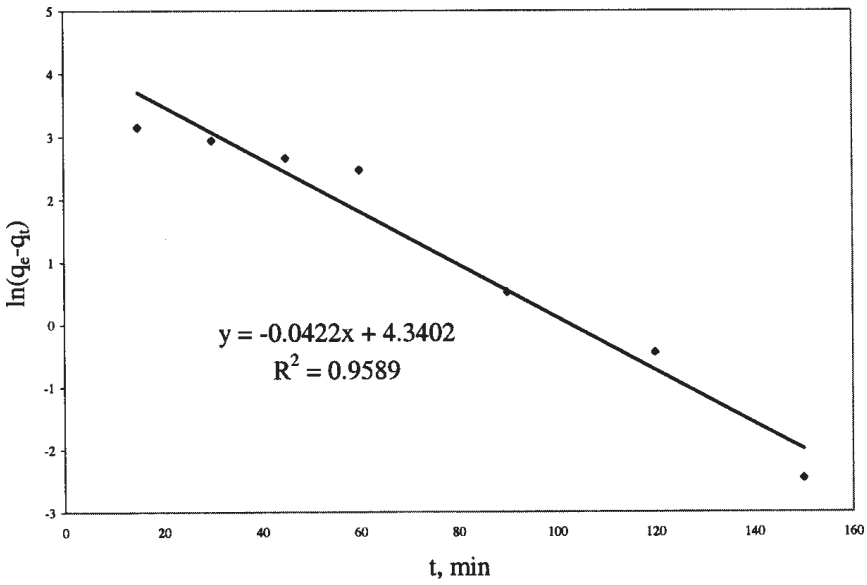

Fig. 2. Pseudo-first-order kinetic plot

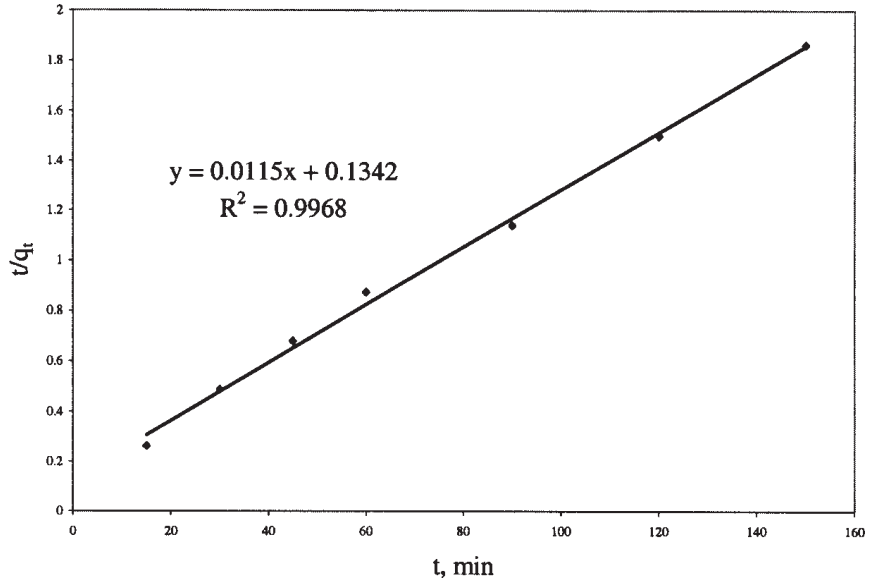

Fig. 3. Pseudo-second-order kinetic plot

Table 1
KINETIC PARAMETERS FOR As(III) SORPTION ONTO BINARY MIXED OXIDE

q_e, exp, μg/g	Pseudo-first-order model			Pseudo-second-order model		
	q_e, kinetic plot, μg/g	k_1, min^{-1}	R^2	q_e, kinetic plot, μg/g	k_2 $min^{-1}(\mu g/g)^{-1}$	R^2
80.6	76.7	0.0422	0.9589	86.95	$9.85 \cdot 10^{-4}$	0.9968

The linear form of the pseudo-second-order rate expression of Ho and McKay, based on the solid phase sorption [3, 7, 16, 17, 21], is given by equation (3):

$$\frac{t}{q_t} = \frac{1}{h} + \frac{t}{q_e} \quad (3)$$

where:

$h = k_{s2} \cdot q_e^2$; k_2 is the pseudo-second-order constant, $min^{-1}(\mu g/g)^{-1}$.

Other terms have their usual meanings. A plot of t/q_t versus t should yield a straight line. From the intercept and slope (fig. 3) are calculated the second-order rate constant (k_2) and the equilibrium adsorption capacity (q_e).

The values of the constants, together with the regression coefficients (R^2) obtained in both cases are summarized in table 1.

The experimental data do not fit the kinetic isotherm of the pseudo-first-order model because the obtained correlation coefficient is not close to 1 and there is a difference between the q_e value experimentally obtained and the value directly obtained from the kinetic plot. In the case of the pseudo-second order model, the theoretically predicted equilibrium adsorption capacity is close to the experimentally determined value. Alongside the correlation coefficient closer to 1, this indicates that the kinetics of As (III) species removal through adsorption on binary mixed oxide Fe_2O_3-SiO_2 is well explained and approximated by the pseudo-second-order kinetic model.

Effect of initial concentration and equilibrium study

The adsorption isotherm of As (III) is presented in figure 4. At arsenic species equilibrium concentrations higher than 200μg/L the value of adsorption capacity remains practically the same. The experimentally determined maximum adsorption capacity of the binary mixed oxide is 340 μg/g.

Several models have been published in the literature to describe experimental data of adsorption isotherms. The Langmuir and Freundlich models are the most frequently used models [3, 5, 7, 9, 16, 17]. In this work, both models were used to describe the relationship between the amount of As (III) ions adsorbed by binary mixed oxide and its equilibrium concentration in solution batch contact time over 90 min as it results from figure 1.

The linear form of the Freundlich isotherm equation can be written as:

$$\ln q_e = \ln K_F + \frac{1}{n} \ln C_e \quad (4)$$

and the linear form of the Langmuir isotherm as the following equation:

$$\frac{C_e}{q_e} = \frac{1}{K_L q_m} + \frac{C_e}{q_m} \quad (5)$$

where:

q_e is the amount of arsenic adsorbed per gram of sorbent, μg/g;

C_e is the equilibrium concentration of arsenic, μg/L;

K_F and 1/n are characteristic constants that can be related to the relative adsorption capacity of the adsorbent and the intensity of adsorption, respectively;

q_m is a measure of monolayer adsorption capacity [μg/g] and K_L is a constant related to the free energy of adsorption.

The curves and parameters, as well as the correlation coefficients (R^2), for As (III) species removal through adsorption onto binary mixed oxide are presented in figures 5 and 6 and table 2.

The Freundlich plot has a very low correlation coefficient; this suggests a restriction on the use of

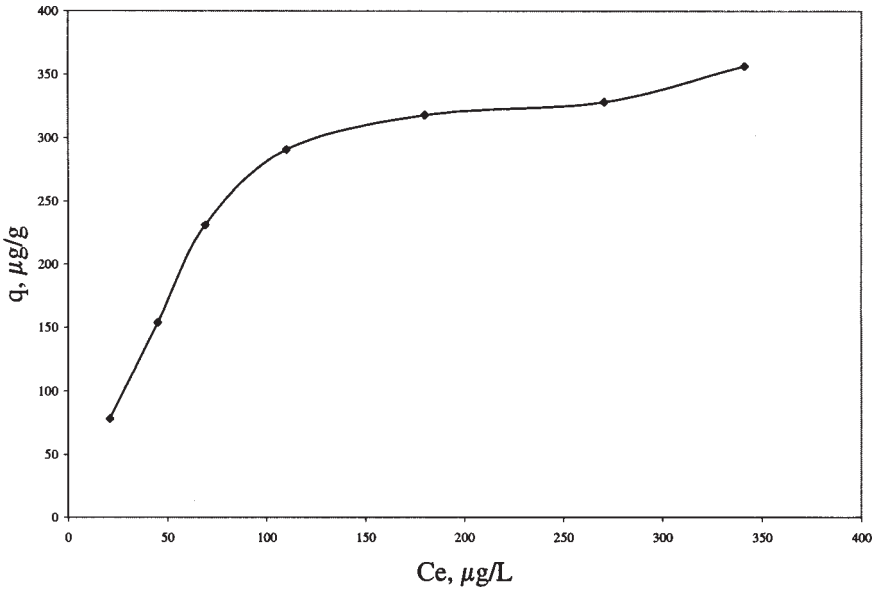

Fig. 4. Adsorption isotherm of As(III) on the binary mixed oxide

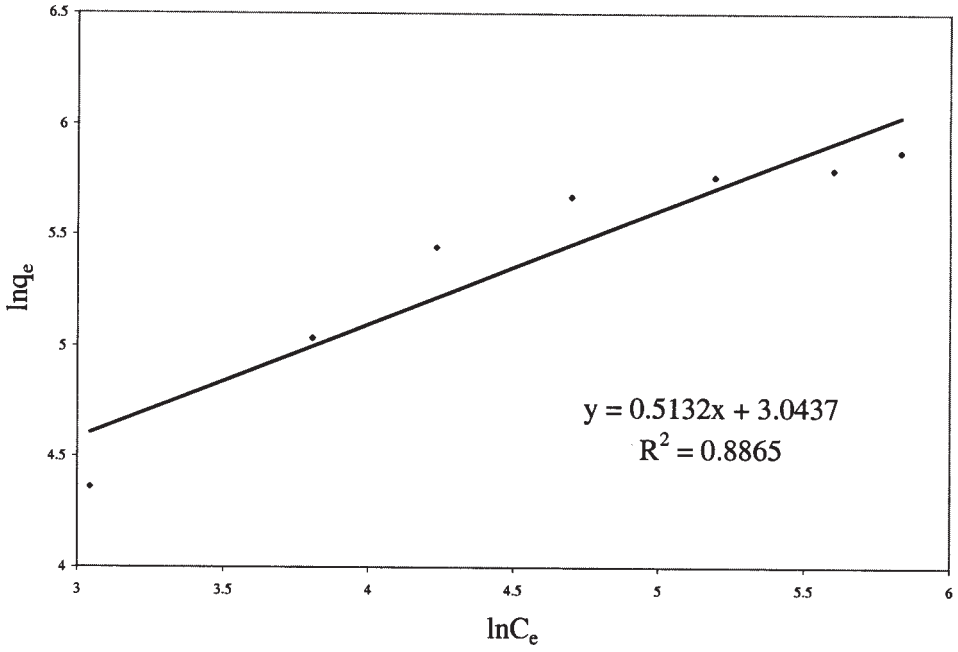

Fig. 5. Freundlich plot of As(III) adsorption on Fe_2O_3-SiO_2

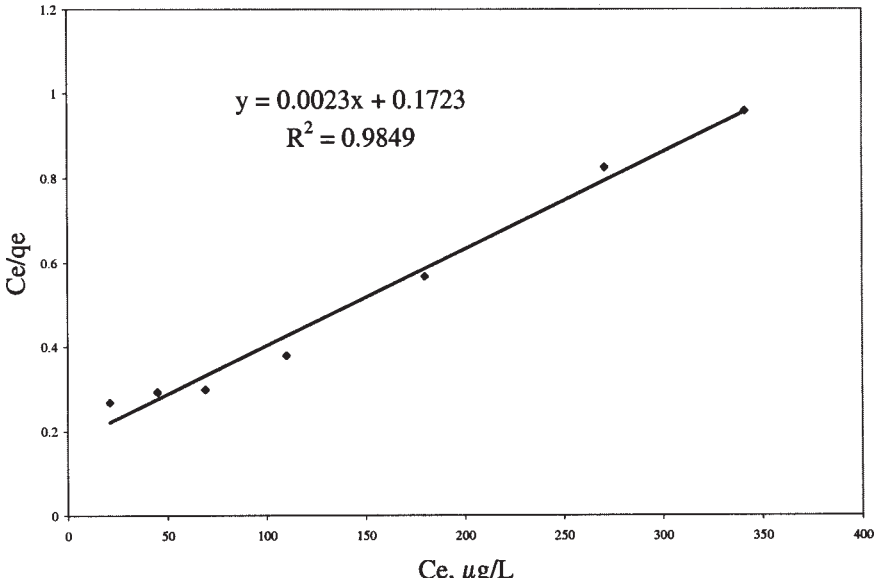

Fig. 6. Langmuir plot of As(III) adsorption Fe_2O_3-SiO_2

Freundlich isotherms. The value of 1/n < 1, which provides information about surface heterogeneity and surface affinity for the solute, indicates a favorable sorption of As (III) species and a very high affinity of the binary mixed oxide for As (III) due to the iron presence in the oxide.

The Langmuir model effectively describes the sorption data with a correlation coefficient of 0.9849. Thus the isotherm follows the sorption process in the entire studied concentration range. Furthermore, the values for the

Table 2
ISOTHERM PARAMETERS FOR As(III) ADSORPTION ON Fe_2O_3-SiO_2

Freundlich isotherm			Langmuir isotherm		
K_F, µg/g	1/n	R^2	K_L, L/µg	$q_{m\ calc}$, µg/g	R^2
20.98	0.5132	0.8865	0.0133	434.78	0.9849

calculated (from the Langmuir plot) and experimental maximum adsorption capacity are very close.

The dimensional constant, called separation factor (R_L), is used to describe the essential characteristics of Langmuir isotherm ($R_L > 1$, unfavorable; $R_L = 1$, linear; $0 < R_L < 1$, favorable; and $R_L = 0$, irreversible):

$$R_L = \frac{1}{1 + K_L C_o} \quad (6)$$

In fact, the separation factor is a measure of the used adsorbent capacity. R_L values were calculated for the studied concentration range and found to be $0 < R_L < 1$, showing favorable adsorption.

Conclusions

The sorption performance of a synthetic binary mixed oxide Fe_2O_3-SiO_2 for the As (III) species removal from water was evaluated. This material was chosen as potential adsorbent for arsenic removal because it was observed that the addition of the SiO_2 to the Fe_2O_3 samples leads to the increase of Fe_2O_3 active surface area.

The effect of contact time on As (III) sorption on the binary mixed oxide revealed that the equilibrium is reached in 90 min , with a typical adsorption performance of about 90%. The adsorption process followed a pseudo-second-order kinetics and the theoretically predicted equilibrium adsorption capacity was close to the experimentally determined value (80.6 mg/g).

Equilibrium adsorption data were modeled using Freundlich and Langmuir adsorption isotherms, and it was observed that the Langmuir model effectively describes the sorption data. The value of the calculated maximum adsorption capacity is close to the experimental value (340 µg/g). The dimensional separation factor used to predict the essential characteristics of Langmuir isotherm indicates favorable adsorption in the studied concentration range (100-700 µg As (III) /L).

The studied binary mixed oxide develops promising adsorbent properties concerning the arsenic (III) removal from aqueous medium.

Acknowledgements: The authors gratefully acknowledge the financial support provided by the UEFISCSU, under grant no. 694/19.01.2009, Code 927, "Integrated concept about depollution of waters with arsenic content, through adsorption on oxide materials, followed by immobilization of the resulted waste in crystalline matrices".

References

1. STREAT, M., HELLGARDT, K., NEWTON, N.L.R., Process Saf. Environ. Prot., **86**, 2008, p. 11
2. JONSSON, J., SHERMAN, D.M., Chem. Geol., **255**, 2008, p. 173
3. D. BORAH, D., SATOKAWA, S., KATO, S., KOJIMA, T., J. Hazard. Mater., **162**, 2009, p. 1269
4. CHUTIA, P., KATO, S., KOJIMA, T., SATOKAWA, S., J. Hazard. Mater., **162**, 2009, p. 204
5. BORAH, D., SATOKAWA, S., KATO, S., KOJIMA, T., J. Colloid Interface Sci., **319**, 2008, p. 53
6. MAJI, S.K., PAL, A., PAL, T., J. Hazard. Mater., **151**, 2008, p. 811
7. GUPTA, K., GHOSH, U.C., J. Hazard. Mater., **161**, 2009, p. 884
8. BANERJEE, K., AMY, G.L., PREVOST, M., NOUR, S., JEKEL, M., GALLAGHER, P.M., BLUMENSCHEIN, C.D., Water Res., **42**, 2008, p. 3371
9. PARTEY, F., NORMAN, D., NDUR, S., NARTEY, R., J. Colloid Interface Sci., **321**, 2008, p. 493
10. THIRUNAVUKKARASU, O.S., VIRARAGHAVAN, T., SUBRAMANIAN, K.S., Water SA, 2003, p. 161
11. SMEDLEY, P.L., KINNIBURGH, G., Appl. Geochem., **17**, 2002, p. 517
12. CIARDELLI, M.C., XU, H., SAHAI, N., Water Res., **42**, 2008, p. 615
13. MONDAL, P., MAJUMDER, C.B., MOHANTY, B., J. Hazard. Mater., **150**, 2008, p. 695
14. GUO, H., STUBEN, D., BERNER, Z., J. Colloid Interface Sci., **315**, 2007, p. 47
15. ZENG, L., Water Res., **37**, 2003, p. 4351
16. NEGREA, A., LUPA, L., CIOPEC, M., LAZĂU, R., Proceedings of the 11th International Conference on Environmental Science and Technology, Chania, Crete, Greece, Sept. 3-5 2009, B-655
17. NEGREA, A., CIOPEC, M., LUPA, L., MUNTEAN, C., LAZĂU, R., NEGREA, P., 10th International Conference on Modelling, Monitoring and Management of Water Pollution, 9-11 June 2010, Bucharest, Romania, accepted
18. LAZĂU, R., NEGREA, A., LUPA, L., IANOŞ, R, LAZĂU, I., PĂCURARIU, C., Rev. Rom. Mater., 2010, in press
19. OHE, K., TAGAI, Y., NAKAMURA, S., OSHIMA, T., BABA, Y., J. Chem. Eng. Jpn., **38**, 2005, p. 671
20. HO, Y.S., Scientometrics, **59**, 2004, p. 171
21. HO, Y.S., MCKAY, G., Process Biochem. (Amsterdam, Neth.), **34**, 1999, p. 451

Manuscript received: 19.05.2010

Adsorption of As(III) Ions onto Iron-containing Waste Sludge

Adina Negrea, Lavinia Lupa*, Mihaela Ciopec, Radu Lazau, Cornelia Muntean and Petru Negrea *Faculty of Industrial Chemistry and Environmental Engineering, University "Politehnica" Timisoara, 2 Piata Victoriei, 300006 Timisoara, Romania.*

(Received 29 July 2010; revised form accepted 27 October 2010)

ABSTRACT: The adsorption performance of a low-cost adsorbent (IS), viz. an iron-containing waste sludge arising during a hot-dip galvanizing process, towards the removal of As(III) ions from synthetic aqueous solutions and natural underground water was examined. The adsorption process was best described by the pseudo-second-order kinetic equation. The equilibrium adsorption data were well described by the Langmuir model. The value of the dimensional separation factor, R_L, indicated favourable adsorption. The maximum adsorption capacity of IS was 625 μg As(III)/g. The variation in the extent of adsorption with temperature was used to evaluate the thermodynamic parameters for the adsorption process. The values of ΔH^0 and ΔG^0 obtained demonstrated that the adsorption process was exothermic and spontaneous. The studied material exhibited an excellent As(III) ion adsorption performance from both synthetic solutions and a natural water sample. Moreover, no secondary contaminated substances arise if the exhausted adsorbent is recycled (e.g. in glass applications).

INTRODUCTION

Contamination of drinking water sources with arsenic is a matter of worldwide concern. High doses of arsenic are known to be toxic to humans, but chronic long-term exposure to inorganic arsenic compounds can also be detrimental to health. The symptoms of chronic poisoning in human beings are numerous: skin cancer, liver, lung, kidney and bladder cancer, as well as conjunctivitis, hyperkeratosis and — in severe cases — gangrene in the limbs and malignant neoplasm (Borah *et al*. 2008, 2009; Chutia *et al*. 2009). For this reason, the maximum permissible limit in drinking water has been set at 10 μg/ℓ according to the World Health Organization (WHO) (Gupta and Ghosh 2009; Maji *et al*. 2008; Banerjee *et al*. 2008; Partey *et al*. 2008). In Romania, the arsenic concentrations in some underground waters vary between 0.05 and 3.7 mg/ℓ, thereby exceeding the maximum limit set by the international standards. Highly concentrated arsenic waters in Romania were identified in the Saru Dornei region and in the Western Plain (Negrea *et al*. 2008). On the one hand, water becomes contaminated with arsenic as a consequence of natural processes such as weathering, biological activity and volcanic emission and, on the other hand, as a result of various industrial discharges, such as waste incineration, petroleum refinery by-products and wastes, fertilizers, insecticides and herbicides (Borah *et al*. 2009; Negrea *et al*. 2008; Jeong *et al*. 2007; Ohe *et al*. 2005).

The toxicity of arsenic depends strongly on its oxidation state. It has been reported that inorganic As(III) combinations are more toxic than As(V) and organic arsenic compounds (Maji *et al*. 2008).

*Author to whom all correspondence should be addressed. E-mail: lavinia.lupa@chim.upt.ro.

Thus, choosing a technology for the removal of As(III) from drinking water often represents a challenge. Numerous methods have been proposed to reduce arsenic levels in natural waters, including oxidation–reduction, precipitation, co-precipitation, adsorption, electrolysis and cementation, solvent extraction, ion-exchange, ion flotation and biological processing (Gupta and Ghosh 2009; Nguyen *et al*. 2009; Borah *et al*. 2008; Banerjee *et al*. 2008; Partey *et al*. 2008; Hsu *et al*. 2008; Chen *et al*. 2008). Although coagulation and co-precipitation processes are widely used at present for arsenic removal, they yield large amounts of sludge and demonstrate low removal efficiencies (Bilici Baskan and Pala 2009; Song *et al*. 2006; Parga *et al*. 2005). Membrane filtration processes lower the arsenic concentration in water from 48 to 1–2 μg/ℓ (Bissen and Frimmel 2003), while ion-exchange methods can lower the arsenic concentration in natural waters down to 5 μg/ℓ (Wang *et al*. 2002). However, the application of membrane techniques, reverse osmosis and nano-filtration is expensive and requires highly qualified personnel for operation and maintenance purposes (Qu *et al*. 2009; Parga *et al*. 2005). Furthermore, the removal efficiency of arsenic via these methods is strongly influenced by the solution pH and type of membrane employed (Kosutic and Furac 2005; Ning 2002). Similarly, the use of ion-exchange resins is an unattractive option because of the high costs involved and the short life cycle of the resin. This is rapidly exhausted if the water contains substantial concentrations of sulphates or nitrates (Parga *et al*. 2005; Kim and Benjamin 2004). Other treatment methods such electro-coagulation and electrodialysis have limited applications in this field because of the expensive equipment required and the high energy consumption involved (Balasubramanian *et al*. 2009; Parga *et al*. 2005).

Adsorption has proved to be the most effective procedure for the removal of arsenic even when present in very low concentrations in aqueous solutions. To date, various adsorbents — both natural and synthetic — have been developed for arsenic removal. These include metal oxides/hydroxides (Gupta and Ghosh 2009; Banerjee *et al*. 2008; Partey *et al*. 2008; Jonsson and Sherman 2008; Jeong *et al*. 2007; Ohe *et al*. 2005), natural and synthetic zeolites (Chutia *et al*. 2009), laterite soil (Maji *et al*. 2008; Partey *et al*. 2008), calcite (So *et al*. 2008) and activated carbon (Borah *et al*. 2008, 2009; Mondal *et al*. 2008). However, the effective removal of arsenic from aqueous media is costly and requires expensive synthetic arsenic adsorbents. Consequently, there is a real need in developing countries for alternative low-cost solutions.

The goal for our research is to develop an arsenic-removal system using a low-cost adsorbent. This requires high arsenic affinity and good adsorption capacity. The material tested in the present work was an iron-containing waste sludge (IS) resulting from the hot-dip galvanizing process. According to literature data, iron compounds in general and particularly iron hydroxides are very efficient adsorbents for the removal of arsenic (Banerjee *et al*. 2008; Hsu *et al*. 2008; Mondal *et al*. 2008; Partey *et al*. 2008; Jeong *et al*. 2007; Yudovich and Ketris 2005; Nikolaidis *et al*. 2003; Thirunavukkarasu *et al*. 2003; Zeng 2003).

Hot-dip galvanization is a coating process applied in order to prevent iron-based materials from corroding. Hot-dip galvanizing is one of the most common coating methods and is particularly used to coat steel. Before hot-dip galvanizing, samples are subjected to a preparation process which consists of degreasing, chemical cleaning, rinsing, fluidizer treatment and pre-warming. The wastewaters resulting from these operations are neutralized with lime. This method can efficiently remove heavy metals from wastewaters, but it generates a secondary product – iron-containing sludge — which is classified as an industrial waste and causes disposal problems (Lupa *et al*. 2006).

In the work described herein, arsenic removal from aqueous media using the hot-dip galvanizing sludge was tested in an attempt to provide an appropriate environmental and economical solution. In future work it is intended to further recycle the exhausted adsorbent (e.g. in iron glass applications — as As_2O_3 is an effective O_2 carrier at high temperatures) and

hence the method presented should generate no secondary contaminated substances at the end of the waste recycling/de-pollution process.

EXPERIMENTAL

Adsorbent characterization

Iron-containing waste sludge (IS) resulting from hot-dip galvanizing was dried in the open air at room temperature and then ground and sieved. In subsequent studies, the fraction possessing particles with diameters less than 0.32 mm but larger than 0.063 mm was employed.

IS was submitted to thermal analysis in order to determine both its thermal behaviour and the most appropriate drying temperature. For such purposes, a 17 mg IS sample placed in a Pt crucible was examined using a Perkin Elmer Diamond TG/DTA Analyzer, employing a linear heating rate of 10 ºC/min in a dynamic atmosphere (air, 100 mℓ/min flow rate) with Al_2O_3 being used as the DTA reference material. After analyzing the results, a temperature of 105 ºC was chosen for drying purposes.

Thus, IS was dried at 105 ºC for 24 h and characterized by scanning electron microscopy (SEM), energy dispersive X-ray analysis (EDX), X-ray diffractometry (XRD) and BET–accelerated surface area analysis.

SEM micrographs were obtained and EDX studies performed on a FEI Inspect S scanning electron microscope, thereby allowing the surface morphology of IS to be observed and its chemical composition analyzed. X-Ray powder diffraction patterns in Bragg–Brentano geometry were recorded on a Bruker D8 Advance automated powder diffractometer fitted with a NaI(Tl) scintillation detector and a graphite monochromator employing Cu Kα diffracted radiation (λ = 1.5418 Å). The specific surface area and the pore volume of an IS sample annealed at 200 ºC were measured using a Micromeritics ASAP 2020 BET surface area analyzer via nitrogen adsorption/desorption isotherms measured at –196 ºC. Thermal treatment was performed using a Nabertherm B 150 oven, the sample being heated at a rate of 10 ºC/min up to 200 ºC with the temperature being then maintained at this value for 1 h.

To understand the characteristics of the surface charge generated on IS in aqueous media, the point of zero charge, pH_{pzc}, of IS was determined by batch equilibration techniques (Borah *et al*. 2008, 2009; Cerovic *et al*. 2007). In such experiments, a known amount of IS (0.2 g) was suspended in 100 mℓ of a 0.005 M NaCl solution employed as an inert background electrolyte. All experiments were performed at laboratory temperature (20 ± 1 ºC). The value of the initial pH of the NaCl solution (pH_i) was varied between 2 and 12, being adjusted to the desired value using 0.1 M/2 M NaOH or 0.1 M/2 M HNO_3, thereby keeping the volume variation of the solution to a value as low as possible. The pH values of the solutions were measured by means of a CRISON MultiMeter MM41 fitted with a glass electrode which had been calibrated using various buffer solutions. The suspensions were stirred for 1 h at 300 rpm by an IKA RTC basic magnetic stirrer. After the necessary stirring time, the suspensions were filtered and the final pH values of the solutions (pH_f) determined. The pH_{pzc} was determined via a plot of pH_f versus pH_i.

Adsorption performance

The influence of different physicochemical parameters [contact time, initial concentration of As(III) ions and temperature] upon the adsorption of As(III) ions onto IS was investigated.

For all adsorption experiments, the initial pH of the solutions was maintained within the range 6.7–7.0, i.e. at the mid-point of the plateau obtained in the plot of pH_f versus pH_i mentioned above. This also corresponds to the most common pH value found in natural waters. In all cases, the same adsorbent dosage (0.1 g IS) was employed in 100 mℓ of As(III) ion solution. The suspensions were stirred using a device fitted with a glass rod at a stirring speed of 200 rpm.

Prior to such experiments, a stock solution of arsenic was prepared by diluting an appropriate amount of 0.05 M $NaAsO_2$ solution (Merck TitriPUR). Other solutions of As(III) ions were prepared from the stock solution by appropriate dilution.

The effect of contact time at 20 ± 1 ºC was initially studied employing 100 mℓ of a 100 µg/ℓ As(III) ion solution with an IS adsorbent dosage of 0.1 g, the resulting suspensions being stirred for different contact times (15, 30, 45, 60, 90, 120 and 150 min). Similar batch experiments were performed at 20 ± 1 ºC to study the influence of the initial As(III) ion concentration (100, 200, 300, 400, 500, 600 and 700 µg/ℓ) on the adsorption process, while the influence of temperature was investigated by studying the adsorption process in a 0.1 g IS/100 µg/ℓ As(III) ion solution system at three different temperatures: 20 ± 1, 25 ± 1 and 30 ± 1 ºC, respectively.

After stirring, the samples were centrifuged at 1200 rpm for 0.5 h using a Hettich ROTINA 420 centrifuge. The residual concentration of As(III) ions in the resulting solutions was determined using atomic absorption spectrometry with hydride generation (Negrea *et al*. 2006; Niedzielski 2005). This method uses the selective reduction of As(III) ions to arsine (H_3As) with sodium borohydride, $NaBH_4$ (Merck-Schuchardt; 0.6 w/v% solution), in a NaOH buffer (Chemapol, Prague, Czech Republic; 0.5 w/v%). The arsine gas generated was introduced into the flame of the atomic absorption spectrometer and the absorbance value measured at 193.7 nm was compared with a calibration curve obtained using As(III) ion solutions of various known concentrations prepared from the stock solution. The carrier solution employed in the flow injection system was prepared using HCl (37%, Corozin, Romania; 1:3). A Varian SpectrAA 110 atomic absorption spectrometer with a Varian VGA 77 hydride generation system was used for all measurements.

The various chemicals employed in the experiments were of A.R. grade and used without further purification. Distilled water was used throughout.

The extent of adsorption was quantified in terms of the adsorption capacity, q_t (µg/g), of the adsorbent, corresponding to the amount of As(III) ions sorbed per g adsorbent at a known time t, as calculated from the following equation (Borah *et al*. 2009; Faghihian and Nejati-Yazdinejad 2009a,b; Gupta and Ghosh 2009; Kul and Caliskan 2009; Gopal and Elango 2007; Ohe *et al*. 2005):

$$q_t = \frac{(C_0 - C_t)V}{m} \quad (1)$$

where C_0 and C_t are the concentrations of As(III) ions (µg/ℓ) in the solution initially, (t = 0) and after a time t (min), respectively, V is the volume of the solution (ℓ) and m is the mass of adsorbent employed (g).

Another parameter of interest was the removal degree of As(III) ions, η (%), which may be calculated from the relationship:

$$\eta\,(\%) = \frac{(C_0 - C_t)}{C_0} \times 100 \quad (2)$$

where C_0 and C_t have the same meanings as above.

To evaluate the potential use of IS as an adsorbent for As(III) ion removal from natural waters, we treated a sample collected from a well with a known high As(III) ion concentration situated in the western area of Romania (Negrea *et al*. 2009). The sample of water (100 mℓ) was treated with the necessary amount of adsorbent (0.1 g) under the optimal conditions established employing synthetic As(III) ion solutions. The initial and residual concentrations of As(III) ions, as well as other metal ions, were determined by atomic absorption spectrometric methods. The experimental results cited below are the average of three sets of data obtained under identical working conditions.

Adsorption kinetics

Kinetic adsorption experiments were carried out with a view to finding out the time necessary for adsorption equilibrium to be established and the mechanism of the adsorption process. To examine the kinetics for As(III) ion adsorption onto IS, the experimental data were analyzed employing the following models:
(a) A first-order reaction model expressed as an integrated concentration function and written as follows (Banerjee *et al*. 2008):

$$\ln C_t = \ln C_0 - k_1 t \tag{3}$$

where k_1 is the specific adsorption rate constant (min^{-1}).
(b) The pseudo-first-order kinetic model proposed by Lagergren (1898). The linear form of this model can be expressed as (Borah *et al*. 2009; Gupta and Ghosh 2009; Kul and Caliskan 2009; Chen *et al*. 2008; Shan 2004):

$$\ln(q_e - q_t) = \ln q_e - k_{s1} t \tag{4}$$

where q_e (µg/g) corresponds to the amount of As(III) ions sorbed per unit mass of IS at equilibrium and k_{s1} is the specific adsorption rate constant (min^{-1}).
(c) A second-order reaction model based on the solution concentration as widely used for metal ion adsorption processes. The integrated form of this model may be expressed by the following equation (Banerjee *et al*. 2008):

$$\frac{1}{C_t} = \frac{1}{C_0} + k_2 t \tag{5}$$

where k_2 is the second-order rate constant [$min^{-1}(\mu g/\ell)^{-1}$].
(d) The linear form of the pseudo-second-order rate expression of Ho and McKay (Borah *et al*. 2009; Gupta and Ghosh 2009; Kul and Caliskan 2009; Jeong *et al*. 2007) which may be written as:

$$\frac{t}{q_t} = \frac{1}{h} + \frac{t}{q_e} \tag{6}$$

where $h = k_{s2} q_e^2$, with k_{s2} being the pseudo-second-order rate constant [$min^{-1}(\mu g/g)^{-1}$].
(e) Intra-particle diffusion, which is an important phenomenon for adsorption processes in porous materials. The functional relationship for this process which has been used by many authors (Bhattacharyya and Gupta 2009; Borah *et al*. 2009; Gupta and Ghosh 2009; Chen *et al*. 2008;

Gopal and Elango 2007; Ho *et al*. 2000; Juang *et al*. 1996; Juang and Swei 1996; Singh *et al*. 1988) may be written as:

$$q_t = k_{id} t^{0.5} \tag{7}$$

where k_{id} is the intra-particle diffusion rate constant [μg/(g $min^{0.5}$)] which may be calculated from the slope of the linear plot of q_t versus $t^{0.5}$.

Adsorption equilibrium

Langmuir and Freundlich isotherm studies were undertaken in order to determine the maximum adsorption capacity, q_m (μg/g), of IS towards As(III) ions.

The linear form of the Freundlich equation may be written as:

$$\ln q_e = \ln K_F + \tfrac{1}{n} \ln C_e \tag{8}$$

while the Langmuir isotherm may be written as:

$$\frac{C_e}{q_e} = \frac{1}{K_L q_m} + \frac{C_e}{q_m} \tag{9}$$

where C_e corresponds to the residual concentration of As(III) ions in the solution at equilibrium (μg/ℓ), K_F and 1/n are characteristic constants that can be related to the relative adsorption capacity of the adsorbent and the intensity of adsorption, respectively, q_m is a measure of monolayer adsorption capacity (μg/g) and K_L is a constant related to the free energy of adsorption (Borah *et al*. 2008, 2009; Chutia *et al*. 2009; Faghihian and Nejati-Yazdinejad 2009a,b; Gupta and Ghosh 2009; Kul and Caliskan 2009; Banerjee *et al*. 2008; Hsu *et al*. 2008; Partey *et al*. 2008; So *et al*. 2008; Jeong *et al*. 2007; Ohe *et al*. 2005; Thirunavukkarasu *et al*. 2003).

To assess the extent to which the kinetic and adsorption isotherms equations fit the experimental data, two different error functions were examined.

The normalized standard deviation, Δq (%), was estimated using the equation (Lv *et al*. 2007; El-Kamash *et al*. 2005):

$$\Delta q\,(\%) = \sqrt{\frac{1}{p-1}\sum_{i=1}^{p}\left(\frac{q_{exp} - q_{calc}}{q_{exp}}\right)_i^2} \times 100 \tag{10}$$

where q_{exp} is the experimentally determined adsorption capacity (μg/g), q_{calc} is the adsorption capacity calculated according to the model equation (μg/g) and p is the number of experimental data points.

The average relative error E (%), which minimizes the fractional error distribution across the entire concentration range, was estimated via the equation (Allen *et al*. 2004; Ho *et al*. 2000):

$$E\,(\%) = \left(\frac{1}{p-1}\right)\sum_{i=1}^{p}\left(\frac{q_{calc} - q_{exp}}{q_{exp}}\right)_i^2 \times 100 \tag{11}$$

Thermodynamics of adsorption

Thermodynamic parameters such as the Gibbs' free energy (ΔG^0) can be obtained from the Gibbs–Helmholtz relationship (Bhattacharyya and Gupta 2009; Borah *et al*. 2009; Gupta and Ghosh 2009; Faghihian and Nejati-Yazdinejad 2009a,b; Kul and Caliskan 2009; Banerjee *et al*. 2008; Partey *et al*. 2008; Gopal and Elango 2007; Singh *et al*. 1988), viz.

$$\Delta G^0 = \Delta H^0 - T\Delta S^0 \tag{12}$$

where ΔH^0 and ΔS^0 are the standard enthalpy change and the standard entropy change, respectively. The corresponding values of ΔH^0 and ΔS^0 can be estimated from the relationship between the equilibrium constant (or distribution coefficient, K_d) and ΔH^0 as defined by the Clausius–Clapeyron equation which is the thermodynamic basis for predicting the change in the value of the equilibrium constant with temperature:

$$\ln K_d = \frac{\Delta S^0}{R} - \frac{\Delta H^0}{RT} \tag{13}$$

where K_d may be defined (Bhattacharyya and Gupta 2009; Borah *et al*. 2009; Faghihian and Nejati-Yazdinejad 2009a,b; Gupta and Ghosh 2009) as:

$$K_d = \frac{(C_0 - C_e)}{C_e} \bullet \frac{V}{m} \tag{14}$$

with the other terms in the equation having their usual meanings. A plot of $\ln K_d$ versus 1/T should be linear with the values of ΔH^0 and ΔS^0 being obtained from the slope ($\Delta H^0/R$) and the intercept ($\Delta S^0/R$), respectively.

RESULTS AND DISCUSSION

Adsorbent characterization

Figure 1 illustrates the thermal behaviour of IS. Heating up to 1000 ºC at a constant heating rate of 10 ºC/min led to decomposition of the sample, accompanied by a corresponding mass loss. Up to 180 ºC, the sample lost 28.0% of its weight in two steps, with maximum rates at 100 ºC (shoulder at 90 ºC) and 130 ºC, both with endothermic effects. This mass loss can be assigned to the elimination of adsorbed water. Between 180 ºC and 300 ºC, the sample lost a further 5.2% of its weight, with a maximum rate at 260 ºC (shoulder at 275 ºC) accompanied by an endothermic effect; between 300 ºC and 720 ºC, the sample slowly lost a further 3.9% of its weight. These mass losses can be assigned to dehydroxylation of the material, i.e. the transformation of FeO(OH) to Fe_2O_3 and the dehydration of $Ca(OH)_2$ which was present in a small proportion in the sample. At 720 ºC, another process begins with an accompanying mass loss leading to the residue being only 52.8% of its initial weight at 1000 ºC. Thus, in order to remove most of the water from IS and to avoid the other processes taking place at higher temperatures, the drying temperature for the material was chosen as 105 ºC.

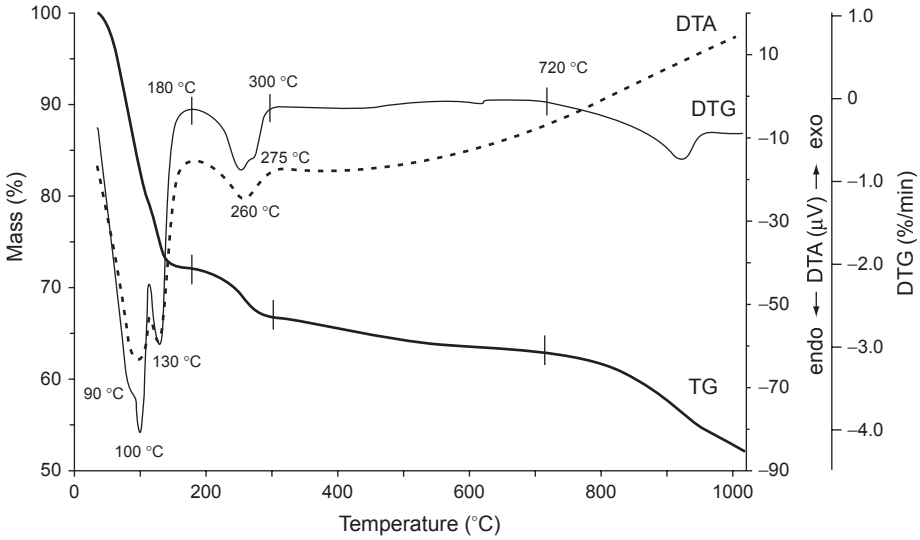

Figure 1. TG, DTG and DTA curves for IS.

EDX data concerning the composition of IS dried at 105 ºC are presented in Figure 2. It will be seen from the EDX plot and corresponding data that the major component in IS was iron, thereby making it suitable for the removal of As(III) ions from water due to the high affinity of arsenic towards iron (Banerjee *et al*. 2008; Hsu *et al*. 2008; Mondal *et al*. 2008; Partey *et al*. 2008; Jeong *et al*. 2007; Yudovich *et al*. 2005; Thirunavukkarasu *et al*. 2003; Nikolaidis *et al*. 2003; Zeng 2003). The chloride ions indicated in the plot arose from the hydrochloric acid used for chemical cleaning of steel parts, while the calcium ions came from the neutralizing agent used in the residual water treatment. The other ions found in smaller proportions either came from the solution used for degreasing the steel parts, or from the water used in various stages of the

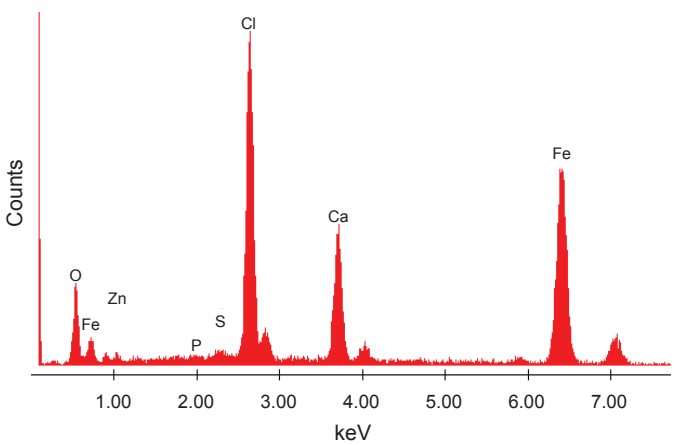

Element	Wt.%
O	28.63
P	0.45
S	0.71
Cl	22.86
Ca	11.20
Fe	33.45
Zn	2.70
Total	100.00

Figure 2. EDX plot and corresponding chemical composition of IS dried at 105 ºC.

technological process. The zinc ions resulted from de-zincing of those parts which had been badly coated during the technological process. All the metals recorded in Figure 2 as present in IS were in the form of oxides or hydroxides.

A scanning electron micrograph of IS dried at 105 ºC is presented in Figure 3. The morphology of the sample consisted of rough conglomerates with a highly open porosity. Hence, the sample was expected to exhibit a relatively high surface area and an associated high adsorption capacity.

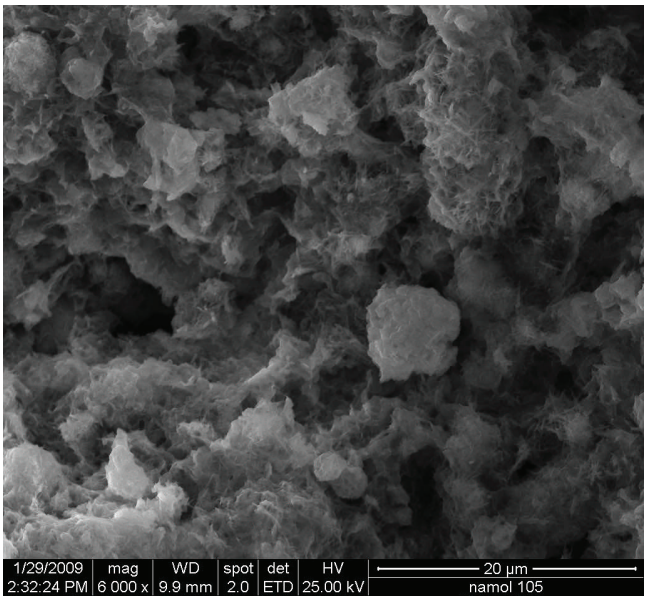

Figure 3. Scanning electron micrograph of IS dried at 105 ºC.

The XRD pattern of IS (Figure 4) shows that the material was mainly amorphous with lines corresponding to poorly crystallized iron oxy-hydroxides present as goethite and lepidocrocite.

The BET surface area of the IS sample annealed at 200 ºC was 50.5 m^2/g, with a pore volume of 0.168 cm^3/g and an average pore size of 111.5 Å. Because of its phase composition, the sample dried at 105 ºC could not be degassed to a satisfactory extent to allow surface area analysis to be performed; however, it may be assumed that it possessed an even higher surface area.

The acid–base properties of IS play an important role in the use of the material as an adsorbent. Figure 5 shows the corresponding plot of pH_f versus pH_i allowing the determination of the point of zero charge (pH_{pzc}) for the material. The pH value of the plateau exhibited in this plot corresponds to pH_{pzc} = 6.2. The presence of such a plateau indicates that IS was an ampholyte and behaved as an acid–base buffer (Borah *et al*. 2008, 2009; Cerovic *et al*. 2007). This plateau corresponds to the pH range where buffering of the IS surface occurs, thereby making all values of pH_i between 4 and 9 equal to the corresponding value of pH_f. The pH_{pzc} value for IS suggests that the surface of the material was predominantly positive at pH values lower than 6.2 and negative at pH values higher than 6.2. The surface charge density of the material should increase or decrease as the pH value of the system decreases below pH_{pzc} or increases above this value.

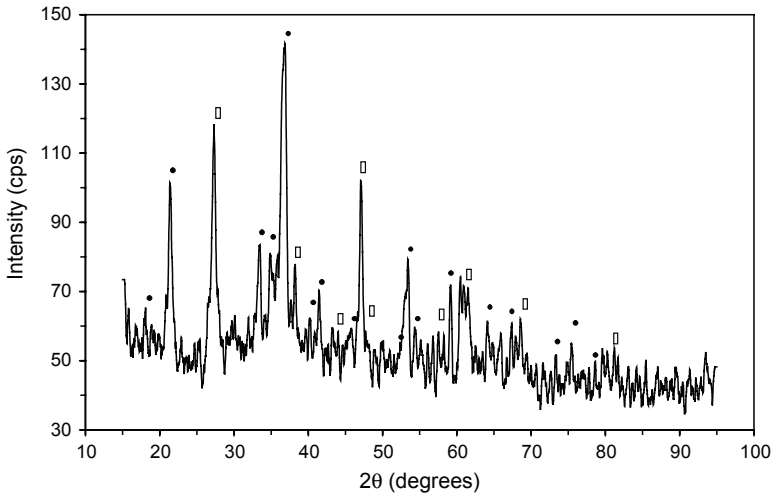

Figure 4. XRD pattern of IS dried at 105 ºC. Peaks marked as • correspond to goethite, i.e. *syn*-FeO(OH) (JCPDS file 81-0464), while those marked as □ correspond to lepidocrocite, i.e. FeO(OH) (JCPDS file 76-2301).

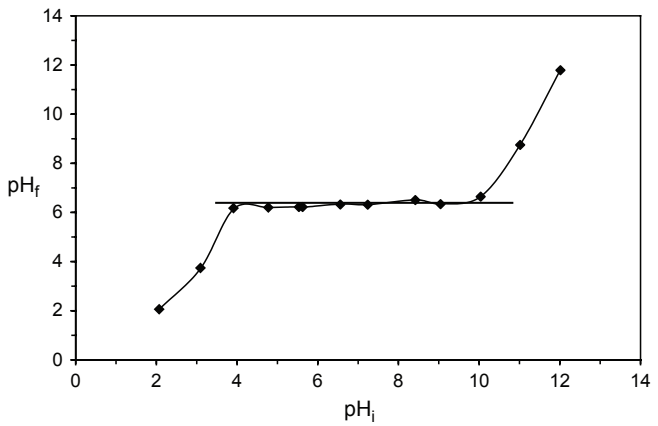

Figure 5. Plot of the final pH (pH_f) versus the initial pH (pH_i) allowing the determination of the value of pH_{pzc} for IS dried at 105 ºC.

Effect of contact time and adsorption kinetics

The effect of contact time on As(III) ion adsorption onto IS is presented in Figure 6. It should be noted that both the adsorption capacity and removal degree increased abruptly as the contact time was increased up to 90 min, but then remained constant. This high initial adsorption rate was due to the availability of a large number of adsorption sites on the adsorbent at the onset of the process. The plateau in the figure corresponds to the attainment of equilibrium when more than 95% of the

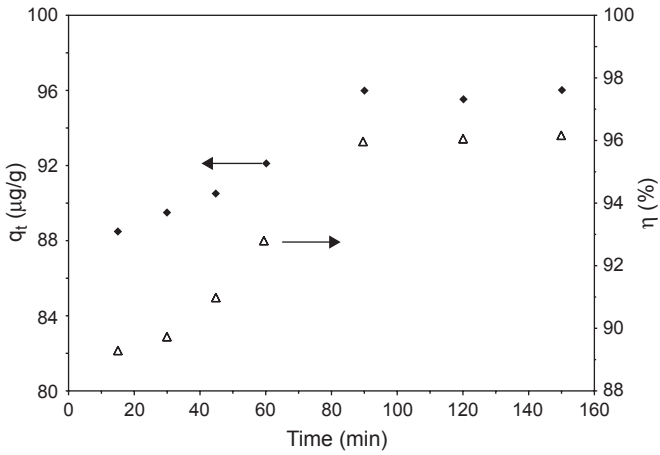

Figure 6. Effect of contact time on the adsorption capacity, q_t (μg/g), and the degree of As(III) ion removal, η (%), by IS dried at 105 ºC. Experimental conditions: initial conc. of As(III) ion solution, C_0 = 100 μg/ℓ; pH = 6.7–7.0; temp. = 20 ± 1 ºC. Data points correspond to the following: ◆, q_t; Δ, η.

initial amount of As(III) ions in the system had been adsorbed. The removal rate of As(III) ions was rather high compared with other results reported in the literature (Chutia *et al*. 2009; Gupta and Ghosh 2009; Chen *et al*. 2008; Jeong *et al*. 2007), where equilibrium times of 3, 8, 12 and even 24 h have been cited. The rapid removal of As(III) ions coupled with a low equilibration time indicates the existence of highly favourable sorptive interactions. In addition, the removal degree was rather high compared to the results of other workers (Borah *et al*. 2009; Chen *et al*. 2008; Hsu *et al*. 2008; Mondal *et al*. 2008; Thirunavukkarasu *et al*. 2003) who have reported values in the range 50–80%. The residual concentration of As(III) ions in the aqueous phase at equilibrium was less than 4 μg/ℓ, a value comparable with other results reported in the literature (Thirunavukkarasu *et al*. 2003).

If the process follows first-order kinetics, the linear plot of ln C_t versus t may be employed to estimate the corresponding rate constant. The pseudo-first-order rate constant may be determined from the linear plot of $\ln(q_e - q_t)$ versus t, while the linear plot of $1/C_t$ versus t may be used to determine the second-order rate constant. Finally, the pseudo-second-order rate constant can be estimated from the linear plot of t/q_t versus t. The values of all these constants determined as indicated, together with the corresponding regression coefficients (R^2), are listed in Table 1.

The only plot exhibiting good linearity with a good correlation coefficient (close to 1) was obtained for the case of the pseudo-second-order model (Figure 7). The other models did not describe the kinetics of the adsorption process in a satisfactory manner and the corresponding plots have therefore not been included here. Furthermore, in the case of the pseudo-first-order model, there was a large difference between the value of q_e as determined experimentally and that calculated from the kinetic plot. At the same time, the value of the estimated error was very high, indicating that the kinetic isotherm equation gave a very poor fit to the experimental data. However, in the case of the pseudo-second-order model, the theoretically predicted equilibrium adsorption capacity was close to the experimentally determined value [q_e (experimental) = 96.1 μg/g; q_e (kinetic plot) = 98.0 μg/g]. In addition, the fact that the correlation coefficient was close

TABLE 1. Kinetic Parameters for As(III) Ion Adsorption by IS

Model/parameter	Value	Model/parameter	Value
First-order model		*Second-order model*	
k_1 (min^{-1})	9×10^{-3}	k_2 [$min^{-1}/(\mu g/\ell)$]	1.5×10^{-3}
$t_{1/2}$ (min)	77	R^2	0.8899
R^2	0.8909	*Pseudo-second-order model*	
Pseudo-first-order model		k_{s2} [$min^{-1}/(\mu g/g)$]	3.87×10^{-3}
k_{s1} (min^{-1})	3.85×10^{-2}	R^2	0.9997
$t_{1/2}$ (min)	18	q_e (experimental) (μg/g)	96.1
R^2	0.8513	q_e (kinetic plot) (μg/g)	98.0
q_e (experimental) (μg/g)	96.1	Δq (%)	6.5
q_e (kinetic plot) (μg/g)	20.4	E (%)	0.4
Δq (%)	88.5	*Intra-particle diffusion model*	
E (%)	78.3	k_{id} [$\mu g/(g\ min^{-0.5})$]	1.31

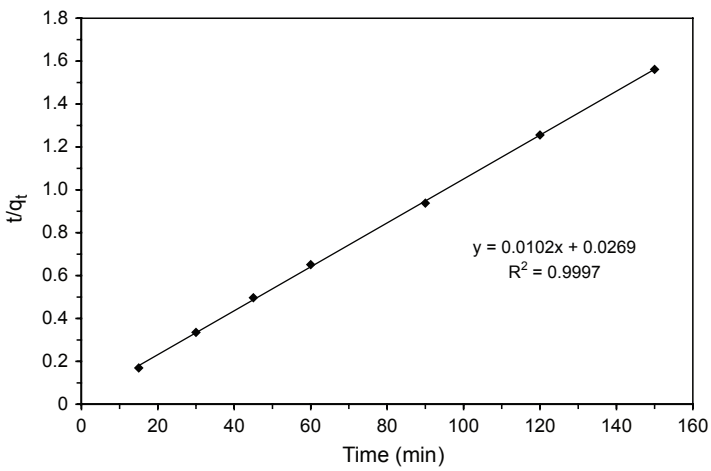

Figure 7. Pseudo-second-order kinetic plot for the adsorption of As(III) ions onto IS.

to unity and that the estimated error was lower indicates that the kinetics for the removal of As(III) ions via adsorption onto IS could be well explained and approximated by the pseudo-second-order kinetic model.

However, such results provide no information regarding the rate-limiting step in the process. The rate-limiting step (i.e. the slowest step in the process) may either be boundary layer (film) diffusion or intra-particle (pore) diffusion of the solute towards the solid surface. If the rate-limiting step is intra-particle diffusion, the plot of q_t versus the square root of time should be linear and pass through the origin. Any deviation of the plot from linearity would indicate that the rate-limiting step should be controlled by boundary layer (film) diffusion. The plot of q_t versus $t^{0.5}$ depicted in Figure 8 shows two linear sections. The first may be attributed to intra-particle

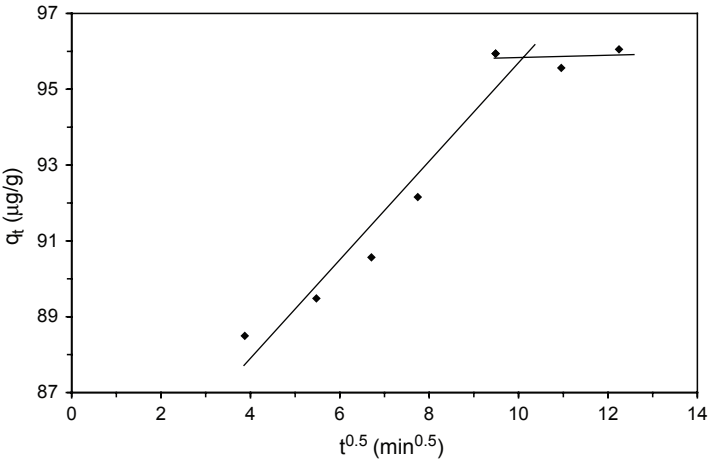

Figure 8. Weber–Morris plot for the intra-particle diffusion of As(III) ions onto IS.

diffusion, the fact that the line does not pass through the origin indicating that the mechanism of As(III) ion adsorption onto IS is complex, with both surface adsorption and intra-particle diffusion contributing to the rate-limiting step. The second linear section represents the final equilibrium stage (Bhattacharyya and Gupta 2009; Borah *et al*. 2009; Gupta and Ghosh 2009; Chen *et al*. 2008; Gopal and Elango 2007; Juang *et al*. 1996; Juang and Swei 1996; Singh *et al*. 1988).

Effect of the initial As(III) ion concentration and adsorption equilibrium

The adsorption isotherm for As(III) ions onto IS is presented in Figure 9. It will be seen that, at high equilibrium concentrations, the adsorption capacity approached a limiting value. This value

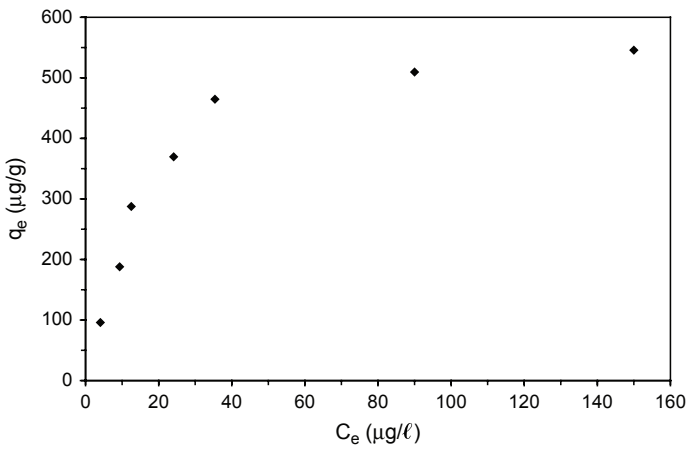

Figure 9. Adsorption isotherm of As(III) ions onto IS. Experimental conditions: C_0 = 100–700 µg/ℓ; contact time = 90 min; temp. = 20 ± 1 ºC; pH = 6.7–7.0.

represents the experimentally-determined maximum adsorption capacity of As(III) ions onto IS [q_m (experimental) > 550 μg/g] and is close to the value calculated using the Langmuir model (Table 2).

The adsorption equilibrium data were correlated with the Freundlich and Langmuir isotherms. The calculated parameters, as well as the correlation coefficients (R^2) and the

TABLE 2. Freundlich and Langmuir Isotherm Parameters for As(III) Ion Adsorption by IS

Isotherm/parameter	Value	Isotherm/parameter	Value
Freundlich isotherm		*Langmuir isotherm*	
K_F (μg/g)	70.32	K_L (ℓ/μg)	0.0569
1/n	0.4584	q_m (μg/g)	625
R^2	0.8550	R^2	0.9952
Δq (%)	25	Δq (%)	12.3
E (%)	6.25	E (%)	1.52

estimated errors for As(III) ion removal through adsorption onto IS are presented in Table 2. It will be seen that the Freundlich plot had a lower correlation coefficient and a higher absolute error than the Langmuir plot. This suggests that the Freundlich isotherm was not suitable for describing the experimental data obtained and its plot has, accordingly, been omitted. However, the Langmuir model effectively described the equilibrium adsorption data (Figure 10), since the linear plot had a good correlation coefficient (> 0.99) and a low absolute error. The isotherm gave a reasonable fit to the experimental data over the entire concentration range studied, thereby suggesting that monolayer adsorption of As(III) ions onto IS was the principal mechanism in the process.

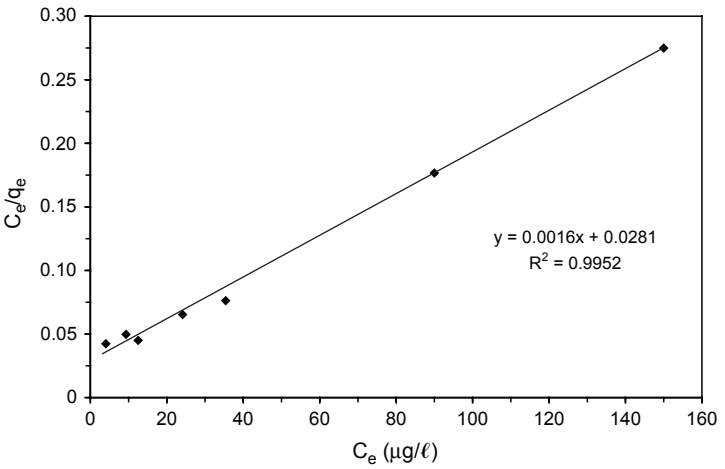

Figure 10. Linear Langmuir plot for the adsorption of As(III) ions onto IS.

The equilibrium parameter, called the separation factor (R_L), was used to describe the essential characteristics of the Langmuir isotherm ($R_L > 1$, unfavourable; $R_L = 1$, linear; $0 < R_L < 1$, favourable; and $R_L = 0$, irreversible) (Borah *et al*. 2008, 2009; Thirunavukkarasu *et al*. 2003):

$$R_L = \frac{1}{1 + K_L C_0} \tag{15}$$

The values of R_L were calculated for the entire concentration range studied and found to be greater than 0 and smaller than 1, showing that the adsorption process was favourable. However, the values of R_L decreased as the initial As(III) ion concentration increased, viz. from 0.149 (for C_0 = 100 μg/ℓ) to 0.024 (for C_0 = 700 μg/ℓ). This indicates that adsorption was more favourable for higher initial As(III) ion concentrations.

Table 3 provides a comparison of the IS adsorption capacity to that of other materials mentioned in the literature. For the same class of materials, IS exhibited a high adsorption capacity. However, it should be noted that there are highly specialized, more expensive synthetic materials available which exhibit higher adsorption capacities.

TABLE 3. Comparison of As(III) Ion Adsorption Performance of IS with that of Other Adsorbents Mentioned in the Literature

Adsorbent	pH	q_m (μg/g)	Reference
Hydrous nanostructure iron(III)–titanium(IV) (NHITO)	7.0	85.0×10^3	Gupta and Ghosh (2009)
Crystalline hydrous ferric oxide	7.0	33.3×10^3	Gupta and Ghosh (2009)
Crystalline hydrous titanium oxide	7.0	31.7×10^3	Gupta and Ghosh (2009)
Magnetite	6.0	20.7×10^3	Ohe *et al*. (2005)
Nanoscale zero-valent iron	7.0	2.47×10^3	Gupta and Ghosh (2009)
Laterite iron concretions	7.0	909	Partey *et al*. (2008)
Iron oxide-coated sand (IOCS)	5.0	12.6	Hsu *et al*. (2008)
Granular ferric hydroxide (GFH)	7.0	112	Thirunavukkarasu *et al*. (2003)
Haematite	7.0	198	Singh *et al*. (1988)
IS (iron-containing waste sludge)	6.7–7.0	625	Present work

Thermodynamic parameters

The plot of ln K_d versus 1/T illustrated in Figure 11 is linear with a good correlation coefficient ($R^2 > 0.98$). The thermodynamic parameters as calculated from the linear plot and from equation (12) are listed in Table 4.

The overall free energy change during the adsorption process was negative for the range of temperatures studied, corresponding to a spontaneous physical process for As(III) ion adsorption. On decreasing the temperature from 303 K to 293 K, the standard free energy change became even more negative, suggesting that the adsorption process was favoured at lower temperatures. This represents an economic advantage, since no heat input would be necessary during the adsorption process. The negative value of ΔH^0 shows that the adsorption process was exothermal. The negative value of ΔS^0 indicates that the adsorbed species undergoes a decrease in its degrees of freedom.

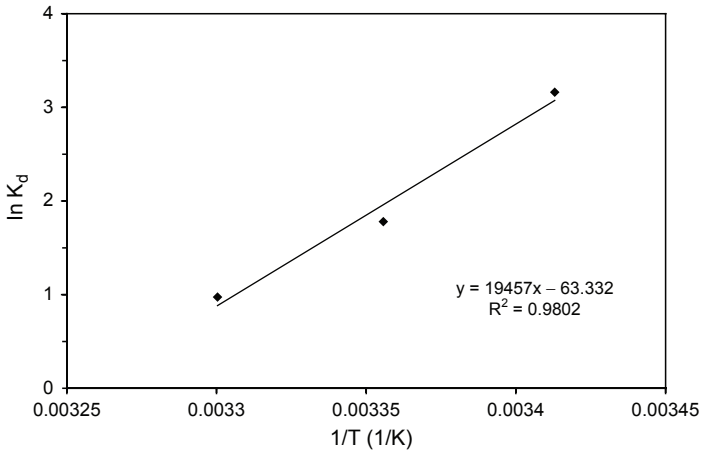

Figure 11. Effect of temperature on the adsorption of As(III) ions onto IS. Experimental conditions: initial conc. of As(III) ion solution, C_0 = 100 μg/ℓ; contact time = 90 min; pH = 6.7–7.0.

TABLE 4. Thermodynamic Parameters for As(III) Ion Adsorption by IS

Temp. (K)	ΔG^0 (kJ/mol)	ΔS^0 [kJ/(mol K)]	ΔH^0 (kJ/mol)
293	–7.68	–0.526	–161.8
298	–5.05		
303	–2.42		

TABLE 5. Composition of Natural Ground Water Before and After Treatment with IS

Parameter	Initial value	Residual value
pH	6.7	6.2
Turbidity (NTU)	9	8.7
Conductivity (μS)	398	376
Ca(II) (ppm)	65	55
Mg(II) (ppm)	47	45
Na(I) (ppm)	105	98
K(I) (ppm)	1.65	1.55
Fe(III) (ppm)	5	< 0.01[a]
Mn(II) (ppm)	0.5	< 0.01[a]
Zn(II) (ppm)	< 0.01[a]	< 0.01[a]
As(III) (ppb)	60.4	< 0.01[a]

[a]Detection limit.

Arsenic(III) ion adsorption from natural water

The composition of the natural ground water before and after treatment with IS is presented in Table 5. It will be seen from the data listed that As(III) ions were almost totally removed from the water together with iron and manganese ions (the residual concentrations in all cases were below the detection limit). Treatment with IS did not lead to any increase in pH value, or any increase in the concentrations of other metallic ions as a result of leaching. These results indicate that IS would be a suitable adsorbent for the removal of As(III) ions from natural waters.

CONCLUSIONS

The adsorption performance of a low-cost adsorbent, viz. iron-containing waste sludge (IS), towards the removal of As(III) ions from aqueous solutions was examined as a means of removing such ions from synthetic aqueous solutions and natural underground water. The major component of IS was iron, thereby making it suitable for the removal of As(III) ions due to the high affinity between such ions and iron. The morphology and high surface area of IS led to a high adsorption capacity for the material. Batch adsorption experiments revealed that equilibrium was reached after 90 min, with an overall adsorption performance greater than 95%. The kinetics of As(III) ion removal through adsorption onto IS was well explained and approximated by the pseudo-second-order kinetic model. The equilibrium adsorption data were well described by the Langmuir model. The values of the dimensional separation factor, R_L, indicated favourable adsorption. The maximum adsorption capacity of IS was 625 μg As(III)/g. The variation in the extent of adsorption with temperature was used to evaluate the thermodynamic parameters for the process. The adsorption was found to be exothermic and spontaneous in nature.

The studies reported showed that iron-containing waste sludge is suitable for use as an adsorbent for the removal of As(III) ions from natural ground water. The results reported recommend the use of IS as a cost-efficient solution for both waste disposal and water treatment, in accordance with the principles of sustainable development. Moreover, the exhausted adsorbent can be immobilized in glass applications. This will remove the need for any recycling process for IS in water treatment, with the added advantage that no secondary contaminated substances are formed.

ACKNOWLEDGEMENTS

The authors gratefully acknowledge financial support provided by the UEFISCSU, under Grant No. 694/19.01.2009, Code 927, “Integrated Concept about Depollution of Waters with Arsenic Content, through Adsorption on Oxide Materials, followed by Immobilization of the Resulted Waste in Crystalline Matrices”.

REFERENCES

Allen, S.J., McKay, G. and Porter, J.F. (2004) *J. Colloid Interface Sci*. **280,** 322.

Balasubramanian, N., Kojima, T., Basha, C.A. and Srinivasakannan, C. (2009) *J. Hazard. Mater*. **167,** 966.

Banerjee, K., Amy, G.L., Prevost, M., Nour, S., Jekel, M., Gallagher, P.M. and Blumenschein, C.D. (2008) *Water Res*. **42,** 3371.

Bhattacharyya, K.G. and Sen Gupta, S. (2009) *Adsorpt. Sci. Technol.* **27,** 47.
Bilici Baskan, M. and Pala, A. (2009) *J. Hazard. Mater.* **166,** 796.
Bissen, M. and Frimmel, F.H. (2003) *Acta Hydroch. Hydrob.* **31,** 97.
Borah, D., Satokawa, S., Kato, S. and Kojima, K. (2008) *J. Colloid Interface Sci.* **319,** 53.
Borah, D., Satokawa, S., Kato, S. and Kojima, T. (2009) *J. Hazard. Mater.* **16,** 1269.
Cerovic, Lj.S., Milonjic, S.K., Todorovic, M.B., Trtanj, M.I., Pogozhev, Y.S., Blagoveschenskii, Y. and Levashov, E.A. (2007) *Colloids Surf. A* **297,** 1.
Chen, Y.N., Chai, L.Y. and Shu, Y.D. (2008) *J. Hazard. Mater.* **160,** 168.
Chutia, P., Kato, S., Kojima, T. and Satokawa, S. (2009) *J. Hazard. Mater.* **162,** 204.
El-Kamash, A.M., Zaki, A.A., Abdel, M. and Geleel, E. (2005) *J. Hazard. Mater. B* **127,** 211.
Faghihian, H. and Nejati-Yazdinejad, M. (2009a) *Adsorpt. Sci. Technol.* **27,** 19.
Faghihian, H. and Nejati-Yazdinejad, M. (2009b) *Adsorpt. Sci. Technol.* **27,** 107.
Gopal, V. and Elango, K.P. (2007) *J. Hazard. Mater.* **141,** 98.
Gupta, K. and Ghosh, U.C. (2009) *J. Hazard. Mater.* **161,** 884.
Ho, Y.S., Ng, J.C.Y. and McKay, G. (2000) *Sep. Purif. Rev.* **29,** 189.
Hsu, J.C., Lin, C.J., Liao, C.H. and Chen, S.T. (2008) *J. Hazard. Mater.* **153,** 817.
Jeong, Y., Fan, M., Singh, S., Chuang, C.L., Saha, B. and van Leeuwen, J.H. (2007) *Chem. Eng. Process.* **46,** 1030.
Jonsson, J. and Sherman, D.M. (2008) *Chem. Geol.* **255,** 173.
Juang, R.-S. and Swei, S.-L. (1996) *Sep. Sci. Technol.* **31,** 2143.
Juang, R.-S., Tseng, R.-L., Wu, F.-C. and Lee, S.-H. (1996) *Sep. Sci. Technol.* **31,** 1915.
Kim, J. and Benjamin, M.M. (2004) *Water Res.* **38,** 2053.
Kosutic, K. and Furac, L. (2005) *Sep. Purif. Technol.* **42,** 137.
Kul, A.R and Caliskan, N. (2009) *Adsorpt. Sci. Technol.* **27,** 85.
Lagergren, S. (1898) *K. Sven. Vetenskapsakad. Handl.* **24,** 1.
Lupa, L., Iovi, A., Negrea, P., Negrea, A. and Szabo, G. (2006) *Environ. Eng. Manage. J.* **5,** 1099.
Lv, L., He, J., Wei, M., Evans, D.G. and Zhou, Z. (2007) *Water Res.* **41,** 1534.
Maji, S.K., Pal, A. and Pal, T. (2008) *J. Hazard. Mater.* **151,** 811.
Mondal, P., Majumder, C.B. and Mohanty, B. (2008) *J. Hazard. Mater.* **150,** 695.
Negrea, A., Muntean, C., Ciopec, M., Lupa, L. and Negrea, P. (2009) *Chem. Bull. "Politehnica" Univ. Timisoara* **54(68),** 82.
Negrea, P., Baltacescu, D., Molnar, B. and Urban, C. (2008) *AGIR Bull.* **1/2,** 201 (in Romanian).
Negrea, P., Negrea, A., Lupa, L. and Mitoi, L. (2006) *Proc. Int. Symp. "Trace Elements in the Food Chain"*, Budapest, Hungary, May 25–27.
Nguyen, V.T., Vigneswaran, S., Ngo, H.H., Shon, H.K. and Kandasamy, J. (2009) *Desalination* **236,** 363.
Niedzielski, P. (2005) *Anal. Chim. Acta* **551,** 199.
Nikolaidis, N.P., Dobbs, G.M. and Lackovic, J.A. (2003) *Water Res.* **37,** 1417.
Ning, R.Y. (2002) *Desalination* **143,** 237.
Ohe, K., Tagai, Y., Nakamura, S., Oshima, T. and Baba, Y. (2005) *J. Chem. Eng. Jpn.* **38,** 671.
Parga, J.R., Cocke, D.L., Valenzuela, J.L., Gomes, J.A., Kesmez, M., Irwin, G., Moreno, H. and Weir, M. (2005) *J. Hazard. Mater. B* **124,** 247.
Partey, F., Norman, D., Ndur, S. and Nartey, R. (2008) *J. Colloid Interface Sci.* **321,** 493.
Qu, D., Wang, J., Hou, D., Luan, Z., Fan, B. and Zhao, C. (2009) *J. Hazard. Mater.* **163,** 874.
Shan, H.Y. (2004) *Scientometrics* **59,** 171.
Singh, D.B., Prasad, G., Rupainwar, D.C. and Singh, N. (1988) *Water Air Soil Pollut.* **42,** 373.
So, H.U., Postma, D., Jakobsen, R. and Larsen, F. (2008) *Geochim. Cosmochim. Acta* **72,** 5871.
Song, S., Lopez-Valdivieso, A., Hernandez-Campos, D.J., Peng, C., Monroy-Fernandez, M.G. and Razo-Soto, I. (2006) *Water Res.* **40,** 364.
Thirunavukkarasu, O.S., Viraraghavan, T. and Subramanian, K.S. (2003) *Water SA* **29,** 161.
Wang, L., Chen, A.S.C., Sorg, T.J. and Fields, K.A. (2002) *J. Am. Water Works Assoc.* **94,** 161.
Yudovich, Y.E. and Ketris, M.P. (2005) *Int. J. Coal Geol.* **61,** 141.
Zeng, L. (2003) *Water Res.* **37,** 4351.

Adsorption of Arsenate Anions from Aqueous Medium by Using Fe(III) Loaded XAD7-DEHPA Impregnated Resin

ADINA NEGREA[1], MIHAELA CIOPEC[1], LAVINIA LUPA[1]*, CORNELIU MIRCEA DAVIDESCU[1], ADRIANA POPA[2], PETRU NEGREA[1], MARILENA MOTOC[3]

[1] University „Politehnica" Timisoara, Faculty of Industrial Chemistry and Environmental Engineering, 2 Piata Victoriei, 300006 Timisoara, Romania,

[2] Romanian Academy, Institute of Chemistry, 24 Mihai Viteazul Blv., 300223 Timisoara, Romania

[3] "Victor Babes" University of Medicine and Pharmacy, 2 Piata Eftimie Murgu, 300041, Timisoara, Romania

This study is aimed to remove arsenate anions from aqueous solution by adsorption. As adsorbent a polymeric resin was used. The resin was prepared by impregnation of the Amberlite XAD7 resin with di(2-ethylhexyl) phosphoric acid (DEHPA) trough the dynamic column method of impregnation. Because of the high affinity of iron towards arsenic the XAD7-DEHPA resin was loaded with Fe(III) ions. The adsorption experiments were conducted at different parameters such as, contact time and initial concentration of As(V) from solution. The Langmuir and Freundlich isotherm models by non-linear regression analysis, were used to represent the experimental data and these could be relatively well interpreted by the Langmuir isotherm. The maximum As(V) adsorption capacity calculated from Langmuir model was 21.7 μg/g. By applying the kinetic models to the experimental data it was found that the removal of As(V) ions by adsorption onto Fe-XAD7-DEHPA follows the pseudo-second-order rate kinetics.

Key words: Fe-XAD7-DEHPA, dynamic column method of impregnation, arsenate anions removal, isotherm, kinetic

Contamination of groundwater resources by arsenic is a well-known environmental problem that can have severe human health implications [1, 2]. Arsenic is released from soil environments into groundwater through natural processes and as a consequence of anthropogenic activities [3-5].

So far numerous technologies have been developed for arsenic removal from the aqueous environment among which adsorption is becoming an attractive and promising technology because of its simplicity, ease of operation and handling, sludge free operation, and regeneration capacity [5-8]. Sorbents of different types like biomaterials [2, 7, 9], metal oxide/hydroxide [3, 6, 10-14], zeolite [5], activated carbon [5, 16], laterite [17] etc. have been used by workers to achieve the goal.

In the recent papers strong cation exchange resins, macroporous polymers, chelating resins and polymeric ligand exchangers have been used for metal ions removal from aqueous solutions [18-26]. In this study, very low-cost amberlite resin chemically modified by impregnation with di(2-ethylhexyl) phosphoric acid (DEHPA) and by Fe(III) ions including was chosen as adsorbent for arsenate anions removal from aqueous solution. The impregnation of the resin with di(2-ethylhexyl) phosphoric acid (DEHPA) was realised trough the dynamic column method of impregnation. Most of the research papers use the dry method of impregnation and none of these use the dynamic column of impregnation. The dynamic column method has the advantages of short impregnation time and high efficiency, which can be obtained not only in laboratory test but also on industrial scale [27]. Many researchers have shown that Fe(III) exhibits high affinity to both arsenate and arsenite [10-14, 16, 17, 28]. Therefore, the Fe(III) ions were immobilized to the functional group of the hosting resin. The optimum conditions for removing arsenate from a synthetic solution, by using Fe-XAD7-DEHPA resin as adsorbent, was investigate.

Theoretical background

Adsorption isotherm models

The sorption process considered here involves trivalent metal loaded impregnated resin as the solid phase and an aqueous phase containing dissolved species to be sorbed. Due to the higher affinity of the arsenate anions for the Fe(III) ions, they are attracted and bound to the solid by different mechanisms. This process take place until equilibrium between the amount of solid-bound ions and their concentration in solution is reached.

The Langmuir isotherm assumes that all adsorbed species interact only with a site, adsorption is limited to a monolayer, and adsorption energy of all sites is identical and independent of the presence of adsorbed species on neighboring sites. It is presented by the following equation [5, 13-15, 23, 26, 28]:

$$q_e = \frac{bq_m C_e}{1 + bC_e} \quad (1)$$

where: q_m is the maximum adsorption capacity (μg/g), q_e is the amount of the metal ions adsorbed at equilibrium (μg/g); C_e is the equilibrium concentration of metal ions (μg/L); b is the equilibrium constant. A curve with an abrupt initial slope indicates a resin with a high affinity for the ionic species at low concentration. The affinity is measured by the coefficient b in the Langmuir equation, the higher value of b, the higher the affinity.

The Freundlich equation is purely empirical based on sorption on heterogeneous surface, which is commonly presented as [5, 13-15, 23, 26, 28]:

$$q_e = K_f C_e^{1/n} \quad (2)$$

where, K_f and n are Freundlich constants which feature the system.

Kinetic models

Kinetic studies provide information relating to time required for the establishment of sorption equilibrium. They

* *email address: lavinia.lupa@chim.upt.ro*

also give information about the reactant species that govern the rate of the reaction and up to what order. Various models can describe the transient behaviour of an adsorption process. Most of these have been reported as pseudo-first-order and some as pseudo-second order kinetic process.

The pseudo-first-order kinetic model is known as the Lagergren equation [5, 7, 13, 22-24]:

$$\ln(q_e - q_t) = \ln q_t - k_1 t \quad (3)$$

where, q_t and q_e are the metal concentration in the adsorbent phase at time t and at equilibrium, respectively and k_1 is the rate constant of first-order sorption.

The pseudo-second-order kinetic model is written as follows:

$$\frac{t}{q_t} = \frac{1}{k_2 q_e^2} + \frac{t}{q_e} \quad (4)$$

where, k_2 is the rate constant of pseudo-second-order sorption.

Experimental part

Materials and methods

Adsorbent preparation and characterization

The Amberlite XAD7 resin (supplied by Rohm and Hass Co.) was impregnated with di(2-ethylhexyl)phosphoric acid (DEHPA) and ethylic alcohol as solvent by dynamic column method [29, 30]. The DEHPA ~ 98.5% used as extractant, was supplied by England and used as received. A certain amount of polymer fully swollen by the solvent was packed in a glass column of 4 cm diameter and 15 cm height. Then the extractant solution was fed into the column with a 0.1 L/h flow rate until the extractant concentration in the outlet was equal to the feed one. The polymeric beads were separated through a porous filter using a vacuum pump, washed with water and dried at 50°C for 24 h [28]. The resulting SIRs were finally washed with distilled water. For the immobilization of the Fe(III) ions onto the XAD7-DEHPA hosting resin 5 g of the hosting resin was equilibrated with 200 mL of 50 mg/L Fe^{3+} solution for 24 h. Fe-XAD7-DEHPA resin were separated through a porous filter using a vacuum pump, washed with distilled water until pH was neutral and dried at 50°C for 24 h. The obtained product after impregnation and Fe(III) loaded was submitted to physico-chemical methods of analysis (FTIR spectroscopy and energy dispersive Xray analyse) in order to establish if the impregnation with DEHPA and the iron loading occurred. The FTIR spectra was recorded using a Shimadzu FTIR spectrophotometer in the range 4000-400 cm^{-1} with 2 cm^{-1} resolution and 40 scans using KBr discs. SEM micrographs and EDX studies were performed using a FEI Inspect S scanning electron microscope.

Adsorption experiments

Adsorption experiments were conducted in 100 mL Erlenmeyer glasses. A measured amount (0.1 g) of Fe-XAD7-DEHPA resin was placed in the glases, which contained 25 mL of various concentrations of As(V) at *p*H=9. The samples were kept in contact for a prescribed length of time to attain equilibrium at 25±1°C. The effect of As(V) initial concentration (30-300μg/L) and contact time (1-24 h), were studied. After filtration the concentration of As(V) was analyzed using a Varian SpectrAA 110 atomic absorption spectrometer with a Varian VGA 77 hydride generation system.

From the concentration measured before and after adsorption (C_0 and C_e, respectively) and dry weight of adsorbent (m), as well as volume of aqueous solution (v), the adsorption capacity was calculated according to eq. (5):

$$q_t = \frac{(C_0 - C_t)V}{m} \quad (5)$$

All experiments were performed at a initial *p*H of As(V) solution of 9, because the predominant anionic species of As(V) [$H_2AsO_4^-$ or $HAsO_4^{2-}$] are found in the environment samples at this *p*H value [5, 13, 14]. The *p*H of the solutions was adjusted to this value using a 1 M NaOH solution, thereby keeping the volume variation of the solution to a value as low as possible. The *p*H of the solutions was measured via a CRISON MultiMeter MM41 fitted with a glass electrode which had been calibrated using various buffer solutions. The stock solution of arsenic was prepared by diluting an appropriate amount of H_3AsO_4 in 0.5 M HNO_3 solution (Merck Standard Solutions). Other solutions of As(V) ions were prepared from the stock solution by appropriate dilution.

Results and discussion

Adsorbent characterization

A FT-IR spectrum of the Fe-XAD7-DEHPA impregnated resin was recorded and is presented in figure 1.

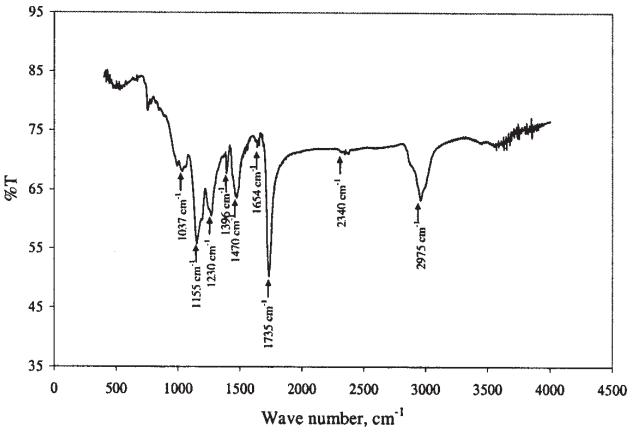

Fig. 1. FTIR spectra of Fe-XAD7-DEHPA resin

IR peak assignments for the matrix are listed in table 1. Amberlite XAD7 is an acrylic ester that contains ester groups O-C=O. All esters give rise to three strong infrared bands that appear at approximately 1700, 1200 and 110 cm^{-1}. The spectrum for our sample exhibits a strong band at 1735 cm^{-1} which represent the C=O stretch of the ester group. The IR spectrum exhibit a band at 2975 (strong sharp) which is attributed to the stretching modes (asymmetric and symmetric) of aliphatic C-H groups. The absorption band 1390 cm^{-1} is due to C-H deformation of $-CH_3$. From the analysis of the FTIR spectra can be observed that the characteristic vibrations originated from DEHPA in which the sorbent was impregnated are: P-OH, P=O and P-O-C which are observed in the spectrum at the wavelengths: 2340 cm^{-1}/1654 cm^{-1}, 1230 cm^{-1} and 1155 cm^{-1} (figure 1). The loading of Fe(III) ions onto the XAD7-DEHPA impregnated resin is put in evidence by the specific band of Fe-OH stretching attributed at the 1037 cm^{-1} wave length.

The energy dispersive XRay spectrum for the Fe-XAD7-DEHPA impregnated resin is presented in figure 2. One may notice the presence of the characteristic peak of phosphorous and iron ions.

All these proves the adsorption of DEHPA and the loading of the Fe(III) ions, respectively onto the XAD7 support.

Adsorption isotherm

The adsorption isotherm of As(V) onto Fe-XAD7-DEHPA resin was conducted using various initial As(V)

Table 1
FUNDAMENTAL FREQUENCY OF THE Fe-XAD7-DEHPA IMPREGNATED RESIN

Frequency, cm^{-1}	Assignments
2975	C-H stretching of CH_3
2340	P-OH stretching
1735	C=O stretching
1654	P-OH stretching
1470	P-CH_2 and C-H bending
1394	C-H deformation of the –CH_3 group
1230	P=O stretching (-O-P=O)
1155	P-O-C stretching
1037	Fe-OH stretching

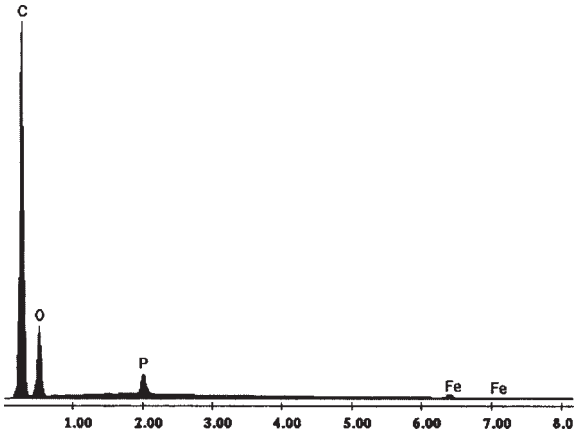

Fig. 2. EDX diagram of Fe-XAD7-DEHPA

concentrations raging from 30 to 300 µg/L at 25±1°C and at a contact time of 10 h. The experimental data were fitted with the Langmuir and Freundlich isotherms by non-linear regression analysis. The results are presented in figure 3 and the values of the correlation coefficients R^2 and the parameter q_m, b, K_f and 1/n are reported in table 2.

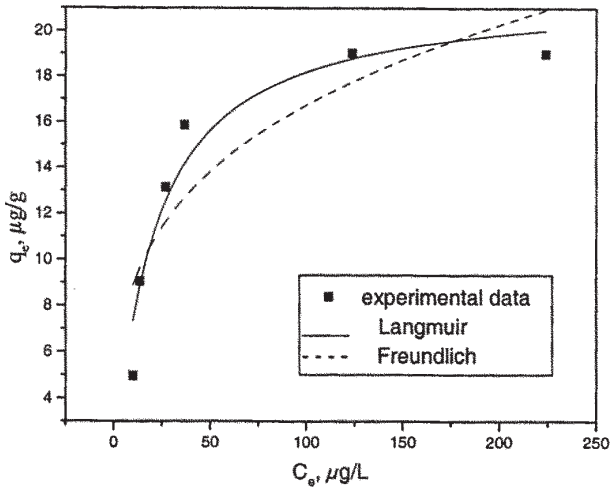

Fig. 3. Adsorption isotherms of As(V) onto Fe-XAD7-DEHPA (m=0.1 g; v=0.025 L; t=10 h; pH=9; T=298 K)

The adsorption capacity increased with increasing equilibrium concentration of arsenic. Then, they approached a constant value at the high equilibrium concentration. The maximum adsorption capacity of the studied material experimentally obtained, in the removal process of As(V) from aqueous solution, is 19µg/g.

Table 2
PARAMETERS OF DIFFERENT ISOTHERM FOR THE As(V) ADSORPTION ONTO Fe-XAD7-DEHPA

Freundlich isotherm			Langmuir isotherm		
K_F, µg/g	1/n	R^2	b, L/µg	$q_{m\,calc}$, µg/g	R^2
4,6886	0.2763	0.7562	0.051	21.7	0.9919

The Freundlich plot has a correlation coefficient very low; this suggests a restriction on the use of Freundlich isotherms. The numerical value of 1/n< 1, which provides information about surface heterogeneity and surface affinity for the solute, indicates a favourable sorption of As(V) and a very high affinity of the Fe-XAD7-DEHPA for As(V).

The Langmuir model effectively describes the sorption data with a correlation coefficient of 0.9919. Thus the isotherm follows the sorption process in the entire concentration range studied. Furthermore, the maximum adsorption capacity from the Langmuir plot is almost the same with the maximum adsorption capacity experimentally obtained. The dimensional constant, called separation factor (R_L), was used to describe the essential characteristics of Langmuir isotherm (R_L >1, unfavourable; R_L = 1, linear; 0<R_L<1, favorable; and R_L=0, irreversible),

$$R_L = \frac{1}{1 + K_L \cdot C_0} \qquad (6)$$

In fact, the separation factor is a measure of the adsorbent capacity used. R_L values were calculated for the entire concentration range studied and found to be higher than 0 and less than 1, showing favourable adsorption.

Adsorption kinetic

Figure 4 shows the effect of the contact time on the As(V) adsorption onto the studied material. It is evident that the adsorption capacity increased initially as contact time increased, and then became almost stable, denoting attainment of equilibrium. To ensure enough time to reach equilibrium, 24 h of contact time was used.

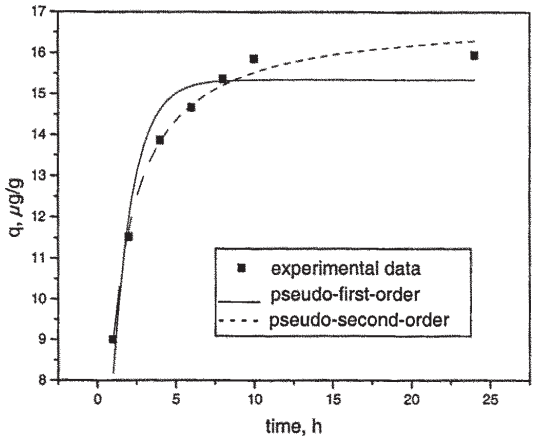

Fig. 4. Effect of adsorption time on As(V) adsorption onto Fe-XAD7-DEHPA. Fitting of the pseudo-first-order and pseudo-second-order kinetic models to the experimental data (C_0 = 100 mg/L; m=0.1 g; V=25mL; pH = 9; T=298 K)

q_e, exp, µg/g	Pseudo-first-order model			Pseudo-second-order model		
	q_e, kinetic plot, µg/g	k_1, h^{-1}	R^2	q_e, kinetic plot, µg/g	k_2 $min^{-1}(µg/g)^{-1}$	R^2
16	4.74	0.2143	0.8577	16.5	0.0819[4]	0.9996

Table 3
KINETIC MODEL PARAMETERS FOR As(V) IONS REMOVAL BY Fe-XAD7-DEHPA

Kinetic data of arsenate adsorption were fitted to the pseudo-first-order and pseudo-second order kinetics models by non-linear regression analysis. Model parameters including kinetic constants, adsorption capacity and the correlation coefficients are presented in table 3.

Data presented in table 3 show that the correlation coefficient for the pseudo-first-order kinetic model is lower than that obtained for the pseudo-second-order model, where the correlation coefficient is very close to 1. Furthermore, the value of the equilibrium sorption capacity calculated ($q_{e,kinetic\ plot}$) using the first-order model, is not close to the experimental value ($q_{e,\ exp}$). In the case of the pseudo-second-order model the theoretically predicted equilibrium sorption capacity is close to the value experimentally determined. This shows that the kinetics of As(V) removal by sorption on the Fe-XAD7-DEHPA is described by a pseudo-second-order expression.

Conclusion

In the present paper the performance of the Fe-XAD7-DEHPA resin, in the removal process of As(V) from aqueous solution, has been investigated. The studied materials have been obtained by impregnation of Amberlite XAD7 resin with DEHPA through dynamic column of impregnation and because of the high affinity of arsenic towards iron the Fe(III) ions were loaded onto the functionalized resin. The FTIR and the EDX analysis of the materials proved the adsorption of DEHPA and the loading of Fe(III) ions on the XAD7 support. The studied material showed good performance in the removal process of As(V) from aqueous solutions. The Langmuir and Freundlich isotherm models by non-linear regression analysis, were used to represent the experimental data and these could be relatively well interpreted by the Langmuir isotherm. R_L values between 0 and 1.0 further indicate a favourable adsorption of As(V) ions onto Fe-XAD7-DEHPA. The maximum As(V) adsorption capacity calculated from Langmuir model was 21.7 μg/g. By applying the kinetic models to the experimental data it was found that the removal of As(V) ions by Fe-XAD7-DEHPA follows the pseudo-second-order rate kinetics.

Acknowledgement: This work was supported by CNCSIS- UEFISCDI, project number PN II-IDEI 927/2008, "Integrated Concept about Depollution of Waters with Arsenic Content, through Adsorption on Oxide Materials, followed by Immobilization of the Resulted Waste in Crystalline Matrices".

References

1. STREAT, M., HELLGARDT, K., NEWTON N.L.R., Process Saf. Environ. Prot., 86, no. 1, 2008, p. 11.
2. JONSSON, J., SHERMAN, D.M., Chem. Geol., 255, no. 1-2, 2008, p. 173.
3. MAMINDY-PAJANY, Y., HUREL, C., MARMIER, N., ROMEO, M., Comptes Rendys Chimie, 12, no. 8, 2009, p. 876.
4. HARTLEY, W., LEPP, N.W., Sci. Total Environ., 390, no. 1, 2008, p. 35.
5. Borah, D., Satokawa, S., Kato, S., Kojima, T., J. Hazard. Mater., 162, no. 2-3, 2009, p. 1269.
6. CAMACHO, J., WEE, H.Y., KRAMER, T.A., AUTENRIETH, R., J. Hazard. Mater., 165, nr. 1-3, 2009, p. 599.
7. CHEN, Y.N., CHAI, L.Y., SHU, Y.D., J. Hazard. Mater., 160, no.1, 2008, p. 168.
8. NGUYEN, V.T., VIGNESWARAN, S., NGO, H.H., SHON, H.K., KANDASAMY, J., Desalination, 236, no. 1-3, 2009, p. 363.
9. SO, H.U., POSTMA, D., JAKOBSEN, R., LARSEN, F., Geochim. Cosmochim. Acta, 72, no. 24, 2008, p. 5871.
10. JEONG, Y., FAN, M., SINGH, S., CHUANG, C.L., SAHA, B., VAN LEEUWEN, J.H., Chem. Eng. Process, 46, no. 10, 2007, p. 1030.
11. ZENG, L., Water Res., 37, no. 18, 2003, p. 4351.
12.THIRUNAVUKKARASU, O. S., VIRARAGHAVAN, T., SUBRAMANIAN, K.S., Water SA, 29, no.1, 2003, p. 161.
13.GUPTA, K., GHOSH, U.C., J. Hazard. Mater., 161, no. 2-3, 2009, p. 884.
14.BANERJEE, K., AMY, G.L., PREVOST, M., NOUR, S., JEKEL, M., GALLAGHER, P.M., BLUMENSCHEIN, C.D., Water Res., 42, no. 13, 2008, p. 3371.
15.CHUTIA, P., KATO, S., KOJIMA, T., SATOKAWA, S., J. Hazard. Mater., 162, no.1, 2009, p. 204.
16.MONDAL, P., MAJUMDER, C.B., MOHANTY, B., J. Hazard. Mater., 150, no.3, 2008, p. 695.
17.PARTEY, F., NORMAN, D., NDUR, S., NARTEY, R., J. Colloid Interface Sci., 321, no.2, 2008, p. 493.
18. BELKHOUCHE, N.E., DIDI, M.A., Hydrometallurgy, 103, no. 1-4, 2010, p. 60.
19.CHABANI, M., AMRANE, A., BENSMAILI, A., Desalination, 206, no.1-3, 2007, p. 560.
20.HOSSEINI-BANDEGHARAEI, A., HOSSEINI, M.S., SARW-GHADI, M., ZOWGHI, S., HOSSEINI, E., HOSSEINI-BANDEGHARAEI, H., Chem. Eng. J.,. 160 (2010) 190-198.
21.MUSTAFA, S., SHAH, K.H., NAEEM, A., WASEEM, M., TAHIR, M., J. Hazard. Mater., 160, no. 1, 2008, p. 1.
22.SAHA, B., GILL, R.J., BAILEY, D.G., KABAY, N., ARDA, M., React. Funct. Polym., 60, 2004, p. 223.
23.SHAO, W., LI, X., CAO, Q., LUO, F., LI, J., DU, Y., Hydrometallurgy, 91, no. 1-4, 2008, p. 138.
24.ZHU, X., JYO, A., Sep. Sci. Technol., 36, no. 14, 2001, p. 3175.
25.CHANDA, M., O'DRISCOLL, K.F., REMPEL, G.L. React., Polym., 8, no.1, 1988, p. 85.
26.AN, B., STEINWINDER, T.R., ZHAO, D., Water Res., 39, no. 20, 2005, p. 4993.
27.BENAMOR, M., BOUARICHE, Z., BELAID, T., DRAA, M.T., Sep. Purif. Technol., 59, no.1, 2008, p. 74.
28. NEGREA, A., LUPA, L., CIOPEC, M., LAZAU, R., MUNTEAN, C., NEGREA, P., Adsorpt. Sci. Technol., 28, no. 6, 2010, p. 467.
29. JUANG, R.S., Proc. Natl. Sci. Counc. ROC(A), 23, no.3, 1999, p. 353
30. DAVIDESCU, C.M., CIOPEC, M., NEGREA, A., POPA, A., LUPA, L., NEGREA, P., MUNTEAN, C., MOTOC, M., Rev. Chim. (Bucharest), 62, no. 7, 2011, p. 712

Manuscript received: 31.05.2011

JOURNAL OF CHEMICAL & ENGINEERING DATA

ARTICLE

pubs.acs.org/jced

Removal of As^V by Fe^{III}-Loaded XAD7 Impregnated Resin Containing Di(2-ethylhexyl) Phosphoric Acid (DEHPA): Equilibrium, Kinetic, and Thermodynamic Modeling Studies

Adina Negrea,[†] Mihaela Ciopec,[†] Lavinia Lupa,[*,†] Corneliu M. Davidescu,[†] Adriana Popa,[‡] Gheorghe Ilia,[‡] and Petru Negrea[†]

[†]Faculty of Industrial Chemistry and Environmental Engineering, Politehnica University, 2 Piata Victoriei, 300006, Timisoara, Romania

[‡]Institute of Chemistry Timisoara of Romanian Academy, Romanian Academy, 24 Mihai Viteazul Blv., 300223, Timisoara, Romania

ABSTRACT: In this paper, we studied the feasibility of using Fe^{III}-loaded Amberlite XAD7 impregnated resin containing di(2-ethylhexyl) phosphoric acid (DEHPA) as adsorbents for the removal of As^V from aqueous solution. The XAD7-DEHPA resins are obtained by the dry method (DM) and column method (CM) of impregnation, respectively. Equilibrium, kinetic, and thermodynamic studies are carried out to study the adsorption performance of both types of Fe-XAD7-DEHPA resins for the removal process of As^V from aqueous solution. The effects of initial As^V concentration, contact time, and temperature of the solution on the adsorption were studied. The Langmuir and Dubinin−Kaganer−Radushkevich (DKR) isotherm models fit the equilibrium data better than Freundlich and Temkin isotherm models, which are used to describe the adsorption of As^V onto Fe-XAD7-DEHPA resins. The pseudosecond-order model is suitable for describing the adsorption kinetics for As^V removal from aqueous solutions onto Fe-XAD7-DEHPA resins. Thermodynamic parameters, such as the Gibbs energy ($\Delta G^{\#}$), enthalpy ($\Delta H^{\#}$), entropy ($\Delta S^{\#}$), and equilibrium constant of activation ($K^{\#}$) are calculated. The adsorption capacities of the both studied materials are found to be almost the same. However, the Fe-XAD7-DEHPA obtained through the CM is the most advantageous as this is obtained in a shorter time than the resin obtained through the DM.

INTRODUCTION

The presence of dissolved arsenic in groundwater has created significant concern on a global basis. The consumption of arsenic-containing water causes serious health-related problems because of its toxicity.[1−6] Thus, choosing a technology for the removal of arsenic from drinking water represents a challenge.

The chemistry of arsenic in aquatic systems is complex and consists of oxidation−reduction, precipitation, adsorption, and ligand exchange. The principal aqueous forms of inorganic arsenic are arsenate [As^V] and arsenit [As^{III}], and their relative distributions are influenced by pH and redox conditions.[5−8] As^V species are found in oxidizing environments at a pH between 6 and 9 as oxyanions of arsenic acid [$H_2AsO_4^-$ or $HAsO_4^{2-}$],[3,8,9] while As^{III} species exist as uncharged arsenious acid [$H_3AsO_3^0$] at pH below 9.[3,8,10]

A literature survey reveals that there are a good number of approaches for arsenic remediation from drinking water. Among the various methods like oxidation−reduction, precipitation, coagulation and coprecipitation, adsorption, electrolysis and cementation, solvent extraction, ion exchange, ion flotation, biological processing, and membrane filtration[1,2,8,9,11−19] proposed to negotiate the problem of arsenic contamination in drinking water, the sorption technique is, however, the most common and is considered to be an effective method. This method is simple and convenient and also has the potential for regeneration and a sludge-free operation.

To date, various adsorbents like metal oxides/hydroxides,[6,8,9,12,20−25] natural and synthetic zeolites,[7,20] laterite soil,[12,20,26] calcite,[27] and activated carbon[2,3,20,28] have been developed for arsenic removal.

The adsorption in porous solid adsorbent is a complex process with respect to the nature of the solid adsorbent surface adsorbate.[29] The use of macroporous organic polymer supports, with a high specific surface area and good mechanical stability, is found to be more suitable for the removal of toxic elements from dilute solution, due to their faster kinetics, ease of regeneration, and high adsorption capacity.[30−38] Impregnating appropriate solid supports, such as Amberlite XAD series, is one of the well-known and effective solid sorbent preparation methods for treatment purposes.[20,30,32,33,35] There are four methods available for the impregnation of the desired extractant into the polymeric supporting structure: the dry method (DM), wet method, modifier addition method, and dynamic column method (CM).[34,39−42]

The most widely used method of impregnation, cited in literature, is the DM, while the CM is very rarely mentioned. In the present work a comparison between the adsorption performance of the XAD7 resin impregnated with di(2-ethylhexyl) phosphoric acid (DEHPA) through the DM and the adsorption performance of XAD7 resin impregnated through CM in the process of As^V ion removal from aqueous solutions was studied. Because the iron compounds in general were found to be very efficient adsorbents for arsenic removal from water, due to the high affinity of arsenic toward iron,[1,4−6,8,12,23,28,37,43] the XAD7 resins impregnated with DEHPA, employing the both mentioned methods, were loaded with Fe^{III} ions.

Received: May 15, 2011
Accepted: August 12, 2011

dx.doi.org/10.1021/je200476u | *J. Chem. Eng. Data* XXXX, XXX, 000–000

Due to the fact that the column method of impregnation (CM, an effective method of impregnation, which is not studied and cited in the specialty literature) needs a lower time of impregnation than the DM of impregnation, the objective of this study is to determine and compare the adsorption performances of the Fe-XAD7-DEHPA resins (obtained via the both mentioned methods of impregnation) in the removal process of As^V from aqueous solutions. To determine the adsorption performances of Fe-XAD7-DEHPA resins, equilibrium, kinetic, and thermodynamic studies were performed.

MATERIALS AND METHODS

Adsorbent Preparation. The Amberlite XAD7 resin (supplied by Rohm and Hass Co.) was impregnated with DEHPA through the DM and CM. The DEHPA (~ 98.5 %) used as the extractant was supplied by BHD Chemicals Ltd. (Poole, England) and used as received. For the DM impregnation 1 g of fresh XAD7 was placed for 24 h in ethanol containing 0.1 $g \cdot mL^{-1}$ extractant (DEHPA). The polymeric beads were separated through a porous filter using a vacuum pump, washed with water, and dried at 323.15 ± 1 K for 24 h.[41] For the Amberlite XAD7 resin impregnation with DEHPA and ethylic alcohol as solvent by the dynamic column impregnation method,[41] a certain amount of polymer fully swollen by the solvent was packed in a glass column of 4 cm diameter and 15 cm height. Then the extractant solution was fed into the column with a 0.1 $L \cdot h^{-1}$ flow rate until the extractant (at the outlet) and feed concentrations were equal. The polymeric beads were separated through a porous filter using a vacuum pump, washed with water, and dried at 323.15 ± 1 K for 24 h.[42] The resulting SIRs were finally washed with distilled water. The extractant content of the impregnated resins was determined after washing a given amount of the resins with ethanol, which completely elutes the ligand and subsequent titration with 0.1 M NaOH.

In this form the XAD7-DEHPA resins are anionic resins, which can be used as adsorbents for divalent and trivalent metal ion removal from aquatic solutions. They cannot be used for the removal of anionic species of arsenate from water. From this reason a metal ion like iron, manganese, zirconium, or aluminum must be loaded on the XAD7-DEHPA resins. The best metal ion for the arsenic removal is considered to be the iron ion because of the high affinity of Fe toward inorganic arsenic.[1,4−6,8,12,23,25,28,37,43] Therefore, the XAD7 resins impregnated with DEHPA through DM and CM were loaded with Fe^{III} ions ($Fe(NO_3)_3$ in 0.5 $mol \cdot L^{-1}$ HNO_3 solution). In this aim 5 g of each XAD7-DEHPA resins was equilibrated with 200 mL of 50 $mg \cdot L^{-1}$ Fe^{III} solution for 24 h. Fe-XAD7-DEHPA resins were separated through a porous filter using a vacuum pump, washed with distilled water until pH was neutral, and dried at 323.15 ± 1 K for 24 h. The residual concentration of the Fe^{III} ions in the resulting solutions after filtration has been determined using a Varian SpectrAA 280 fast sequential atomic absorption spectrometer with an air-acetylene flame.

Adsorption Experiments. The experiments were performed with both resins at an initial pH of As^V solution of 9 ± 0.1, because the predominant anionic species of As^V [$H_2AsO_4^-$ or $HAsO_4^{2-}$] are found in the environment samples at this pH value.[3,8,9] The pH of the solutions was adjusted to this value using a 1 M NaOH solutions, thereby keeping the volume variation of the solution to a value as low as possible. The pH of the solutions was measured via a CRISON MultiMeter MM41 fitted with a glass electrode which had been calibrated using various buffer solutions.

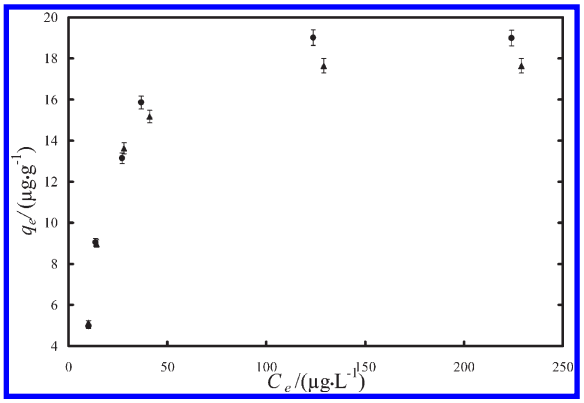

Figure 1. Adsorption isotherm of As^V ions onto Fe-XAD7-DEHPA resins C_0 = (30 ± 0.01 to 300 ± 0.01) $\mu g \cdot L^{-1}$; m = 0.1 ± 0.0001 g; V = 25 ± 0.1 mL; t = 10 h; T = 298.15 ± 1 K; pH = 9 ± 0.1; ▲, DM; ●, CM. Error bars represent the relative standard deviation.

Prior to such experiments, a stock solution of arsenic was prepared by diluting an appropriate amount of H_3AsO_4 in 0.5 M HNO_3 solution (Merck Standard Solutions). Other solutions of As^V ions were prepared from the stock solution by appropriate dilution.

In the first instance, the effect of the initial As^V concentration (C_0 = (30 ± 0.01 to 300 ± 0.01) $\mu g \cdot L^{-1}$) was studied. In each experiment 0.1 ± 0.0001 g of sorbent was suspended in 25 ± 0.1 mL of As^V solution of different concentrations. The samples were kept in contact for 10 h at room temperature, 298.15 ± 1 K. The filtrate was collected for As^V analysis.

To study the effect of contact time on adsorption at three temperatures 298.15 ± 1 K, 303.15 ± 1 K, and 318 ± 1 K, the experiments were carried out with samples of 0.1 ± 0.0001 g of Fe-XAD7-DEHPA in 25 ± 0.1 mL of 100 ± 0.01 $\mu g \cdot L^{-1}$ As^V solutions. The suspensions were kept in contact for different times: (1, 2, 4, 6, 8, 10, and 24) h. To maintain the temperature of the suspensions at the desired value, the samples were immersed in a bath of a mechanical shaker bath (without shaking) MTA Kutesz 609/A, Hungary with a standard thermocouple. After contact time elapsed, the suspensions were filtered, and the residual concentration of As^V ions in the filtrates was determined by means of atomic absorption spectrometry using a Varian SpectrAA 110 atomic absorption spectrometer with a Varian VGA 77 hydride generation system.

The various chemicals employed in the experiments were of analytical reagent (A.R.) grade and used without further purification. Distilled water was used throughout. The adsorption performance is expressed as metal uptake, $q_e/\mu g \cdot g^{-1}$, and the corresponding mass balance expression is:[3,9,22,34,38,44]

$$q_t = \frac{(C_0 - C_t) \cdot V}{m} \quad (1)$$

where C_0 and C_t are the concentrations of As^V ions ($\mu g \cdot L^{-1}$) in the solution initially (t = 0) and after a time t (h), respectively, V is the volume of the solution (V = (25 ± 0.1) · 1000^{-1} L), and m is the mass of adsorbent (m = 0.1 ± 0.0001 g). The experimental results are given as an average of five sets of data obtained in identical working conditions.

dx.doi.org/10.1021/je200476u |J. Chem. Eng. Data XXXX, XXX, 000–000

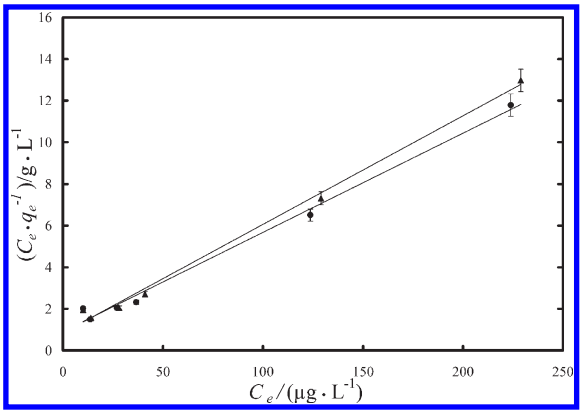

Figure 2. Langmuir plot of As^V adsorption onto Fe-XAD7-DEHPA resins: ▲, DM; ●, CM. Error bars represent the average relative error.

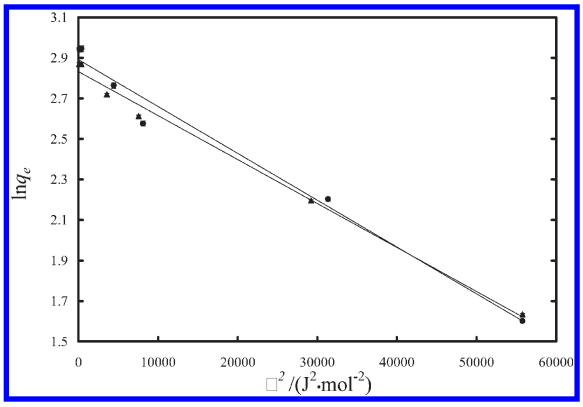

Figure 3. Dubinin−Kaganer−Radushkevich plot of As^V adsorption onto Fe-XAD7-DEHPA resins; ▲, DM; ●, CM. Error bars represent the average relative error.

RESULTS AND DISCUSSION

The extractant content of the XAD7-DEHPA obtained through the DM of impregnation determined by titration with 0.1 M NaOH was 0.35 g DEHPA/g SIR, and the extractant content of the XAD7-DEHPA obtained through the CM of impregnation was 0.352 g DEHPA/g SIR. The analysis of the residual concentration of the Fe^{III} in the resulting solution after filtration showed that the entire quantity of Fe^{III} ions from the solutions was loaded on the studied resins.

Concentration Dependence and Adsorption Isotherms. The adsorption isotherm for As^V ions onto Fe-XAD7-DEHPA resins are presented in Figure 1.

The adsorption capacity increased with increasing equilibrium concentration of arsenic for the both studied resins. Then, it approached a constant value at the high equilibrium concentrations. One can be observed that the Fe-XAD7-DEHPA obtained through DM develops a maximum adsorption capacity of As^V of 17.6 $\mu g \cdot g^{-1}$, while the maximum adsorption capacity of As^V developed by the Fe-XAD7-DEHPA obtained via CM is 19 $\mu g \cdot g^{-1}$.

Four important isotherm models were chosen to fit the experimental data in this study: Langmuir, Freundlich, Temkin, and Dubinin−Kaganer−Radushkevich.

The linear form of the Langmuir equation[2−7,9,22−25,35,37,38] is expressed by:

$$\frac{C_e}{q_e} = \frac{1}{K_L q_m} + \frac{C_e}{q_m} \tag{2}$$

where K_L denotes the Langmuir isotherm constant related to the affinity between adsorbent and the adsorbate ($L \cdot \mu g^{-1}$) and q_m denotes the Langmuir monomolecular adsorption capacity ($\mu g \cdot g^{-1}$). The values of q_m and K_L can be determined by plotting $C_e \cdot q_e^{-1}$ versus C_e (Figure 2).

The Freundlich isotherm[2−7,9,22,23,25,35,37,38] equation can be written as:

$$\ln q_e = \ln K_F + \frac{1}{n} \cdot \ln C_e \tag{3}$$

where q_e is the amount of As^V adsorbed per gram of adsorbent, that is, metal uptake ($\mu g \cdot g^{-1}$), and C_e is the equilibrium concentration of adsorbate in the bulk solution after adsorption ($\mu g \cdot L^{-1}$). K_F and $1/n$ are characteristic constants that can be related to the relative adsorption capacity of the adsorbent ($\mu g \cdot g^{-1}$) and the intensity of the adsorption, respectively, and can be determined from the plot of ln q_e versus ln C_e.

The equation of the Temkin model[44,45] is given by:

$$q_e = \left(\frac{RT}{b_T}\right) \cdot \ln K_T + \left(\frac{RT}{b_T}\right) \cdot \ln C_e \tag{4}$$

where b_T is the adsorption potential of the adsorbent and K_T is the equilibrium constant corresponding to maximum binding energy ($L \cdot \mu g^{-1}$), R is the universal gas constant ($J \cdot (mol \cdot K)^{-1}$), and T is the absolute temperature (K).

K_T, determined from the plot of q_e versus ln C_e, can be used to determine the value of the standard free enthalpy $\Delta G°$ as follows:

$$K_T = \exp\left(\frac{-\Delta G^0}{RT}\right) \tag{5}$$

The Dubinin−Kaganer−Radushkevich (DKR) isotherm equation[2] is based on the concept of heterogeneous surface of the adsorbent and can be written as:

$$\ln q_e = \ln q_m - \beta \cdot \varepsilon^2 \tag{6}$$

where the quantities q_e and q_m are the amount of As^V adsorbed per gram of adsorbent, that is, metal uptake ($\mu g \cdot g^{-1}$) and the measurement of the monolayer adsorption capacity ($\mu g \cdot g^{-1}$), respectively. β is the activity coefficient related to the mean sorption energy, and ε is the Polanyi potential and can be calculated using the following relation:

$$\varepsilon = RT \ln\left(1 + \frac{1}{C_e}\right) \tag{7}$$

where R is the universal gas constant, T is the temperature in Kelvin, and C_e is the equilibrium concentration of adsorbate in the bulk solution after adsorption ($\mu g \cdot L^{-1}$).

A plot of ln q_e versus ε^2 (Figure 3) yields a straight line, confirming the model. The mean free energy of adsorption E ($kJ \cdot mol^{-1}$) per molecule of the adsorbate when it is transferred from the solution to the powder surface can be calculated using the following equation:[2]

$$E = \frac{1}{\sqrt{2\beta}} \tag{8}$$

dx.doi.org/10.1021/je200476u |J. Chem. Eng. Data XXXX, XXX, 000–000

Table 1. Parameters of Different Isotherms for As^V Ion Adsorption onto Fe-XAD7-DEHPA Resins

isotherm	adsorbent Fe-XAD7-DEHPA	isotherm parameters			R^2	Δq/%	E/%
Langmuir		$K_L/(L\cdot\mu g^{-1})$	q_m (calc.)/($\mu g\cdot g^{-1}$)				
	DM	0.062	19.2		0.9943	20.5	4.2
	CM	0.052	21.0		0.9919	21.3	4.5
Freundlich		$K_F/(\mu g\cdot g^{-1})$	$1/n$				
	DM	3.395	0.3396		0.7413	26.5	7.0
	CM	3.136	0.3711		0.7562	28.1	7.9
Temkin		$K_T/(L\cdot mol^{-1})$	$\Delta G°/(kJ\cdot mol^{-1})$				
	DM	0.775	0.63		0.8496	24.9	6.2
	CM	0.585	1.33		0.8745	25.8	6.7
DKR		$\beta/(mol^2\cdot J^{-2})$	q_m(calc.)/($\mu g\cdot g^{-1}$)	$E/(kJ\cdot mol^{-1})$			
	DM	$2.2\cdot10^{-5}$	17	0.15	0.9929	4.2	0.2
	CM	$2.3\cdot10^{-5}$	18	0.147	0.9814	7.4	0.5

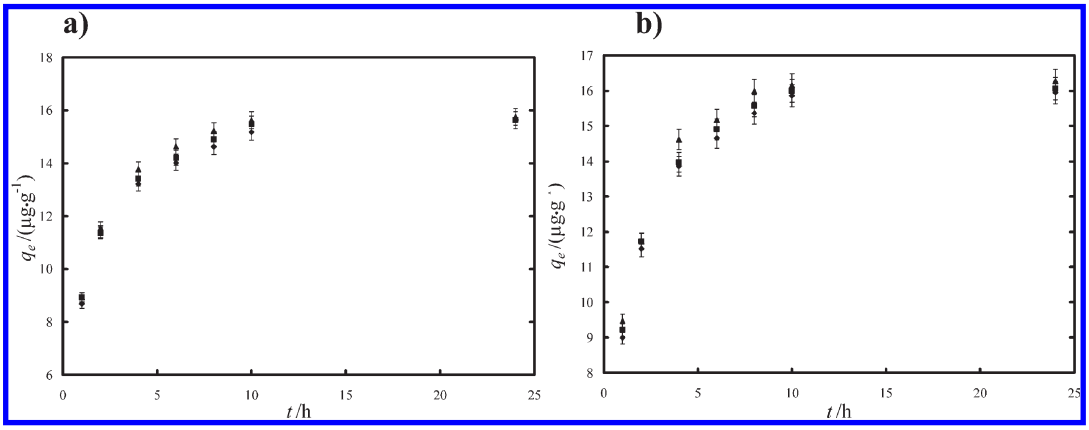

Figure 4. Effect of contact time on the adsorption capacity of the studied materials at different temperatures; $C_0 = 100 \pm 0.01\ \mu g\cdot L^{-1}$; $m = 0.1 \pm 0.0001$ g; $V = 25 \pm 0.1$ mL; pH = 9 ± 0.1; a, DM; b, CM; ♦, 298.15 ± 1 K; ■, 303.15 ± 1 K; ▲, 318.15 ± 1 K. Error bars represent the relative standard deviation.

The isotherm equation parameters of Langmuir, Freundlich, Temkin, and Dubinin−Kaganer−Radushkevich are summarized in Table 1.

To assess the extent to which the adsorption isotherm equations fit the experimental data, two different error functions were examined.

The normalized standard deviation Δq/% was estimated using the equation:[4,46,47]

$$\Delta q = 100\cdot\sqrt{\frac{1}{p-1}\sum_{i=1}^{p}\left(\frac{q_{exp}-q_{calc}}{q_{exp}}\right)_i^2} \quad (9)$$

where q_{exp} is the experimentally determined adsorption capacity ($\mu g\cdot g^{-1}$), q_{calc} is the adsorption capacity calculated according to the model equation ($\mu g\cdot g^{-1}$), and p is the number of experimental data.

The average relative error E/%, which minimizes the fractional error distribution across the entire concentration range, was estimated with the equation:[4,48]

$$E = \frac{100}{p-1}\cdot\sum_{i=1}^{p}\left(\frac{q_{calc}-q_{exp}}{q_{exp}}\right)_i^2 \quad (10)$$

An analysis of R^2 and of the absolute error values (Table 1) showed that the Langmuir and Dubinin−Kaganer−Radushkevich equations have more precise coefficients and lower absolute error than the Freundlich and Temkin equations for modeling the As^V adsorption onto Fe-XAD7-DEHPA resins obtained through DM and CM, respectively.

The Langmuir adsorption isotherm provided an excellent fit to the equilibrium adsorption data, giving correlation coefficients >0.99 and maximum adsorption capacities close to that determined experimentally. The maximum adsorption capacity of the Fe-XAD7-DEHPA resin obtained through the CM is higher than the maximum adsorption capacity of the Fe-XAD7-DEHPA resin obtained through the DM (Table 1). The essential feature of the Langmuir equation can be expressed in terms of a dimensionless separation factor, R_L, defined as:

$$R_L = \frac{1}{1 + K_L\cdot C_0} \quad (11)$$

The value of R_L indicates the shape of the isotherm to be unfavorable, $R_L > 1$; linear, $R_L = 1$; favorable $0 < R_L < 1$; and irreversible, $R_L = 0$.[2−4,28,30,32] R_L values were found to be between 0 and 1 for all of the concentrations of As^V ions and for both studied materials, showing that the adsorption is favorable.

dx.doi.org/10.1021/je200476u |J. Chem. Eng. Data XXXX, XXX, 000–000

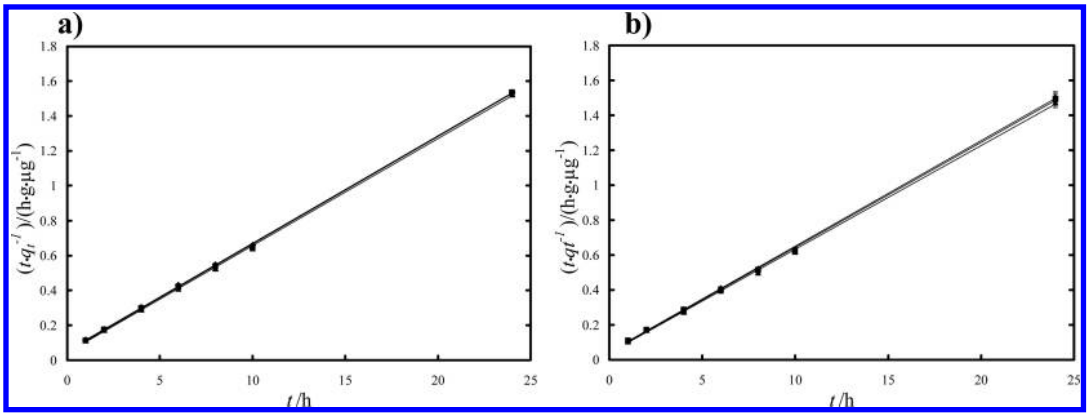

Figure 5. Pseudosecond-order kinetic plot for the adsorption of As^V onto studied materials; a, DM; b, CM; ♦, 298.15 ± 1 K; ■, 303.15 ± 1 K; ▲, 318.15 ± 1 K. Error bars represent the average relative error.

The Langmuir model indicates a homogeneous and monomolecular adsorption mechanism.

The Freundlich plots have a correlation coefficient very low; this suggests a restriction on the use of Freundlich isotherms. The constant K_F can be defined as an adsorption coefficient which represents the quantity of adsorbed metal ions for a unit equilibrium concentration. The slope $1/n$ is a measure of the adsorption intensity or surface heterogeneity. For $1/n = 1$, the partition between the two phases is independent of the concentration. The situation $1/n < 1$ is the most common and corresponds to a normal L-type Langmuir isotherm, while $1/n > 1$ indicates a cooperative adsorption, which involves strong interactions between the molecules of adsorbate.[45] Values of $1/n < 1$ indicate a very high affinity of the both Fe-XAD7-DEHPA resins for As^V ions.

The Temkin isotherm model was chosen to determine the adsorption potentials of the adsorbents for adsorbates. The Temkin adsorption potentials K_T is 0.775 $L\cdot mol^{-1}$ for Fe-XAD7-DEHPA obtained by DM and 0.585 $L\cdot mol^{-1}$ for Fe-XAD7-DEHPA obtained by CM, respectively. The values for the standard free enthalpy, $\Delta G°$, were calculated according to eq 5 for both studied materials (Table 1). These results show that, in the Temkin isotherm model, the binding energy is higher for the adsorbent obtained employing the CM than the binding energy for the adsorbent obtained through the DM. However, the Temkin model is not able to describe the experimental data properly because of the poor linear correlation coefficients.

The Dubinin−Kaganer−Radushkevich model (which presents the lowest absolute errors) was used to determine the characteristic porosity and the apparent free energy of adsorption. The monomolecular adsorption capacities q_m for Fe-XAD7-DEHPA obtained through DM and for Fe-XAD7-DEHPA obtained through CM were 17 and 18 $\mu g\cdot g^{-1}$, respectively; values which are very close to that determined experimentally. The values of the porosity factors β less than unity (Table 1) imply that Fe-XAD7-DEHPA resins consist of fine micropores and indicate a surface heterogeneity may arise from the pore structure as well as adsorbate−adsorbent interaction.[44] The apparent free energy from the Dubinin−Kaganer−Raduskevich is a parameter used in predicting the type of adsorption. If the value of E is between (8 and 16) $kJ\cdot mol^{-1}$, then the adsorption process follows by chemical ion exchange, and if $E < 8$ $kJ\cdot mol^{-1}$, the adsorption process is of a physical nature.[7,42] The apparent free energy values for the studied materials are in the region of 0.15 $kJ\cdot mol^{-1}$; these results indicate that the adsorption of As^V onto Fe-XAD7-DEHPA resins is governed by physisorption.

Contact Time Dependence and Adsorption Kinetics. The effects of contact time on equilibrium adsorption capacities of As^V for the studied materials at (298.15 ± 1, 303.15 ± 1, and 318.15 ± 1) K are presented in Figure 4.

Both materials reached the saturation level in approximately 10 h. At the initial As^V concentration of 100 ppb, the equilibrium adsorption capacities were determined to be (15.7 and 16) $\mu g\cdot g^{-1}$ of As^V adsorption onto Fe-XAD7-DEHPA obtained via DM and Fe-XAD7-DEHPA obtained via CM in 10 h, respectively. After 10 h of contact between adsorbent and adsorbate, the adsorption capacity hardly changed during the adsorption time.

The experimental kinetic data of the adsorption studies were used in the Lagergren pseudofirst-order, pseudosecond-order, and intraparticle diffusion models. The integrated forms of the models are shown below:

The pseudofirst-order kinetic model is defined by the equation:[3,9,14,25,32,35,37,38,45,49]

$$\ln(q_e - q_t) = \ln q_t - k_1\cdot t \tag{12}$$

where q_e and q_t are the amount of the As^V adsorbed onto the studied materials ($\mu g\cdot g^{-1}$) at equilibrium and at time t, respectively. t is the contact time (h), and k_1 is the specific sorption rate constant (h^{-1}). The values of the adsorption rate constant (k_1) were determined from $\ln(q_e - q_t)$ in terms of t.

The linear form of the pseudosecond-order model is defined by:[3,6,7,9,14,25,32,35,37,38,44,49]

$$\frac{t}{q_t} = \frac{1}{k_2\cdot q_e^{\,2}} + \frac{t}{q_e} \tag{13}$$

where q_e and q_t are the amount of the As^V adsorbed onto the studied materials ($\mu g\cdot g^{-1}$) at equilibrium and at time t, respectively. t is the contact time (h), and k_2 is the pseudosecond-order adsorption rate constant ($g\cdot\mu g^{-1}\cdot h^{-1}$). The values q_e and k_2 are determined from the slope and intercept of $(t\cdot q_t^{-1})$ versus t (Figure 5). In eq 13, the expression $k_2\cdot q_e^{\,2}$ in the intercept term describes the initial sorption rate $h/(\mu g\cdot(g\cdot h)^{-1})$ as $t\rightarrow 0$.

Intraparticle Diffusion Model. The adsorption of As^V ions onto the studied materials may be controlled via external film diffusion at earlier stages and later by the particle diffusion. The possibility of intraparticle diffusion resistance was identified by

dx.doi.org/10.1021/je200476u |J. Chem. Eng. Data XXXX, XXX, 000–000

Table 2. Kinetic Parameters for As^V Ion Adsorption onto Fe-XAD7-DEHPA Resins

	q_{exp}	k_1	q_{calc}		Δq	E
pseudofirst-order	$\mu g \cdot q^{-1}$	h^{-1}	$\mu g \cdot g^{-1}$	R^2	%	%
			$T = 298.15 \pm 1$ K			
DM	15.7	0.1907	5.69	0.9647	11.1	1.2
CM	16.0	0.2143	4.74	0.8577	15.3	2.3
			$T = 303.15 \pm 1$ K			
DM	15.7	0.1937	4.81	0.8796	13.5	1.8
CM	16.3	0.1547	4.05	0.7494	17.1	2.9
			$T = 318.15 \pm 1$ K			
DM	15.8	0.2108	4.58	0.8764	15.2	2.3
CM	16.5	0.1439	3.64	0.7202	18.2	3.3
	q_{exp}	k_2	q_{calc}		Δq	E
pseudosecond-order	$\mu g \cdot g^{-1}$	$g \cdot \mu g^{-1} \cdot h^{-1}$	$\mu g \cdot g^{-1}$	R^2	%	%
			$T = 298.15 \pm 1$ K			
DM	15.7	0.0719	16.2	0.9999	0.97	0.01
CM	16.0	0.0819	16.5	0.9996	3.2	0.10
			$T = 303.15 \pm 1$ K			
DM	15.7	0.0799	16.2	0.9997	2.06	0.04
CM	16.3	0.0861	16.6	0.9995	3.5	0.12
			$T = 318.15 \pm 1$ K			
DM	15.8	0.0873	16.3	0.9996	3.69	0.13
CM	16.5	0.0961	16.8	0.9994	5.6	0.31
	q_{exp}	K_{dif}			Δq	E
intraparticle diffusion model	$\mu g \cdot g^{-1}$	$\mu g \cdot g^{-1} \cdot h^{-1/2}$	C	R^2	%	%
			$T = 298.15 \pm 1$ K			
DM	15.7	1.6032	9.11	0.7346	11.6	1.3
CM	16.0	1.6695	9.51	0.6903	12.4	1.5
			$T = 303.15 \pm 1$ K			
DM	15.7	1.6126	9.32	0.7139	12.1	1.5
CM	16.3	1.6497	9.71	0.6927	12.1	1.4
			$T = 318.15 \pm 1$ K			
DM	15.8	1.6168	9.54	0.6776	12.6	1.6
CM	16.5	1.6426	10.0	0.6580	12.3	1.5

using the following intraparticle diffusion model:[3,9,14,44]

$$q_t = k_{dif} \cdot t^{1/2} + C \quad (14)$$

where K_{dif} is the intraparticle diffusion rate constant ($\mu g \cdot g^{-1} \cdot h^{-1/2}$) and C is the intercept. The values of q_t versus $t^{1/2}$ and the rate constant K_{dif} are directly evaluated from the slope of the regression line.

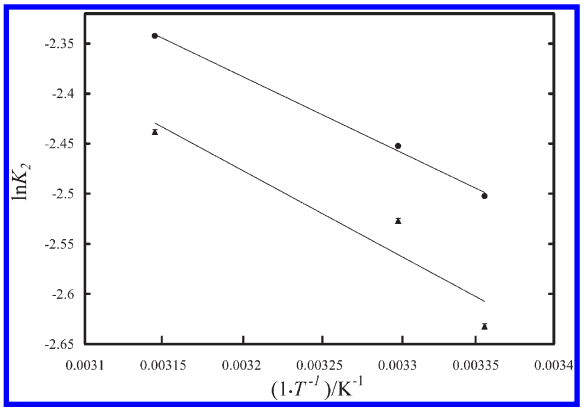

Figure 6. Arrhenius plots for the adsorption of As^V onto Fe-XAD7-DEHPA resins; ▲, DM; ●, CM. Error bars represent the relative standard deviation.

The models were tested by the normalized standard deviation (eq 9) and average relative error (eq 10) to determine which equation best describes the data. The values of the constants, together with the regression coefficients (R^2) and the absolute error values obtained in all the cases, are summarized in Table 2.

The only plot exhibiting good linearity with a good correlation coefficient (close to 1) and the lower value of the estimated errors was obtained for the case of the pseudosecond-order model (Figure 5). Also, in this case, the theoretically predicted equilibrium adsorption capacity was close to the experimentally determined value. The other models did not describe the kinetics of the adsorption process in a satisfactory manner, and the corresponding plots have therefore not been included here. This process was suitable for the description of the adsorption kinetics for the removal of As^V from aqueous solution onto Fe-XAD7-DEHPA resins. The adsorption can be seen as the rate-limiting step that controls the adsorption process. The rate constant k_2 increased with temperature increasing (Table 2), which shows that the process is endothermic.

As seen in Table 2, which shows the K_{dif} values and coefficient constant, the intraparticle diffusion model cannot be the dominating mechanism for the adsorption of the As^V from aqueous solution by the studied adsorbents.

Adsorption Thermodynamics. The rate constants k_2 calculated from eq 13 at different temperatures were used to estimate the activation energy of As^V onto Fe-XAD7-DEHPA resins. The rate constant is expressed as a function of temperature according to the well-known Arrhenius equation:[3,5,32,44,49]

$$\ln k_2 = \ln A - \frac{E^{\#}}{RT} \quad (15)$$

where $E^{\#}$ ($kJ \cdot mol^{-1}$) is the activation energy of adsorption, A is a constant called the frequency factor, and T and R have the same meanings as before. The activation energy $E^{\#}$ and the frequency factor A were calculated, respectively, from the slope and the intercept of the straight line obtained from the plot of $\ln K_2$ versus $1 \cdot T^{-1}/(1 \cdot K^{-1})$ as seen in Figure 6.

The magnitude of the activate energy $E^{\#}$ may provide a clue in the type of adsorption, physical or chemical.[2,44,49] The $E^{\#}$ values, calculated from the plot of ln k_2 versus $(1 \cdot T^{-1})/(1 \cdot K^{-1})$ (Figure 6), were found to be (7.012 and 6.21) $kJ \cdot mol^{-1}$ for the adsorption of As^V onto Fe-XAD7-DEHPA obtained through DM and CM, respectively. These values are of the same magnitude

dx.doi.org/10.1021/je200476u |J. Chem. Eng. Data XXXX, XXX, 000–000

Table 3. Thermodynamic Parameters for As^V Ion Adsorption onto Fe-XAD7-DEHPA Resins Obtained Through the Dry Method (DM) and the Column Method (CM)

T	k_2	$K^{\#}\cdot 10^{14}$	$\Delta H^{\#}$	$\Delta G^{\#}$	$\Delta S^{\#}$
K	$g\cdot mol^{-1}\cdot s^{-1}$	$g\cdot mol^{-1}$	$kJ\cdot mol^{-1}$	$kJ\cdot mol^{-1}$	$J\cdot mol^{-1}\cdot K^{-1}$
			DM		
298.15 ± 1	0.266	4.28	2.06	76.3	−249.0
303.15 ± 1	0.296	4.69	1.97	77.3	−249.0
318.15 ± 1	0.323	4.87	1.72	81.1	−249.4
			CM		
298.15 ± 1	0.303	4.88	1.26	75.9	−250.6
303.15 ± 1	0.319	5.05	1.17	77.1	−250.7
318.15 ± 1	0.356	5.37	0.92	80.8	−251.1

as the activation energy of the physisorption. The positive values of $E^{\#}$ indicate the endothermic nature of the adsorption process.

The relation between rate constant (k_2) and equilibrium constant ($K^{\#}$) can be given in the form:[49]

$$k_2 = \left(\frac{k_B\cdot T}{h}\right)\cdot K^{\#} \tag{16}$$

where $k_B = 1.381\cdot 10^{-23}\ J\cdot K^{-1}$ is the Boltzmann constant, $h = 6.626\cdot 10^{-34}\ J\cdot s$ is the Planck constant, and T is the absolute temperature. The value of $K^{\#}$ was calculated for each temperature for both studied adsorbents.

The relation between the activation energy and internal energy of activation ($\Delta U^{\#}$) can be derived by using the well-known Arrhenius ($d\ln k\cdot dT^{-1} = E^{\#}\cdot(RT^2)^{-1}$) and van't Hoff ($d\ln K^{\#}\cdot dT^{-1} = \Delta U^{\#}\cdot(RT^2)^{-1}$) equations in the temperature derivative of the last equation as follows:

$$d\ln\frac{k}{dT} = \left(\frac{1}{T}\right) + d\ln\frac{K^{\#}}{dT} \tag{17}$$

$$\frac{E^{\#}}{RT^2} = \left(\frac{1}{T}\right) + \frac{\Delta U^{\#}}{RT} \tag{18}$$

$$\Delta U^{\#} = E^{\#} - RT \tag{19}$$

The relation between the enthalpy ($\Delta H^{\#}$) and the internal energy of activation ($\Delta U^{\#}$) can be given in the form:

$$\begin{aligned}\Delta H^{\#} &= \Delta U^{\#} + \Delta v^{\#}RT \\ &= E^{\#} - RT + (1-m)RT = E^{\#} - mRT\end{aligned} \tag{20}$$

where $\Delta H^{\#}$ is the enthalpy of activation, $\Delta v^{\#} = 1 - m$ is the stoichiometric value of the activation reaction, and m is the molecularity, which is equal to the order.

The $\Delta H^{\#}$ value for each temperature was calculated from the last equation. The Gibbs energy for activation ($\Delta G^{\#}$) and entropy of activation ($\Delta S^{\#}$) were calculated from the equation:

$$\Delta G^{\#} = \Delta H^{\#} - T\Delta S^{\#} = -RT\ln K^{\#} \tag{21}$$

All of the thermodynamic parameters for the adsorption of As^V onto Fe-XAD7-DEHPA resins, obtained via DM and CM, are presented in Table 3.

As can be seen from Table 3, the positive $\Delta G^{\#}$ values indicate that the instability activation complex of the adsorption reaction increases with increasing temperature. Also, the positive $\Delta H^{\#}$ indicates the endothermic nature of adsorption at $T = (298.15 \pm 1$ to $318.15 \pm 1)$ K. The values of the negative activation entropy $\Delta S^{\#}$ confirm the decreased randomness at the solid−solution interface during adsorption.

CONCLUSIONS

XAD7-DEHPA resins were prepared through the DM and the CM. The both resins were loaded with iron to be used as adsorbents in the removal process of arsenate anions from aqueous solutions. The ability of the Fe-XAD7-DEHPA resins to remove As^V was examined, including equilibrium, kinetic, and thermodynamic studies of adsorption. Experiments were performed as a function of time, temperature, and initial concentration of As^V from solution.

The Langmuir, Freundlich, Temkin, and Dubinin−Kaganer−Radushkevich adsorption models were used for the mathematical explanations of the adsorption equilibrium of As^V. The R^2 values indicated that the adsorption of As^V onto Fe-XAD7-DEHPA fit the Langmuir and DKR isotherm model. The maximum adsorption capacities of Fe-XAD7-DEHPA obtained via DM and CM for As^V were (17 and 18) $\mu g\cdot g^{-1}$, respectively, obtained from the DKR isotherm model, which provided the best estimated error values.

The pseudofirst-order and pseudosecond-order kinetic and intraparticle diffusion models were used to model the adsorption of the As^V onto Fe-XAD7-DEHPA resins. It was determined that the interactions could be explained on the basis of the second-order kinetic model. The kinetic studies at the initial As^V concentration showed that the greatest adsorption capacity was achieved in 10 h of contact for the both studied materials.

The activation energies of As^V over the Fe-XAD7-DEHPA obtained through DM and CM were calculated as (7.012 and 6.21) $kJ\cdot mol^{-1}$, respectively. The positive values of $E^{\#}$ indicate that the adsorption process is an endothermic process of a physical nature.

The above results confirmed the potential of Fe-XAD7-DEHPA resins, obtained through DM and CM, as an adsorbent for As^V as well as other adsorbate. The adsorption capacities of the both studied materials are almost the same, but we can conclude that the Fe-XAD7-DEHPA obtained through the column method is most advantageous because this is obtained in a shorter time than the resin obtained via the DM.

AUTHOR INFORMATION

Corresponding Author

*Tel./Fax: +4 0256 404192. E-mail address: lavinia.lupa@chim.upt.ro.

Funding Sources

This work was supported by CNCSIS-UEFISCDI, Project No. PN II-IDEI 927/2008, "Integrated Concept about Depollution of Waters with Arsenic Content, through Adsorption on Oxide Materials, followed by Immobilization of the Resulted Waste in Crystalline Matrices". This work was partially supported by the strategic grant POSDRU/89/1.5/S/57649, Project ID 57649 (PERFORM-ERA), cofinanced by the European Social Fund—Investing in People, within the Sectoral Operational Programme, Human Resources Development, 2007−2013.

REFERENCES

(1) Kundu, S.; Gupta, A. K. Adsorptive removal of As(III) from aqueous solution using iron oxide coated cement (IOCC): Evaluation of kinetic, equilibrium and thermodynamic models. *Sep. Purif. Technol.* **2006**, *51*, 165–172.

(2) Borah, D.; Satokawa, S.; Kato, S.; Kojima, T. Surface-modified carbon black for As(V) removal. *J. Colloid Interface Sci.* **2008**, *319*, 53–62.

(3) Borah, D.; Satokawa, S.; Kato, S.; Kojima, T. Sorption of As(V) from aqueous solution using acid modified carbon black. *J. Hazard. Mater.* **2009**, *162*, 1269–1277.

(4) Negrea, A.; Lupa, L.; Ciopec, M.; Lazau, R.; Muntean, C.; Negrea, P. Adsorption of As(III) ions onto iron-containing waste sludge. *Adsorpt. Sci. Technol.* **2010**, *28*, 467–484.

(5) Ramesh, A.; Hasegawa, H.; Maki, T.; Ueda, K. Adsorption of inorganic and organic arsenic from aqueous solution by polymeric Al/Fe modified montmorillonite. *Sep. Purif. Technol.* **2007**, *56*, 90–100.

(6) Goswami, R.; Deb, P.; Thakur, R.; Sarma, K. P.; Bsumalick, A. Removal of As(III) from aqueous solution using functionalized ultrafine iron oxide nanoparticles. *Sep. Sci. Technol.* **2011**, *46*, 1017–1022.

(7) Ahmad, R. A.; Awwad, A. M. Thermodynamics of As(V) adsorption onto treated granular zeolitic tuff from aqueous solutions. *J. Chem. Eng. Data* **2010**, *55*, 3170–3173.

(8) Banerjee, K.; Amy, G. L.; Prevost, M.; Nour, S.; Jekel, M.; Gallagher, P. M.; Blumenschein, C. D. Kinetic and thermodynamic aspects of adsorption of arsenic onto granular ferric hydroxide (GFH). *Water Res.* **2008**, *42*, 3371–3378.

(9) Gupta, K.; Ghosh, U. C. Arsenic removal using hydrous nanostructure iron(III)-titanium(IV) binary mixed oxide from aqueous solution. *J. Hazard. Mater.* **2009**, *161*, 884–892.

(10) Hlavay, J.; Polyak, K. Determination of surface properties of iron hydroxide coated alumina adsorbent prepared from drinking water. *J. Colloid Interface Sci.* **2005**, *284*, 71–77.

(11) Nguyen, V. T.; Vigneswaran, S.; Ngo, H. H.; Shon, H. K.; Kandasamy, J. Arsenic removal by a membrane hybrid filtration system. *Desalination* **2009**, *236*, 363–369.

(12) Partey, F.; Norman, D.; Ndur, S.; Nartey, R. Arsenic sorption onto laterite iron concretions: Temperature effect. *J. Colloid Interface Sci.* **2008**, *321*, 493–500.

(13) Hsu, J. C.; Lin, C. J.; Liao, C. H.; Chen, S. T. Removal of As(V) and As(III) by reclaimed iron-oxide coated sands. *J. Hazard. Mater.* **2008**, *153*, 817–826.

(14) Chen, Y. N.; Chai, L. Y.; Shu, Y. D. Study of arsenic(V) adsorption on bone char from aqueous solution. *J. Hazard. Mater.* **2008**, *160*, 168–172.

(15) Bilici Baskan, M.; Pala, A. Determination of arsenic removal efficiency by ferric ions using response surface methodology. *J. Hazard. Mater.* **2009**, *166*, 796–801.

(16) Parga, J. R.; Cocke, D. L.; Valenzuela, J. L.; Gomes, J. A.; Kesmez, M.; Irwin, G.; Moreno, H.; Weir, M. Arsenic removal via electrocoagulation from heavy metal contaminated groundwater in La Comarca Lagunera Mexico. *J. Hazard. Mater.* **2005**, *B124*, 247–254.

(17) Bissen, M.; Frimmel, F. H. Arsenic-a review. Part II: oxidation of arsenic and its removal in water treatment. *Acta Hydrochim. Hydrobiol.* **2003**, *31*, 97–107.

(18) Song, S.; Lopez-Valdivieso, A.; Hernandez-Campos, D. J.; Peng, C.; Monroy-Fernandez, M. G.; Razo-Soto, I. Arsenic removal from high-arsenic water by enhanced coagulation with ferric ions and coarse calcite. *Water Res.* **2006**, *40*, 364–372.

(19) Wang, L.; Chen, A. S. C.; Sorg, T. J.; Fields, K. A. Field evaluation of As removal by IX and AA. *J. Am. Water Works Assoc.* **2002**, *94*, 161–173.

(20) Monah, D.; Pittman, C. U. Arsenic removal from water/wastewater using adsorbents- a critical review. *J. Hazard. Mater.* **2007**, *142*, 1–53.

(21) Jonsson, J.; Sherman, D. M. Sorption of As(III) and As(V) to siderite, green rust (fougerite) and magnetite; Implications for arsenic release in anoxic groundwaters. *Chem. Geol.* **2008**, *255*, 173–181.

(22) Ohe, K.; Tagai, Y.; Nakamura, S.; Oshima, T.; Baba, Y. Adsorption behaviour of arsenic(III) and arsenic(V) using magnetite. *J. Chem. Eng. Jpn.* **2005**, *38*, 671–676.

(23) Jeong, Y.; Fan, M.; Singh, S.; Chuang, C. L.; Saha, B.; van Leeuwen, J. H. Evaluation of iron oxide and aluminium oxide as potential arsenic(V) adsorbents. *Chem. Eng. Process* **2007**, *46*, 1030–1039.

(24) Gupta, K.; Basu, T.; Ghosh, U. C. Sorption characteristics of arsenic(V) for removal from water using agglomerated nanostructure iron(III)−zirconium(IV) bimetal mixed oxide. *J. Chem. Eng. Data* **2009**, *54*, 2222–2228.

(25) Ren, Z.; Zhang, G.; Chen, J. P. Adsorptive removal of arsenic from water by an iron-zirconium binary oxide adsorbent. *J. Colloid Interface Sci.* **2011**, *358*, 230–237.

(26) Maji, S. K.; Pal, A.; Pal, T. Arsenic removal from real-life groundwater by adsorption on laterite soil. *J. Hazard. Mater.* **2008**, *151*, 811–820.

(27) So, H. U.; Postma, D.; Jakobsen, R.; Larsen, F. Sorption and desorption of arsenate and arsenite on calcite. *Geochim. Cosmochim. Acta* **2008**, *72*, 5871–5884.

(28) Mondal, P.; Majumder, C. B.; Mohanty, B. Effects of adsorbent dose, its particle size and initial arsenic concentration on the removal of arsenic, iron and manganese from simulated ground water by FeIII impregnated activated carbon. *J. Hazard. Mater.* **2008**, *150*, 695–702.

(29) Chakraborty, A.; Saha, B. B.; Ng, K. C.; Koyama, S.; Srinivasan, K. Theoretical insight of physical adsorption for a single component adsorbent+adsorbate system: II The Henry region. *Langmuir* **2009**, *25*, 7359–7367.

(30) Belkhouche, N. E.; Didi, M. A. Extraction of Bi(III) from nitrate medium by D2EHPA impregnated onto Amberlite XAD-1180. *Hydrometallurgy* **2010**, *103*, 60–67.

(31) Chabani, M.; Amrane, A.; Bensmaili, A. Kinetics of nitrates adsorption on Amberlite IRA-400 resin. *Desalination* **2007**, *206*, 560–567.

(32) Hosseini-Bandegharaei, A.; Hosseini, M. S.; Sarw-Ghadi, M.; Zowghi, S.; Hosseini, E.; Hosseini-Bandegharaei, H. Kinetics, equilibrium and thermodynamic study of Cr(VI) sorption into toluidine blue o-impregnated XAD-7 resin beads and its application for the treatment of wastewaters containing Cr(VI). *Chem. Eng. J.* **2010**, *160*, 190–198.

(33) Mustafa, S.; Shah, K. H.; Naeem, A.; Waseem, M.; Tahir, M. Chromium (III) removal by weak acid exchanger Amberlite IRC-50 (Na). *J. Hazard. Mater.* **2008**, *160*, 1–5.

(34) Saha, B.; Gill, R. J.; Bailey, D. G.; Kabay, N.; Arda, M. Sorption of Cr(VI) from aqueous solution by Amberlite XAD-7 resin impregnated with Aliquat 336. *React. Funct. Polym.* **2004**, *60*, 223–244.

(35) Shao, W.; Li, X.; Cao, Q.; Luo, F.; Li, J.; Du, Y. Adsorption of arsenate and arsenite anions from aqueous medium by using metal (III)-loaded Amberlite resins. *Hydrometallurgy* **2008**, *91*, 138–143.

(36) Zhu, X.; Jyo, A. Removal of arsenic(V) by zirconium(IV)-loaded phosphoric acid chelating resin. *Sep. Sci. Technol.* **2001**, *36*, 3175–3189.

(37) Chanda, M.; O'Driscoll, K. F.; Rempel, G. L. Ligand exchange sorption of arsenate and arsenite anions by chelatin resins in ferric ion form: II. Iminodiacetic chelatin resin Chelex 100. *React. Polym.* **1988**, *8*, 85–95.

(38) An., B.; Steinwinder, T. R.; Zhao, D. Selective removal of arsenate from drinking water using a polymeric ligand exchanger. *Water Res.* **2005**, *39*, 4993–5004.

(39) Mendoza, R. N.; Medina, I. S.; Vera, A.; Rodriguez, M. A. Study of the sorption of Cr(III) with XAD-2 resin impregnated with di-(2,4,4-trimethylpentyl)phosphinic acid (Cyanex 272). *Solvent Extr. Ion Exch.* **2000**, *18*, 319–343.

(40) Muraviev, D.; Ghantous, L.; Valiente, M. Stabilization of solvent impregnated resin capacities by different techniques. *React. Funct. Polym.* **1998**, *38*, 259–268.

(41) Juang, R. S. Preparation, properties and sorption behaviour of impregnated resin containing acidic organophosphorus extractants. *Proc. Natl. Sci. Counc. ROC(A)* **1999**, *23*, 353–364.

(42) Benamor, M.; Bouariche, Z.; Belaid, T.; Draa, M. T. Kinetic studies on cadmium ions by Amberlite XAD7 impregnated resin containing di(2-ethylhexyl) phosphoric acid as extractant. *Sep. Purif. Technol.* **2008**, *59*, 74–84.

(43) Guo, X.; Fuhua, C. Removal of arsenic by bead cellulose loaded with iron oxyhydroxide from groundwater. *Environ. Sci. Technol.* **2005**, *39*, 6808–6818.

(44) Ada, K.; Ergene, A.; Tan, S.; Yalcin, E. Adsorption of Remazol Brilliant Blue R using ZnO fine powder: equilibrium, kinetic and thermodynamic modelling studies. *J. Hazard. Mater.* **2009**, *165*, 637–644.

(45) Mohad Din, A. T.; Hameed, B. H. Adsorption of methyl violet dye on acid modified activated carbon: isotherms and thermodynamics. *J. Appl. Sci. Environ. Sanit.* **2010**, *5*, 161–170.

(46) Lv, L.; He, J.; Wei, M.; Evans, D. G.; Zhou, Z. Treatment of high fluoride concentration water by MgAl-CO_3 layered double hydroxides: Kinetic and equilibrium studies. *Water Res.* **2007**, *41*, 1534–1542.

(47) El-Kamash, A. M.; Zaki, A. A.; Abdel, M.; Geleel, E. Modeling batch kinetics and thermodynamics of zinc and cadmium ions removal from waste solutions using synthetic zeolite. *J. Hazard. Mater.* **2005**, *B127*, 211–220.

(48) Allen, S. J.; Mckay, G.; Porter, J. F. Adsorption isotherm models for basic dye adsorption by peat in single and binary component systems. *J. Colloid Interface Sci.* **2004**, *280*, 322–333.

(49) Yu, Z.; Qi, T.; Qu, J.; Wang, L.; Chu, J. Removal of Ca(II) and Mg(II) from potassium chromate solution on Amberlite IRC 748 synthetic resin by ion exchange. *J. Hazard. Mater.* **2009**, *167*, 406–412.

Bambino Gesù
OSPEDALE PEDIATRICO

GENE EXPRESSION – MICROARRAYS LABORATORY

IRCCS-Children's Hospital Bambino Gesù

Ph.D. Andrea Masotti

Rome, 1st December 2011

To whom it may concern.

I hereby certify that the chapter entitled "CLOSED CYCLE PROCESS INVESTIGATIONS FOR ARSENIC REMOVAL FROM WATERS USING ADSORPTION ON IRON-CONTAINING MATERIALS FOLLOWED BY WASTE IMMOBILIZATION" by L. Lupa, M. Ciopec, A. Negrea and R. Lazău has been accepted for publication in the book "*Arsenic: Sources, Environmental Impact and Human Health – A Medical Geology Perspective*" (Nova Science Publishers).

Sincerely,

Andrea Masotti

Guest Editor of the Book

"*Arsenic: Sources, Environmental Impact*

and Human Health – A Medical Geology Perspective" (Nova Science Publishers)

Piazza Sant'Onofrio, 4
00165 Roma
Tel. +39 06 6859 2650
Fax +39 06 6859 2904
e-mail andrea.masotti@opbg.net

Bambino Gesù
Ospedale Pediatrico
Istituto di Ricovero e Cura
a Carattere Scientifico
www.ospedalebambinogesu.it

Joint Commission International

Chapter

CLOSED CYCLE PROCESS INVESTIGATIONS FOR ARSENIC REMOVAL FROM WATERS USING ADSORPTION ON IRON-CONTAINING MATERIALS FOLLOWED BY WASTE IMMOBILIZATION

L. Lupa*, M. Ciopec, A. Negrea and R. Lazău
University "Politehnica" Timisoara, Faculty of Industrial Chemistry and Environmental Engineering, Timisoara, Romania

ABSTRACT

The chapter deals with adsorption process evaluation for removing arsenic from water using different iron containing materials, including an industrial waste. Adsorption is one of the most widely used techniques for arsenic removal from water and iron-based adsorbent materials proved to be very efficient. Therefore, kinetic, equilibrium, thermodynamic and column studies were performed for Fe_2O_3, Fe_2O_3:SiO_2 mixtures and an industrial sludge mostly containing Fe_2O_3 from hot dip galvanizing industry. Competing anions effect upon adsorption performance was also followed. All the studied materials showed good adsorption performance in both synthetic solutions and natural waters. The most suitable amongst the tested materials for arsenic

* E-mail address: lavinia.lupa@chim.upt.ro (L. Lupa).

adsorption remains the iron containing waste sludge (IS), due to economic reasons and high adsorption capacity. Thus, it has also been explored the possibility of immobilization of the exhausted adsorbent (IS) in vitreous matrices. This has been successfully done in frits/ ceramic decorative glazes. Considering the chosen solutions, the results are in full agreement with the sustainable development principles and comply with the closed-cycle technologies.

INTRODUCTION

The presence of dissolved arsenic in groundwater has created significant concern on a global scale, because of its toxic and carcinogenic effects on human beings [1, 2]. Unfortunately, there is no known cure for As poisoning and therefore providing As free drinking water is the only way to eliminate its adverse health effects [3]. The World Health Organization (WHO) recommends a maximum admissible concentration of arsenic of 10 µg/L in drinking water [4]. It is well known from the chemistry of arsenic that As(III) is more toxic and mobile than As(V) [5]. The removal of As(III) from aqueous solution is usually more difficult compared to that of As(V), by almost all of the methods developed. It is because the predominant As(III) species are of neutral charge, whilst the As(V) species are negatively charged in the pH range of 4-10 [2, 5]. So sometimes pre-oxidation step is required to convert As(III) to As(V) in order to achieve the removal of As(III). A variety of technologies have been used to remove arsenic from water including conventional co-precipitation, lime softening, filtration, ion exchange, reverse osmosis and membrane filtration [6-9], but due to the extended use of chemicals, bulky sludge, high cost, these techniques are not feasible at small-scale or household level [5, 10]. The adsorption technique is regarded as very attractive and promising due to its simplicity, ease of operation and handling, sludge free operation, and regeneration capacity [11, 12]. Many types of adsorbents have been used including activated carbon [13-15], calcite [16], natural and synthetic zeolites [17], etc. However because of the selectivity and affinity of Fe(III) toward inorganic arsenic species, zero valent-iron[18], Fe(III) bearing mixed oxide [19-22], iron oxide-coated materials [12, 22-25], iron (hydr)oxide [1, 26, 27], laterite [2, 28] and Fe(III)-loaded resins [29-33] are the most used in arsenic adsorption. Arsenic is strongly attracted to the sorption site of these solids and thus can be effectively removed from solution. The purpose of the work presented within this chapter was to evaluate the adsorption performances of Fe_2O_3 obtained after annealing different iron salts:

iron oxalate – $Fe(COO)_2 \cdot 2H_2O$, ammonium ferric alum – $Fe^{3+}(NH_4)(SO_4)_2 \cdot 12H_2O$ and Mohr salt – $Fe^{2+}(NH_4)_2(SO_4)_2 \cdot 6H_2O$ in the removal process of As(III) from aqueous solution. In order to resolve the issue of the resulted sludge after adsorption we proposed the recycling of the exhausted adsorbent with arsenic content in iron glass applications and thus, the presented method generates no secondary contaminated substances at the end of the waste recycling/ depollution process. This approach starts from the fact that in glass applications arsenic is used under As_2O_3 form. Even if this is very toxic, it is practically irreplaceable in these mixtures, due to its acting as an effective O_2 carrier at high temperatures [34-36]. In order to make it more suitable for this purpose we added SiO_2, as Ultrasil VN3 (Degussa), in the obtained Fe_2O_3 adsorbent composition. The focus was on these oxide mixtures because the iron oxide is responsible for arsenic removal and the presence of SiO_2 during adsorbent preparation leads to higher surface area, so we expect to obtain higher adsorption capacities. Although these materials are selective and efficient in removing arsenic, their applicability is limited because of their cost. Hence the goal for our research is to develop an arsenic removal system by using a low cost adsorbent. The material tested in the present chapter is an iron containing waste sludge (IS) resulted from the hot-dip galvanizing process. The main points described in this chapter are: (a) obtaining the Fe_2O_3 and the Fe_2O_3:SiO_2 mixtures; (b) characterization of the obtained synthetic adsorbents and the low cost adsorbent (IS); (c) investigation of As(III) adsorption using the new adsorbents in batch tests; (d) study of the multi-component presence influence in the solution; (e) characterization of As (III) uptake on the columns packed with the new adsorbents under different operating conditions; (f) imobilization of the exhausted adsorbents in vitreous matrices.

1. ADSORBENTS PREPARATION AND CHARACTERIZATION

The iron containing sludge (IS) formed during hot-dip galvanizing process was tested as a low cost adsorbent. Hot-dip galvanizing is a coating process applied in order to prevent iron-based materials from corroding. Hot-dip galvanizing is one of the most common coating methods and it is particularly being used to coat steel. Before the hot-dip galvanizing, pieces are being subjected to a preparation process, which consists of degreasing, chemical cleaning, rinsing, fluidizer treatment and pre-warming. Waste waters result from these operations and they are neutralized with lime. This method can

efficiently remove heavy metals from wastewaters, but it generates an iron containing sludge classified as industrial waste, which often causes disposal problems [37]. Arsenic removal from water using the above mentioned iron sludge has been tested, as an appropriate environmental and economical solution, in accordance with the sustainable development principles. The IS used for arsenic removal, dried at 105°C has the particle size below 0.32 µm. The chemical composition of the IS resulted from energy dispersive X-ray analysis (EDX) is presented in table 1.

Table 1. Chemical composition of the IS

No.	Element	Composition (wt,%)
1.	Fe	33.5
2.	Ca	11.2
3.	Cl	22.8
4.	P	0.45
5.	S	0.71
6.	Zn	2.74
7.	O	28.6

The major component of the IS is iron, which makes it suitable for arsenic removal from water, due to the high affinity of arsenic towards iron. The chlorine ions come from the hydrochloric acid used at the chemical cleaning of the steel parts and the calcium ions come from the neutralization agent used for the residual waters treatment [38]. The other ions evidenced by the analysis in low proportion come either from the degreasing solution of the steel parts, or from the water used in various stages of the technological process. The zinc ions result from the parts, which were poorly coated, subjected to de-zincking and then re-entered in the technological process. The IS was characterized through: XRD, and BET – accelerated surface area analysis.

The adsorbents based on Fe_2O_3 and Fe_2O_3:SiO_2 mixtures were obtained by annealing at 550°C of the iron oxalate – $Fe(COO)_2 \cdot 2H_2O$, and at 800°C of the ammonium ferric alum – $Fe^{3+}(NH_4)(SO_4)_2 \cdot 12H_2O$ and Mohr salt – $Fe^{2+}(NH_4)_2(SO_4)_2 \cdot 6H_2O$. In the case of samples with SiO_2 content, these have been wet homogenized with the iron salts prior to annealing, in the mass ratio 1:1, in a porcelain dish, dried at 110ºC and the resulted mixtures have been grinded in a mortar. The iron salts and the mixtures with Ultrasil have been loaded in porcelain crucibles and annealed in an electric kiln at the minimum temperatures necessary for their decomposition with the formation of Fe_2O_3. After annealing the obtained iron oxides have been characterized through

XRD phase analysis, and BET – accelerated surface area analysis. The XRD patterns were recorded on a Bruker D8 Advance System with monochromator, Cu $_{K\alpha}$ radiation. The specific surface area and the pore volume of the studied materials were measured using a Micrometrics ASAP 2020 BET surface area analyzer, by cold nitrogen adsorption.

The characteristic of the studied adsorbents are presented in table 2. The XRD pattern of the IS reveals the predominance of the iron oxy-hydroxides as goethite and lepidocrocite. Can be observed that the IS sample dried at 105°C is more amorphous then the sample annealed at 200°C (figure 1). The XRD pattern of the samples obtained by annealing of the iron salts alone or mixed with SiO_2 reveals that the only crystalline phase present in the sample is the hematite (figure 2).

The BET surface area analysis of the IS sample was carried out after degasing at 200°C in order to remove the volatile compounds from the sample. The BET surface area of the IS is higher than the BET surface area of the iron oxide obtained after annealing of the iron salts. This is explained by the fact that IS is more amorphous then the synthetic oxides. The presence of SiO_2 leads to the increase of the surface area of the synthetic iron oxides. From the BET surface area one can aspect that the materials with the highest adsorption capacity are the IS and the mixtures Fe_2O_3:SiO_2.

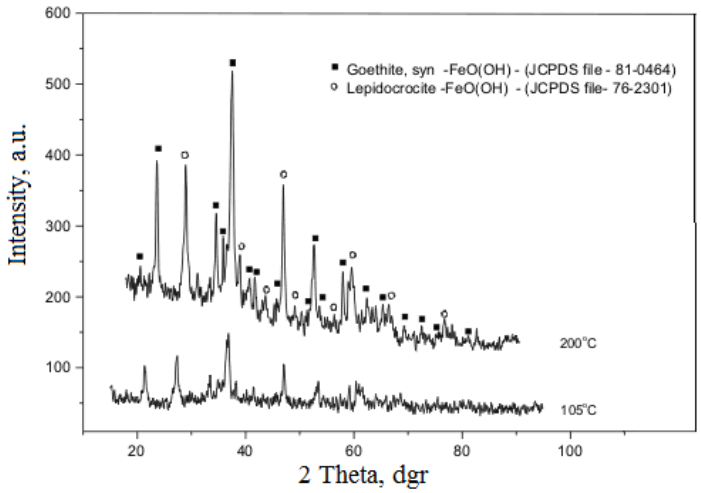

Figure 1. X-Ray diffraction patterns of the IS samples dried at 105°C and annealed at 200°C.

Table 2. Characteristics of the studied adsorbents

Sample no. and symbol	Salt used	SiO_2 content (Fe_2O_3:SiO_2 mass ratio)	Anealing temperature °C	BET surface area (m^2/g)	Pore volume cm^3/g	Average pore size (Å)
1.×	IS	-	200	50.5	0.168	111.5
2.▼	$Fe(COO)_2 \cdot 2H_2O$	-	550	14.6	0.089	255
3. ▽	$Fe(COO)_2 \cdot 2H_2O$	1:1	550	78.0	0.556	287
4.■	$Fe^{3+}(NH_4)(SO_4)_2 \cdot 12H_2O$	-	800	11.1	0.035	133
5.□	$Fe^{3+}(NH_4)(SO_4)_2 \cdot 12H_2O$	1:1	800	57.0	0.467	309
6.●	$Fe^{2+}(NH_4)_2(SO_4)_2 \cdot 6H_2O$	-	800	8.22	0.037	178
7.○	$Fe^{2+}(NH_4)_2(SO_4)_2 \cdot 6H_2O$	1:1	800	57.0	0.427	287

In order to understand the characteristics of the surface charge for the studied adsorbents, the pH_{pzc} of the IS and of the iron oxide obtained from the annealing of iron oxalate was determined by mass titration method [13, 14]. For the determination of the pH_{pzc} a definite amount (0.2 g) of sorbent was suspended in 100 mL 0.005 M NaCl solution, used as an inert/background electrolyte with initial pH varying between 2 and 12. The initial pH of the NaCl solution was adjusted to the desired value using 0.1M/2M NaOH or 0.1M/2M HNO_3, so that the volume variation of the solution was as low as possible. The pH of the suspension was measured using a CRISON MultiMeter MM41. The suspensions were stirred for 1 h at 300 rpm, using a magnetic stirring device IKA RTC and then the final pH was read. The pH_{pzc} was determined through the plot of the pH_f versus pH_i (figure 3).

The acid–base properties of the studied material play an important role in the use of the materials as adsorbents. Figure 5 shows the corresponding plot of pH_i versus pH_f allowing the determination of the point of zero charge (pH_{pzc}) for the IS and for the Fe_2O_3 obtained by annealing of iron oxalate. The pH value of the plateau exhibited in this plot corresponds to $pH_{pzc} = 6.2$ for IS and $pH_{pzc} = 6.1$ for the Fe_2O_3. The presence of such a plateau indicates that the studied materials were ampholytes and behaved as acid–base buffers [13, 14, 39]. These plateaus correspond to the pH range where buffering of the studied materials surface occur, thereby making all values of pH_i between 4 and 9 equal to the corresponding value of pH_f. The pH_{pzc} value suggest that the surface of the material was predominantly positive at pH values lower than 6.2 for IS and 6.1 for Fe_2O_3, respectively and negative at pH values higher than these values. The surface charge density of the materials should increase/decrease as the pH value of the system decreased below pH_{pzc} or increased above these values [38, 40].

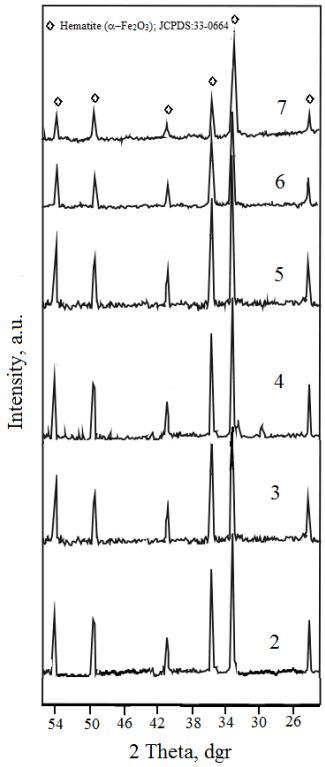

Figure 2. X-Ray diffraction patterns of the Fe_2O_3 samples and Fe_2O_3-SiO_2 mixtures.

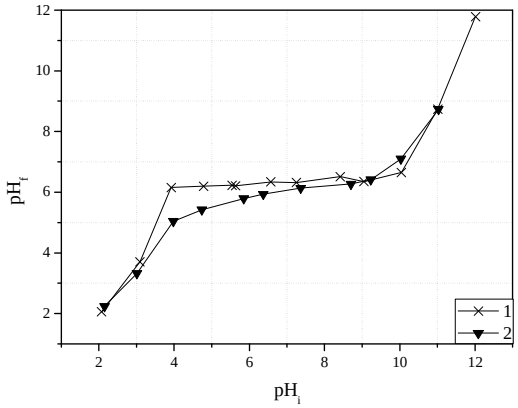

Figure 3. Plot of the final pH (pH_f) versus the initial pH (pH_i) allowing the determination of the value of pH_{pzc} for the IS and iron oxide obtained from iron oxalate.

2. KINETIC, EQUILIBRIUM AND THERMODYNAMIC STUDIES REGARDING THE AS(III) ADSORPTION ONTO THE STUDIED MATERIALS

In order to establish the adsorption performance of the studied materials in the removal process of As(III) from solution equilibrium, kinetic and thermodynamic studies were performed. The influence of different physicochemical parameters (stirring rate, contact time, arsenic initial concentration and temperature) upon the arsenic adsorption onto the studied materials was investigated.

For all adsorption experiments, the initial pH of the solutions was maintained within the range 6.5–7.0, i.e. at the mid-point of the plateau obtained in the plot of pH_f versus pH_i mentioned above. This also corresponded to the most common pH value found in natural waters.

Prior to such experiments a stock solution was prepared by diluting an appropriate amount of 0.05 M $NaAsO_2$ solution (Merck TitriPUR). Other solutions of As(III) ions were prepared from the stock solution by appropriated dilution. The adsorption experiments were conducted using agitating device with glass rod to obtain the data for the equilibrium, kinetic and thermodynamic parameters for As(III) adsorption onto the studied materials. The experiments were performed with 0.1 g of adsorbent in 100 mL of As(III) solution of desired concentration and pH. The samples were stirred at the established temperature and time intervals for the various experimental studies. After stirring, the samples were centrifuged at 1200 rpm for 0.5 h using a Hettich ROTINA 420 centrifuge. The residual concentration of As(III) ions in the resulting solutions was determined using atomic absorption spectrometry with hydride generation [41, 42]. This method uses the selective reduction of As(III) ions to arsine (H_3As) with sodium boron hydride $NaBH_4$ (Merck-Schuchardt; 0.6 w/v% solution) in a NaOH buffer (Chemapol, Prague, Czech Republic; 0.5 w/v%). The arsine gas generated was introduced into the flame of the atomic absorption spectrometer and the absorbance value measured at 193.7 nm was compared with a calibration curve obtained using As(III) ion solutions of various known concentrations prepared from the stock solution. The carrier solution employed in the flow injection system was prepared using HCl (37%, Corozin, Romania; 1:3). A Varian SpectrAA 110 atomic absorption spectrometer with a Varian VGA 77 hydride generation system was used for all measurements.

The extent of adsorption is quantified in terms of the adsorption capacity q_t (µg/g) of the adsorbent, corresponding to the amount of As(III) ions sorbed per g of adsorbent at a known time, t, as calculated from the following equation [13, 21, 38]:

$$q_t = \frac{(C_0 - C_t)V}{m} \quad (1)$$

where C_0 and C_t are the concentrations of As(III) ions (µg/L) in the solution initially (t = 0) and after a time t (min), respectively, V is the volume of the solution (L) and m is the mass of adsorbent employed (g).

The effect of stirring rate (50-250 rpm) on As(III) removal was studied with initial As(III) concentration of 100 µg/L and adsorbent dose of 1 g/L at a contact time of 90 min. The effect of contact time at ambient temperatures (20-25 °C) was initially studied employing a 100 µg/L As(III) ion solution with an adsorbent dosage of 0.1 g, the resulting suspensions being stirred for different contact times (15, 30, 45, 60, 90, 120 and 150 min). Adsorption isotherm studies were done by varying the initial concentration of As(III) (100, 200, 300, 400, 500, 600 and 700 µg/L) and keeping the adsorbent dose fixed (1 g/L) at the ambient temperature (20-25 °C), while the influence of temperature was investigated by studying the adsorption process in a 0.1 g of adsorbent/100 µg/L As(III) ion solution system at three different temperatures: 20, 25 and 30 ºC, respectively for first sample, 18, 20 and 40°C for second and third samples and 25, 30 and 45 °C for the last four samples. Equilibrium time for the isotherm and thermodynamic studies was kept as 90 minutes.

2.1. Effect of Stirring Rate

The adsorption of As(III) onto the studied materials was influenced by the rate of stirring. The influence of stirring rate on adsorption of As(III) onto the studied materials was studied by changing the speed of stirring from 50 to 250 rpm and results are given in figure 4.

From the figures it is obvious that the removal of As(III) increases with the increase in stirring rate from 50 to 200 rpm, for all the studied materials. This may be explained by the fact that the increasing stirring rate decreases the boundary layer resistance to mass transfer in the bulk and increases the driving force of As(III) ions. It may be, therefore, assumed that the film diffusion does

not dominantly control the overall adsorption process [24]. It is further noted that there was no significant increase in uptake above 200 rpm.

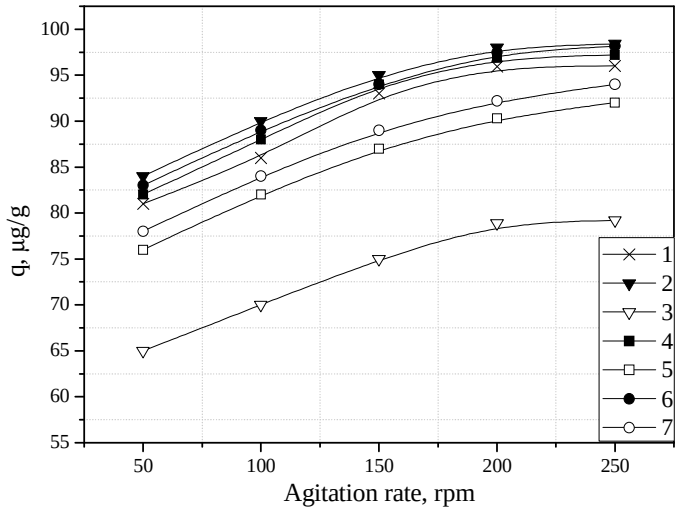

Figure 4. Effect of stirring rate on As(III) uptake by the studied materials. C_0 = 100µg/L; T=20-25°C; t = 90 min; pH=6.5 – 7; sorbent dose, 1 g/L.

2.2. Effect of Contact Time and Kinetic Studies

In equilibrium sorption experiments, kinetic study is very important to find out the contact time of the adsorbent with adsorbate and for evaluating reaction coefficients, in order to establish the mechanism of adsorption process. The stirring time effect on the adsorption capacity of the studied material in the process of As(III) removal from water are presented in figure 5. Experimental results indicate that the adsorption capacity of all studied materials increased as the contact time was increased up to 90 minutes, and remained constant afterwards. This high initial adsorption rate was due to the local availability of a large number of adsorption sites on the adsorbents. After 90 minutes of contact between adsorbents and adsorbate, the adsorption capacity changed. The rapid removal of As(III) ions coupled with a low equilibration time indicates the existence of highly favorable sorptive interactions. For subsequent experiments, an equilibration time of 90 minutes was chosen.

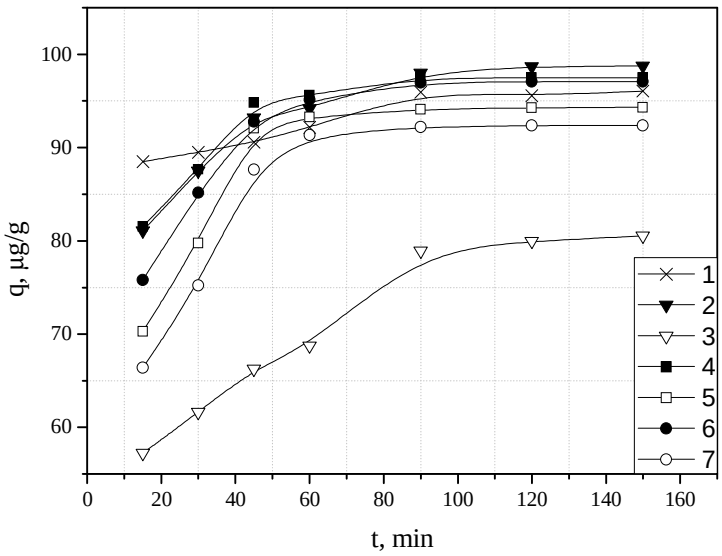

Figure 5. Effect of contact time on the adsorption capacitiy of the studied materials. C_0 = 100µg/L; T=20-25°C; pH=6.5 – 7; sorbent dose, 1 g/L; stirring rate 200 rpm.

The kinetics of the adsorption describing the rate of the arsenic removal is one of the important features that define the adsorption efficiency. In order to express the kinetics of arsenic adsorption onto the studied materials the results were analyzed using the models presented as follows.

The pseudo-first-order kinetic model based on the solid capacity and proposed by Lagergren can be used to determine the rate constant for the adsorption process and the integrated form is expressed by the following equation [13, 21, 38-40, 43]:

$$\ln(q_e - q_t) = \ln q_e - k_1 t \qquad (2)$$

where: q_t and q_e represent the amounts of the arsenic adsorbed onto the studied materials at *t* time and at equilibrium time, respectively, µg/g; k_1 is the specific adsorption rate constant, min^{-1}.

The linear form of the pseudo-second-order rate expression of Ho and Mckay, based on the solid phase sorption, is given by [1, 19, 21, 44]:

$$\frac{t}{q_t} = \frac{1}{h} + \frac{t}{q_e} \quad (3)$$

where: $h=k_2 \cdot q_e^2$; k_2 is the pseudo-second-order constant, $min^{-1}(\mu g/g)^{-1}$. Other terms have their usual meanings.

Intra-particle diffusion is an important phenomenon for adsorption processes in porous materials. The functional relationship for this process, which has been used by many authors [11, 13, 21, 44] may be written as:

$$q_t = k_{id} t^{0.5} \quad (4)$$

where k_{id} is the intra-particle diffusion rate constant [$\mu g/(g\ min^{0.5})$], which may be calculated from the slope of the linear plot of q_t versus $t^{0.5}$.

The application of the different kinetic models revealed some interesting features regarding the mechanism and rate-controlling step in the overall sorption process. The pseudo-first-order rate constant may be determined from the linear plot of $\ln(q_e - q_t)$ versus t (figure 6), whilst the pseudo-second-order rate constant can be estimated from the linear plot of t/q_t versus t (figure 7). The values of all these constants determined as indicated, together with the corresponding regression coefficients (R^2), are listed in table 3.

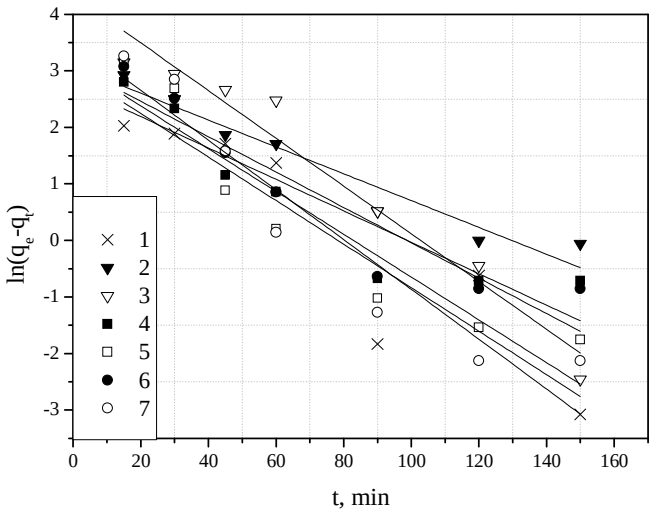

Figure 6. Pseudo-first order kinetic plot.

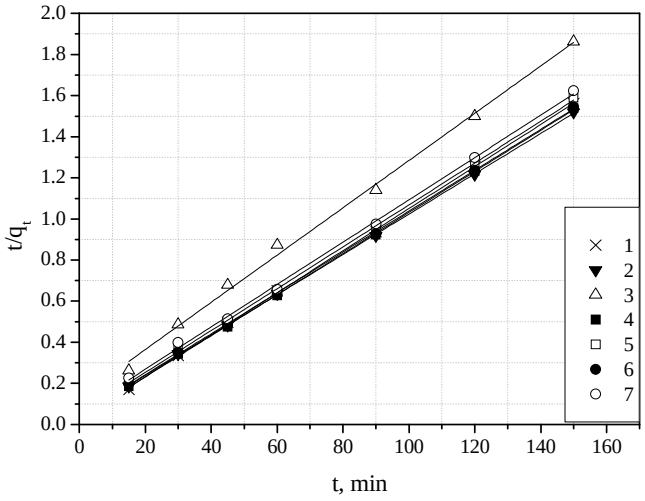

Figure 7. Pseudo-second order kinetic plot.

It was observed that the pseudo-first-order model does not describe in a satisfying manner the kinetics of the sorption process, since the correlation coefficients were much lower than those for the pseudo-second-order rate, for all the studied materials. Furthermore, the calculated equilibrium sorption capacity for the pseudo-first order model, for all the studied materials, $q_{e,calc}$, values differ from the experimental values $q_{e,\ exp}$, whilst the theoretically predicted equilibrium sorption capacity in the case of the pseudo-second-order model is close to the experimentally determined one, for all studied materials. This shows that the kinetics of As(III) removal using the studied materials with iron oxide content is described by a pseudo-second-order expression, instead of a pseudo-first-order.

However, such results provide no information regarding the rate-limiting step in the process. The rate-limiting step (i.e. the slowest step in the process) may either be boundary layer (film) diffusion or intra-particle (pore) diffusion of the solute towards the solid surface. If the rate-limiting step is intra-particle diffusion, the plot of q_t versus the square root of time should be linear and pass through the origin. Any deviation of the plot from the linearity would indicate that the rate-limiting step should be controlled by boundary layer (film) diffusion. The plot of q_t versus $t^{0.5}$ (figure 8) shows two linear sections for all the studied materials. The first may be assigned to intra-particle diffusion, the fact that the line does not pass through the origin indicating that the mechanism of As(III) ion adsorption onto the studied materials is complex,

with both surface adsorption and intra-particle diffusion contributing to the rate-limiting step. The second linear section represents the final equilibrium stage [5, 11, 13, 21, 39].

Table 3. Kinetic parameters for As(III) sorption onto iron oxide

Sample no.	q_e (exp), µg/g	Pseudo-first-order			Pseudo-second-order			Intra-particle diffusion
		q_e (calc), µg/g	k_1, min^{-1}	R^2	q_e (calc), µg/g	k_2, min^{-1} $(µg/g)^{-1}$	R^2	K_{id}, µg/g/ $min^{-0.5}$
1.	96.1	20.4	0.0381	0.8513	98.0	0.00387	0.9997	1.31
2.	98.8	21.8	0.0237	0.9925	102	0.00227	0.9999	3.01
3.	80.3	76.7	0.0422	0.9589	86.9	$9.85 \cdot 10^{-4}$	0.9968	3.77
4.	98	21.3	0.0320	0.9366	100	$2.75 \cdot 10^{-3}$	0.9998	3.04
5.	93	23.2	0.0216	0.8191	97.1	$1.63 \cdot 10^{-3}$	0.9990	4.89
6.	97	28.8	0.0411	0.8474	100	$2.18 \cdot 10^{-3}$	0.9997	3.98
7.	91	26.3	0.0312	0.8713	95.2	$1.65 \cdot 10^{-3}$	0.9988	4.89

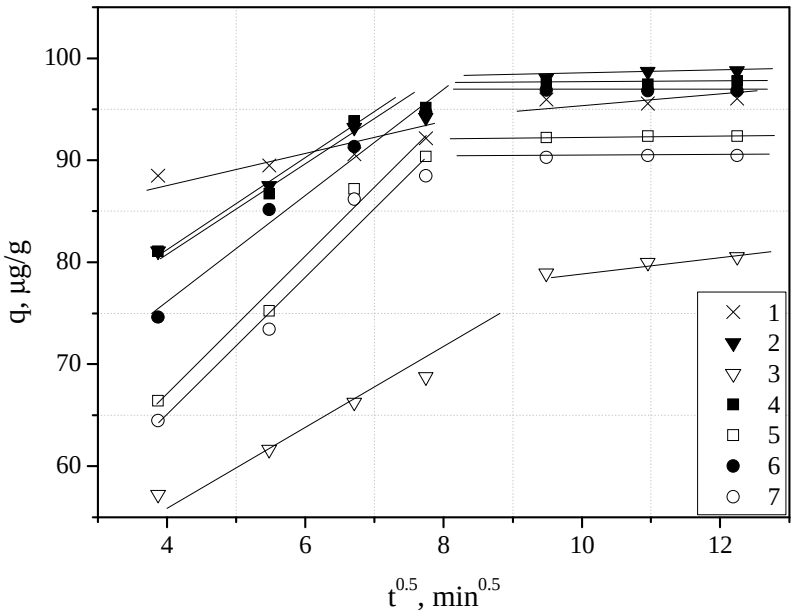

Figure 8. The Weber-Morris plot for intra-particle diffusion of the arsenic sorption kinetic data onto IS and Fe_2O_3 samples.

2.3. Effect of Arsenic Initial Concentration and Adsorption Equilibrium Studies

The adsorption isotherms of As(III) removal by the studied materials are presented in figure 9.

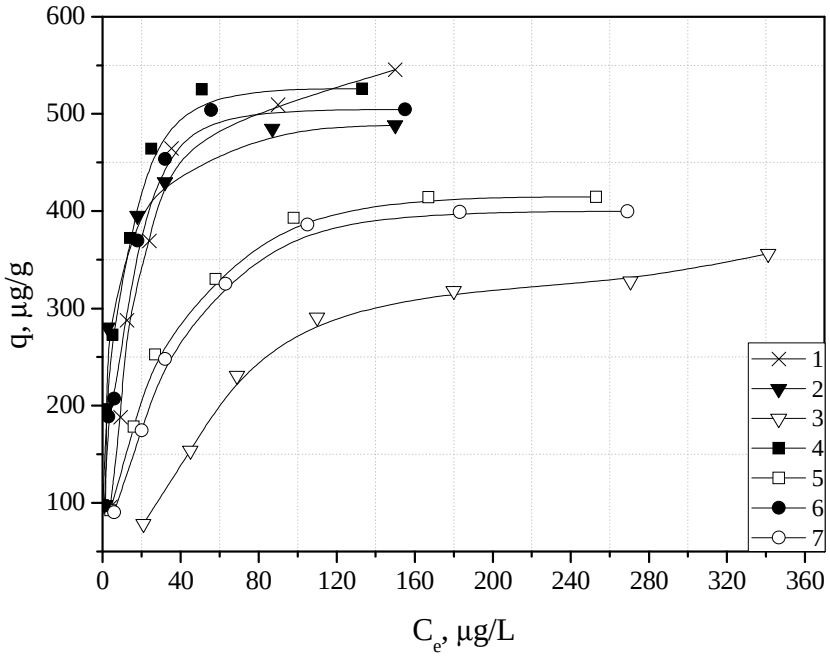

Figure 9. Adsorption isotherms of As(III) onto the studied materials. t=90 min; T=20-25°C; pH=6.5 – 7; sorbent dose, 1 g/L; stirring rate, 200 rpm.

The adsorption capacity increased with the increasing equilibrium concentration of arsenic for all the studied materials. At high equilibrium concentrations, the adsorption capacity approached a limit value. This value represents the experimentally-determined maximum adsorption capacity of As(III) ions onto the studied materials.

Several models are mentioned in the literature to describe experimental data of adsorption isotherms. The Langmuir and Freundlich models are the most frequently employed models. In this chapter, both models were used to describe the relationship between the amount of As(III) adsorbed by studied materials and its equilibrium concentration in solution for 90 minutes [13, 14, 21, 45, 46].

The linear form of the Freundlich isotherm equation can be written as:

$$\ln q_e = \ln K_F + \frac{1}{n}\ln C_e \quad (5)$$

and the Langmuir isotherm as the following equation:

$$\frac{C_e}{q_e} = \frac{1}{K_L q_m} + \frac{C_e}{q_m} \quad (6)$$

where: q_e is the amount of arsenic adsorbed per gram of sorbent, µg/g; C_e is the equilibrium concentration of arsenic, µg/L; K_f and 1/n are specific constants concerning the relative adsorption capacity of the adsorbent and the intensity of adsorption, respectively; q_m is a measure of monolayer adsorption capacity, µg/g and K_L is a constant related to the free energy of adsorption.

The curves and parameters, as well as the correlation coefficients (R^2), for As(III) removal trough adsorption onto the studied adsorbent are presented in figures 10, 11 and table 4.

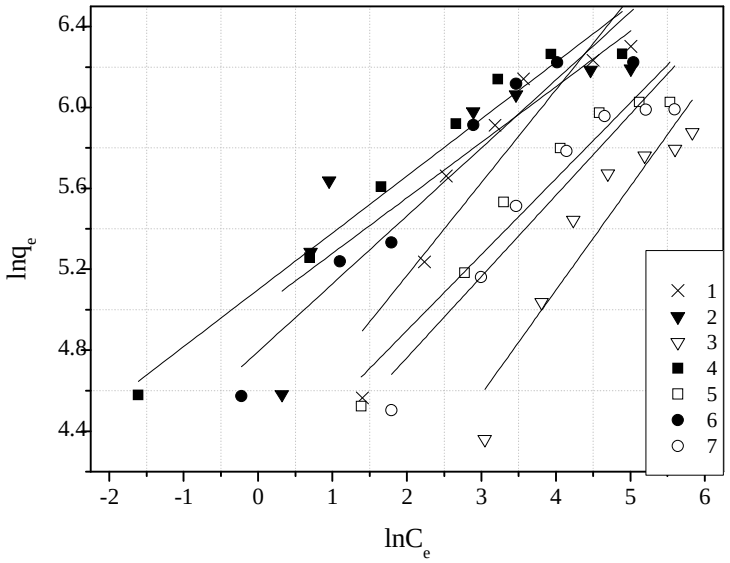

Figure 10. Freundlich plot of As(III) adsorption onto the studied materials.

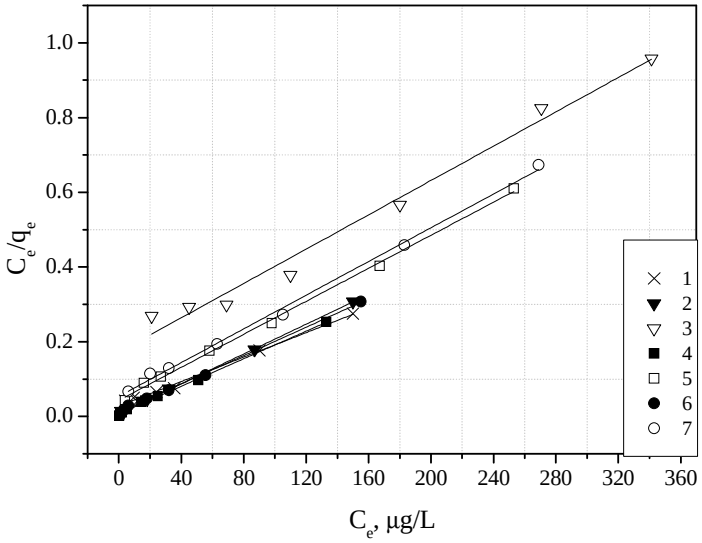

Figure 11. Langmuir plot of As(III) adsorption onto the studied materials.

Table 4. Parameters of Freundlich and Langmuir isotherms for the As(III) adsorption onto the studied materials

Sample no.	q_m(exp), µg/g	Freundlich isotherm			Langmuir isotherm		
		K_F, µg/g	1/n	R^2	q_m(calc), µg/g	K_L, L/µg	R^2
1.	550	70.32	0.4584	0.8550	625	0.0569	0.9952
2.	490	149	0.2744	0.7689	500	0.2470	0.9994
3.	341	20.9	0.5132	0.8865	434.8	0.0133	0.9849
4.	526	164	0.2812	0.9662	555	0.2611	0.9983
5.	415	63.3	0.3751	0.9413	454	0.0511	0.9980
6.	505	121	0.3356	0.9350	526	0.1744	0.9982
7.	400	52.6	0.4007	0.9193	434	0.0427	0.9971

The Freundlich plots (figure 10) have very low regression coefficients suggesting a restricted use of Freundlich isotherm. The constants K_F and 1/n computed from the linear plot are presented in table 4. The constant K_F can be defined as an adsorption coefficient, which represents the quantity of adsorbed metal ions for a unit equilibrium concentration. The slope 1/n is a measure of the adsorption intensity or surface heterogeneity. For 1/n = 1, the partition between the two phases does not depend on the concentration. The situation 1/n < 1 is the most common and correspond to a normal L-type Langmuir isotherm, whilst 1/n > 1 indicates a cooperative adsorption, which involves

strong interactions between the molecules of adsorbate. Values of 1/n < 1 show favorable adsorption of As(III) ions related to all the studied materials. The Langmuir model effectively describes the sorption data for all the studied materials with correlation coefficient closer to 1. Thus, the isotherm follows the sorption process in the entire concentration range studied for all four materials. Moreover the maximum adsorption capacities of the studied materials obtained from the Langmuir plot are very close to those obtained experimentally. The maximum adsorption capacities of As(III) developed by Fe_2O_3 obtained by annealing of the iron salts are higher than the adsorption capacities of As(III) developed by the mixtures Fe_2O_3:SiO_2. This is in contradiction with the conclusion resulted from the BET surface area. If one refers the adsorbent properties only to the Fe_2O_3 content (the active phase responsible for arsenic removal) of the samples 3, 5 and 7, it may be said that the presence of SiO_2 improves the adsorption capacity of the powders. A possible explanation for this situation refers to the hydroxylate character of the Ultrasil particles (even after annealing at 550°C or 800°C), which leads to their hydration and dispersion of the Fe_2O_3 agglomerations in the presence of the aqueous solutions with As(III) content [47]. This behavior is very favorable for the perspective of the waste immobilization in vitreous matrices.

The dimensionless constant, called separation factor (R_L) can be used to describe the essential characteristics of a Langmuir isotherm.

$$R_L = \frac{1}{1 + K_L \cdot C_0} \tag{7}$$

where the terms have their meanings as stated above. In fact, the separation factor is a measure of the adsorbent capacity used. Its value decreases with increasing "K_L" as well as initial concentration. R_L values can be related to the equilibrium isotherm as follows: unfavorable, $R_L > 1$; linear, $R_L = 1$; favorable $0 < R_L < 1$; and irreversible, $R_L = 0$ [13, 14, 16]. The values were calculated for the entire concentration range studied and the results are found to lie in between 0 and 1, in all the cases, demonstrating a favorable sorption process.

Since the IS develop the highest adsorption capacity (amongst the samples tested) in the removal process of As(III) from aqueous solution, its use represent an appropriate environmental and economical solution.

2.4. Effect of Temperature and Thermodynamic Studies

In general, the experimental conditions such as metal ion concentration and temperature have strong effects on the equilibrium distribution coefficient value (K_d), so they can be used to compare the efficiency of various adsorbents. Equilibrium distribution coefficient value (K_d) represents the amount of removed As(III) ions per gram of adsorbent, divided by their concentration in the liquid phase:

$$K_d = \frac{q_e}{C_e} \tag{8}$$

Temperature dependence of the adsorption process is associated with several thermodynamic parameters. Thermodynamic considerations of an adsorption process are necessary to conclude whether the process is spontaneous or not. Thermodynamic parameters such as Gibbs free energy change (ΔG°), enthalpy change (ΔH°) and entropy change (ΔS°) can be estimated using equilibrium constant changing with temperature. The Gibbs free energy change of the adsorption reaction is given by the following equation [1, 13, 21, 45]:

$$\Delta G^\circ = -RT \ln K_d \tag{9}$$

where R represents the universal gas constant (8.314 J/(mol·K)), T represents the absolute temperature (K) and K_d represents the distribution coefficient.

Relation between ΔG°, ΔH° and ΔS° can be expressed by the following equations:

$$\Delta G^o = \Delta H^o - T\Delta S^o \tag{10}$$

$$\ln K_d = \frac{\Delta S^\circ}{R} - \frac{\Delta H^\circ}{RT} \tag{11}$$

The thermodynamic parameters were determined from the slope and intercept of the plot of $\ln K_d$ versus 1/T (figure omitted). The values of ΔG°, ΔH° and ΔS° for all the studied temperature are given in table 5.

In case of the obtained Fe_2O_3 and Fe_2O_3:SiO_2 mixtures the negative values of ΔG° and positive values of ΔH° indicate that the adsorption of As(III) onto the studied materials is a spontaneous and endothermic process. The more negative value of ΔG° imply a greater driving force to the adsorption process. The values of ΔH° are high enough to ensure the strong interaction between the As(III) and the studied materials. The positive values of ΔS° indicate an increased randomness at the solid-solution interface during the adsorption of As(III) onto the studied materials [1, 13, 21, 38, 45]. The increasing of the adsorption capacities of the studied materials at higher temperatures may be due to the enlargement of pore size and/or activation of the adsorbent surface.

Table 5. Thermodynamic parameters for As(III) adsorption onto the studied materials

Sample no.	Temperature, K	ΔG°, kJ/mol	ΔH°, kJ/mol	ΔS°, kJ/mol·K	R^2
1.	293	-7.68	-161.8	-0.526	0.9802
	298	-5.05			
	303	-2.42			
2.	291	-8.79	131.7	0.483	0.9915
	295	-10.7			
	313	-19.4			
3.	293	-3.16	36.15	0.134	0.9817
	298	-3.83			
	303	-4.50			
4.	298	-15.1	55.8	0.239	0.9963
	303	-16.6			
	308	-20.2			
5.	298	-8.75	58.3	0.225	0.9964
	303	-9.88			
	308	-13.3			
6.	298	-11.9	81.1	0.312	0.9959
	303	-13.4			
	308	-18.1			
7.	298	-7.51	64.9	0.243	0.9964
	303	-8.73			
	308	-12.4			

In case of the IS, the overall free energy change during the adsorption process was also negative for the range of temperatures studied, corresponding to a spontaneous physical process for As(III) ion adsorption. As decreasing the

temperature from 303 K to 293 K, the standard free energy change became even more negative, suggesting that the adsorption process was favored at lower temperatures. *This represents an economic advantage, since no heat input would be necessary during the adsorption process.* The negative value of ΔH^0 shows that the adsorption process was exothermal. The negative value of ΔS^0 indicates that the adsorbed species suffers a decrease in its freedom degrees.

3. EFFECTS OF COMPETING ANIONS ONTO AS(III) ADSORPTION PROCESS

The existence of multi-component in the solution, as usually found in real-world systems, is of particular importance in practical applications, where competition between different components for the available adsorption sites occurs [3, 48, 49]. Anions directly compete for available surface binding sites and indirectly influence adsorption by alteration of the electrostatic charge at the solid surface. Both direct and indirect effects are caused by solution pH, the relative anions concentrations and intrinsic binding affinities [50, 51].

The present chapter deals with the effect of the presence of some anionic species (nitrate NO_3^-, phosphate PO_4^{3-}, sulphate SO_4^{2-}, chloride Cl^- and carbonate CO_3^{2-}) in the arsenic containing water on the adsorption of As(III) onto the first two studied materials. These two materials were chosen in order to compare the effects of the anions on the arsenic adsorption when a waste material and a synthetic material are used as adsorbents.

For the studies 100 µg/L As(III) synthetic solutions with/without anionic species (NO_3^-, PO_4^{3-}, SO_4^{2-}, Cl^- and CO_3^{2-}) have been used. It has been separately studied the influence of each anionic species and the influence of all mixed anionic species at two concentrations: 10 mg/L and 100 mg/L, respectively. All reagents used to prepare the solutions were in analytical reagent grade. The adsorbents were kept in contact with the arsenic solution in the solid:liquid ratio of 1g/L at laboratory temperature (23°C) for different contact periods (1, 2, 3, 4, 8 and 24 h). After the contact time elapsed the suspensions were filtered and the residual concentration of arsenic in the filtrate was determined. During the adsorption experiments the pH of the suspensions was maintained at a constant value (range between: 6.5-7), due to the natural buffer capacity of the sorbent materials [52].

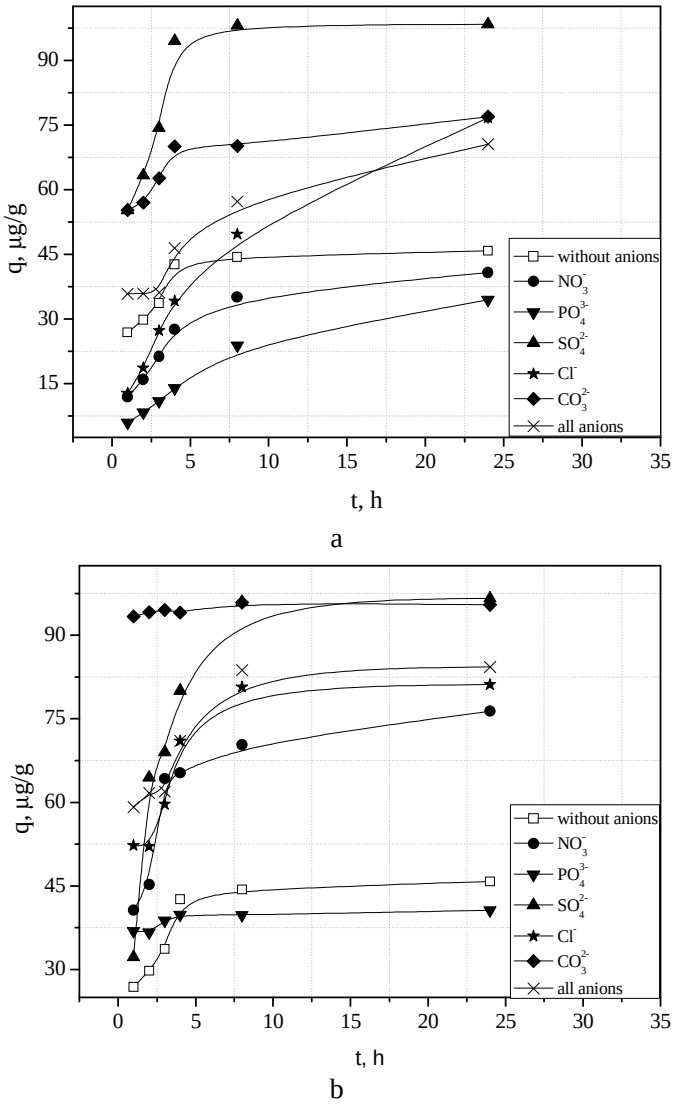

Figure 12. Influence of contact time on the IS adsorption capacity. anionic species concentrations: (a) 10mg/L; (b) 100mg/L.

Experimental data regarding the dependence of the adsorption capacities of the studied materials versus time for two anion concentration are presented in figure 12 for IS and in figure 13 for Fe_2O_3 obtained by annealing the iron oxalate. One may notice that in all situations the adsorption capacity of the

studied materials increase as contact time increases. In most cases the increase rate is lower after 6 h of contact time and one may consider that the equilibrium was reached. The figures also show that the adsorption capacities of the studied materials in the removal process of As(III) from water is influenced by the solutions composition.

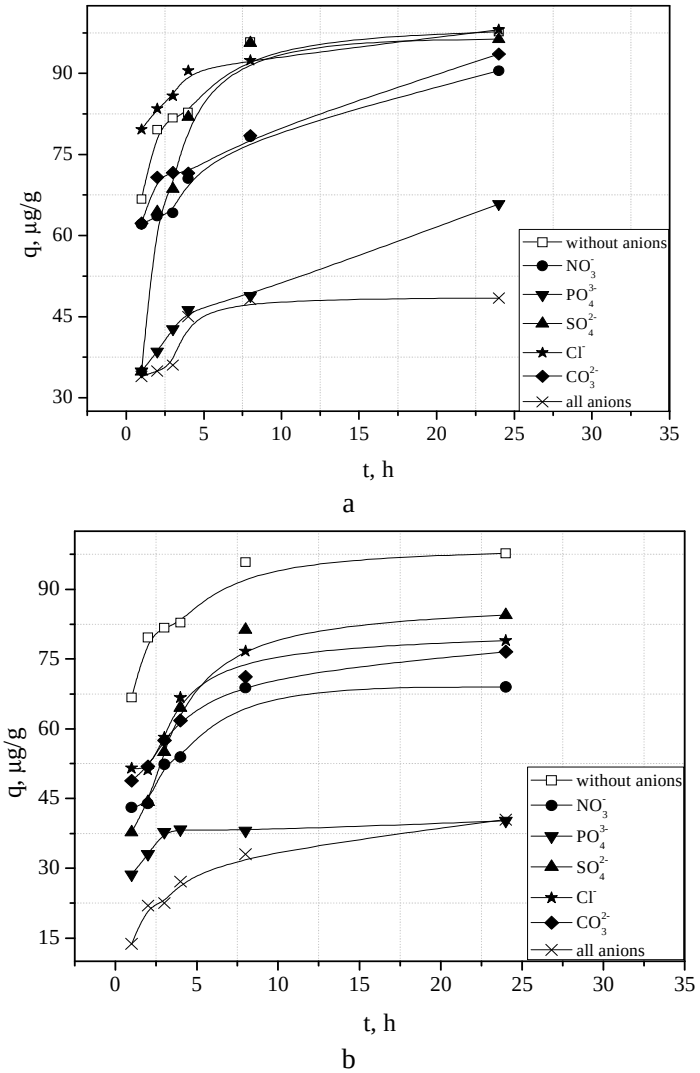

Figure 13. Influence of contact time on the Fe_2O_3 adsorption capacity. anionic species concentrations: (a) 10mg/L; (b) 100mg/L.

Figure 12 shows the adsorption of As(III) onto the IS is mainly influenced by the solution composition, according to the following sequence: PO_4^{3-}>NO_3^- >Cl^->CO_3^{2-}>SO_4^{2-}, regardless the concentration of anionic species (10 mg/L and 100 mg/L).

One may notice that the presence of phosphate anions has a negative influence on the As(III) adsorption in the case of IS, leading to a reduced adsorption capacity. This observation is consistent with literature data, which indicate that arsenic adsorption is seriously reduced by the presence of phosphate, because of the competition for the binding sites of the sorbent material, which appears between arsenic and phosphate [49, 53]. The individual presence of SO_4^{2-} and CO_3^{2-} has a positive effect on As(III) adsorption, leading to adsorption capacities higher than those obtained in their absence. Other researchers also concluded that the sulphate and carbonate do not affect the As(III) adsorption [49]. The NO_3^-, Cl^- were found to have a negligible effect or even positive effect (when they are in a higher concentration) on the removal of As(III) through adsorption onto IS. The adsorption capacities of the IS is higher in the individual presence of these anions when their concentration is higher (100 mg/L). The simultaneous presence of all anions develops an overall positive effect on arsenic adsorption, but the adsorption capacities were somehow lower that in the presence of SO_4^{2-} and CO_3^{2-} alone, due to the negative influence of PO_4^{3-}.

From figure 13 one may notice that when anions are individually present in the sample matrix at concentrations of 10 mg/L, it's only Cl^- and SO_4^{2-} that have no obvious influence on As(III) adsorption on Fe_2O_3. All other anions have negative influence according to the following sequence: PO_4^{3-}>NO_3^- >CO_3^{2-}>SO_4^{2-}>Cl^-. The negative competitive effect of all the studied anions is more visible at higher concentration (100 mg/L). When all anions are present together in solutions, their negative effect on arsenic adsorption remains and adsorption capacities are slightly reduced than compared with the individual anions presence.

If we compare the efficiency of the two studied materials we can notice that in the absence of the studied anions Fe_2O_3 develop a higher adsorption capacity than IS. The same observation is true for the individual presence of the studied anions in the samples, in a concentration of 10 mg/L. But when the anions are individually present in the solutions in concentrations 10 times higher (100mg/L) the adsorption capacity developed by the Fe_2O_3 is lower than in the case of IS. At the same time, if the As(III) solution contains simultaneously all anions, regardless their concentration, the IS is a more efficient adsorbent for As(III) than Fe_2O_3.

For this reasons we recommend the IS to be used as adsorbent material in the removal process of arsenic from water, since there is highly unlikely to find the studied anions individually in natural underground water. Using the sludge is also advantageous from the economic and environmental protection point of view, since this utilization turns into account a waste resulting from another technological process.

4. ARSENIC ADSORPTION FROM NATURAL UNDERGROUND WATERS

To evaluate the potential use of the studied material as adsorbents for As(III) removal from natural underground waters, we treated 5 sample collected from wells with a known high As(III) concentrations situated in the western area of Romania. The samples of water (100 mL) were treated with the necessary amount of adsorbent (0.1 g) under the optimal conditions established employing synthetic As(III) ion solutions (T=20-25°C, t=90 min, stirring rate=200 rpm, pH=6.5-7). The initial and residual concentrations of As(III) ions, as well as other metal ions, were determined by atomic absorption spectrometric methods. The concentration of chloride has been determined by $AgNO_3$ titration, using K_2CrO_4 as indicator. Nitrite, nitrate, ammonoum, and phosphate concentrations have been determined by UV-VIS spectrophotometric method using a carry 50 spectrophotometer. The sulphate anion has been determined by direct titration with barium chloride in etilic alchool medium and in presence of barium sulphate using thorin as indicator.

The compositions of natural underground water samples are presented in table 6. After treatment of the underground water samples with the studied materials the water quality parameters were determined. It was observed that in all the underground water samples for all the studied adsorbents As(III) was practically totally removed from the waters together with iron and manganese ions (residual concentrations were under the detection limit).

In all the cases the pH of the treated waters remained rather unchanged, suggesting that no post treatment is necessary. Treatment with IS did not lead to any increase in the concentration of other metallic ions as a result of possible leaching. All these facts lead to the conclusion that the studied materials could be used as potential adsorbents for As(III) removal from natural underground water.

Table 6. The initial compositions of the underground water samples

Parameter	Sample 1	Sample 2	Sample 3	Sample 4	Sample 5
pH	6.7	6.8	6.64	6.74	7
Turbidity (NTU)	9	8.7	8.5	8.7	9
Conductivity (μS)	398	385	378	395	383
P_2O_5 (ppm)	31.6	46.7	32.5	41.2	36.2
NO_2^- (ppm)	0.5	0.3	0.6	0.7	0.4
NO_3^- (ppm)	BDL*	22	BDL*	BDL*	20.2
NH_4^+ (ppm)	1.2	6.6	0.5	0.46	1.1
Cl^- (ppm)	13.8	31.1	10.4	20.7	17.3
SO_4^{2-} (ppm)	48.1	11.1	10.5	12.4	22.8
Ca (ppm)	65	30.8	35	27.4	7.5
Mg (ppm)	47	18.2	11.6	7.39	23.5
Na (ppm)	105	118	98.1	103	81
K (ppm)	1.65	1.67	0.89	1.44	3.78
Fe (ppm)	5	2	1.28	0.75	2
Mn (ppm)	0.5	0.51	0.17	0.2	0.35
As III (ppb)	60.4	80	45.4	62.9	73.5

*BDL= below detection limit.

5. COLUMN STUDIES REGARDING AS(III) ADSORPTION

Batch operation is very easy to be used in the laboratory studies, but less convenient for field applications. Moreover, accurate scale-up data for fixed bed systems cannot be obtained from the adsorption isotherms of batch results, so practical applicability of the adsorbent should be ascertained in column operations. Adsorption on fixed bed columns presents numerous advantages. It is simple to operate, gives high yields and can be easily scaled up from laboratory process [23].

Generally, an arsenic adsorbent should meet several requirements: (1) low cost; (2) granular type; high capacity, selectivity, and rate of adsorption; (3) high physical strength (not disintegrating) in water and (4) able to be regenerated if required [20]. In order to accomplish the first requirement we used the IS in the column test as adsorbent for arsenic removal from water. Since the adsorbent is a powder, in order to avoid the clogging of the column we mixed the adsorbent with quartz sand. From previous studies we concluded the best IS:sand ratio is 1:1, when the highest adsorption capacity was reached [54]. Due to very small size of particles, IS penetrated between the grains of sand, and thus a high contact surface was created, the adsorption process

occurred in good conditions. For a larger amount of IS the column was clogged after a short time. For a larger amount of sand, the mixture contains a too small amount of IS active phase responsible for arsenic adsorption, and consequently the adsorption capacity lowers.

Fixed bed adsorption studies were conducted in a 1.5 cm i.d., 20 cm length vertical down flow glass column packed with IS:sand adsorbent for different bed height (5, 7.5 and 10 cm). the experiments were conducted with a 100 μg/L As(III) solution. The column was charged with arsenic solution in the down-flow mode with an influent flow rate, which was supplied and maintained throughout the experiments by the use of variable flow peristaltic pump (Heidolph 6201). The samples were collected at certain time intervals and were analysed for the remaining arsenic concentrations. The shape of the breakthrough curve and the time for the breakthrough appearance are the predominant factors for determining the operation and the dynamic response of an adsorption column. Effects of adsorbent bed height (5-10 cm) and inlet feed flow rate 0.033-0.16 cm^3/s) were investigated on the performance of breakthrough for the adsorption of As(III) by the IS:sand mixture.

Empty bed contact time is a critical parameter that determines the residence time during which the solution being treated is in contact with the adsorbent. Hence, EBCT may strongly affect adsorption, especially if the adsorption mainly depends on the contact time between the adsorbent and adsorbate [55]. The corresponding EBCT in the bed was in the range 55-535 s.

5.1. Effect of Bed Depth

The breakthrough curves obtained for As(III) adsorption onto IS:sand at different bed depth, at a constant linear flow rate of 10 cm^3/min are shown in figure 14.

Sorbent bed height strongly affects the volume of the solution treated or throughput volume. The curves followed characteristic S-shape profile, which is associated with adsorbate of smaller molecular diameter and more simple structure. As it is evident from figure 14, an increase in column depth increased the treated volume due to high contact time. The exhaust time (corresponding to an effluent concentration=$0.9C_0$) increased with increasing bed height, as more binding sites were available for sorption. The increase in adsorption with bed depth was due to the increase in adsorbent doses in larger beds which provided greater adsorption sites for As(III). The breakthrough time also increased with increasing bed depth, suggesting that it is the

determing parameter of the process (table 7). The larger the breakthrough time, better is the intra-particulate phenomena.

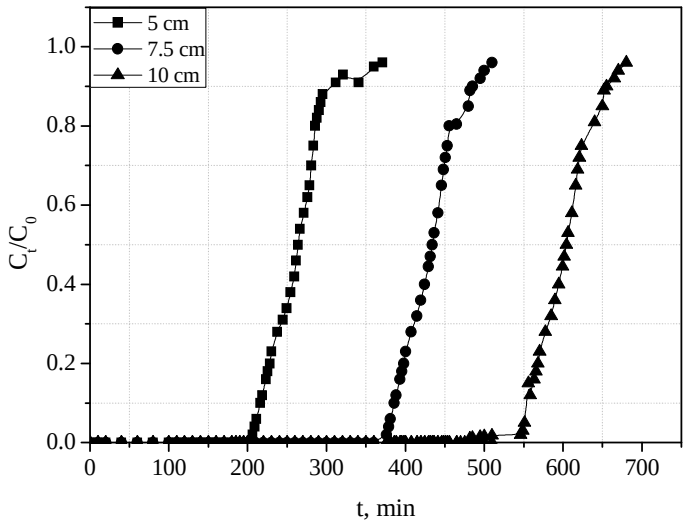

Figure 14. Effect of bed height on breakthrough curves for As(III) adsorption onto IS:sand. C_0=100μg/L, flow rate=10 mL/min, pH=6.8.

5.2. Effect of Flow Rate

The effect of flow rate on As(III) adsorption by IS:sand was investigated by varying the flow rate from 2 to 10 mL/min and keeping the initial As(III) concentration (100 μg/L), bed depth (10 cm) and column diameter (1.5 cm) constant. Breakthrough plots between C_t/C_0 versus time at different flow rate are given in figure 15.

At low flow rate, relatively high volume was observed whilst much sharper breakthrough was obtained at higher flow rates. The time required to reach the breakthrough decreased with an increased flow rate (table 7). This is certainly because of the reduced contact time causes a poor distribution of the liquid inside the column, which leads to a lower diffusivity of the solute through the adsorbent particles [23]. As seen from the results presented in table 7, an increased flow rate reduces the volume treated efficiently until breakthrough and thereby decreases the service time of the bed. This is due to the decrease in the residence time of the As(III) ions within the bed at higher flow rates.

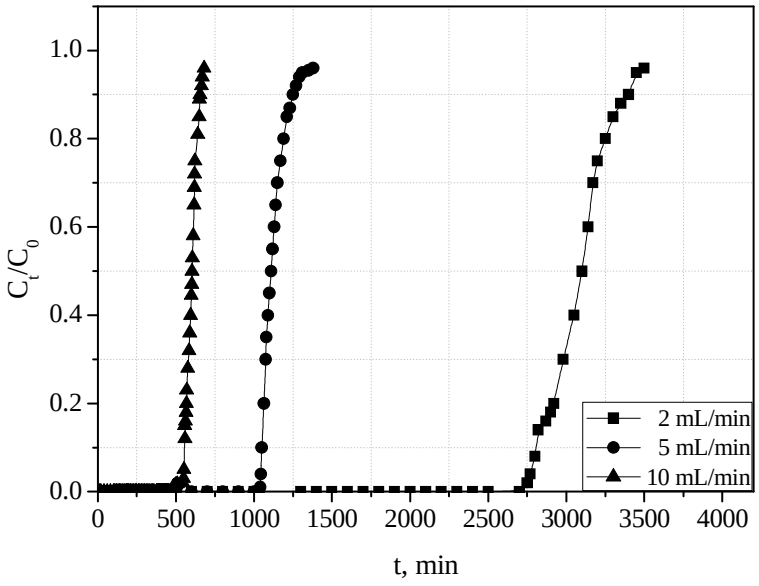

Figure 15. Effect of flow rate on breakthrough curves for As(III) adsorption onto IS:sand. C_0=100µg/L, h=10 cm, pH=6.8.

Table 7. Adsorption data for fixed bed IS:sand column for As(III) adsorption at different process parameters

Process parameters	Breakthrough time, min	Exhaust time, min	Volume of arsenic solution treated, L
Bed depth, h (cm)			
5	200	371	2/3.71
7.5	376	510	3.76/5.1
10	482	680	4.82/6.8
Flow rate, Q(mL/min)			
2	2750	3500	5.5/7
5	1040	1380	5.2/6.9
10	482	680	4.82/6.8

One may notice that the best performance of the IS:sand mixture in the removal process of As(III) on column studies occurs under the process parameters of 10 cm bed depth and 2 mL/min flow rate.

5.3. Modelling of Breakthrough Curve

The fixed bed column was designed by logit method [2]. The logit equation can be written as:

$$\ln\left[\frac{C}{C_0 - C}\right] = -\frac{KNX}{V} + KC_0 t \qquad (15)$$

where C is the solute concentration at any time t, C_0 the initial solute concentration (100 µg/L), V the approach velocity (~ 0.033 mL/h), X the bed depth (10 cm), K the adsorption rate constant (L/(mg·h)), and N is the adsorption capacity coefficient (mg/L). Plot of ln[C·(C_0 – C)] versus t was shown in figure 16. The value of adsorption rate coefficient (K) and adsorption capacity coefficient (N) was obtained as 0.084,L/(mg·h) and 1.03, mg/L. These values could be used for the design of adsorption column.

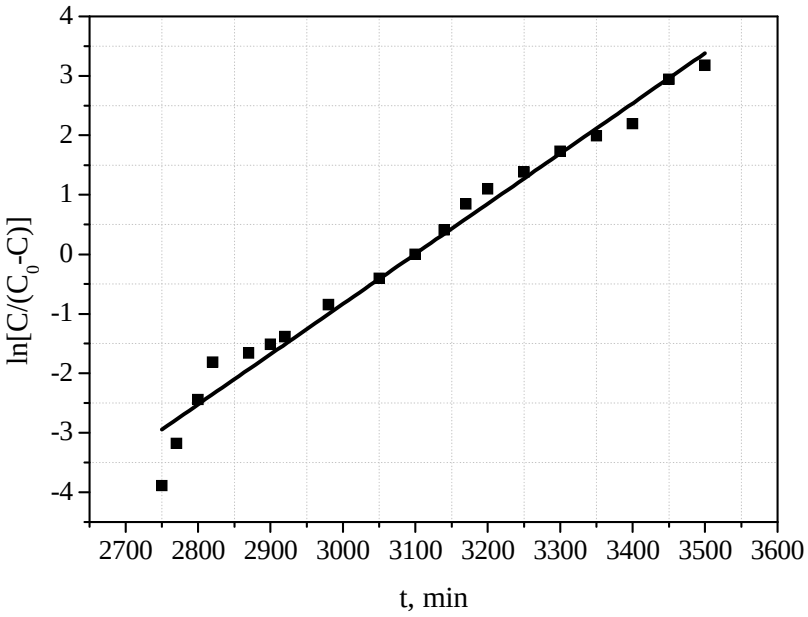

Figure 16. Linearized form of logit model.

6. IMMOBILISATION OF THE EXHAUSTED IS ADSORBENT IN VITREOUS MATRICES

In order to test the possibility of the exhausted IS adsorbent immobilization in vitreous matrices, this has been introduced in the composition of some frits, for further storage in appropriate conditions or reuse in decorative glass applications. 20g of arsenic containing IS were used for 100g frit. The oxide compounds were homogenized and fired at 1250°C, for 30 minutes. The molten glass obtained was poured in cold water, than grinded and classified in different grain size classes. The oxide composition of the obtained frit is presented in table 8:

Table 8. The oxide composition of the obtained frit

Component	Content, % wt.
SiO_2	39,5
B_2O_3	23,6
Na_2O	10,5
PbO	6,7
CaO	3,83
ZnO	0,38
Fe_2O_3	15,3
Al_2O_3	0,14
As_2O_3	0,03

The frit was tested for leaching, as follows: 5g of frit, grain size between 1 and 3 mm were treated with different acids at pH 4÷5 simultaing the effect of acid rains, for 60 days. The pH of the solutions was monitored, and the results are presented in table 9.

One may notice that the pH of the solutions raises up to 7 in the first week and remains constant until week 4. At the end of the test period the pH of the solutions is between 8 and 9, which may be assigned to the sodium leaching from the frits enhanced by the increased contact with the solutions, due to previous grinding. This assumption was confirmed by the chemical analysis of the solution performed by atomic absorption spectrometry (VARIAN Spectr AA 280FS) aimed to establish the metal content. The results are presented in table 10.

Table 9. pH variation of the solutions

Sample	Initial pH	pH variation							
		Week 1	Week 2	Week 3	Week 4	Week 5	Week 6	Week 7	Week 8
Frit + H_2O	5.21	7.10	7.01	7.06	7.13	8.12	8.40	8.47	8.55
Frit + HNO_3	4.64	7.04	7.01	7.06	7.15	8.21	8.34	8.43	8.53
Frit + HCl	4.30	7.03	6.95	7.09	7.19	8.13	8.35	8.57	8.56
Frit + H_2SO_4	4.00	7.09	6.99	7.12	7.23	8.24	8.36	8.46	8.56
Frit + CH_3COOH	4.19	7.10	7.04	7.21	7.56	8.22	8.41	8.43	8.54
Frit + carbonated water	5.47	7.09	6.97	7.12	7.47	8.56	8.99	8.96	9.02

Table 10. The metal content in the leaching solutions

Sample	Metal content, mg/L				
	Ca^{2+}	Na^{+}	Pb^{2+}	Fe^{n+}	As^{3+}
Frit + H_2O	0.45	63.2	BDL*	BDL	BDL
Frit + HNO_3	0.52	68.2	BDL	BDL	BDL
Frit + HCl	0.63	65.1	BDL	BDL	BDL
Frit + H_2SO_4	0.45	64.2	BDL	BDL	BDL
Frit + CH_3COOH	0.53	68.4	BDL	BDL	BDL
Frit + carbonated water	0.25	88.6	BDL	BDL	BDL

*BDL = below detection limit.

No dangerous species were noticed in the leaching solutions, so one may conclude the exhausted adsorbent IS containig arsenic was succesfully immobilized in the glassy matrix of the frit and it doesn't represent an environmental threat anylonger. Yet, further tests were performed to explore the possibility of actually reclaiming the materials envolved in arsenic adsorption and than immobilized in glass, meaning to find some applications for the resulted frits. For this purpose, another waste was used. CRT waste glass from old TV/ computer screens is available in large amounts and raises disposal issues. Since the CRT glass has high melting temperature (around 1350°C), the need of a fluxing agent occurred. Sodium silicate ($Na_2O \cdot 1.5SiO_2$) has been used as fluxing agent. The CRT glass oxide composition is presented in table 11.

Table 11. CRT glass oxide composition

Oxide	Composition, % wt.
SiO_2	62
Na_2O	6.3
K_2O	9
SrO	10
BaO	7
PbO	1
Al_2O_3	2
Al_2O_3 +Sb_2O_3	0.5
TiO_2+ZrO_2	2
CeO_2	0.2

The raw materials mixture ratio for obtaining the frit was IS exhausted adsorbent: CRT glass: fluxing agent ($Na_2O \cdot 1.5SiO_2$) = 1:1:1. After melting at 1200°C for one hour, the glass melt was poured in cold water and the frit obtained consisted of smooth glass wires or grains, with no incomplete molten solid inclusions or air bubbles, which all indicate a proper melting. An image of the as-obtained frit is presented in figure 14.

Figure 14. Image of the obtained frit.

In order to assess the arsenic and other dangerous elements leaching, the frit was treated with 4% wt. acetic acid solution, according to STAS 708/2-83 [56] for 24h at room temperature. The result of the chemical analysis performed by atomic absorption spectrometry with hydride generation,

including the Na^+ content (a good indicator of glass solubility) is presented in table 12:

Table 12. Chemical analysis result of the leaching solution

Leached elements (mg/g frit)			
As	Pb	Fe	Na
BDL *	BDL *	0,35	0,23

*BDL = below detection limit.

The result shows a slight solubility of the frit, but no possible dangerous elements (As or Pb) were noticed in the solution, so the arsenic containing IS immobilization was considered successful. At the same time, using CRT waste glass for this purpose proved to be a viable solution. The frit was further processed in order to obtain a ceramic decorative glaze, since the overall iron content of the frit makes it suitable for obtaining aventurine glazes (generally 10-30% Fe_2O_3 in glaze). After grinding, it was mixed with 5% wt. kaolin and subjected to wet homogenization in a Fritsch Pulverisette ball mill. The slip obtained was applied on a tableware faience ceramic support and after drying, it was fired at 1150°C for 1 hour, followed by a 30 minutes thermal treatment at 780°C, designed to develop the hematite crystals, which impart a certain decorative effect due to their flaky golden appearance. The samples were investigated by optical microscopy in reflected light using a Guangzhou L2020A China microscope with digital camera and by X-Ray diffraction, using a DRON 3 instrument, Cu $_{K\alpha}$ radiation.

Figure 15 presents the glazed samples, as well as optical microscopy images of the hematite crystals developed in the samples, with different magnifications.

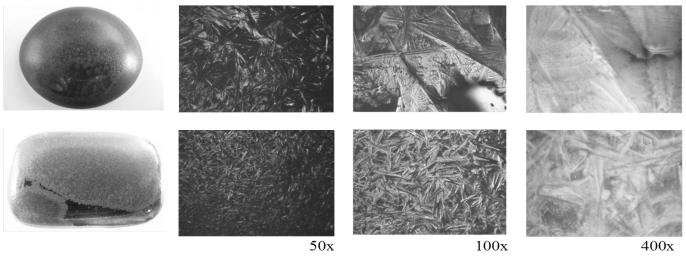

Figure 15. Images of the glazed samples showing the decorative effect and the hematite crystals.

Figure 16 presents the X-ray diffraction spectrum of the glaze showing hematite as the single crystalline phase.

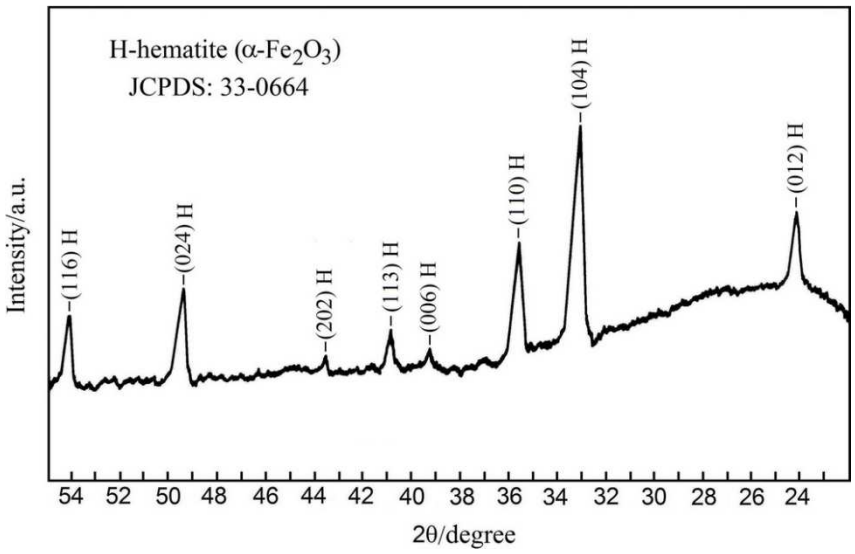

Figure 16. The X-ray diffraction spectrum of the glaze.

Considering the positive results obtained we consider that using the iron containing waste sludge in arsenic adsorption followed by the immobilization of the exhausted adsorbent in vitreous matrices represents a viable solution framed in the direction of closed cycle technologies.

ACKNOWLEDGMENTS

This work was supported by CNCSIS- UEFISCDI, project number PN II-IDEI 927/2008, “Integrated Concept about Depollution of Waters with Arsenic Content, through Adsorption on Oxide Materials, followed by Immobilization of the Resulted Waste in Crystalline Matrices”. This work was partially supported by the strategic grant POSDRU/89/1.5/S/57649, Project ID 57649 (PERFORM-ERA), co-financed by the European Social Fund – Investing in People, within the Sectoral Operational Programme Human Resources Development 2007-2013.

REFERENCES

[1] K. Banerjee, G.L. Amy, M. Prevost, S. Nour, M. Jekel, P.M. Gallagher and C.D. Blumenshein, *Wat. Res.* 42, 3371 (2008).

[2] S.K. Maji, A. Pal and T. Pal, *J. Hazard. Mater.* 151, 811 (2008).

[3] H. Guo, D. Stuben and Z. Berner, *Sci. Total Environ.* 377, 142 (2007).

[4] WHO, Guidelines for drinking-water quality, third ed. Vol. 1: Recommendations, *World Health Organization* (2004).

[5] T. S. Singh and K.K. Pant, *Sep. Purif. Technol.* 48, 288 (2006).

[6] V.T. Nguyen, S. Vigneswaran, H.H. Ngo, H.K. Shon and J. Kandasamy, *Desalination* 236, 363 (2009).

[7] J.R. Parga, D.L. Cocke, J.L. Valenzuela, J.A. Gomes, M. Kesmez, G. Irwin, H. Moreno and M.Weir, *J. Hazard. Mater.* B124, 247 (2005).

[8] R.Y. Ning, *Desalination* 143, 237 (2002).

[9] J.Kim and M.M. Benjamin, *Wat. Res.* 38, 2053 (2004).

[10] T. Tuuutijarvi, J. Lu, M. Sillanpaa and G. Chen, *J. Env. Eng.* 136, (2010).

[11] C.Y. Chen, T.H. Chang, J.T. Kuo, Y.F. Chen and Y.C. Chung, *Bioresource Technol.* 99, 7487 (2008).

[12] S. Kundu and A.K. Gupta, *J. Hazard. Mater.* 142, 97 (2007).

[13] D. Borah, S. Satokawa, S. Kato and T. Kojima, *J. Hazard. Mater.* 162, 1269 (2009).

[14] D. Borah, S. Satokawa, S. Kato and K. Kojima, *J. Colloid Interface Sci.* 319, 53 (2008).

[15] P. Mondal, C.B. Majumder and B.Mohanty, *J. Hazard. Mater.* 150, 695 (2008).

[16] H.U. So, D. Postma, R. Jakobsen and F. Larsen, *Geochim. Cosmochim. Ac.* 72, 5871 (2008).

[17] P. Chutia, S. Kato, T. Kojima, S. Satokawa, *J. Hazard. Mater.* 162, 204 (2009).

[18] H.L. Lien and R. T. Wilkin, *Chemosphere* 59, 377 (2005).

[19] Y. Jeong, M. Fan, S. Singh, C.L. Chuang, B. Saha and J. H. Leeuwen, *Chem. Eng. Process.* 46, 1030 (2007).

[20] L. Zeng, *Wat. Res.* 37, 4351 (2003).

[21] K. Gupta and U.C. Ghosh, *J. Hazard. Mater.* 161, 884 (2009).

[22] Z. Ren, G. Zhang and J.P. Chen, *J. Colloid Interf. Sci.* 358, 230 (2011).

[23] S. Kundu and A.K. Gupta, *Chem. Eng. J.* 129, 123 (2007).

[24] S. Kundu and A.K. Gupta, *Sep. Purif. Technol.* 51, 165 (2006).

[25] O.S. Thirunavukkarasu, T. Viraraghavan and K.S. Subramanian, *Water Air Soil Poll.* 142, 95 (2003).
[26] J.C. Hsu, C.J. Lin, C.H. Liao and S.T. Chen, *J. Hazard. Mater.* 153, 817 (2008).
[27] O.S. Thirunavukkarasu, T. Viraraghavan and K.S. Subramanian, *Water SA* 29, 161 (2003).
[28] B.J. Lafferty and R.H. Loeppert, *Environ. Sci. Technol.* 39, 2120 (2005).
[29] M. Vithanage, R. Chandrajith, A. Bandara and R. Weerasooriya, *J. Colloid Interf. Sci.* 294, 265 (2006).
[30] X. Guo and F. Chen, *Environ. Sci. Technol.* 39, 6808 (2005).
[31] B.R. White, B.T. Stackhouse and J.A. Holcombe, *J. Hazard. Mater.* 161, 848 (2009).
[32] T. Moller and P. Sylvester, *Wat. Res.* 42, 1760 (2008).
[33] A. Gupta, V.S. Chauhan and N. Sankararamakrishnan, *Wat. Res.* 43, 3862 (2009).
[34] S. Dakhai, L.A. Orlova and N.Yu. Mikhailenko, *Glass and Ceramics 56*, 177 (1999).
[35] I. A. Levitskii, *Glass and Ceramics 58*, 223 (2001).
[36] I. N. Dvornichenko and S.V. Matsenko, *Glass and Ceramics*, *57*, 67 (2000).
[37] L. Lupa, A. Iovi, P. Negrea, A. Negrea and G. Szabo, *Environ. Eng. Manage. J.* 5, 1099 (2006).
[38] A. Negrea, L. Lupa, M. Ciopec, R. Lazau, C. Muntean and P. Negrea, *Adosrb. Sci. Technol.* 28, 467 (2010).
[39] Lj.S.Cerovic, S.K. Milonjic, M.B. Todorovic, M.I. Trtanj, Y.S. Pogozhev, Y. Blagoveschenskii and E.A. Levashov, *Colloids Surf. A* 297, 1 (2007).
[40] A. Negrea, M. Ciopec, L. Lupa, C. Muntean, R. Lazau, P. Negrea, *Water pollution X, WIT Transaction on Ecology and Environment*, 135, 117 (2010).
[41] P. Negrea, A. Negrea, L. Lupa, and L. Mitoi, *Proc. Int. Symp. "Trace Elements in the Food Chain"*, Budapest, Hungary, May 25–27 (2006).
[42] P. Niedzielski, *Anal. Chim. Acta* 551, 199 (2005).
[43] H.Y. Shan, *Scientometrics* 59, 171 (2004).
[44] Y.S. Ho and G. McKay, *Process Biochem.* 34, 451 (1999).
[45] F. Partey, D. Norman, S. Ndur and R. Nartey, *J. Colloid Interface Sci.* 321, 493 (2008).
[46] A. Negrea, L. Lupa, M. Ciopec, C. Muntean, R. Lazau, M. Motoc, *Rev Chim-Bucharest* 61, 691 (2010).

[47] R. Lazau, L. Lupa, I. Lazau, P. Negrea and C. Pacurariu, *Rom. J. Mater*. 40, 71 (2010).
[48] K. Tyrovola, N.P. Nikolaidis, N. Veranis, N. Kallithrakas-Kontos and P.E. Koulouiridakis, *Wat. Res.* 40, 2375 (2006).
[49] X. Meng, S. Bang and G.P. Korfiatis, *Wat. Res.* 34, 1255 (2000).
[50] X. Guan, H. Dong, J. Ma and L. Jiang, *Wat. Res.* 43, 3891 (2009).
[51] F. Frau, R. Biddau and L. Fanfani, *Appl. Geochem.* 23, 1451 (2008).
[52] A. Negrea, C. Muntean, L. Lupa, R. Lazau, M. Ciopec and P. Negrea, *Chem. Bull. "Politehnica" Univ. (Timisoara),* 55, 46 (2010).
[53] S. Wang and C.N. Mulligan, *J. Hazard. Mater.* B138, 459 (2006).
[54] A. Negrea, L. Lupa, C. Muntean, M. Ciopec, P. Negrea and R. Istratie, *Chem. Bull. "Politehnica" Univ. (Timisoara)* 55, 123 (2010).
[55] H. Guo, D. Stuben, Z. Berner, U. Kramar, *J. Hazard. Mater*. 151, 628 (2008).
[56] STAS 708/2-83, Porcelain and tableware faience – chemical tests, acid resistence (Romanian language).

Effect of Matrix Solution on As(V) Adsorption onto Iron-containing Materials

*p*H and kinetic studies

ADINA NEGREA[1], CORNELIA MUNTEAN[1*], IOANA BOTNARESCU[1], MIHAELA CIOPEC[1], MARILENA MOTOC[2]

[1] University Politehnica Timişoara, Faculty of Industrial Chemistry and Environmental Engineering, 2 Piaţa Victoriei, 300006, ,Timişoara, Romania

[2] "Victor Babes "University of Medicine and Pharmacy Timisoara, 2 Piata Eftimie Murgu, 300041, Timisoara, Romania

In the present paper is investigated the effect of the presence of some competing anionic (NO_3^-, PO_4^{3-}, Cl^- and CO_3^{2-}) and cationic (Mg^{2+} and Mn^{n+}) species on the adsorption of arsenic (V) on two iron containing materials: a waste material and a synthetic material. The waste material was an iron containing sludge (IS) resulting from hot-dip galvanization. The synthetic material was Fe_2O_3 obtained through annealing of $Fe(COO)_2 \cdot 2H_2O$ at 550 °C. For the studies, a synthetic solution containing 100 μg As(V)/L was used. The adsorption of As(V) over the initial pH range 2-11 for IS and 2-8 for Fe_2O_3 was not strongly dependent on pH. The influence of ionic species was investigated in single and in multicomponent competing ion solutions at two concentrations: 10 mg/L and 100 mg/L, respectively. Adsorption experiments were also carried out on a real groundwater containing the studied ions. The adsorption experiments were performed at different contact times (1, 2, 3, 4, 8 and 24 h). The presence of any ionic species has a negative effect on As(V) adsorption onto Fe_2O_3. Only PO_4^{3-} showed a negative effect on the adsorption of As(V) onto IS. The other studied ions, in single and in multicomponent solutions had a positive effect on the adsorption of As(V) onto IS. Fe_2O_3 proved to be more efficient than IS for the adsorption of As(V) from solutions containing only this species (adsorption capacities of 97 μg/g and 45 μg/g, respectively). The presence of other species was benefic for the adsorption of As(V) onto IS from solutions containing all ions and the real underground water. The values of the adsorption capacity reached in these cases were very close for both adsorbent materials (~85 μg/g for the real water and ~80 μg/g for the all ions synthetic solution). These results indicate that IS would be a suitable adsorbent for the removal of As(V) ions from natural waters. The adsorption process followed a pseudo-second-order kinetics and the theoretically predicted equilibrium adsorption capacities were close to the experimentally determined values.

Keywords: arsenic, adsorption, iron sludge, anion, cation, kinetics

The effects of pollution of natural systems with arsenic are serious and dangerous to human life. Especially contamination of drinking water sources with arsenic is a matter of worldwide concern. The symptoms of chronic poisoning in human beings are numerous: skin cancer, liver, lung, kidney and bladder cancer, as well as conjunctivitis, hyperkeratosis and, in severe cases, gangrene in the limbs and malignant neoplasm [1-3].

For this reason, World Health Organization (WHO) set the maximum permissible limit in drinking water at 10μg/L [4]. Due to the high toxicity of arsenic, remediation of arsenic contaminated soils and groundwater is necessary to protect the environment and the public health [5].

A variety of treatment processes has been studied for arsenic removal from water. One of the most used methods is the adsorption. The most efficient adsorbent materials are those with iron content considering the affinity of arsenic towards iron [6-10].

Since underground water and surface water usually contains some soluble solutes, the effect of these species on the removal of As(V) through adsorption should be studied. Many researchers reported that competing solutes affect the removal of As(V) by adsorbents.

The literature data indicate that arsenic adsorption is strongly decreased by the presence of phosphate; due to their structural resemblances, they compete for the binding sites of the adsorbent [5, 11-15].

Some studies found that the presence of NO_3^-, Cl^- and SO_4^{2-} has negligible effects on As(V) uptake, these ions forming outer-sphere complexes that do not interfere with the inner-sphere complex formed by As(V) at the adsorbent surface [11-13]. As a potential competitor or extractor of arsenic, CO_3^{2-} has a negligible to moderate effect [16, 17], a moderate to notable effect [13, 18] or equivocal results were obtained [19]. Some studies revealed the cooperative effect of metal cations such as Ca^{2+}, Mg^{2+} and Fe^{3+} on adsorption of arsenic, which could be attributed to the favorable electrostatic effects, as the adsorption of metal cations increases the amount of positive charge on the adsorbent surface [5, 7, 20].

The difference and sometimes even the contradiction between the results reported by different researchers may be due to different experimental conditions (*p*H value, anion concentration, adsorbent, solid:liquid ratio).

The present paper reports studies on the effect of the presence of some competing anionic (NO^{3-}, PO_4^{3-}, Cl^- and CO_3^{2-}) and cationic (Mg^{2+} and Mn^{n+}) species on the adsorption of arsenic (V) on two iron containing materials: an iron containing sludge (IS) resulting from hot-dip galvanization and synthetic Fe_2O_3.

Experimental part

The adsorption of As(V) was studied in batch experiments using two iron containing materials: a

* email: cornelia.muntean@chim.upt.ro,; Tel.: +40 256 404164

synthetic material and a by-product resulting from another technology. The synthetic material used as adsorbent was Fe_2O_3 obtained through annealing of analytical grade $Fe(COO)_2 \cdot 2H_2O$ at 550°C. The by-product is an iron sludge (IS) resulting during the neutralization with lime of wastewaters from hot dip galvanization. IS was grinded and sieved. The fraction with particles size between 0.1 and 0.2 mm was used after drying at 105°C.

The influence of *p*H on the adsorption performance of the IS and Fe_2O_3 was studied by batch equilibration technique [1, 9, 10, 21]. A known amount of IS (0.1 g) was suspended in 100 mL of a 100 μg/L As(V) solution. The value of the initial *p*H of the As(V) solution (pH_i) was varied between 2 and 12, being adjusted to the desired value using 0.1 M/2 M NaOH or 0.1 M/2 M HNO_3, thereby keeping the volume variation of the solution to a value as low as possible. The *p*H values of the solutions were measured by means of a CRISON MultiMeter MM41 fitted with a glass electrode, which was calibrated using various buffer solutions. The suspensions were left to equilibrate for 24 h at laboratory temperature (23 ± 1 °C), then were filtered and the final *p*H values of the solutions (pH_f) determined.

The adsorption experiments were carried out using a 100 mg As(V)/L synthetic solutions without or with ionic species (NO_3^-, PO_4^{3-}, Cl^-, CO_3^{2-}, Mg^{2+} and Mn^{n+}). The influence of each ionic species was studied at two concentrations: 10 mg/L and 100 mg/L respectively, in single component solutions (containing only one anionic species at the time). It was also studied the influence of all mixed anionic species and respectively all species (anionic and cationic) at two total concentrations: 10 mg/L and 100 mg/L. Concentration range of ionic species was chosen to fit the concentrations usually found in groundwater. Adsorption experiments were also carried out on a real groundwater with the following composition: As – 70 μg/L; Mn^{n+} - 0.17 mg/L; PO_4^{3-} - 5 mg/L; NO_3^- - 40 mg/L; Cl^- - 15 mg/L; CO_3^{2-} - 50 mg/L. During the batch adsorption experiments, the *p*H of the suspensions was left to drift freely.

All reagents used to prepare the synthetic solutions were in analytical reagent grade. Samples of 0.1 g adsorbent material were treated with 100 mL solution and left at laboratory temperature (23 ± 1°C) at different contact times (1, 2, 3, 4, 8 and 24 h). After contact time elapsed, the suspensions were filtered and the residual concentration of arsenic in the filtrate was determined through atomic absorption spectrometry with hydride generation, using a VARIAN SPECTR AA110 spectrophotometer with hydride system VGA 77.

Results and discussions

The experimental data for the composition of IS resulting from chemical analysis are: Fe – 31.6%, Zn – 1.91%, Pb – 0.03%, Ca – 15.6% and Cl – 24.3% [9, 22]. The major component of this material is iron, which makes it suitable for arsenic removal from water, due to the high affinity of arsenic towards iron [6-10]. The difference up to 100% is represented by hydrogen and oxygen, because metallic ions are present in the material mainly as oxides, hydroxides and chlorides.

The adsorption capacity (adsorption performance) is expressed as the amount of As(V) adsorbed per gram of adsorbent q_t (μg/g) at a moment *t* and is calculated using the following equation [8, 9, 21, 22]:

$$q_t = (C_o - C_t)\frac{V}{m} \quad (1)$$

where:

C_o is the initial concentration of arsenic in solution, μg/L;

C_e – residual concentration of arsenic in solution at a moment *t*, μg/L;

V - volume of solution, L;

m - amount of adsorbent, g.

Influence of pH

To understand the characteristics of the surface charge generated on IS and Fe_2O_3 in aqueous media, the point of zero charge, pH_{pzc}, of these materials was determined by batch equilibration technique. In the case of IS this value was pH_{pzc} = 6.2 for initial solutions having *p*H values in the range 4-10 [9]. For Fe_2O_3 the value was pH_{pzc} = 6.1 in the initial pH range 6-9.5 [21] The fact that both materials have nearly neutral point of zero charge suggests that both negatively and positively charged ions could be adsorbed [23].

The experimental results of effect of *p*H on sorption performance are shown in figure 1a where As(V) equilibrium uptake (q_e) and equilibrium solution *p*H (pH_f) are plotted against the initial solution *p*H (pH_i). As is evident from figure 1a, the adsorption of As(V) over the pH_i range 2-11 for IS and 2-8 for Fe_2O_3 is not strongly dependent on pH, which is highly advantageous for practical operation [20].

The *p*H dependence of As(V) adsorption is influenced by the distribution of metal species in the solution phase, which, on the other hand, depends on the *p*H of the medium. Pentavalent arsenic exists in the form of H_3AsO_4, $H_2AsO_4^-$, $HAsO_4^{2-}$, and AsO_4^{3-}, depending on the solution *p*H. The distribution of these species as a function of solution *p*H is presented in figure 2. The values of relative proportions of the species (α_i) were calculated based on the three dissociation equilibriums of arsenic acid and their respective acidity constants [24]:

$$H_3AsO_4 \rightleftharpoons H_2AsO_4^- + H^+ \qquad pK_{a1} = 2.24$$

$$H_2AsO_4^- \rightleftharpoons HAsO_4^{2-} + H^+ \qquad pK_{a2} = 6.96$$

$$HAsO_4^{2-} \rightleftharpoons AsO_4^{3-} + H^+ \qquad pK_{a3} = 11.50$$

The *p*H dependence of As adsorption is usually explained in terms of ionization of both adsorbates and adsorbents [25]. In the pH_f range 2.30 – 6.80, the predominant species $H_2AsO_4^-$ is primarily responsible for adsorption and maximum As(V) removal was reached for both sorbents (fig. 1b) [1]. This *p*H range is below the pH_{pzc} of both materials (IS – 6.2; Fe_2O_3 – 6.1); sorbed protons on the functional groups of the surface cause an overall positive surface charge [26], and adsorption of anionic As(V) is enhanced by Coulombic attractions (non-specific adsorption) (eq. 2) [25]. Surface protonation and the number of positively charged sites decreases as the pH increases and therefore arsenic uptake should decrease [17, 26], but such effect was not observed in this study. The probable cause is that as *p*H increases and approaches the almost neutral pH_{pzc}, the second type of mechanism (eq. 3) becomes predominant.

Although at pH_f values higher than pH_{pzc} the surfaces exhibit a net negative charge due to the dissociation of proton of the hydroxide group [8], a significant adsorption still takes place. The adsorption of As(V) species is favoured electrostatically up to the pH_{pzc} of the adsorbents but beyond this point specific adsorption (ligand exchange) plays an important role [27].

When the *p*H is above 7, the negatively charged $HAsNO_4^{2-}$ becomes predominant, whereas the oxide surface also

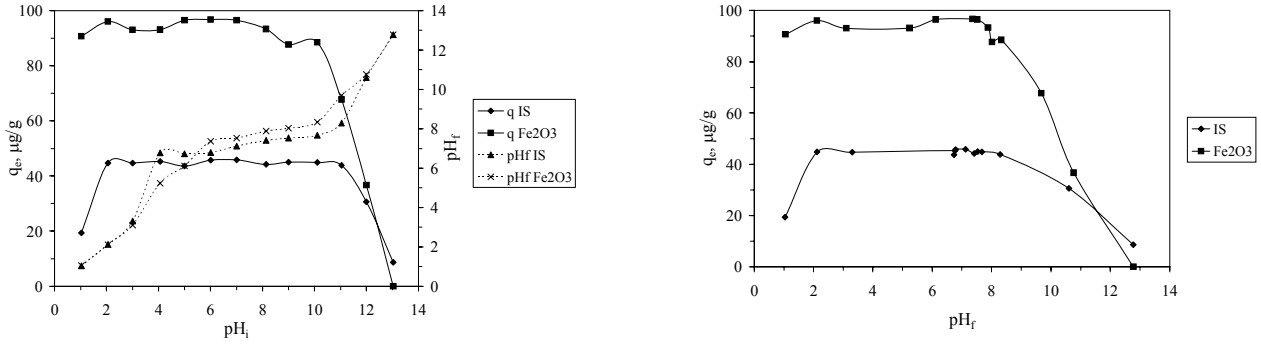

Fig. 1. Influence of *p*H on As(V) adsorption onto IS and Fe_2O_3

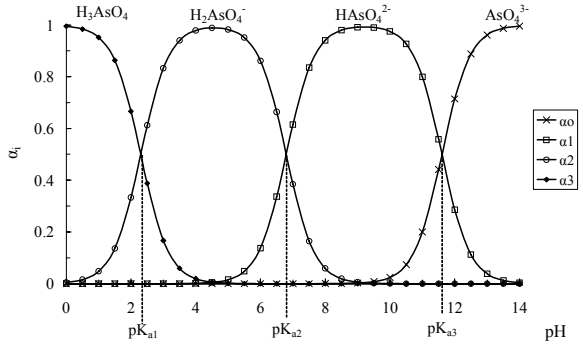

Fig. 2. Distribution of As(V) species as a function of solution pH

becomes negatively charged; thus, electrostatic repulsion results in decreased adsorption [1, 8, 17]. Beyond *p*H 9.5 AsO_4^{3-} is formed (above 11.60 becomes predominant) and arsenic uptake decreases abruptly. Besides the electrostatic repulsion, the decrease of adsorption performance under basic conditions may also be caused by the fact that the hydroxyl groups become more plentiful on the surface of the adsorbents with the increase of *p*H, thereby limiting adsorption [1].

At *p*H values lower than 2.3, although H_3AsO_4 predominates over $H_2AsO_4^-$, $H_2AsO_4^-$ can be preferentially sorbed [26]. As(V) predominant species H_3AsO_4 is neutral and exhibits no electrostatic interactions with adsorbents surface, and $H_2AsO_4^-$ concentration is lower in this *p*H range. As a result, the arsenic uptake decreased. In the case of IS, the decrease in the extent of adsorption may be also attributed to the partial dissolution of the material and a consequent decrease in the number of adsorption sites [27, 28].

It was also observed that the initial *p*H of the suspensions was shifted during adsorption (fig. 1a). However, there is no regular trend in the change of *p*H. In the lower *p*H range of 2–7, the *p*H of the solutions shifted toward higher *p*H (i.e., basic) after adsorption for both adsorbents. Above *p*H 7, the shifts are toward the acidic region. One may notice that both $pH_f - pH_i$ plots show a plateau for pH_i values in the range 4-10 for IS and 6-10 for Fe_2O_3. The presence of such a plateau indicates that the materials are ampholytes and behaved as acid–base buffers [1, 9, 21]. The plateau corresponds to the *p*H range where buffering of the materials surface occurs.

The shape of $pH_f - pH_i$ curves is similar to the $pH_f - pH_f$ plots obtained in view of pH_{pzc} determination for both materials, in the presence of NaCl as background electrolyte and without As(V) [9, 21]. In the presence of As(V), the *p*H value of the plateau shifted to higher values: from pH_{pzc} = 6.2 to pH_f ~7.2 for IS and from pH_{pzc} = 6.1 to pH_f ~7.8 for Fe_2O_3. This shift in *p*H may be attributed to the sorption reactions of As(V) which releases OH groups from sorbent (eq. 3), as a result of ligand exchange [1, 15].

The results demonstrate the operation of two types of mechanisms: (1) non-specific adsorption – surface complexion due to electrostatic attractive interaction (eq. 2), and (2) specific adsorption in a two-step process resulting in the formation of an inner-sphere bidentate surface complex (eq. 3) [1, 3]:

- surface complexion, $pH < pH_{pzc}$:

$$\text{Surface (Fe)} - OH_2^+ + H_2AsO_4^- \rightarrow \text{Surface (Fe)} - OH_2^+ - H_2AsO_4^- \quad (2)$$

- anion exchange, near neutral pH:

$$2\ \text{Surface (Fe)} - OH + H_2AsO_4^- \rightarrow (\text{Surface (Fe)})_2 - HAsO_3 + H_2O + OH^- \quad (3)$$

Influence of contact time and competing ions

The influence of contact time on the adsorption capacity towards As(V) of the two studied adsorbent materials is shown in figures 3 and 4. Initially sorption takes place more quickly (in the first four hours) and then it continued slowly up to the maximum sorption. The equilibrium was reached for most of the systems after 8 h, and thereafter the amount of adsorbed As(V) did not change significantly with the increase of contact time. For some systems, especially for ion concentration of 10 mg/L, the adsorption capacity still increased at 24 h contact time showing that the equilibrium was not reached. Curves are single, smooth and continuous, leading to saturation, and suggests the possible

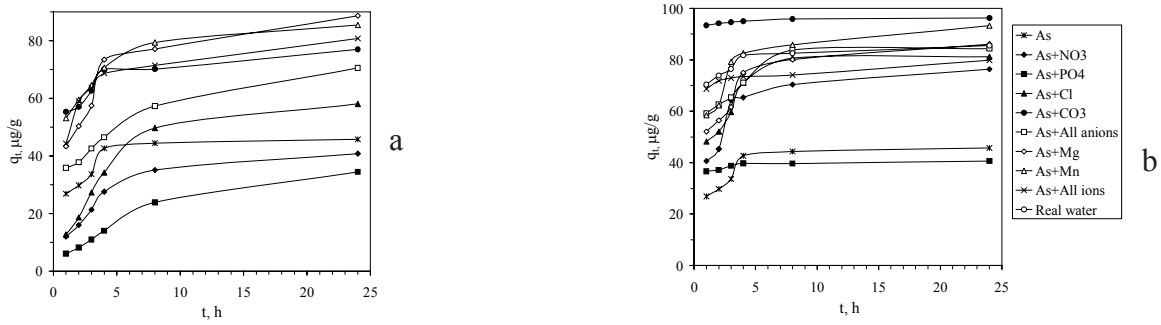

Fig. 3. Influence of contact time on As(V) adsorption capacity of IS
(a) – ion concentration 10 mg/L; (b) – ion concentration 100 mg/L

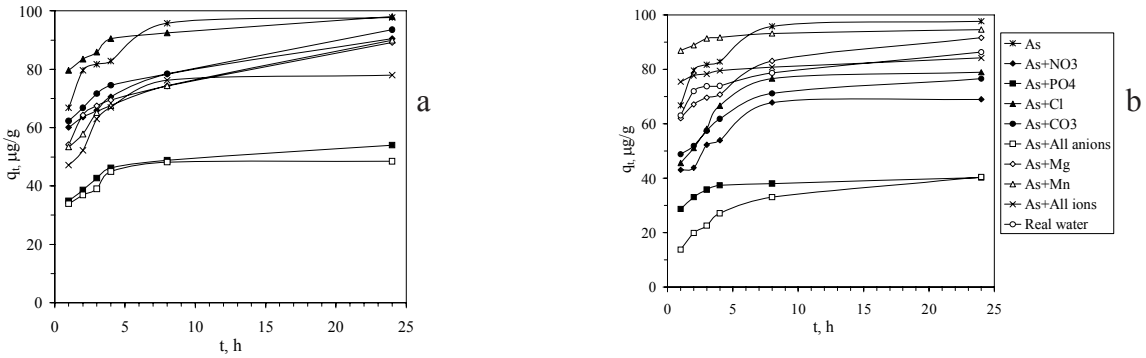

Fig. 4. Influence of contact time on As(V) adsorption capacity of Fe_2O_3
(a) – ion concentration 10 mg/L; (b) – ion concentration 100 mg/L

monolayer coverage of As(V) on the IS and Fe_2O_3 surface [29].

The mechanism of solute transfer to the solid includes diffusion through the boundary layer or fluid film around the adsorbent particle and diffusion through the pores to the internal adsorption sites. At the onset of the process, the concentration gradient between the layer or film and the solid surface is large, and hence the transfer of solute onto the solid surface is faster. The fast diffusion on to the external surface is followed by slow diffusion into the intra particle matrix. In this stage, solute takes more time to transfer from the solid surface to internal adsorption sites through the pores. Finally, the equilibrium is attained [29].

Figure 3a shows that the individual presence of some of the studied species (Cl^-, CO_3^{2-}, Mg^{2+} and Mn^{n+}) in a concentration of 10 mg/L has a positive effect on the As(V) adsorption onto IS, the adsorption capacities reached after 24 h being higher than the value obtained for As(V) alone. The same effect is present when the solution contains the mixture of all studied anions or the mixture of all studied ions. For these systems, the pseudo-second order kinetic model predicted even higher values of the adsorption capacities (table 3), because after 24 h contact time the equilibrium was not reached. In the case of solutions containing NO_3^- and PO_4^{3-} respectively, although at 24 h contact time the experimental adsorption capacities were lower than the value reached for As(V), the pseudo-second order kinetic model predicted higher values and closer to the value obtained for As(V) alone.

At an ionic species concentration of 100 mg/L, after 24 h contact time the equilibrium was reached for most systems (fig. 3b). The experimental adsorption capacities were higher than for the 10 mg/L concentration in the systems containing Cl^-, CO_3^{2-}, NO_3^-, Mn^{n+} and the mixture of all anions. For systems containing Mg^{2+} and the mixture of all ions, the values were almost the same as for 10 mg/L. For 100 mg/L PO_4^{3-} was reached a lower adsorption capacity (40.7 µg/L) than the value predicted by the pseudo-second order kinetic model in the case of 10 mg/L solution (47.0 µg/L) and lower than that for the As(V) alone (45.8 µg/L). The experimental results show that in the case of IS used as adsorbent material, all studied ions had a positive influence on As(V) uptake increasing the adsorption capacity, with the exception of PO_4^{3-} which lowered the adsorption capacity, but only for the higher concentration (100 mg/L). This observation is consistent with literature data, which indicate that arsenic adsorption is strongly decreased by the presence of phosphate, because of the competition for the binding sites of the adsorbent material between arsenic and phosphate. These ions compete because of the structural resemblances – they are tetrahedral anions that form inner-sphere complexes via a ligand-exchange mechanism with the functional groups at the surfaces of iron containing materials such as iron oxides and hydrous iron oxides [5, 11-15].

In the case of IS, the decrease of the adsorption capacity was not strong, probably due to the fact that IS has a complex composition and PO_4^{3-} may interact with some of the IS components. Ionic species, CO_3^{3-}, Mg^{2+} and Mn^{n+} had the most positive influence on As(V) uptake by the IS. The cooperative effect of metal cations such as Ca^{2+}, Mg^{2+} and Fe^{3+} on adsorption of As(V) and As(III) was previously observed by other researchers and could be attributed to the favorable electrostatic effects, as the adsorption of metal cations increases the amount of positive charge on the adsorbent surface [5, 7, 20]. Previously published studies found that as a potential competitor of arsenic, CO_3^{2-} has a negligible to moderate effect [16, 17], a moderate to notable effect [18] or equivocal results were obtained [19]. In our study, we found that the individual presence of CO_3^{2-} had a positive effect on As(V) uptake by IS, especially for higher concentration (100 mg/L), when the highest adsorption capacity was reached (96.3 µg/L).

As(V) uptake onto IS from the real underground water (~85µg/g) was close to that reached for the both synthetic solutions (~80µg/g), and was much higher than the value obtained for the solution containing As(V) alone (~45 µg/g) (fig. 3a).

Figure 4a,b shows that for both studied concentrations, the presence of any ionic species (either in single or multicomponent solution) has a negative effect on As(V) adsorption onto Fe_2O_3. For some of the species, after 24 h contact time the equilibrium was not reached, especially for the lower concentration. At higher contact time an increase in As(V) uptake in the presence of these species may be expected and the values to become closer to that obtained for arsenic alone (~ 97 µg/g).

The most negative impact on As(V) uptake was found for the presence of and for the solutions containing all anions. In the case of Fe_2O_3 as opposite to IS, the results are consistent with literature data, which indicate that arsenic adsorption is strongly decreased by the presence of phosphate.

The effect of cationic species on As(V) adsorption onto Fe_2O_3 is less evident. Their influence compensates the negative effect of PO_4^{3-} and for the solutions containing all ions and for the real water were reached good adsorption capacities (~84 µg/g for 100 mg/L solution and ~86 µg/g, respectively).

Comparing the efficiencies of the adsorbent materials used in this study, although Fe_2O_3 proved to be more efficient than IS for the adsorption of As(V) from solutions containing only this species, the presence of other species was benefic for the adsorption of As(V) onto IS from solutions containing all ions and real underground water. The values of the

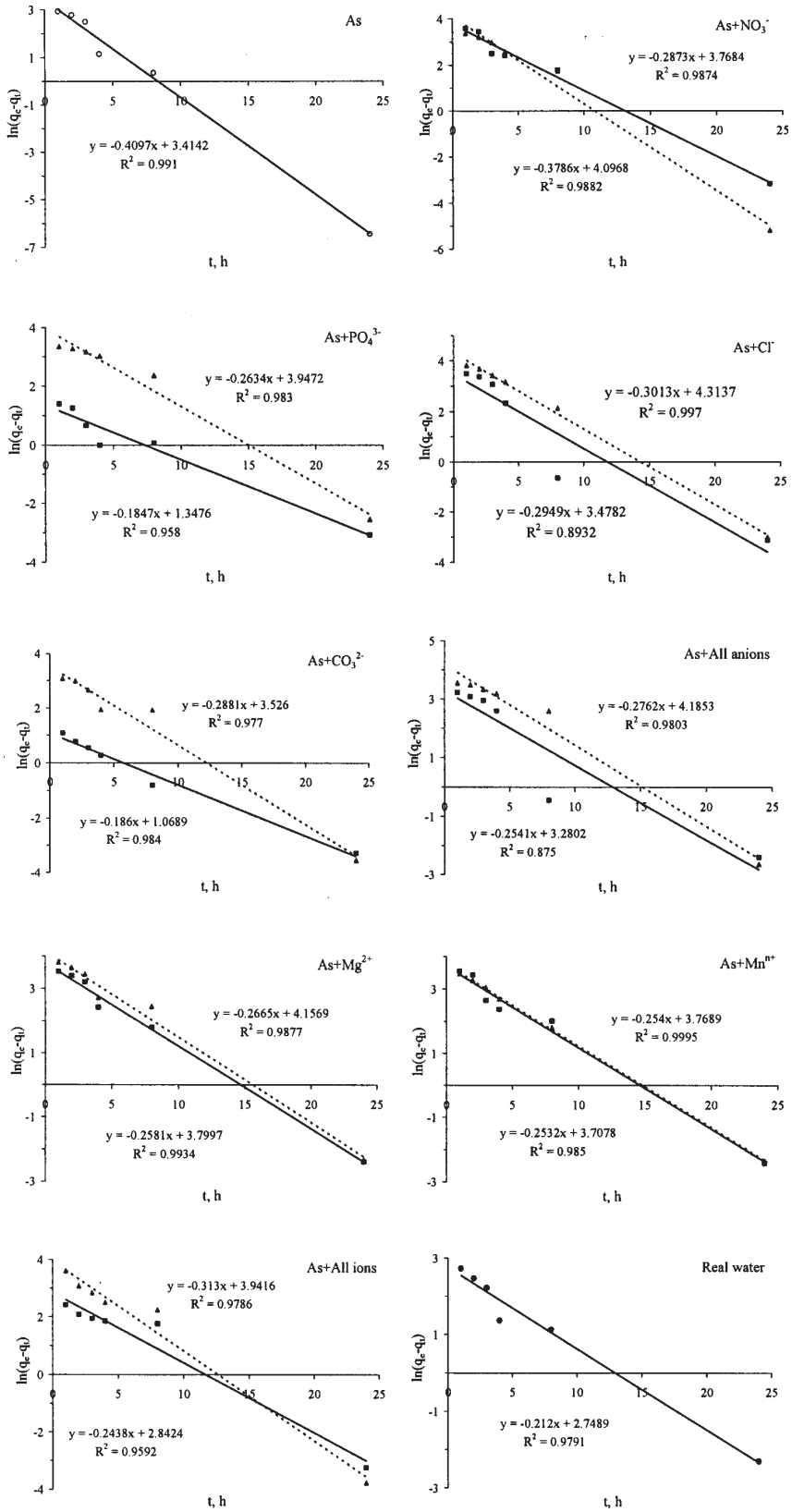

Fig. 5. Pseudo-first-order kinetic plots for As(V) adsorption onto IS (- ▲ -) 10 mg/L; (-■-) 100 mg/L

adsorption capacities reached in these cases were very close for both adsorbent materials.

Kinetic studies

Various models can describe the transient behaviour of a batch adsorption process. Most of these have been reported as pseudo-first-order and some as pseudo-second-order kinetic processes. In order to express the kinetics of arsenic adsorption on the two studied adsorbent materials the data were analyzed using both models.

The pseudo-first-order kinetic model based on the solid capacity and proposed by Lagergren can be used to determine the rate constant for the adsorption process and the integrated form is expressed by the following equation [1, 9, 10]:

$$\ln(q_e - q_t) = \ln q_e - k_1 t \quad (4)$$

where q_t and q_e represent the amounts of the arsenic adsorbed on the iron oxide at time t and at equilibrium time, respectively, μg/g; k_1 is the specific adsorption rate constant, h^{-1}.

The linear form of the pseudo-second-order rate expression of Ho and McKay, based on the solid phase sorption, is given by [1, 9, 10, 30]:

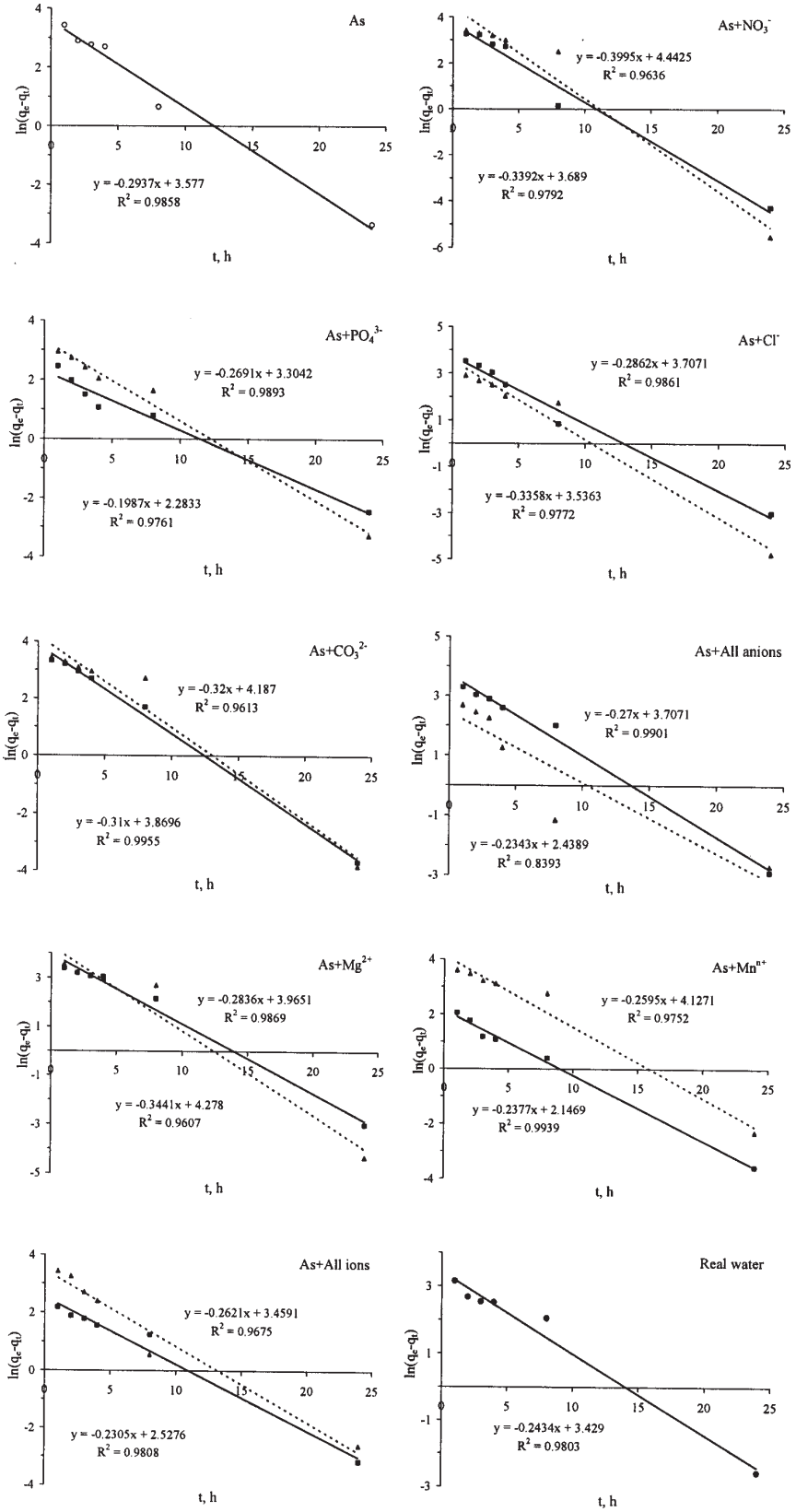

Fig. 6. Pseudo-first-order kinetic plots for As(V) adsorption onto Fe_2O_3 (- ▲ -) 10 mg/L; (-■-) 100 mg/L

$$\frac{t}{q_t} = \frac{1}{h} + \frac{t}{q_e} \quad (5)$$

where $h = k_{s2} \cdot q_e^2$; k_2 is the pseudo-second-order constant, $h^{-1}(\mu g/g)^{-1}$; q_t and q_e have the meanings mentioned before.

To assess the extent to which the kinetic equations fit the experimental data, two different error functions were examined.

The normalized standard deviation, Δq (%), was estimated using the equation [9, 31, 32]:

$$\Delta q(\%) = 100\sqrt{\frac{1}{p-1}\sum_{i=1}^{p}\left(\frac{q_{exp} - q_{calc}}{q_{exp}}\right)_i^2} \quad (6)$$

where q_{exp} is the experimentally determined adsorption capacity (μg/g), q_{calc} is the adsorption capacity calculated according to the model equation (μg/g) and p is the number of experimental data points.

The average relative error E (%), which minimizes the fractional error distribution across the entire concentration range, was estimated via the equation [9, 33, 34]:

Table 1
KINETIC PARAMETERS FOR As(V) SORPTION ONTO IS, PSEUDO-FIRST-ORDER KINETIC MODEL

Sample	Ion concentration 10 mg/L						Ion concentration 100 mg/L					
	q_e, exp., μg/g	q_e, kinetic plot, μg/g	k_1, h^{-1}	R^2	Δq, %	E, %	q_e, exp., μg/g	q_e, kinetic plot, μg/g	k_1, h^{-1}	R^2	Δq, %	E, %
As	45.8	30.4	0.4097	0.9910	47.1	22.2						
As+ NO_3^-	40.8	60.1	0.3786	0.9882	81.0	65.6	76.4	43.3	0.2873	0.9874	38.7	62.2
As+ PO_4^{3-}	34.4	51.8	0.2634	0.9830	135	183	40.7	3.85	0.1847	0.9580	104	108
As+ Cl^-	58.1	74.7	0.3013	0.9970	60.6	36.7	81.2	32.4	0.2949	0.8932	76.2	58.1
As+ CO_3^{2-}	77.0	34.0	0.2881	0.9770	74.9	56.2	96.3	2.91	0.1860	0.9840	108	116
As+All anions	70.5	65.7	0.2762	0.9803	28.4	8.01	84.3	26.6	0.2541	0.8750	85.8	73.7
As+ Mg^{2+}	88.6	63.9	0.2665	0.9877	47.8	22.8	86.1	44.7	0.2581	0.9934	68.6	47.1
As+ Mn^{n+}	85.4	43.3	0.2540	0.9995	70.4	49.5	93.2	40.8	0.2532	0.9850	76.4	58.3
As+All ions	80.8	51.5	0.3130	0.9786	55.5	30.9	79.9	17.2	0.2438	0.9592	94.6	89.5
Real water	85.5	15.6	0.2120	0.9791	97.7	95.4						

Table 2
KINETIC PARAMETERS FOR As(V) SORPTION ONTO Fe_2O_3, PSEUDO-FIRST-ORDER KINETIC MODEL

Sample	Ion concentration 10 mg/L						Ion concentration 100 mg/L					
	q_e, exp., μg/g	q_e, kinetic plot, μg/g	k_1, h^{-1}	R^2	Δq, %	E, %	q_e, exp., μg/g	q_e, kinetic plot, μg/g	k_1, h^{-1}	R^2	Δq, %	E, %
As	97.7	35.8	0.2937	0.9858	80.9	65.4						
As+ NO_3^-	90.5	85.0	0.3995	0.9636	27.3	7.45	69.0	40.0	0.3392	0.9792	58.0	33.7
As+ PO_4^{3-}	54.0	27.2	0.2691	0.9893	70.2	49.2	40.2	9.81	0.1987	0.9761	93.8	88.1
As+ Cl^-	98.1	34.3	0.3358	0.9772	81.6	66.6	79.0	40.7	0.2862	0.9861	66.9	44.7
As+ CO_3^{2-}	93.6	65.8	0.3200	0.9613	50.0	25.0	76.6	47.9	0.3100	0.9955	56.7	32.2
As+All anions	48.4	11.5	0.2343	0.8393	92.8	86.1	40.4	40.7	0.2700	0.9901	15.4	2.37
As+ Mg^{2+}	89.2	72.1	0.3441	0.9607	39.1	15.3	91.7	52.7	0.2836	0.9869	63.1	39.8
As+ Mn^{n+}	90.0	62.0	0.2595	0.9752	53.5	28.6	94.7	8.56	0.2377	0.9939	104	107
As+All ions	77.9	31.8	0.2621	0.9675	77.9	60.7	84.2	12.5	0.2305	0.9808	99.7	99.3
Real water	86.3	30.8	0.2434	0.9803	83.8	70.3						

$$E(\%) = \frac{100}{p-1} \cdot \sum_{i=1}^{p} \left(\frac{q_{calc} - q_{exp}}{q_{exp}} \right)_i^2 , \qquad (7)$$

Figures 5 and 6 present the plots of $\ln(q_e - q_t)$ versus t for As(V) adsorption onto IS and Fe_2O_3 respectively, for all studied solutions. The slopes and intercepts of the plots are used to estimate the pseudo-first-order rate constant (k_1) and the equilibrium adsorption capacity (q_e), respectively. Tables 1 and 2 summarize the values of the kinetic parameters, together with the regression coefficients (R^2) and the estimated errors obtained from the pseudo-first-order kinetic plots for both studied adsorbent materials.

In the case of the pseudo-second-order kinetic model, a plot of t/q_t versus t should yield a straight line. From the intercept and slope (figs. 7 and 8) are calculated the second-order rate constant (k_2) and the equilibrium adsorption capacity (q_e). The values of the kinetic parameters, together with the regression coefficients (R^2) and the estimated errors obtained for both studied adsorbent materials from the pseudo-second-order kinetic plots are summarized in tables 3 and 4, respectively.

The values of the correlation coefficient R^2 were higher and closer to 1 and the estimated errors were smaller in the case of the pseudo-second-order kinetic model. For the pseudo-first-order model there was a difference between the q_e values experimentally obtained and the values calculated from the kinetic plots. In the case of the

Table 3
KINETIC PARAMETERS FOR AS(V) SORPTION ONTO IS, PSEUDO-SECOND-ORDER KINETIC MODEL

Sample	Ion concentration 10 mg/L						Ion concentration 100 mg/L					
	q_e, exp., μg/g	q_e, kinetic plot, μg/g	k_2, h^{-1} $(\mu g/g)^{-1}$	R^2	Δq, %	E, %	q_e, exp., μg/g	q_e, kinetic plot, μg/g	k_2, h^{-1} $(\mu g/g)^{-1}$	R^2	Δq, %	E, %
As	45.8	47.6	0.02402	0.9987	8.10	0.66						
As+ NO_3^-	40.8	46.4	0.006870	0.9969	7.82	0.61	76.4	79.7	0.01216	0.9990	8.25	0.68
As+ PO_4^{3-}	34.4	47.0	0.002453	0.9817	10.9	1.20	40.7	40.9	0.1458	0.99996	2.20	0.05
As+ Cl^-	58.1	69.7	0.003204	0.9925	8.61	0.74	81.2	84.7	0.01294	0.9985	8.07	0.65
As+ CO_3^{2-}	77.0	78.9	0.01874	0.9994	7.32	0.54	96.3	96.4	0.2068	0.99999	0.75	0.006
As+All anions	70.5	75.9	0.006337	0.9959	14.8	2.18	84.3	87.0	0.01630	0.9991	7.70	0.59
As+ Mg^{2+}	88.6	94.0	0.006980	0.9986	8.54	0.73	86.1	89.7	0.01111	0.9992	8.14	0.66
As+ Mn^{n+}	85.4	88.6	0.01199	0.9997	6.67	0.44	93.2	96.2	0.01311	0.9995	6.39	0.41
As+All ions	80.8	83.7	0.01238	0.9994	3.39	0.11	79.9	80.6	0.03601	0.9995	6.33	0.40
Real water	85.5	86.6	0.03655	0.9999	3.28	0.11						

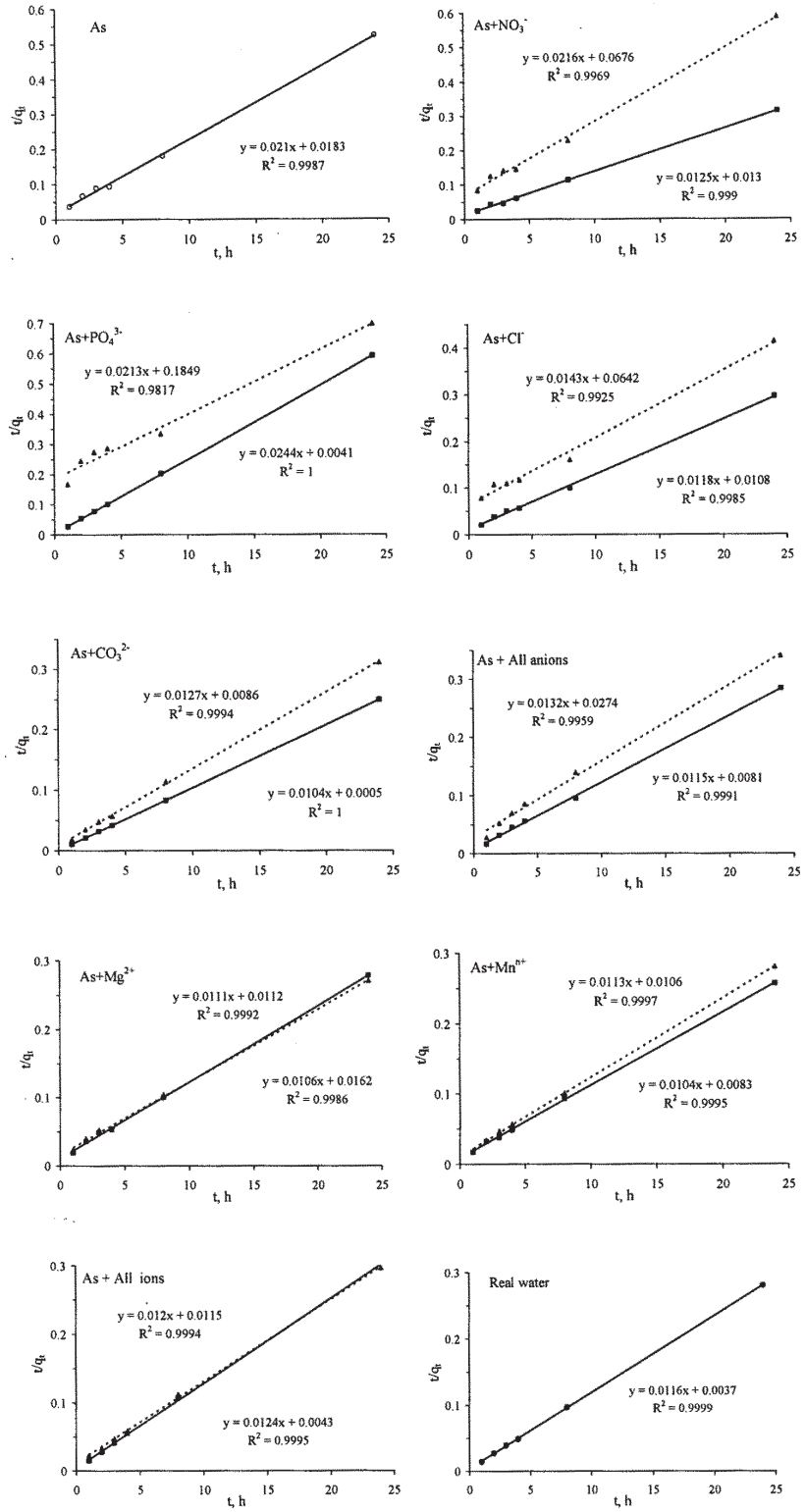

Fig. 7. Pseudo-second-order kinetic plots for As(V) adsorption onto IS
(-▲-) 10 mg/L; (-■-) 100 mg/L

Table 4
KINETIC PARAMETERS FOR As(V) SORPTION ONTO Fe_2O_3, PSEUDO-SECOND-ORDER KINETIC MODEL

Sample	Ion concentration 10 mg/L						Ion concentration 100 mg/L					
	q_e, exp., µg/g	q_e, kinetic plot, µg/g	k_2, h^{-1} $(µg/g)^{-1}$	R^2	Δq, %	E, %	q_e, exp., µg/g	q_e, kinetic plot, µg/g	k_2, h^{-1} $(µg/g)^{-1}$	R^2	Δq, %	E, %
As	97.7	100	0.01700	0.9996	3.99	0.16						
As+ NO_3^-	90.5	94.0	0.009610	0.9982	12.3	1.51	69.0	72.1	0.01378	0.9985	9.46	0.89
As+ PO_4^{3-}	54.0	55.7	0.02119	0.9996	6.34	0.40	40.2	40.9	0.05372	0.9999	1.47	0.02
As+ Cl^-	98.1	99.5	0.02434	0.9998	5.38	0.29	79.0	82.5	0.01229	0.9992	6.42	0.41
As+ CO_3^{2-}	93.6	96.7	0.009755	0.9973	12.0	1.44	76.6	79.6	0.01274	0.9995	8.46	0.72
As+All anions	48.4	49.7	0.03701	0.9994	5.30	0.28	40.4	44.7	0.008596	0.9992	5.39	0.29
As+ Mg^{2+}	89.2	92.5	0.009439	0.9973	10.8	1.16	91.7	95.0	0.01087	0.9989	10.9	1.19
As+ Mn^{n+}	90.0	94.2	0.007805	0.9972	12.2	1.48	94.7	95.1	0.08004	0.99999	1.50	0.02
As+All ions	77.9	80.8	0.01524	0.9994	5.42	0.29	84.2	84.9	0.05010	0.9999	4.24	0.18
Real water	86.3	88.1	0.01875	0.9994	6.84	0.47						

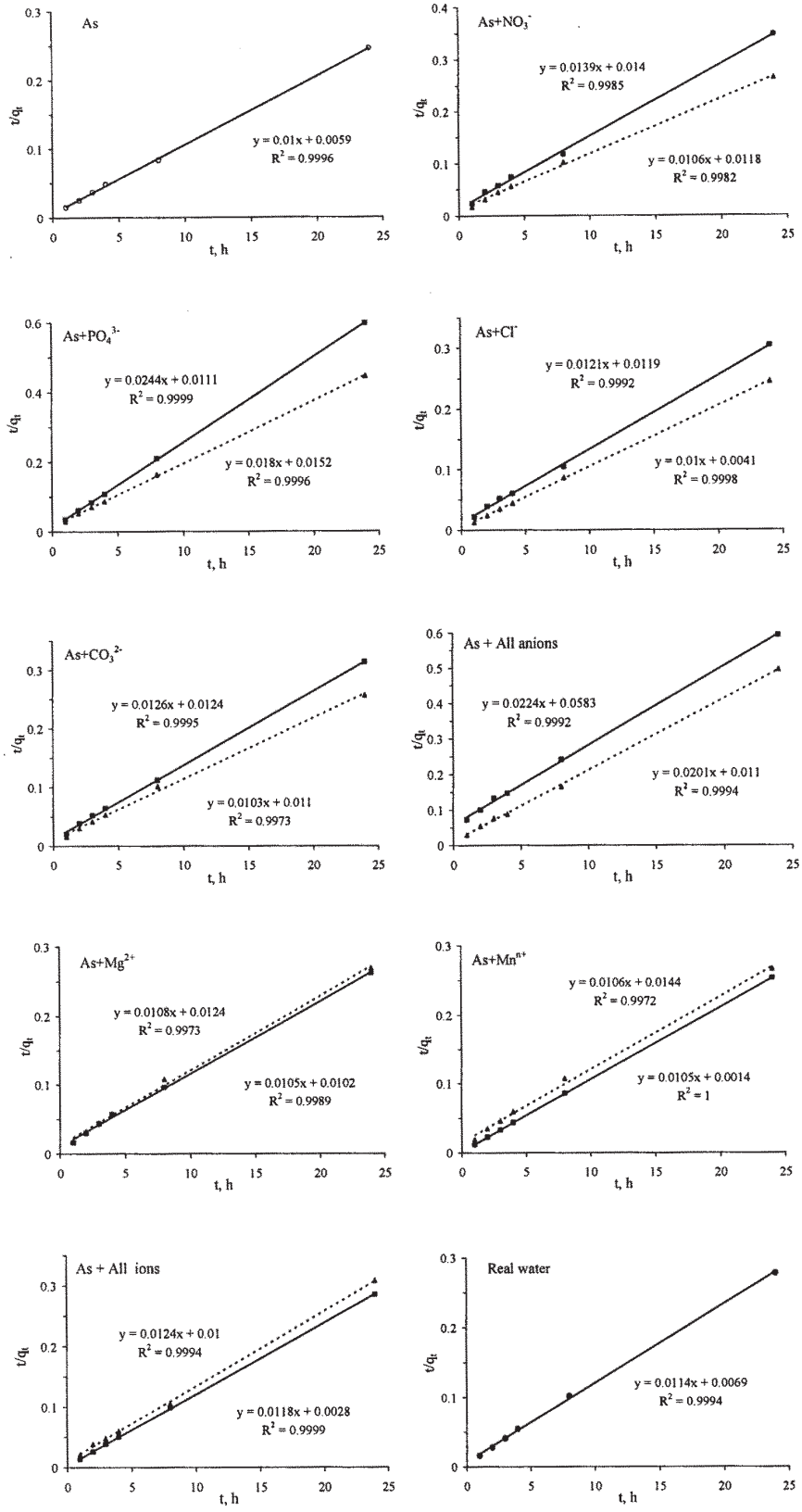

Fig. 8. Pseudo-second-order kinetic plots for As(V) adsorption onto Fe_2O_3 (-▲-) 10 mg/L; (-■-) 100 mg/

pseudo-second order model, the theoretically predicted equilibrium adsorption capacities are close to the experimentally determined values. This indicates that the kinetics of As (V) removal through adsorption onto both adsorbent materials is well explained and approximated by the pseudo-second-order kinetic model. This kinetic model is used to describe chemisorption involving valency forces through the sharing or exchange of electrons between the adsorbent and adsorbate as covalent forces, and ion exchange.

Conclusions

In the present paper is investigated the effect of the presence of some competing anionic (NO_3^-, PO_4^{3-}, Cl^- and CO_3^{2-}) and cationic (Mg^{2+}, Mn^{n+}) species on the adsorption of arsenic (V) on two iron containing materials: a waste material and a synthetic material. The waste material was an iron containing sludge (IS) resulting from hot-dip galvanization. The synthetic material was Fe_2O_3 obtained through annealing of $Fe(COO)_2 \cdot 2H_2O$ at 550°C. For the studies, a synthetic solution containing 100 μg As(V)/L was used.

The effect of *p*H on As(V) adsorption performance was studied in the 2-12 *p*H range. The adsorption of As(V) over the initial *p*H range 2-11 for IS and 2-8 for Fe_2O_3 was not strongly dependent on *p*H, which is highly advantageous for practical operation. The results demonstrated that in adsorption of As(V) onto both IS and Fe_2O_3 operate two types of mechanisms: (1) non-specific adsorption – surface complexion due to electrostatic attractive interaction, and (2) specific adsorption in a two-step process resulting in the formation of an inner-sphere bidentate surface complex.

The influence of ionic species was investigated in single and in multicomponent competing ion solutions at two concentrations: 10 mg/L and 100 mg/L, respectively. Adsorption experiments were also carried out on a real groundwater containing the studied ions. The adsorption experiments were performed at different contact times (1, 2, 3, 4, 8 and 24 h).

The experimental results showed that the presence of any ionic species (either in single or multicomponent solution) has a negative effect on As(V) adsorption onto Fe_2O_3. The most negative effect was observed for PO_4^{3-} solutions and solutions containing all studied anions, due to competition of As(V) and PO_4^{3-} for binding sites.

Only PO_4^{3-} showed a negative effect on the adsorption of As(V) onto IS, but this effect was much diminished compared with the adsorption onto Fe_2O_3, due to the interaction of PO_4^{3-} with some components of the IS. The other studied ions, in single and in multicomponent solutions had a positive effect on the adsorption of As(V) onto IS.

Comparing the efficiencies of the adsorbent materials used in this study, although Fe_2O_3 proved to be more efficient than IS for the adsorption of As(V) from solutions containing only this species (adsorption capacities of 97 μg/g and 45 μg/g, respectively), the presence of other species was benefic for the adsorption of As(V) onto IS from solutions containing all ions and the real underground water. The values of the adsorption capacity reached in these cases were very close for both adsorbent materials (~85 μg/g for the real water and ~80 μg/g for the all ions synthetic solution).These results indicate that although IS is a waste, it has the same efficiency as the synthetic, more expensive Fe_2O_3, and would be a suitable adsorbent for the removal of As(V) ions from underground waters.

The experimental data were fitted to the pseudo-first-order and pseudo-second-order kinetic models. It was found that the adsorption process followed a pseudo-second-order kinetics and the theoretically predicted equilibrium adsorption capacities were close to the experimentally determined values.

Acknowledgements: This paper is supported by the Sectoral Operational Programme Human Resources Development, financed from the European Social Fund and by the Romanian Government under the contract number POSDRU/86/1.2/S/58146 (MASTERMAT)"

References

1. BORAH, D., SATOKAWA, S., KATO, S., KOJIMA, T., J. Colloid Interface Sci., **319**, 2008, p. 53
2. BORAH, D., SATOKAWA, S., KATO, S., KOJIMA, T., J. Hazard. Mater., **162**, 2009, p. 1269
3. CHUTIA, P., KATO, S., KOJIMA, T., SATOKAWA, S., J. Hazard. Mater., **162**, 2009, p. 204
4. WHO, Guidelines for Drinking Water Quality, second ed., Geneva, Switzerland, 1993.
5. WANG, S., MULLIGAN, C.N., J. Hazard. Mater., **B138**, 2006, p. 459
6. THIRUNAVUKKARASU, O.S., VIRARAGHAVAN, T., SUBRAMANIAN, K.S., Water SA, 2003, p. 161
7. MOHAN, D., PITTMAN, C.U., J. Hazard. Mater., **142,** nr. 1-2, 2007, p. 1.
8. OHE, K., TAGAI, Y., NAKAMURA, S., OSHIMA, T., BABA, Y., J. Chem. Eng. Jpn., **38**, 2005, p. 671
9. NEGREA, A, LUPA, L., CIOPEC, M., LAZĂU, R., MUNTEAN, C., NEGREA, P., Adsorpt. Sci. Technol., **28**, nr.6, 2010, p. 467
10. NEGREA, A, LUPA, L., CIOPEC, M., MUNTEAN, C., LAZĂU, R., MOTOC, M., Rev. Chim.(Bucharest), **61**, no. 7, 2010, p. 691
11. FRAU, F., ADDARI, D., ATZEI, D., BIDDAU, R., CIDU, R., ROSSI, A., Water Air Soil Pollut., **205**, 2010, p. 25
12. JEONG, Y., FAN, M., VAN LEEUWEN, J., BELCZYK J.F., J. Environ. Sci, **19**, 2007, p. 910
13. FRAU, F., BIDDAU, R., FANFANI, L., Appl. Geochem., **23**, 2008, p. 1451
14. SMEDLEY, P.L., KINNIBURGH, G., Appl. Geochem., **17**, 2002, p. 517
15. SU, C., PULS, R.W., Environ. Sci. Technol., **35**, 2001, 4562.
16. MENG, X., BANG, S., KORFIATIS, G.P., Wat. Res., **34**, nr.4, 2000, p. 1255
17. MAITI, A., BASU, J.K, DE, S., Chem. Eng. J., **191**, 2010, p. 1
18. ANAWAR, H.M., AKAI, J., SAKUGAWA, H., Chemosphere, **54**, 2004, p. 753
19. ARAI, Y., SPARKS, D.L., DAVIS, J.A., Environ. Sci. Technol., **38**, 2004, p. 817
20. KUNDU, S., GUPTA, A.K., Sep. Purif. Technol., **51**, 2006, p. 165
21. NEGREA, A., CIOPEC, M., LUPA, L., MUNTEAN, C., LAZĂU, R., NEGREA, P., 10th International Conference on Modelling, Monitoring and Management of Water Pollution, 9-11 June 2010, Bucharest, Romania, Water Pollution X, WIT Press, p. 117
22. NEGREA, A., LUPA, L., CIOPEC, M., LAZĂU, R., Proceedings of the 11th International Conference on Environmental Science and Technology, Chania, Crete, Greece, Sept. 3-5, 2009, p. B-655
23. ZACH-MAOR, A., SEMIAT, R., SHEMER, H., Adsorption, **17**, nr.6, 2011, p. 929
24. HARVEY, D., Modern Analytical Chemistry, 2000, McGraw-Hill, New York, p. 733
25. SU, C., PULS, R.W., Environ. Sci. Technol., **35**, 2001, p. 1487
26. ASTA, M.P., CAMA, J., MARTÍNEZ, M., GIMÉNEZ, J., J. Hazard. Mater., **171**, 2009, p. 965
27. SINGH, D.B., PRASAD, G., RUPAINWAR, D.C., Colloids Surf., A, **111**, 1996, p. 49
28. HAQUE, N., MORRISON, G., CANO-AGUILERA, I., GARDEA-TORRESDEY, J.L., Microchem. J., **88**, 2008, p. 7
29. CHANDRASEKHAR, S., PRAMADA, P. N., Adsorption, **12**, 2006, p. 27
30. HO, Y.S., MCKAY, G., Process Biochem. (Amsterdam, Neth.), **34**, 1999, p. 451
31. LV, L., HE, J., WEI, M., EVANS, D.G., ZHOU, Z., Water Res., **41**, 2007, p. 1534
32. EL-KAMASH, A.M., ZAKI, A.A., ABDEL, M., GELEEL, E., J. Hazard. Mater. B, **127**, 2005, p. 211
33. ALLEN, S.J., MCKAY, G., PORTER, J.F., J. Colloid Interface Sci., **280**, 2004, p. 322
34. HO, Y.S., NG, J.C.Y., MCKAY, G., Sep. Purif. Rev., **29**, 2000, p. 189

Manuscript received: 16.10.2012

Adsorption Properties of Fe_2O_3 and Fe_2O_3:SiO_2 Mixtures in the Removal Process of As(III) from Underground Waters

ADINA NEGREA [1], LAVINIA LUPA [1]*, RADU LAZAU [1], MIHAELA CIOPEC [1], OANA POP [1], MARILENA MOTOC[2]

[1]University Politehnica Timisoara, Faculty of Industrial Chemistry and Environmental Engineering, Piata Victoriei, 300006 Timisoara, Romania

ADINA NEGREA*, LAVINIA LUPA*, RADU LAZAU*, MIHAELA CIOPEC*, OANA POP*, MARILENA MOTOC**

[2] **"Victor Babes" University of Medicine and Pharmacy, 2 Piata Eftimie Murgu, 300041, Timisoara, Romania

The effect of SiO_2 addition to the Fe_2O_3 adsorbent composition onto the adsorption performance in the removal process of As(III) from waters was studied. The studied materials (Fe_2O_3 and mixtures Fe_2O_3:SiO_2) were obtained by annealing at 800°C of ammonium ferric alum and Mohr salts, alone or mixed with SiO_2. SiO_2 was added to the Fe_2O_3 exhausted adsorbent with arsenic content in order to make it suitable for recycling in iron glass applications. Equilibrium, kinetic and thermodynamic studies were carried out to study the adsorption performance of the obtained oxides in the removal process of As(III) from aqueous solutions and from natural underground waters. The study revealed that SiO_2 presence significantly improves the adsorption capacity of the powders. All the studied materials are very efficient as adsorbents in the removal process of As(III) from natural underground water. This behaviour is very favourable for the perspective of the waste immobilization in vitreous matrices.

Keywords: arsenic adsorption, kinetic, thermodynamic, Fe_2O_3:SiO_2 mixtures

Many countries in the world use ground water as source of drinking water. However, ground water is often contaminated with Fe, Mn, As and other impurities. The presence of contaminants in the ground water has an adverse effect on human health. Arsenic is one of the known toxic elements found in ground water in many parts of the world. Arsenic in ground water is found in organic and inorganic forms, which are far more toxic than the organic forms, as As(III) and As(V) [1]. At the same time, it is reported that inorganic As(III) combinations are more toxic than As(V) and organic arsenicals [2]. The toxicity of arsenic at high concentration has been known for centuries. However, arsenic is difficult to detect in water, since it has no odour, no taste and has no visible appearance. The presence of arsenic in drinking water has serious adverse effects on human health and other living organisms [3-6].

The issue concerning arsenic presence in drinking water will increase in the coming years. The only ways to avoid the toxicity of arsenic present in drinking water is to use arsenic-free water sources or to remove the arsenic from drinking water. The World Health Organization (WHO) guideline for acceptable arsenic concentration in drinking water is 10 μg/L [1, 2, 7, 8].

There are many techniques for arsenic removal from dinking water. Among these techniques are enhanced coagulation, lime softening, reverse osmosis, nano filtration, in-situ sub-surface arsenic removal, ion exchange and adsorption [1, 2, 7-16].

The choice of an appropriate arsenic removal technique depends on the removal effectiveness, efficiency, cost, suitability for central and point of use, as well as simplicity of technique. Adsorption proved to be the most effective procedure in arsenic removal, even from very low concentration solutions. So far, various adsorbents, either natural or synthetic have been developed for arsenic removal. These include metal oxides/ hydroxides [1, 7, 8, 10, 17-19], natural and synthetic zeolites [6], laterite soil [2, 3, 8], calcite [20], activated carbon [4, 5, 21] or organic polymers [22]. According to literature data, iron compounds in general and particularly iron hydroxides are very efficient adsorbents for arsenic removal [1, 8-10, 17, 19, 21, 23, 24]. In this paper the adsorption performance of the iron oxides, obtained through annealing at 800°C of the ammonium ferric alum – $Fe^{3+}(NH_4)(SO_4)_2 \cdot 12H_2O$ and Mohr salt – $Fe^{2+}(NH_4)_2(SO_4)_2 \cdot 6H_2O$, in the removal process of As(III) from aqueous solution, has been investigated. In order to resolve the issue of the resulted sludge after adsorption we propose the recycling of the exhausted adsorbent with arsenic content in iron glass applications. This idea starts from the fact that in glass application arsenic is used under As_2O_3 form. Even if is very toxic it is practically irreplaceable in these mixtures, because of its role as an effective O_2 carrier at high temperatures [25-28]. In order to make it more suitable for glass applications and for the further studies we added SiO_2, as Ultrasil VN3 (Degussa), in the adsorbent composition. The objective of this paper is to study the effect of the SiO_2 addition to the Fe_2O_3 composition, onto the adsorption performance of the studied materials in the removal process of arsenic from aqueous solutions. In order to determine the adsorption performance of the Fe_2O_3 and Fe_2O_3:SiO_2 powders the equilibrium, kinetic and thermodynamic studies were performed.

Experimental part

Adsorbent preparation and characterization

The iron salts (ammonium ferric alum – $Fe^{3+}(NH_4)(SO_4)_2 \cdot 12H_2O$ and Mohr salt – $Fe^{2+}(NH_4)_2(SO_4)_2 \cdot 6H_2O$) and the mixtures with Ultrasil have been loaded in porcelain crucibles and annealed in an electric kiln at 800°C, which is the lowest temperature necessary for their decomposition with the formation of Fe_2O_3. In the case of samples with SiO_2 content, this has been wet homogenized with the iron salts, in the mass ratio 1:1, in a porcelain dish, dried at 110°C and the resulted mixtures have been grinded in a mortar. After annealing the obtained iron oxides have

* email: lavinia.lupa@chim.upt.ro

Sample Symbol	The used salt	Phase composition	BET surface area (m^2/g)	Pore volume, (cm^3/g)	Average size of the pores, (Å)
S1	$Fe^{3+}(NH_4)(SO_4)_2 \cdot 12H_2O$	H	11.07	0.035	133
S2	$Fe^{2+}(NH_4)_2(SO_4)_2 \cdot 6H_2O$	H	8.22	0.037	178
S3	$Fe^{3+}(NH_4)(SO_4)_2 \cdot 12H_2O:SiO_2$=1:1	H	57.01	0.467	309
S4	$Fe^{2+}(NH_4)_2(SO_4)_2 \cdot 6H_2O:SiO_2$=1:1	H	57.01	0.427	287

Table 1
CHARACTERISTICS OF THE OBTAINED ADSORBENTS

been characterized through XRD phase analysis, and BET – accelerated surface area analysis. The XRD patterns were recorded on a Bruker D8 Advance System with monochromator, Cu $_{K\alpha}$ radiation. The specific surface area and the pore volume of the studied materials were measured using a Micrometrics ASAP 2020 BET surface area analyzer, by cold nitrogen adsorption.

Adsorption experiments

The experiments were performed with all studied materials at an initial *p*H of As(III) solutions between 6.7–7, the most common *p*H value found in the natural waters. The pH of the solutions was measured using a CRISON MultiMeter MM41 fitted with a glass electrode which had been calibrated using various buffer solutions.

Prior to such experiments a stock solution of arsenic was prepared by diluting an appropriate amount of 0.05 mol/L $NaAsO_2$ solution (Merck TitriPUR). Other As(III) solutions-were prepared from the stock solution by appropriate dilution.

In the first instance, the effect of the initial As(III) concentration (range:100 – 700 μg/L) was studied. In each experiments 0.1 g of adsorbent was suspended in 100 cm^3 of As(III) solutions of different concentrations. The samples were stirred 90 (min) using agitating device with glass rod (stirring speed 200 rpm) at room temperature 298 K. After stirring the samples were centrifuged at 1200 rpm for 10 minutes using a ROTINA 420 centrifuge. The arsenic residual concentration was determined from the resulted solution through atomic absorption spectrometry with hydride generation, using a spectrophotometer VARIAN SpectrAA 110 VGA 77. The As(III) content in the samples was analyzed by the selective reduction to arsine with $NaBH_4$ (0.6% w/v) solution in NaOH buffer (0.5%w/v). The arsine gas was carried over the flame of atomic absorption spectrophotometer and absorbance value noted at 193.7 nm was compared to the standard curve obtained from the standard arsenic solution.

To study the effect of contact time on adsorption at three temperatures 298 K, 303 K and 318 K, the experiments were carried out with samples of 0.1 g studied materials in 100 cm^3 of 100 μg/L As(III) solutions. The suspensions were stirred for various periods of time: 15, 30, 45, 60, 90 and 120 (min). After the contact time elapsed, the suspensions were centrifuged and the residual concentration of As(III) ions in the filtrates was determined by means of atomic absorption spectrometry.

The various chemicals employed in the experiments were of A.R. grade and used without further purification. Distilled water was used throughout. The adsorption performance is expressed as the amount of As(III) adsorbed per gram of adsorbent q_e (μg/g) and is calculated using the following equation [4, 7, 17, 29, 30]:

$$q_t = \frac{(C_0 - C_t) \cdot V}{m} \quad (1)$$

where C_0 and C_t are the concentrations of As(III) ions (μg/L) in the solution initially (t = 0) and after a time t (min), respectively, V is the volume of the solution (L) and m is the mass of adsorbent employed (g).

To evaluate the potential use of the studied materials as adsorbents for arsenic removal from natural waters, we treated two samples collected from two wells situated in the western area of Romania and having a known high arsenic concentration. The samples of water (100 cm^3 for each sample) were treated with the necessary amount of adsorbents (0.1 g) under the optimum conditions established by using the synthetic As(III) solutions. The initial and the residual concentrations of arsenic, as well as other metal ions were determined by atomic absorption spectrometric methods.

Results and discussions

Adsorbent characterization

The characteristics of the samples obtained after annealing at 800°C of the iron salts and of the mixture Fe_2O_3: SiO_2 respectively, are presented in table 1.

The XRD pattern of the samples obtained by annealing at 800°C of ammonium ferric alum – $Fe^{3+}(NH_4)(SO_4)_2 \cdot 12H_2O$ and Mohr salt – $Fe^{2+}(NH_4)_2(SO_4)_2 \cdot 6H_2O$, alone or mixed with SiO_2, reveals that the only crystalline phase present in the samples is the hematite (fig. 1).

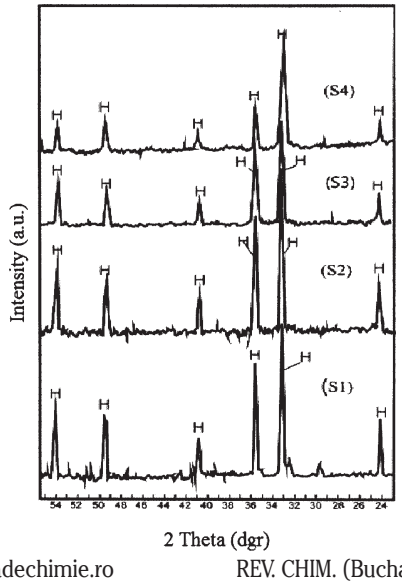

Fig. 1. X-Ray diffraction patterns of obtained iron oxides H-hematite (α-Fe_2O_3); JCPDS:33-0664

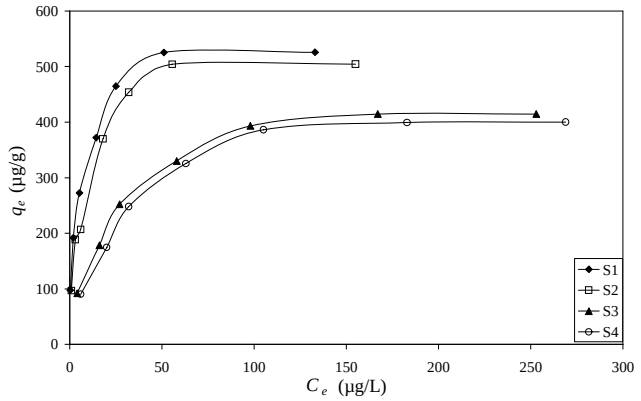

Fig. 2. Adsorption isotherms of As(III) onto studied materials C_o=(100-700 µg/L); V=100 cm^3; m=0.1 g; t=90 min; T=298 K; pH=6.7-7.0

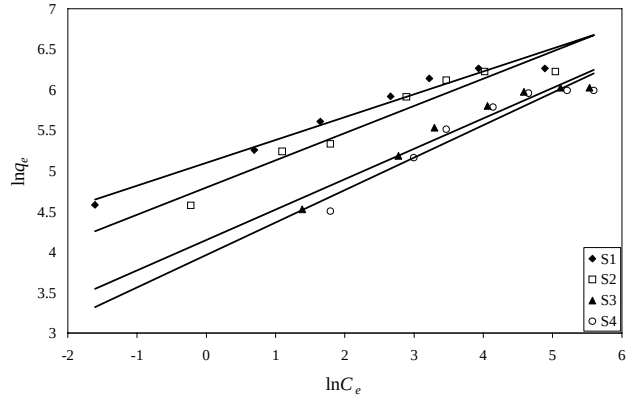

Fig. 3. Freundlich plot for As(III) adsorption onto the studied adsorbents

The BET surface area of the iron oxide obtained by annealing of Fe^{3+} ammoniacal double sulphate (ammonium ferric alum) is higher then the iron oxide obtained by annealing of Fe^{2+} ammoniacal double sulphate (Mohr salt). The presence of SiO_2 leads to the increase of the surface area in both cases, the surface area of the samples with SiO_2 content is practically identical (57.01 m^2/g) (table 1). From the BET surface area one could expect that the materials with the best adsorption capacity will be the mixtures Fe_2O_3:SiO_2.

Adsorption isotherms

The adsorption isotherms of As(III) removal by the studied materials are presented in figure 2.

The adsorption capacity increased with the increasing equilibrium concentration of arsenic for all the studied material and approached a constant value at the highest equilibrium concentration.

The adsorption equilibrium data were correlated with the well-known Freundlich and Langmuir isotherms [1, 5, 10, 19, 22, 29, 30].

The Freundlich isotherm in its linear form can be expressed as follows:

$$\ln q_e = \ln K_F + \frac{1}{n}\ln C_e \quad (2)$$

where q_e is the amount of As(III) adsorbed per gram of adsorbent, i.e., metal uptake (µg/g), and C_e is the equilibrium concentration of adsorbate in the bulk solution after adsorption (µg/L). K and $1/n$ are characteristic constants that can be related to the relative adsorption capacity of the adsorbent (µg/g) and the intensity of the adsorption, respectively. The logarithmic plot of q_e against C_e should result in a straight line that allows computations of $1/n$ and K_F from the slope and intercept, respectively (fig. 3).

The linear form of the Langmuir isotherm can be expressed as follows:

$$\frac{C_e}{q_e} = \frac{1}{K_L \cdot q_m} + \frac{C_e}{q_m} \quad (3)$$

where q_m is the measure of the monolayer sorption capacity (µg/g) and K_L denotes the Langmuir isotherm constant related to the affinity between adsorbent and the adsorbate (L/µg). The rest of the terms have their usual meanings as described above. The values of q_m and K_L can be determined by plotting C_e/q_e versus C_e (fig. 4).

The calculated parameters, as well as the correlation coefficients (R^2) for As(III) removal through adsorption onto the studied materials are presented in table 2.

The Freundlich plots (fig. 3) have very low regression coefficients suggesting a restriction on the use of Freundlich

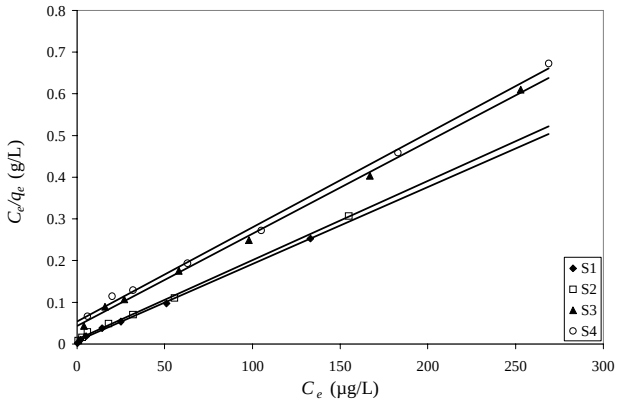

Fig. 4. Langmuir plot for As(III) adsorption onto the studied adsorbents

Adsorbent	$q_{m,exp}$ (µg/g)	Freundlich isotherm			Langmuir isotherm		
		K_F (µg/g)	$1/n$	R^2	K_L (L/µg)	$q_{m,calc}$ (µg/g)	R^2
S1	526	164	0.2812	0.9662	0.2611	555	0.9983
S2	505	121	0.3356	0.9350	0.1744	526	0.9982
S3	415	63.3	0.3751	0.9413	0.0511	454	0.9980
S4	400	52.6	0.4007	0.9193	0.0427	434	0.9971

Table 2
PARAMETERS OF FREUNDLICH AND LANGMUIR ISOTHERMS FOR AS(III) IONS ADSORPTION ONTO THE STUDIED MATERIALS

isotherm. The constants K_F and $1/n$ computed from the linear plot are presented in table 2. The constant K_F can be defined as an adsorption coefficient which represents the quantity of adsorbed metal ions for a unit equilibrium concentration. The slope $1/n$ is a measure of the adsorption intensity or surface heterogeneity. For $1/n = 1$, the partition between the two phases is independent on the concentration. The situation $1/n < 1$ is the most common and corresponds to a normal L-type Langmuir isotherm, whilst $1/n > 1$ is indicative of a cooperative adsorption which involves strong interactions between the molecules of adsorbate. Values of $1/n < 1$ show favourable adsorption of As(III) ions onto the studied materials. The Langmuir model effectively describes the sorption data for all the studied materials with correlation coefficient closer to 1. Thus the isotherm follows the sorption process in the entire concentration range studied for all four materials. Moreover the maximum adsorption capacities of the studied materials obtained from the Langmuir plot are very close to those experimentally obtained. The maximum adsorption capacities of As(III) developed by Fe_2O_3 obtained by annealing of the iron salts are higher than the adsorption capacities of As(III) developed by the mixtures Fe_2O_3:SiO_2. This is in contradiction with the conclusion resulted from the BET surface area. If one relates the adsorbent properties only to the Fe_2O_3 content (which is the active phase responsible for arsenic removal) of the samples S3 and S4, it may be said that the presence of SiO_2 significantly improves the adsorption capacity of the powders. A possible explanation for this situation refers to the hydroxylate character of the Ultrasil particles (even after annealing at 800°C) which leads to their hydration and dispersion of the Fe_2O_3 agglomerations in the presence of the aqueous solutions with As(III) content. This behaviour is very favourable for the perspective of the waste immobilization in vitreous matrices. The samples obtained by annealing of the Fe^{3+} ammoniacal double sulphate (S1 and S3) develop adsorption capacities higher than the samples obtained by annealing of the Fe^{2+} ammoniacal double sulphate (S2 and S4).

The dimensionless constant, called separation factor (R_L) can be used to describe the essential characteristics of a Langmuir isotherm.

$$R_L = \frac{1}{1 + K_L \cdot C_0} \quad (4)$$

where the terms have their meanings as stated above. In fact, the separation factor is a measure of the adsorbent capacity used. Its value decreases with increasing "K_L" as well as initial concentration. R_L values can be related to the equilibrium isotherm as follows: unfavourable, $R_L > 1$; linear, $R_L = 1$; favourable $0 < R_L < 1$; and irreversible, $R_L = 0$ [4, 5, 17, 21].

The values were calculated for the entire concentration range studied and the results are found to lie in between 0 and 1, in all the cases, demonstrating a favourable sorption process.

Adsorption kinetics

The kinetic of the adsorption describing the rate of the removal of arsenic is one of the important characteristic that defines the efficiency of adsorption. Figure 5 shows the time profile of As(III) adsorption onto the studied materials with an initial concentration of 100µg/L at three temperatures 298 K, 303 K and 318 K.

Experimental results indicate that the maximum adsorption is reached in 90 (min) for all the studied materials at all three studied temperatures. After 90 (min) of contact

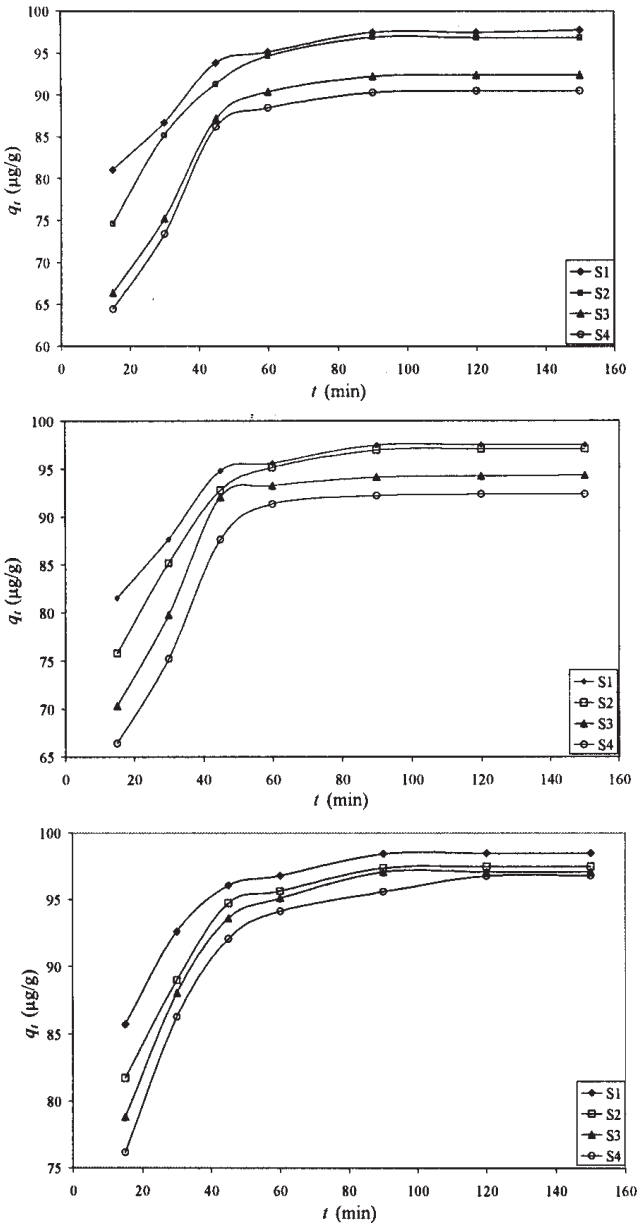

Fig. 5. Effect of contact time on the adsorption capacities of the studied materials
C_o=100 µg/L; V=100 cm^3; m=0.1 g; pH = 6.7-7.0 a) T=298 K; b) T=303 K; c) T=318 K

between adsorbent and adsorbate, the adsorption capacity hardly changed during the adsorption time.

In order to evaluate the kinetic mechanism that controls the adsorption process, the pseudo-first-order, pseudo-second-order and intraparticle diffusion models were tested to interpret the experimental data. Because of the poor regression coefficient (R^2) values of the Lagergren pseudo-first-order model and intra particle diffusion model, the results are not included in the text.

The linear form of the pseudo-second-order rate expression is given by [2, 5, 22,23]:

$$\frac{t}{q_t} = \frac{1}{k_2 \cdot q_e^2} + \frac{t}{q_e} \quad (5)$$

where k_2 is the pseudo-second-order rate constant (g/min . µg). q_e the amount of As(III) adsorbed (µg/g) at equilibrium and q_t is the amount of the adsorption (µg/g) at any time t. The pseudo second-order rate constant k_2 and q_e were calculated from the slope and intercept of the plots of t/q_t versus t (fig. 6). The experimental and calculated q_e values,

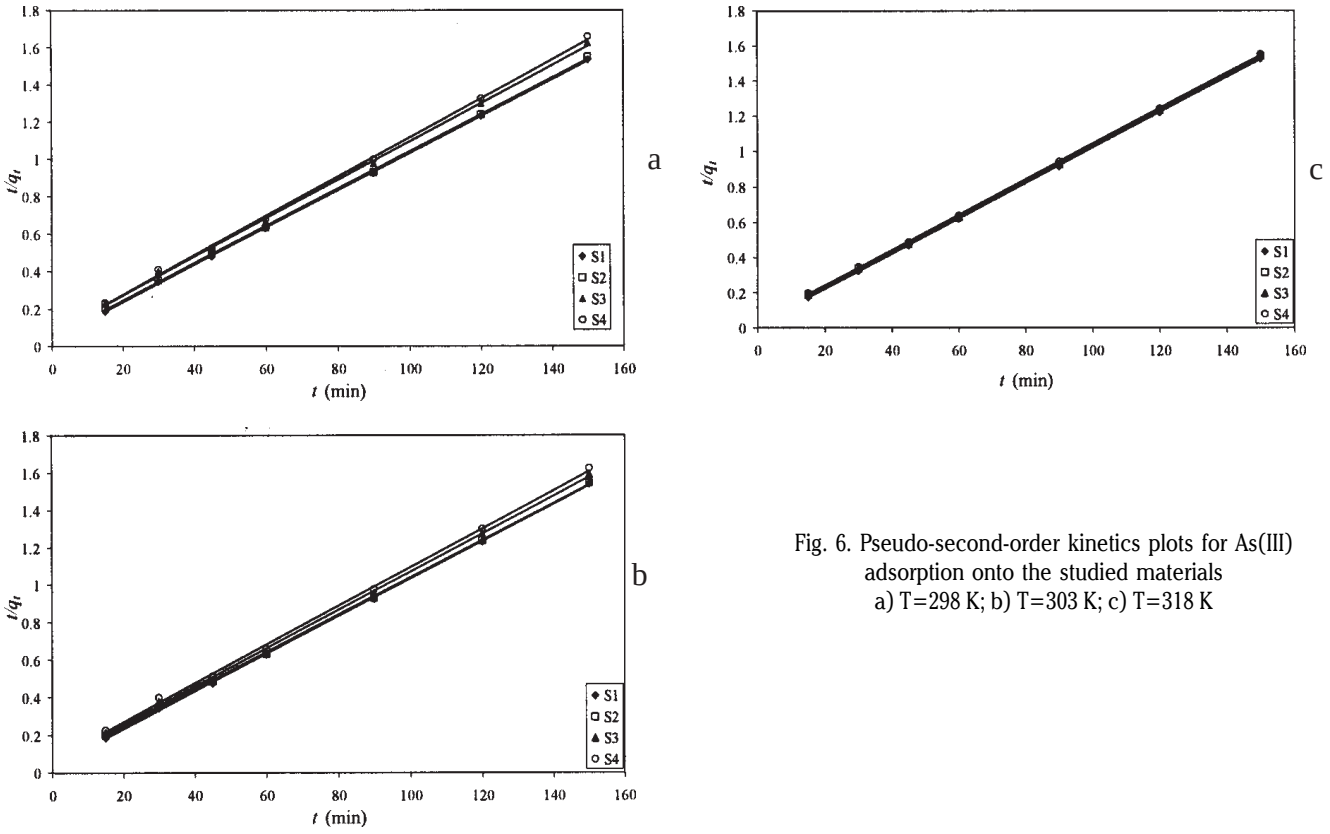

Fig. 6. Pseudo-second-order kinetics plots for As(III) adsorption onto the studied materials
a) T=298 K; b) T=303 K; c) T=318 K

Table 3
PSEUDO-SECOND-ORDER PARAMETERS FOR AS(III) ADSORPTION ONTO THE STUDIED MATERIALS

T (K)	Parameters	S1	S2	S3	S4
298	$q_{e,exp}$ (μg/g)	98	97	93	91
	$q_{e,calc}$ (μg/g)	100	100	97.1	95.2
	k_2 (g/min·μg)	$2.75 \cdot 10^{-3}$	$2.18 \cdot 10^{-3}$	$1.63 \cdot 10^{-3}$	$1.65 \cdot 10^{-3}$
	R^2	0.9998	0.9997	0.9990	0.9988
303	$q_{e,calc}$ (μg/g)	100	100	98	97.1
	k_2(g/min·μg)	$3.17 \cdot 10^{-3}$	$2.34 \cdot 10^{-3}$	$2.13 \cdot 10^{-3}$	$1.68 \cdot 10^{-3}$
	R^2	0.9998	0.9997	0.9990	0.9987
318	$q_{e,calc}$ (μg/g)	100	100	100	100
	k_2(g/min·μg)	$4.52 \cdot 10^{-3}$	$3.39 \cdot 10^{-3}$	$2.92 \cdot 10^{-3}$	$2.35 \cdot 10^{-3}$
	R^2	0.9999	0.9999	0.9998	0.9999

pseudo-second-order rate constants, R^2 values are presented in table 3.

The calculated q_e values are in agreement with the experimental q_e values and the plots show good linearity, with R^2 higher than 0.99 for all the studied adsorbent at all three studied temperatures. Hence, this study suggested that the pseudo-second-order kinetic model better represent the adsorption kinetics, and the adsorption process has the profile of a chemisorption.

The values of the rate constants from the pseudo-second-order model can be used to calculate the activation energy of the sorption process by Arhenius equation:

$$\ln(k_2) = \ln(A) - \frac{E}{RT} \quad (6)$$

where k_2 is the pseudo-second-order rate constant of sorption (g/min . μg), A the Arhenius constant which is a temperature independent factor (min·g/μg), E is the activation energy of sorption (kJ/mol) and T is the absolute temperature (K). The activation energy was calculated from the slope of the plots $\ln k_2$ versus 1/T for all the studied materials (fig. 7).

In this study the activation energy values were found to be 19.4, 17.9, 21.6 and 14.8 (kJ/mol) for S1, S2, S3 and S4, respectively. The magnitude of activation energy can give information on weather the adsorption process is physical or chemical. The activation energy of physisorption is normally not more than 4.2 (kJ/mol) [22]. Hence, the values of activation energy found in this study suggest that the adsorption of As(III) onto the studied materials is a chemical adsorption.

Adsorption thermodynamic

In general, the experimental conditions such as metal ion concentration and temperature have strong effects on the equilibrium distribution coefficient value (K_d); so it can

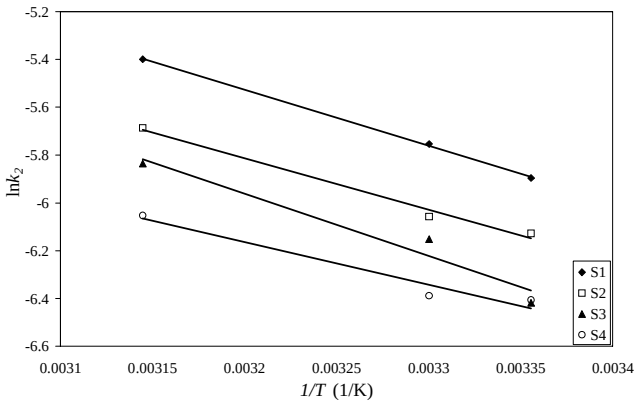

Fig. 7. Arhenius plot of As(III) adsorption onto the studied materials

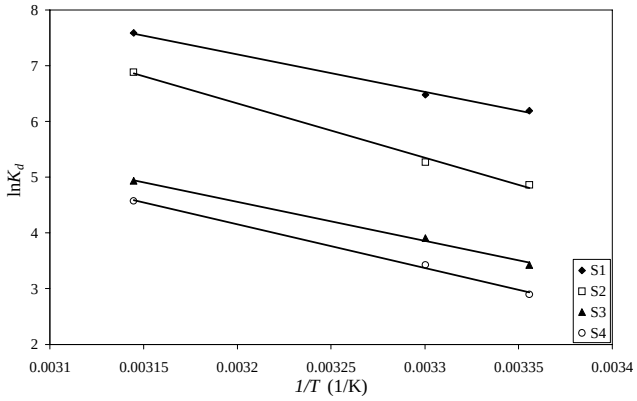

Fig. 8. Effect of temperature on the adsorption of As(III) onto the studied materials C_o = 100 μg/L; T = 90 (min); pH = 6.7-7.0

Adsorbent	$\Delta H°$ (kJ/mol)	$\Delta S°$ (J/mol·K)	ΔG^o (kJ/mol)			R^2
			298 (K)	303 (K)	308 (K)	
S1	55.8	239	-15.1	-16.6	-20.2	0.9963
S2	81.1	312	-11.9	-13.4	-18.1	0.9959
S3	58.3	225	-8.75	-9.88	-13.3	0.9964
S4	64.9	243	-7.51	-8.73	-12.4	0.9964

Table 4
THERMODYNAMIC PARAMETERS FOR AS(III) ADSORPTION ONTO THE STUDIED MATERIALS

be used as a comparative measure to the efficiency of various adsorbents. Equilibrium distribution coefficient value (K_d) is the amount of removed As(III) ions per gram of adsorbent divided by their concentration in the liquid phase:

$$K_d = \frac{q_e}{C_e} \quad (7)$$

Temperature dependence of the adsorption process is associated with several thermodynamic parameters. Thermodynamic considerations of an adsorption process are necessary to conclude whether the process is spontaneous or not. Thermodynamic parameters such as Gibbs free energy change ($\Delta G°$), enthalpy change ($\Delta H°$) and entropy change ($\Delta S°$) can be estimated using equilibrium constant changing with temperature. The Gibbs free energy change of the adsorption reaction is given by the following equation [7, 8, 22]:

$$\Delta G^o = -RT \ln K_d \quad (8)$$

where R is universal gas constant (8.314 J·mol/K), T is absolute temperature (K) and K_d is the distribution coefficient.

Table 5
INITIAL COMPOSITIONS OF THE UNDERGROUND WATER SAMPLES

Parameter	Sample 1	Sample 2
pH	6.7	6.8
Turbidity (NTU)	9	8.7
Conductivity (μS)	398	385
Ca (mg/L)	65	30.8
Mg (mg/L)	47	18.2
Na (mg/L)	105	118
K (mg/L)	1.65	1.67
Fe (mg/L)	5	2
Mn (mg/L)	0.5	0.51
Zn (mg/L)	<0.01*	<0.01*
As III (μg/L)	60.4	80

* detection limit

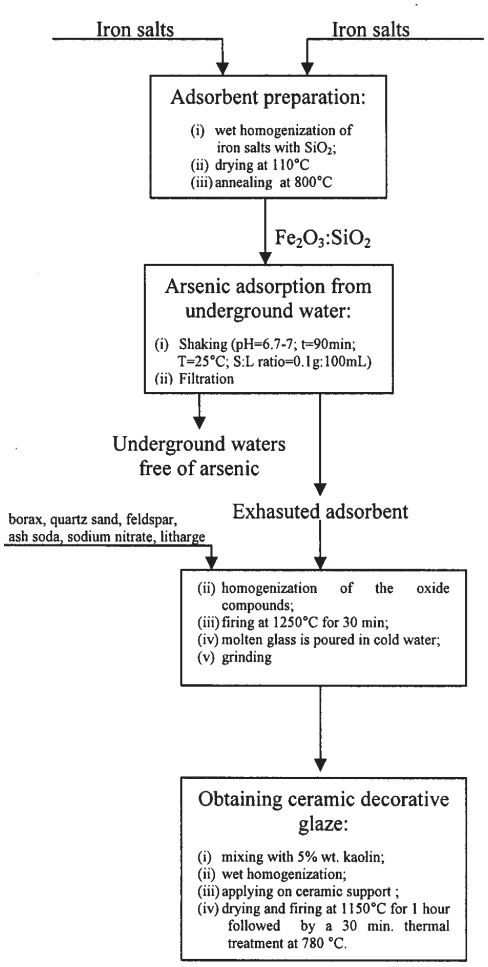

Fig. 9. Closed cycle technology for the treatment of ground water with arsenic content

Relation between ΔG°, ΔH° and ΔS° can be expressed by the following equations:

$$\Delta G^o = \Delta H^o - T\Delta S^o \quad (9)$$

$$\ln K_d = \frac{\Delta S^\circ}{R} - \frac{\Delta H^\circ}{RT} \quad (10)$$

where values of ΔH° and ΔS° can be determined from the slope and intercept of the plot between $\ln K_d$ versus $1/T$.

The thermodynamic parameters were determined from the slope and intercept of the plot of $\ln K_d$ versus 1/T (fig. 8). The values of ΔG°, ΔH° and ΔS° are given in table 4.

The negative values of ΔG° and positive values of ΔH° indicate that the adsorption of As(III) onto the studied materials is a spontaneous and endothermic process. The more negative value of ΔG° implies a greater driving force to the adsorption process. The values of ΔH° are high enough to ensure the strong interaction between the As(III) and studied materials. The positive values of ΔS° indicate an increased randomness at the solid-solution interface during the adsorption of As(III) onto the studied materials [1, 4, 6]. The increasing of the adsorption capacities of the studied materials at higher temperatures may be due to the pore size enlargement and/or activation of the adsorbent surface.

Arsenic adsorption from natural waters

To evaluate the potential use of the studied materials as adsorbents for arsenic removal from natural underground waters, we treated two samples collected from two wells with a known high arsenic concentration, situated in the western area of Romania. The compositions of underground water samples are presented in table 5.

After treatment of the underground water samples with the studied materials the water quality parameters were determined. It was observed that for all the studied adsorbents As(III) was practically totally removed from both of the underground waters, together with iron and manganese ions (residual concentrations were below the detection limit). In all the cases the *p*H of the treated waters remained almost the same as the initial waters suggesting that no post treatment is necessary. All these suggested that the studied materials could be used as an efficient adsorbent for As(III) removal from natural underground water.

Closed cycle technology for the treatment of ground water with arsenic content

Based on the gathered experimental data we propose the following closed cycle technology for the treatment of ground water with arsenic content.

The technological flow of the proposed process is presented in figure 9.

The proposed process of underground water treatment by using Fe_2O_3:SiO_2 adsorbents followed by the immobilization of the exhausted adsorbents in vitreous matrices represents a viable solution in accordance with the closed cycle technologies. The use of the exhausted adsorbent as raw material in frits answers both the environmental (the resulted waste does not raise any storage problem) and the economic issues (the use of some natural raw materials, as feldspar for example is diminished). The frit can be further processed in order to obtain a ceramic decorative glaze, since the overall iron content of the frit makes it suitable for obtaining aventurine glazes (generally 10-30% Fe_2O_3 in glaze). The arsenic presence (from the exhausted adsorbent content) in the raw materials mixture for frit preparation develops a positive effect (as high temperature oxygen carrier) by Fe^{3+} favoring in the crystalline matrices and thus to increase the proportion of hematite separated by crystallization during cooling glazes.

Conclusions

The effect of SiO_2 addition to the Fe_2O_3 adsorbent composition onto the adsorption performance in the removal process of As(III) from aqueous solutions and natural underground waters was studied. The addition of SiO_2 to the Fe_2O_3 samples increased the surface area of the samples, thus their adsorption capacity. At the same time the exhausted adsorbent with arsenic content became suitable for recycling in iron glass applications.

Adsorption data were modeled using Freundlich and Langmuir adsorption isotherms, and it was observed that the Langmuir model effectively describes the sorption data. The dimensional separation factor used to predict the essential characteristics of Langmuir isotherm indicates favorable adsorption in the entire concentration range.

The effect of contact time on As(III) sorption onto the studied materials revealed that the equilibrium is reached in 90 (min). The adsorption process followed a pseudo-second-order kinetic and theoretically predicted equilibrium sorption is close to that determined experimentally. This suggests that the adsorption process has a chemisorption profile. The values of activation energy found in this study suggests, also, that the adsorption of As(III) onto the studied materials is a chemical adsorption.

Temperature dependence of sorption reveals the increase in sorption performance of the adsorbents with temperature. The negative values of Gibbs free energy (ΔG°) show the spontaneous nature of As(III) adsorption and the positive values of the standard enthalpy (ΔH°) show the endothermic nature of As(III) adsorption onto the studied materials. Positive entropy (ΔS°) suggests the affinity of the studied materials for the arsenite in solution.

The studied materials are efficient adsorbents for As(III) removal from natural underground waters. This does not cause any increase in *p*H, suggesting that no post treatment is necessary.

The use of Fe_2O_3:SiO_2 mixtures is a cost-efficient solution for both water treatment and waste disposal, if the exhausted adsorbents will be immobilized in vitreous matrixes. The proposed underground water treatment is in accordance with the principle of sustainable development, being fit in the closed cycle technologies.

Acknowledgement: This paper is supported by the Sectoral Operational Programme Human Resources Development, financed from the European Social Fund and by the Romanian Government under the contract number POSDRU/86/1.2/S/58146 (MASTERMAT)".

References

1.BANERJEE, K., AMY, G. L., PREVOST, M., NOUR, S., JEKEL, M., GALLAGHER, P. M., BLUMENSCHEIN, C. D., Wat. Res., 42, 2008, p. 3371.
2.MAJI, S. K., PAL, A., PAL, T., J. Hazard. Mater., 151, 2008, p. 811.
3.MAITI, A., BASU, J. K., DE, S., Ind. Eng. Chem. Res., 49, 2010, p. 4873.
4.BORAH, D., SATOKAWA, S., KATO, S., KOJIMA, T. J., Colloid Inter. Sci, 319, 2008, p. 53.
5.BORAH, D., SATOKAWA, S., KATO, S., KOJIMA, T., J. Hazard. Mater., 162, 2009, p. 1269.
6.CHUTIA, P., KATO, S., KOJIMA, T., J. Hazard. Mater., 162, 2009, p. 204.
7.GUPTA, K., GHOSH, U. C., J. Hazard. Mater., 161, 2009, p.884.
8.PARTEY, F., NORMAN, D., NDUR, S., NARTEY, R., J. Colloid. Inter. Sci., 321, 2008, p. 493.
9.ZOUBOULIS, A.I., KATSOYIANNIS, I.A., Ind. Eng. Chem. Res., 41, no 24, 2002, p. 6149.
10.HSU, J. C., LIN, C. J., LIAO, C. H., CHEN, S. T., J. Hazard. Mater., 153, 2008, p. 817.
11.CHEN, Y. N., CHAI, L. Y., SHU, Y. D., J. Hazard. Mater., 160, 2008, p. 168.
12.SONG, S., LOPEZ-VALDIVIESO, A., HERNANDEZ-CAMPOS, D. J., PENG, C., MONROY-FERNANDEZ, M. G., RAZO-SOTO, I., Wat. Res., 40, 2006, p. 364.
13.BILICI BASKAN, M., PALA, A., Desalination, 254, 2010, p. 42.
14.BISSEN, M., FRIMMEL, F. H., 31, 2003, p. 97.
15.QU, D., WANG, J., HOU, D., LUAN, Z., FAN, B., ZHAO, C., J. Hazard. Mater., 163, 2009, p. 874.
16.KOSUTIC, K., FURAC, L., Sep.Purif. Technol., 42, 2005, p. 137.
17.NEGREA, A., LUPA, L., CIOPEC, M., MUNTEAN, C., LAZAU, R., MOTOC, M., Rev. Chim. (Bucharest), **61**, no.7, 2010, p. 691
18.JONSSON, J., SHERMAN, D. M., Chem. Geol., 255, 2008 p. 173.
19.VUKASINOVIC-PESIC, V. L., RAJAKOVIC-OGNJANOVIC, V. N., BLAGOJEVIC, N. Z., GRUDIC, V. V., JOVANOVIC, B. M., RAJAKOVIC, L. V. Chem. Eng. Commun., 199, no. 7, 2012, p. 849.
20.SO, H. U., POSTMA, D., JAKOBSEN, R., LARSEN, F., Geochim. Cosmochim. Acta., 72, 2008, p. 5871.
21.MONDAL, P., MAJUMDER, C.B., MOHANTY, B., J. Hazard. Mater., 150, 2008, p. 695.
22.RAMESH, A., HASEGAWA, H., MAKI, T., UEDA, K., Sep. Purif. Technol., 56, 2007, p.90.
23.MAITI, A., DASGUTA, S., BASU, J.K., DE, S., Ind. Eng. Chem. Res., 47, no 5, 2008, p. 1620.
24.YUDOVICH, Y. E., KETRIS, M. P., J. Coal Geol., 61, 2005, p. 141.
25.DAKHAI, S., ORLOVA, L. A., MIKHAILENKO, N. Yu., Glass and Ceramics, 58, 1999, p. 177.
26.LEVITSKII, I. A., Glass and Ceramics, 58, 2001, p. 223.
27.DVORNICHENKO, I. N., MATSENKO, S. V., Glass and Ceramics, 57, 2000, p. 67.
28.BILICI BASKAN, M., PALA, A.,J. Hazard. Mater., 166, 2009, p. 796.
29.NEGREA A., CIOPEC, M., LUPA, L., DAVIDESCU, C., M., POPA, A., NEGREA, P., MOTOC., M., Rev. Chim. (Bucharest), **62**, no.10, 2011, p. 1008
30.NEGREA, A., LUPA, L., CIOPEC, M., LAZAU, R., MUNTEAN, C., NEGREA, P. Adsorp. Sci. Technol., 28, 2010, p. 467

Manuscript received:13.11.2012

Conference paper

Adina Negrea, Adriana Popa*, Mihaela Ciopec, Lavinia Lupa, Petru Negrea, Corneliu M. Davidescu, Marinela Motoc and Vasile Mînzatu

Phosphonium grafted styrene–divinylbenzene resins impregnated with iron(III) and crown ethers for arsenic removal

Abstract: In the present work a polymer with phosphonium pendant groups impregnated with crown ether (dibenzo-18-crown-6) and loaded with iron ions was investigated for arsenic removal through adsorption from aqueous solutions. The impregnated polymer was loaded with iron ions due to the high affinity of arsenic to it. The characterization of the surface modification of the obtained new adsorbent material was performed on the basis of energy dispersive X-ray analysis; scanning electron microscopy and Fourier transform infrared spectroscopy. The arsenic adsorption was investigated, including effect of pH, arsenic initial concentration, the shaking time and temperature. The effect of the pH was examined over the range 2–11. The adsorption of As(V) increases with pH increasing reaching a maximum at pH higher than 8. Equilibrium, kinetic and thermodynamic studies were carried out to study the adsorption performance of the obtained material in the removal process of arsenic from aqueous solutions. For the studied materials the equilibrium data closely fitted Langmuir model and was achieved a maximum adsorption capacity of 32.6 μg As(V)/g of material. The pseudo-second order kinetic model is suitable for describing the adsorption system. The obtained results show that the studied adsorbent can be used with efficiency in the arsenic removal from underground water even from low influent arsenic concentration solutions.

Keywords: arsenic removal; crown ether; POC-2014; polymer with phosphonium pendant group.

DOI 10.1515/pac-2014-0806

Introduction

Arsenic is a highly toxic element even at low concentration thus creating potentially serious environmental concerns worldwide [1–5]. Therefore the development of new technologies to remove traces of arsenic from drinking water, wastewaters and industrial effluents in order to reach acceptable levels is still a challenging for the scientific community. Several methods are used to remove arsenic from aqueous solutions like

Article note: A collection of invited papers based on presentations at the 15th International Conference on Polymers and Organic Chemistry (POC-2014), Timisoara, Romania, 10–13 June 2014.

***Corresponding author: Adriana Popa,** Institute of Chemistry Timisoara of Romanian Academy, Romanian Academy, 24 Mihai Viteazu Blv., 300223 Timisoara, Romania, e-mail: apopa_ro@yahoo.com
Adina Negrea, Mihaela Ciopec, Lavinia Lupa, Petru Negrea, Corneliu M. Davidescu and Vasile Mînzatu: Faculty of Industrial Chemistry and Environmental Engineering, University Politehnica Timisoara, 6 V. Parvan Blv., 300223, Timisoara, Romania
Marinela Motoc: Faculty of Medicine, University of Medicine and Pharmacy "Victor Babeş", 2 Eftimie Murgu Square, 300041, Timisoara, Romania

oxidation-reduction, precipitation, coagulation and co precipitation, adsorption, electrolysis and cementation, solvent extraction, ion exchange, etc. Each of the above processes has its own advantages and disadvantages which make the difficulty to select a suitable process. The disadvantages of traditional methods are high cost (coagulation–flocculation–filtration, oxidation and nanofiltration), high sludge production (coagulation–flocculation, electrochemical treatment), membrane fouling (nanofiltration), and constant monitoring of the ions concentration (ion exchange) [6]. From all these technologies sorption technique proved to be the most effective method, especially to remove traces of arsenic from drinking water [1, 2, 7–19]. Various adsorbents have been developed for arsenic removal [2, 3, 5–8, 18–25]. Some of the studied adsorbents developed very high adsorption capacities in the removal process of arsenic from drinking water, of the order of hundreds mg/g, but unfortunately these adsorbents could not remove arsenic from aqueous solutions containing a concentration under 100 μg/L, in such a way to give residual concentrations bellow the maximum admitted value by the World Health Organization (10 μg/L). More expensive technologies are required to achieve arsenic contaminant levels <10 ppb. Therefore the purpose of our research is to obtain an adsorbent which could be efficiently used in the removal process of arsenic from aqueous solutions having concentration under 100 μg/L. These concentrations were the most common found in the underground waters from the west area of Romania and east area of Hungary [26, 27]. Crown ether compounds have a considerable potential to be used as metal-selective reagents in the separation science due to their ability to form stable complexes with metal ions [28–30]. Therefore we focused on the use of dibenzo-18-crown-6-crown ether, in the removal process of arsenic from aqueous solutions, which is the simplest and the cheapest crown ether. The selective separation of elements by crown ether is managed either by the accommodation of ions within their circular cavity or in the three dimensional cavity like structures formed between the macroring and the sidearms [31, 32]. In order that, the use of dibenzo-18-crown-6-crown ether, in the removal process of arsenic from aqueous solutions, to be considered a cost effective option, we thought to attach this compounds to a solid support. The efficiency of such system leads to the development of new separation systems, with the use of solid supported crown ethers, which are capable of high selectivity or recognition towards a particular species of metal or metalloid [32]. Styrene-7%divinylbenzene copolymer with quaternary phosphonium pendant group was used as the macromolecular support. The modification of the polymeric matrix through functionalization of their surface with different phosphorus pendant groups lead to an increase of the adsorption efficiency of the polymers in the removal process of metals ions from various aqueous solutions [33, 34]. Also, in order to enhance the adsorption properties and the selectivity of the studied materials for arsenic removal, the polymer with phosphonium pendant group and impregnated with dibenzo-18-crown-6-crown ether was loaded with iron ions due to the high affinity of arsenic to it [1, 4, 7, 8, 10, 13]. Comparing with the simple ion exchange the metal loaded ligand exchanger develops rapid, selective and great efficiency in the removal process of trace arsenic from aqueous solutions [35–37]. In this way is combined the advantages of the resin such as: excellent hydraulic properties and mechanic strength with the excellent selectivity offered by the loaded metal [38]. Even if the metal ion content (weight %) of the loaded resin is much less than the metal oxide, the resulted adsorbent present a higher efficiency due to its mechanical integrity and its possibility to be used for several cycles [39]. The purpose of this paper is to develop an adsorbent material which presents higher efficiency in the removal process of arsenic from aqueous solutions containing low concentrations. In this way the study was conducting investigating the effect of pH, arsenic initial concentration, shaking time and temperature upon the adsorption capacity of the obtained material.

Experimental

Chemical reagents

Chloromethylated styrene–7%divinylbenzene copolymer (Victoria Chemical Plant, Romania), triphenylphosphine (Merck, p.a.), were used for the preparation of copolymer grafted with phosphonium groups.

The crown ether (dibenzo-18-crown-6) used for the impregnation was purchased from Sigma-Aldrich and $Fe(NO_3)_3$ in 0.5 mol/L HNO_3 solution (Merck Standard Solution) was used for the polymers loading with Fe(III).

The stock solution of arsenic was prepared by diluting an appropriate amount of H_3AsO_4 in 0.5 M HNO_3 solution (Merck Standard Solutions). Other solutions of As(V) ions were prepared from the stock solution by appropriate dilution.

All other chemicals used for experiments were of analytical reagent grade, and were used without further purification. Distilled water was used in all experiments.

Preparation of phosphonium salts grafted on styrene-7%divinylbenzene copolymer impregnated with crown ether and with loaded Fe(III) ions

Quaternary phosphonium pendant groups grafted on St–DVB copolymer was obtained by the method previously described [40] (Scheme 1).

The impregnation of crown ether (dibenzo-18-crown-6) onto the copolymer functionalized with phosphonium pendant groups was realized through a dry method of impregnation [34].

One gram of polymer with pendant groups was impregnated with 0.01 g of crown ether which was previously dissolved in acetone.

After impregnation the samples were treated with 25 mL of Fe(III) solution having a concentration of 100 mg/L.

Instruments

The characterization of the surface modification of the new obtained adsorbent material was performed on the basis of energy dispersive X-ray analysis; scanning electron microscopy and Fourier transform infrared spectroscopy. The FTIR spectra (KBr pellets) of the obtained impregnated solid supports with Cyphos IL-101 were recorded on a Shimadzu Prestige-21 FTIR spectrophotometer in the range 4000–400 cm^{-1}. The surface morphology of the impregnated material was investigated by scanning electron microscopy (SEM) using a Quanta FEG 250 Microscope, equipped with EDAX ZAF quantifier. The residual concentration of As(V) ions was determined by means of atomic absorption spectrometry using a Varian SpectrAA 110 atomic absorption spectrometer with a Varian VGA 77 hydride generation system.

Sorption experiments

In order to determine the efficiency of the obtained adsorbent material in the removal process of arsenic from aqueous solutions the effect of the pH, stirring time, arsenic initial concentration and temperature, was investigated. We focused on the removal of As(V) from aqueous solutions because in the most of the water treatment systems in the first step the arsenite is oxidized to arsenate, due to the fact that arsenic in the pentavalent arsenate form is more readily removed than the trivalent arsenite form [2, 3, 12]. The adsorption performance of the studied material was expressed as arsenic metal uptake (μg/g) eq. 1. [1–5]:

$$q_e = \frac{(C_0 - C_e)\cdot V}{m} \tag{1}$$

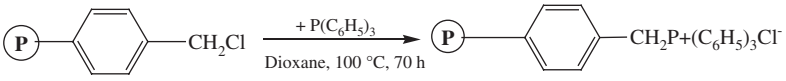

Scheme 1 Synthesis of quaternary phosphonium pendant groups grafted on St-7%DVB copolymer.

where: C_0 and C_e are the concentrations of arsenate (μg/L) in the solution, initially ($t = 0$) and at equilibrium, respectively, V is the volume of the solution and m is the mass of adsorbent.

In all the adsorption experiments the solid-liquid ratio used was 0.1 g of adsorbent in 25 mL of arsenic containing aqueous solutions. The effect of the pH was examined over the range 2–11. The effect of the arsenic initial concentration was examined over the range [25–175 μg/L As(V)]. The effect of stirring time (2, 4, 6, 8 h) was determined at three temperature (298, 308, 318 K). For the samples stirring a Julabo shaker was used.

In order to evaluate the efficiency of the obtained adsorbent it was used for the treatment of real underground water having the next composition: NO^{3-}: 18 mg/L; NO^{2-}: 0.5 mg/L; P_2O_5: 5 mg/L; SO_4^{2-}:11 mg/L; NH_4^+: 6.4 mg/L; Fe^{n+}: 1.8 mg/L; Mn^{2+}: 0.6 mg/L; Na^+: 120 mg/L; K^+: 1.75 mg/L; Ca^{2+}: 30 mg/L; Mg^{2+}: 18 mg/L; As^{n+}: 60 μg/L.

In order to recover and reuse of the adsorbent 0.2 g of exhausted adsorbent was treated with 25 mL of HCl solution having various concentrations (5, 10 and 15 %) under stirring for 4 h at the room temperatures. After the contact time elapsed the filtrate was collected for arsenic analysis.

Results and discussion

Adsorbent characterization

The obtained St-DVB copolymer after grafting with phosphonium pendant groups and impregnating with crown ether and Fe(III) ions was subjected to the FTIR analysis in order to prove that the impregnation occurred. The FTIR spectrum is provided in Fig. 1.

In the IR spectrum of this material the absorption band can be observed of the dibenzo-18-crown-6-crown ether unit [the intense bands about 1000 cm^{-1} and 1100 cm^{-1} are attributed to the $\nu_{sym}(C_{alphatic}\text{-}O\text{-}C_{aromatic})$ respectively $\nu_{asym}(C_{alphatic}\text{-}O\text{-}C_{alphatic})$] [36, 37]. The formation of the PPh_3Cl^- was confirmed by the appearance of the absorption bonds at 1130–1110 and 1440–1390 cm^{-1} associated with the stretching vibrations of the C_{phenyl}-H bonds and with the planar P-C_{phenyl} bonds, respectively [41, 42]. The band at 498 cm^{-1} is attributed to the group of vibrations $\nu_{Fe\text{-}O} + \nu_{C\text{-}C}$. The IR spectrum confirms the fact that the studied solid support was impregnated with the crown ether and loaded with the iron ions.

The SEM image and the EDAX quantification of the obtained material is presented in Fig. 2. From the SEM image can be observed that the smooth surface of the polymer with phosphonium pendant group is covered with a thin film of crown ether on which is bound the iron ions (the white particles). The EDAX quantification

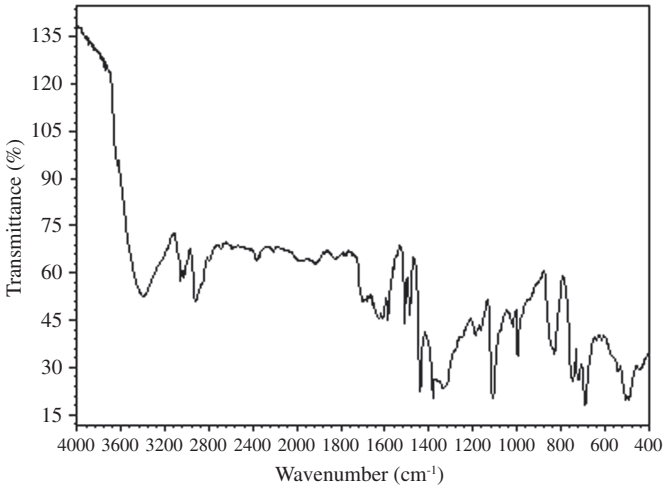

Fig. 1 IR vibrational spectrum of the obtained material.

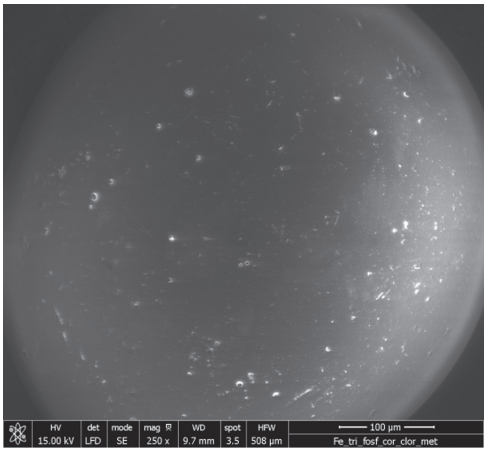

Element	Wt %
C	86.77
O	7.55
P	3.8
Cl	1.56
Fe	0.22
Total	100.00

Fig. 2 SEM image and the EDX quantification of the obtained material.

also proved that the polymer with phosphonium pendant group was impregnated with the crown ether and loaded with iron ions.

The pH influence onto As(V) adsorption process

The influence of pH on the amount of As(V) uptake can be explained by the results given in Fig. 3.

The data obtained indicate that the relative amount of As(V) taken up by the studied adsorbent increases with increasing pH of the medium, reaching a maximum at pH higher than 8. This behavior confirm the fact that As(V) is present in the aqueous solution as anionic species [$H_2AsO_4^-$ or $HAsO_4^{2-}$] [3, 7, 8] and is more easily removed due to the fact that the surface of the studied adsorbent is protonated because of the Fe(III) ions loaded [33, 43]. The further experiments were performed at an initial pH of the As(V) solution around 8.

Equilibrium studies

The equilibrium studies were conducted in order to determine the maximum adsorption capacities of the studied material in the removal process of As(V) from aqueous solutions as a function of its surface prop-

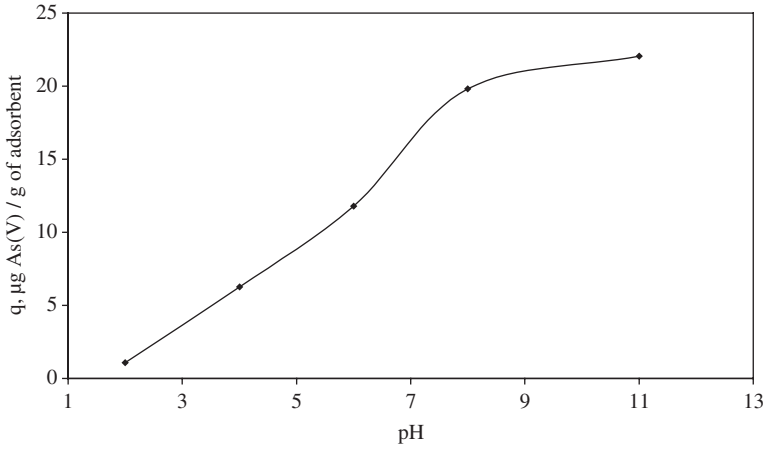

Fig. 3 The dependence of the As(V) uptake versus the pH of the solution.
C_i = 100 µg/L, V = 25 mL, t = 1 h, m = 0.1 g.

erties. The adsorption isotherm of As(V) removal by the studied material is presented in Fig. 4. It can be observed that the initial removal of As(V) is fast and at higher equilibrium concentration the adsorption capacity achieve a constant value.

The profile obtained from the study of As(V) initial concentration was used to obtain Langmuir and Freundlich adsorption isotherms by using well-known adsorption isotherm equation [1–4, 8]. In both cases linear plots were obtained, that reveal the applicability of these isotherms in the outgoing adsorption process. Figures 5 and 6 exhibit Freundlich and Langmuir plots, respectively, for As(V) adsorption onto the studied materials. The regression coefficients together with different Freundlich and Langmuir parameters derived from Freundlich and Langmuir plots are presented in Table 1.

From the experimental data can be observed that the correlation coefficient (R^2) obtained for the Freundlich isotherm is less than that obtained with Langmuir isotherm, where it is closed to unity. This indicate that the Langmuir isotherm describe better the adsorption process of As(V) onto the studied material. Moreover the maximum adsorption capacity of the studied material obtained from the Langmuir plot is very close to that obtained experimentally. The Langmuir mode assumes that the surface of the adsorbent is homogenous and the sorption energy to be equivalent for each sorption site. The essential characteristics of the Langmuir isotherm parameters can be used to predict the affinity between the sorbate and sorbent using separation factor or dimensionless equilibrium parameter, R_L expressed as in the following equation:

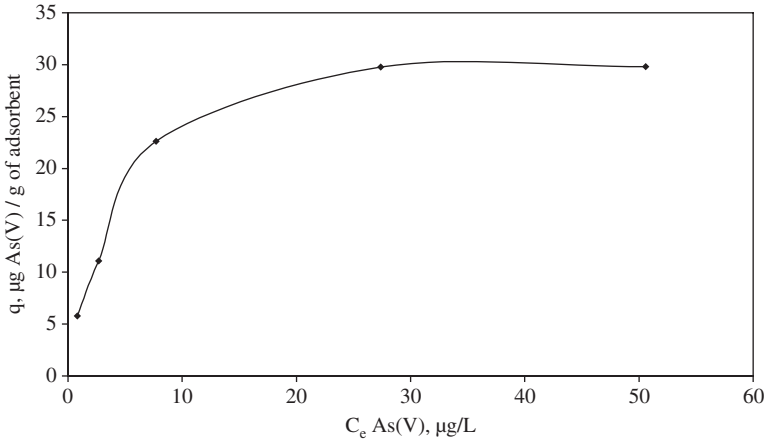

Fig. 4 As(V) adsorption isotherm onto the studied material.
pH = 8, V = 25 mL, t = 4 h, m = 0.1 g.

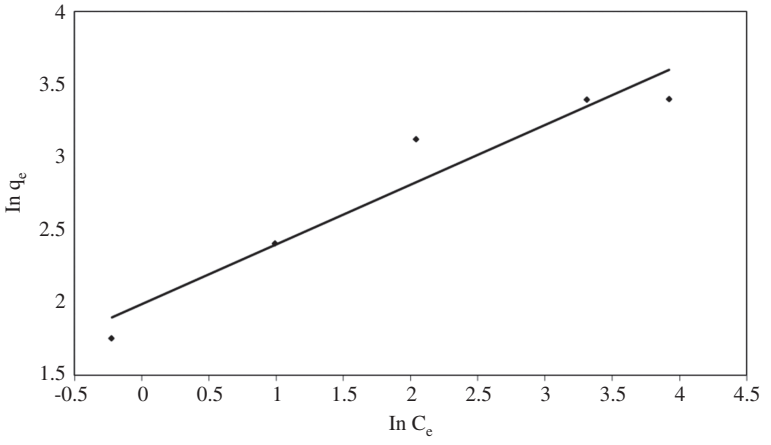

Fig. 5 Freundlich isotherm of As(V) adsorption onto the studied material.

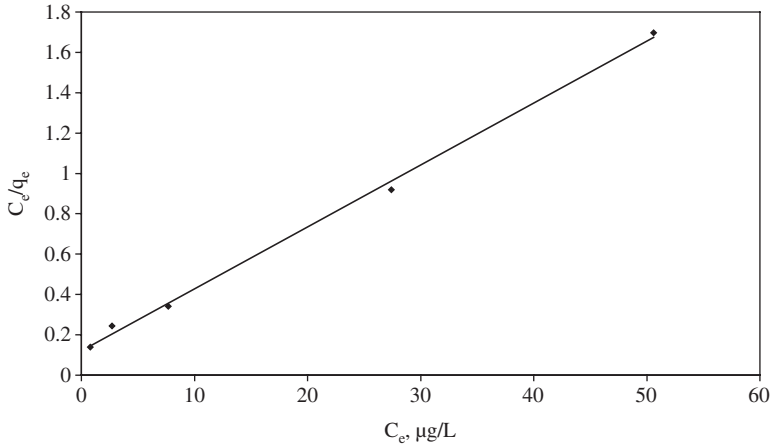

Fig. 6 Langmuir isotherm of As(V) adsorption onto the studied material.

Table 1 Parameters of Langmuir and Freundlich isotherms for As(V) adsorption onto the studied material.

$q_{m,exp}$ µg/g	Langmuir isotherm			Freundlich isotherm		
	K_L L/µg	$q_{m,calc}$ µg/g	R^2	K_F µg/g	1/n	R^2
30	0.2556	32.6	0.9975	7.31	0.4048	0.9271

$$R_L = \frac{1}{1+K_L C_0} \tag{2}$$

where K_L is the Langmuir constant and C_0 is the initial concentration of As(V) ions. The value of separation parameter R_L provides important information about the nature of adsorption. The value of R_L indicated the type of Langmuir isotherm to be irreversible ($R_L = 0$), favorable ($0 < R_L < 1$), linear ($R_L = 1$), or unfavorable ($R_L > 1$). The R_L was found to be between 0 and 1 for the entire concentration range, which indicates the favorable adsorption of As(V) onto the studied material. Due to the fact that the Langmuir isotherm fit the experimental data better than the Freundlich isotherm, it can be mentioned that the arsenic ions are adsorbed uniform onto the surface of the studied adsorbent, because of the homogenous distribution of active site onto the surface. In this case there is no migration of the arsenic ions onto the surface of the studied adsorbent, these suggesting that there is a possible chemisorption between the adsorbent and adsorbate.

Kinetic studies

In the batch experiments, kinetic studies are used to determine the contact time of the adsorbent with adsorbate and to evaluate the reaction coefficients. Adsorption kinetics were evaluated at pH = 8 at an initial As(V) solution concentration of 100 µg/L at three different temperatures (298 K, 308 K, 318 K). Arsenate adsorption onto the studied material was rapid and essentially complete within 4 h for all the studied temperatures (Fig. 7). At higher stirring times the adsorption capacity becomes linearly constant. This may be due the overlapping of active sites with arsenic species and also due to decrease in the effective surface area resulting in the conglomeration of exchange particle [8]. Adsorption capacity increase with the temperature, this indicates that the adsorption is endothermic in nature.

In order to investigate the mechanism of arsenate adsorption onto the studied material the two kinetic models were analysed: pseudo-first-order equation [1–4, 33], based on the solid capacity and pseudo-second-order reaction model [1–4, 33], based on the solid phase adsorption and implying that the chemisorption is

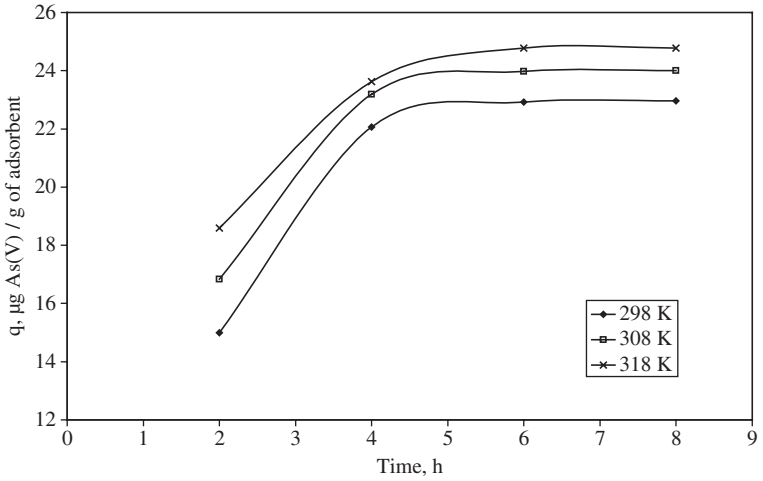

Fig. 7 Effect of contact time on the adsorption capacity of the studied materials. C_0 = 100 μg/L; m = 0.1 g; V = 0.025 L; pH = 8.

the rate controlling step. The pseudo-first-order and pseudo-second-order kinetic models were employed to investigate the mechanism of sorption processes such as mass transfer and chemical reactions. The plots of the both linear equation are presented in Figs. 8 and 9. The slopes and intercepts were used to calculate the adsorption rate constant and theoretical adsorption capacity which were presented in Table 3. From Table 2 it can be observed that the degree of fit R^2 for the pseudo-second-order ($R^2 > 0.99$) is higher than those of the pseudo-first-order model ($R^2 < 0.90$). Accordingly, the pseudo-second-order kinetic model is applicable the plot of t/qt versus t showing a straight line (Fig. 9). Also, the q_e calculated values are fitted the experimental data. This suggests that the pseudo-second-order adsorption mechanism is predominant and that the overall rate of the As(V) adsorption process appeared to be controlled by the chemical process [5, 8].

Thermodynamic studies

Thermodynamic parameters like activation energy, Gibbs free energy (ΔG), entropy (ΔS) and heat of adsorption (enthalpy ΔH) were evaluated by the following equation [7, 8]:

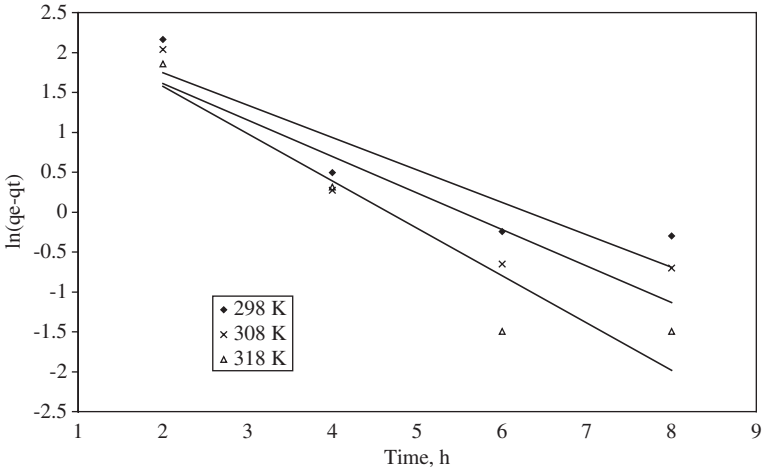

Fig. 8 Pseudo-first-order kinetic model of As(V) adsorption onto the studied material.

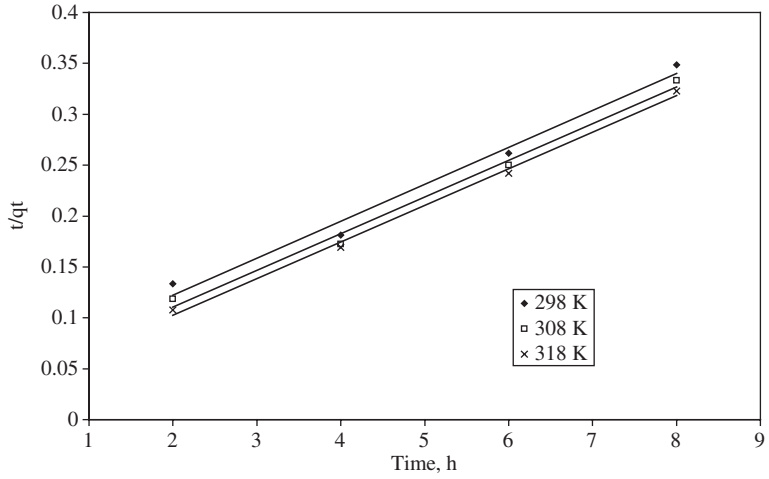

Fig. 9 Pseudo-second-order kinetic model of As(V) adsorption onto the studied material.

Table 2 Kinetic parameters for As(V) sorption onto the studied material at three different temperatures.

Temperature	298 K	308 K	318 K
Model/parameters			
$q_{e,exp}$, μg/g	23.5	24.5	25
Pseudo-first-order model			
$q_{e,calc}$, μg/g	12.4	12.5	15.8
k_1, 1/h	0.4062	0.4571	0.5928
R^2	0.8343	0.8513	0.8967
Pseudo-second-order model			
$q_{e,calc}$, μg/g	27.5	27.7	27.9
k_2, 1/h·1/(μg/g)	0.0265	0.0340	0.0418
R^2	0.9907	0.9912	0.9961

$$\ln(k_2) = \ln(A) - \frac{E}{RT}; \tag{3}$$

$$\Delta G^\circ = -RT \ln K_d; \tag{4}$$

$$\Delta G^\circ = \Delta H^\circ - T\Delta S^\circ; \tag{5}$$

$$\ln K_d = \frac{\Delta S^\circ}{R} - \frac{\Delta H^\circ}{RT}; \tag{6}$$

$$K_d = \frac{q_e}{C_e}; \tag{7}$$

where: k_2 is the pseudo-second-order rate constant of sorption (1/h·1/(μg/g), A the Arhenius constant which is a temperature independent factor (h·g/μg), E is the activation energy of sorption (kJ/mol), T is the absolute temperature (K), R is universal gas constant (8.314 J/mol·K) and K_d is the distribution coefficient.

The activation energy (E) was obtained from the slope of the plot between $\ln(K_2)$ versus $1/T$ (Fig. 10).

The magnitude of activation energy can give information whether the adsorption process is physical or chemical. The activation energy of physical sorption is normally not more than 4.2 kJ·mol^{-1} [5]. In this case was obtained a value of activation energy of 17.9 kJ/mol (Table 3) suggesting that the adsorption of As(V) onto

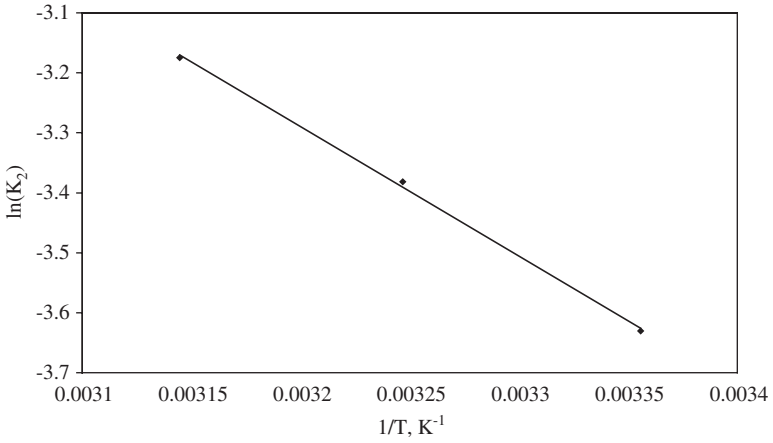

Fig. 10 Arrhenius plot of AS(V) adsorption onto the studied material.

Table 3 Thermodynamic parameters of As(V) adsorption onto the studied material.

Activation energy		Thermodynamic parameters					
E, kJ/mol	R^2	$\Delta H°$, kJ/mol	$\Delta S°$, J/mol·K	$\Delta G°$, kJ/mol			R^2
				298 K	303 K	308 K	
17.9	0.9988	86.3	299	27.5	57.9	87.3	0.9485

the studied material is a chemical adsorption. This is in accordance with the conclusions raised from the equilibrium studies.

The thermodynamic parameters of ΔH, ΔS were also calculated from the linear regression according to the eq. 6. The plot is shown in Fig. 11 and the obtained parameters are listed in Table 3.

The ΔH was observed to be 86.3 kJ/mol, which implies the endothermic nature of As(V) adsorption on the polymer with phosphonium pendant groups impregnated with crown ether and loaded with Fe(III) ions. The Gibbs free energy change (ΔG) was also calculated according to the eq. 5 which indicated the spontaneous nature of the sorption process. In addition, the positive value of ΔS suggested an increase in randomness at the solid/liquid interface during adsorption of As(V) ions onto the studied material [3, 7, 8].

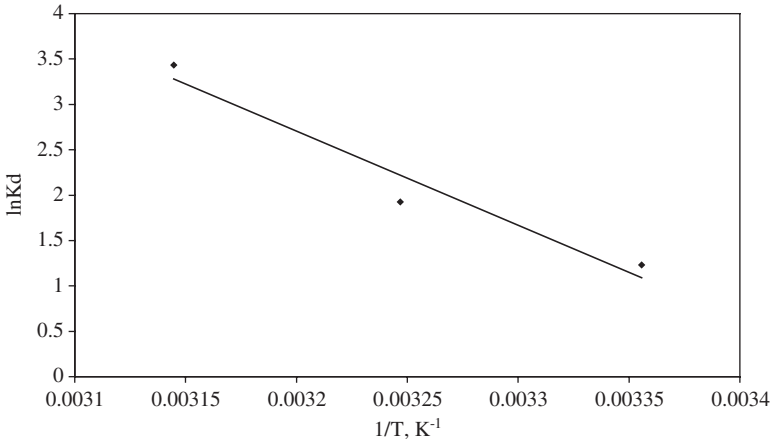

Fig. 11 Effect of temperature on the adsorption of As(V) onto the studied material.

Arsenic removal from real underground water

The efficiency of the treatment technique depends on the concentration and species of arsenic as well as on the presence of other constituents in the water. The studied adsorbent showed good efficiency in the treatment process of the real underground water. It can be notice that the presence of the other constituents in the water sample did not influence the efficiency of the studied adsorbent, the residual concentration of arsenic being under the maximum limit allowed by the World Health Organization of 10 μg/L. In the same time decreased the concentration of sulphate ions, these means that there can be a competition between the phosphate and arsenic ions present in the water samples, but at these concentrations the adsorbent has the capacity to remove the both ions.

Mechanism of arsenic adsorption

Based on the experimental data and their modeling it can be supposed that the mechanism of arsenic removal through chemisorption onto the studied adsorbent is formed from two distinguish parts: in the first step the Fe(III) ions is caught through coordinative bounds inside the macro cycle of the crown ether [44, 45]; and in the second step the arsenate ions are retained through ionic bounds by the formed crown ether-iron ions complex [23]. The proposed mechanism of arsenic adsorption onto the studied material is presented in Scheme 2.

Desorption studies

From the experimental data it was observed that the desorption degree of As(V) from the exhausted adsorbent increase with the increasing of the HCl concentration. The degree of arsenic desorption is over 95 % in all the cases. From the economically point of view is not recommended to be used a solution of HCl having a concentration higher than 5 %. In this case the studied adsorbent material can be used in more cycles of adsorption-desorption.

Conclusions

Polymer with phosphonium pendant group impregnated with dibenzo-18-crown-6-crown ether and loaded with iron ions was investigated for As(V) adsorption from aqueous solutions containing arsenic concentration from 25 to 175 μg/L. The adsorption behaviors were thoroughly studied by Langmuir and Freundlich isotherms. The adsorption was observed to be a chemisorption process. The adsorption kinetics was better described by pseudo-second-order kinetic model compare to pseudo-first-order model. The endothermic

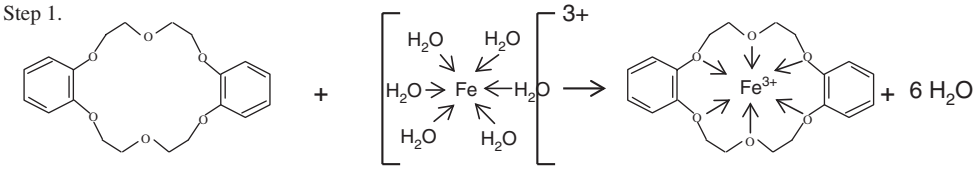

Step 2. $[\text{dibenzo-18-crown-6 Fe}]^{3+} + AsO_4^{3-} \rightarrow (\text{DB-18-C6 Fe})(AsO_4)$

Scheme 2 Mechanism of arsenic adsorption onto the studied material.

and spontaneous nature of adsorption was confirmed by thermodynamic study. The studied material can be effectively used in the removal process of As(V) from aqueous solutions containing trace concentration of arsenic (the most often found concentrations in the real underground waters) and obtaining a residual concentration under the maximum admitted value by the WHO.

References

[1] S. Kundu, A. K. Gupta. *Sep. Purif. Technol.* **51**, 165 (2006).
[2] D. Borah, S. Satokawa, S. Kato, T. Kojima. *J. Colloid Interface Sci.* **319**, 53 (2008).
[3] D. Borah, S. Satokawa, S. Kato, T. Kojima. *J. Hazard. Mater.* **162**, 1269 (2009).
[4] A. Negrea, L. Lupa, M. Ciopec, R. Lazau, C. Muntean, P. Negrea. *Adsorpt. Sci. Technol.* **28**, 467 (2010).
[5] A. Ramesh, H. Hasegawa, T. Maki, K. Ueda. *Sep. Purif. Technol.* **56**, 90 (2007).
[6] L. S. Thakur, P. Semil. *Int. J. Chem. Tech. Res.* **5**, 1299 (2013).
[7] K. Banerjee, G. L. Amy, M. Prevost, S. Nour, M. Jekel, P. M. Gallagher. *Water Res.* **42**, 3371 (2008).
[8] K. Gupta, U. C. Ghosh. *J. Hazard. Mater.* **161**, 884 (2009).
[9] V. T. Nguyen, S. Vigneswaran, H. H. Ngo, H. K. Shon, J. Kandasamy. *Desalination* **236**, 363 (2009).
[10] F. Partey, D. Norman, S. Ndur, R. Nartey. *J. Colloid Interface Sci.* **321**, 493 (2008).
[11] J. C. Hsu, C. J. Lin, C. H. Liao, S. T. Chen. *J. Hazard. Mater.* **153**, 817 (2008).
[12] Y. N. Chen, L. Y. Chai, Y. D. Shu. *J. Hazard. Mater.* **160**, 168 (2008).
[13] M. Bilici Baskan, A. Pala. *J. Hazard. Mater.* **166**, 796 (2009).
[14] J. R. Parga, D. L. Cocke, J. L. Valenzuela, J. A. Gomes, M. Kesmez, G. Irwin, H. Moreno, M. Weir. *J. Hazard. Mater.* **B124**, 247 (2005).
[15] M. Bissen, F. H. Frimmel. *Acta Hydrochimca et Hydrobiologica* **31**, 97 (2003).
[16] S. Song, A. Lopez-Valdivieso, D. J. Hernandez-Campos, C. Peng, M. G. Monroy-Fernandez, I. Razo-Soto. *Water Res.* **40**, 364 (2006).
[17] L. Wang, A. S. C. Chen, T. J. Sorg, K. A. Fields. *J. Am. Water Works Ass.* **94**, 161 (2002).
[18] D. Monah, C. U. Pittman. *J. Hazard. Mater.* **142**, 1 (2007).
[19] J. Jonsson, D. M. Sherman, *Chem. Geol.* **255**, 173 (2008).
[20] K. Ohe, Y. Tagai, S. Nakamura, T. Oshima, Y. Baba. *J. Chem. Eng. Jpn.* **38**, 671 (2005).
[21] Y. Jeong, M. Fan, S. Singh, C. L. Chuang, B. Saha, J. H. van Leeuwen. *Chem. Eng. Process.* **46**, 1030 (2007).
[22] K. Gupta, T. Basu, U. C. Ghosh. *J. Chem. Eng. Data* **54**, 2222 (2009).
[23] S. K. Maji, A. Pal, T. Pal. *J. Hazard. Mater.* **151**, 811 (2008).
[24] H. U. So, D. Postma, R. Jakobsen, F. Larsen. *Geochim. Cosmochim. Acta*. **72**, 5871 (2008).
[25] P. Mondal, C. B. Majumder, B. Mohanty. *J. Hazard. Mater.* **150**, 695 (2008).
[26] A. Mukherjee, M. K. Sengupta, M. A. Hossain, S. Ahamed, B. Das, B. Nayak, D. Lodh, M. M. Rahman, D. Chakraborti. *J. Health. Popul. Nutr.* **24**, 142 (2006).
[27] A. Negrea, C. Muntean, M. Ciopec, L. Lupa, P. Negrea. *Chem. Bull. Politehnica Univ.*, *(Timisoara)* **54**, 82 (2009).
[28] M. Hiraoka. *Crown Compounds: Their Characteristics and Applications*, Elsevier, Amsterdam (1982).
[29] M. Hiraoka. *Crown Ethers and Analogous Compounds*, Elsevier, Amsterdam (1992).
[30] G. W. Gokel. *Crown Ethers and Cryptands*, Royal Society of Chemistry, Cambridge (1991).
[31] B. F. Wang, L. R. Li, Y. M. Zhu, Q. Kang, J. J. Zhang. *J. Coal Sci. Eng. (China)*, **19**, 375 (2013).
[32] I. M. M. Rahman, Z. A. Begum, H. Hasegawa. *Microchem. J.* **110**, 485 (2013).
[33] A. Negrea, M. Ciopec, L. Lupa, C. M. Davidescu, A. Popa, G. Ilia, P. Negrea, *J. Chem. Eng. Data* **56**, 3830 (2011).
[34] T. Oshima, K. Kondo, K. Ohto, K. Inoue, Y. Baba. *React. Func. Polym.* **68**, 376 (2008).
[35] M. R. Awual, M. A. Shenashen, T. Yaita, H. Shiwaku, A. Jyo. *Water Res.* **46**, 5541 (2012).
[36] M. R. Awual, S. A. El-Safty. *J. Environ. Sci*. **23**, 1947 (2011).
[37] M. R. Awual, A. Hossain, M. A. Shenashen, T. Yaita, S. Suzuki, A. Jyo. *Environ. Sci. Pollut. Res.* **20**, 421 (2013).
[38] J. E. Greenleaf, J. C. Lin, A. K. Sengupta. *Environ. Progr.* **25**, 300 (2006).
[39] M. German, H. Seingheng, A. K. Sen Gupta. *Sci. Total Environ*. **488–489**, 547 (2014).
[40] A. Popa, C. M. Davidescu, R. Trif, G. Ilia, S. Iliescu, G. Dehelean. *React. Funct. Polym.* **55**, 151 (2003).
[41] O. A. Raevskii, S. V. Trepalin, V. E. Zubareva, D. G. Batyr. *Russ. Chem. B+* **34**, 1441 (1985).
[42] T. Balaban, M. Banciu, I. I. Pogany. *Applications of Physical Methods in Organic Chemistry*, Scientific and Encyclopedic Publishing, Bucharest (1983).
[43] M. Ciopec, A. Negrea, L. Lupa, C. Davidescu, P. Negrea, P. Sfarloaga. *J. Mater. Sci. Eng.* **B1**, 421 (2011).
[44] C. M. Choi, J. Heo, N. J. Kim. *Chem. Central J.* **6**, 1 (2012).
[45] K. Durr, B. P. Macpherson, R. Warratz, F. Hampel, F. Tuczek, M. Helmreich, N. Jux, I. Ivanovic-Burmazovic. *J. Am. Chem. Soc* **129**, 4217 (2007).

Molecules **2014**, *19*, 16082-16101; doi:10.3390/molecules191016082

OPEN ACCESS

molecules

ISSN 1420-3049

www.mdpi.com/journal/molecules

Article

Studies Regarding As(V) Adsorption from Underground Water by Fe-XAD8-DEHPA Impregnated Resin. Equilibrium Sorption and Fixed-Bed Column Tests

Mihaela Ciopec, Adina Negrea, Lavinia Lupa *, Corneliu M. Davidescu and Petru Negrea

Faculty of Industrial Chemistry and Environmental Engineering Blvd.,
"Politehnica" University of Timisoara, Vasile Parvan No. 6, Timisoara 300223, Romania

* Author to whom correspondence should be addressed; E-Mail: lavinia.lupa@upt.ro;
Tel.: +4-025-640-4192.

External Editor: Derek J. McPhee

Received: 11 July 2014; in revised form: 12 September 2014 / Accepted: 18 September 2014 / Published: 9 October 2014

Abstract: The characteristics of arsenic adsorption onto Fe-XAD8-DEHPA resin were studied on the laboratory scale using aqueous solutions and natural underground waters. Amberlite XAD8 resin was impregnated with di(2-ethylhexyl) phosphoric acid (DEHPA) via the dry method of impregnation. Fe(III) ions were loaded onto the impregnated resin by exploiting the high affinity of arsenic towards iron. The studies were conducted by both in contact and continuous modes. Kinetics data revealed that the removal of arsenic by Fe-XAD8-DEHPA resin is a pseudo-second-order reaction. The equilibrium data were modelled with Freundlich Langmuir and Dubinin Radushkevich (D-R) isotherms and it was found that the Freundlich model give the poorest correlation coefficient. The maximum adsorption capacity obtained from the Langmuir isotherm is 22.6 μg As(V)/g of Fe-XAD8-DEHPA resin. The mean free energy of adsorption was found in this study to be 7.2 kJ/mol and the $\Delta G°$ value negative (−9.2 kJ/mol). This indicates that the sorption process is exothermal, spontaneous and physical in nature. The studied Fe-XAD8-DEHPA resin showed excellent arsenic removal performance by sorption, both from synthetic solution and the natural water sample, and could be regenerated simply by using aqueous NaOH or HCl solutions.

Keywords: arsenic removal; Fe-XAD8-DEHPA; underground water; adsorption isotherm; kinetics; column study

---

1. Introduction

Because in developing countries underground waters represent the main source of drinking water, their contamination with arsenic is a problem which must be solved [1–3]. It is well known that because of its toxicity the presence of arsenic in drinking water above the maximum admitted level has a negative impact on human health [1–8]. In order to reduce its adverse health effects it is necessary to minimize the pollution of underground water with arsenic content or to find some effective methods for their remediation [3]. The valences and inorganic species of arsenic depend on the redox conditions and the pH of the underground waters. In an aqueous solution of As(V) there are four species: H_3AsO_4, $H_2AsO_4^-$, $HAsO_4^{2-}$, AsO_4^{3-} that predominate at pH values between 6 and 9. In the same mode in aqueous solutions at pH values below 9 they exist the As(III) species: H_3AsO_3, $H_2AsO_3^-$, $HAsO_3^{2-}$, AsO_3 [4–6,9,10]. The conventional methods used for the arsenic removal from aqueous solutions are precipitation, coagulation and filtration, reverse osmosis, ion exchange and adsorption. Of the above methods, adsorption is the most promising one as it is economical and highly efficient [1–12]. In the last years solvent impregnated resins (SIR) were used for the recovery and selective separation of metal ions from aqueous solutions with good results [13–22]. In order to improve the adsorption properties of the SIRs four method of impregnation with an organic extractant of the polymeric support were developed. These are: the dry, wet, modifier addition and dynamic column methods [13,16,22–24]. In the present study, the dry method of impregnation was used to impregnate an Amberlite XAD8 resin with di(2-ethylhexyl) phosphoric acid DEHPA in order to obtain an efficient adsorbent for the removal of As(V) from aqueous solutions [22]. We focused on this resin because in our previous studies the Amberlite XAD7 resin displayed good adsorption properties in the process of arsenic removal from aqueous solutions [18]. The advantages of the use as solid support of the Amberlite XAD series are represented by the possibilities of obtaining spherical beads of suitable size. Other researchers used these resins for the arsenic removal, but in other more expensive functionalization systems [20,21]. Due to the shape of these solid supports they are easy to separate from the solutions and also easy to regenerate, avoiding in this way the drawbacks of the adsorption method. On the other hand the purpose of our research was to obtain an adsorbent which could be efficiently used in the process of arsenic removal from aqueous solutions having concentrations under 100 μg/L. These concentrations were the most common found in the underground waters from the west area of Romania and east area of Hungary [25,26]. Awual and co-workers underlined the importance of the preparation of an adsorbent intended to remove arsenic from waters containing low concentrations. They also demonstrated that the metal-loaded ligand exchangers show rapid, selective and great efficiency in the process of trace arsenic removal from aqueous solutions [27–31]. For this reason, in this paper, in order to prepare an efficient adsorbent for the purification of water with trace levels of arsenic, the XAD8-DEHPA impregnated resin was loaded with Fe(III) ions. We used the iron ions for the metal loading of the impregnated resin due to the high affinity of arsenic towards iron [3,4,7–11,24,32]. By using as adsorbent material, in the process of arsenic removal from aqueous solutions, a resin loaded with a polyvalent metal ion, combines the known advantages of the resin such as excellent hydraulic properties and mechanic strength along with the excellent selectivity offered by the loaded metal ion [33]. Even if the metal ion content (weight %) of the loaded resin is much less than the metal oxide, the resulting adsorbent presents a higher efficiency due to its mechanical integrity and its

possibility to be used for several cycles [34]. Taking into account these considerations the purposed adsorbent material is in agreement with the Life Cycle Approach, underlining the sustainability of arsenic removal through adsorption [35]. The objective of this study was to investigate the adsorption characteristic of the Fe-XAD8-DEHPA resin for As(V) removal in aqueous solutions by performing equilibrium sorption tests and fixed-bed column tests.

2. Results and Discussion

2.1. Evaluation of the Adsorbent Preparation Process

The extractant content of the XAD8-DEHPA was found to be 0.28 g DEHPA for each gram of SIR as determined by titration using 0.1 M NaOH. The experimental data regarding the dependence of the Fe(III) ion uptake versus the initial concentration on Fe(III) ions in the loading process of iron onto XAD8-DEHPA resin are presented in Figure 1.

Figure 1. Dependence of the Fe(III) ions uptake versus the initial concentration of Fe(III) pH = 3, t = 24 h, m = 0.1 g, V = 25 mL.

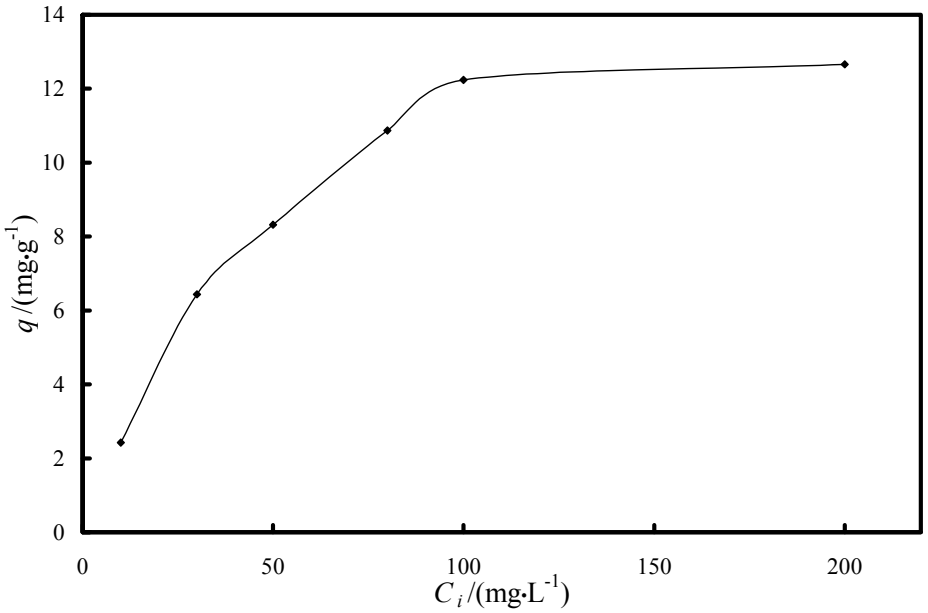

The experimental data shows the increase of the Fe(III) ions uptake as the initial concentration of Fe(III) ions in solution increases. Above 100 mg/L initial Fe(III) concentration, there is no significant increase of the Fe(III) ions loaded onto the XAD8-DEHPA. Therefore it was considered that for the loading of the XAD8-DEHPA resin, using a S:L ratio of 0.1:25, the concentration of the Fe(III) ions in the aqueous solutions should not exceed 100 mg/L. In this way the loading of the highest quantity of iron ions onto the impregnated resin is obtained, which will lead to a higher adsorption of As(V) ions from the aqueous solution, due to the fact that the Fe(III) ions are responsible for the arsenic removal because of its affinity for this pollutant [3,4,7–11,24,32].

The IR spectrum of Fe-XAD8-DEHPA (Figure 2) presents the characteristic bands of XAD8 resin and also illustrated the fact that the resin was impregnated with the studied solvent and loaded with the Fe(III) ions. The peak at 1390 cm^{-1} was assigned to the C-H deformation vibration of CH_3; the

absorption band at 1734 cm^{-1} corresponds to a C=O stretching vibration and the band at 2970 cm^{-1} was attributed to the C-H stretching vibration of CH_3. The impregnated status of the XAD8 resin by DEHPA extractant is manifested in the appearance of the adsorption band at 1235 cm^{-1}, which is the P=O stretching band. P-CH_2 stretching is observed at 1477 cm^{-1}; the O-H bending band was found at 1690 cm^{-1} and the band assigned to P-OH is observed at 2340 cm^{-1}. The iron loading of the XAD8-DEHPA resin is demonstrated by the peaks at 1037 and 2890 cm^{-1} which belong to the Fe-OH stretching band.

Figure 2. IR spectrum of a Fe-XAD8-DEHPA sample.

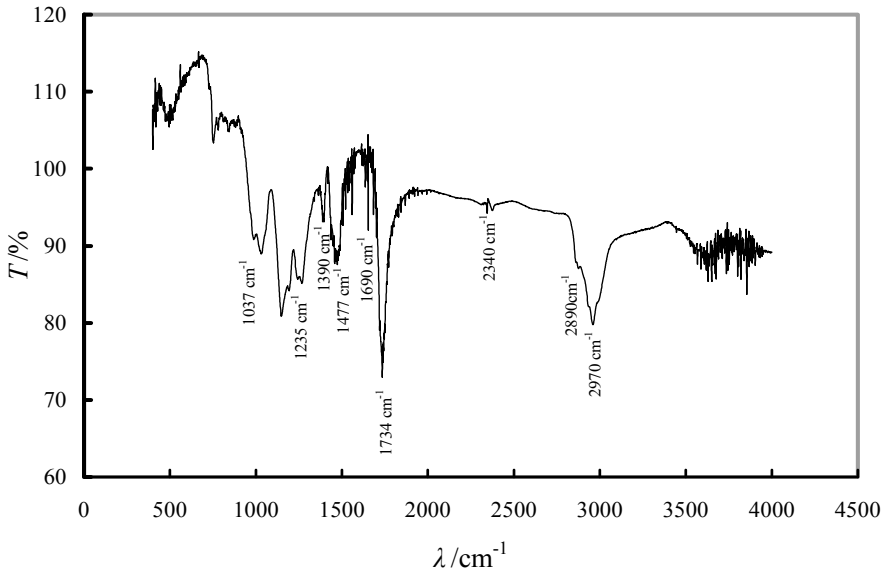

The impregnation of the resin with DEHPA and the loading of the impregnated resin with Fe(III) ions is also demonstrated by the EDX spectra, where characteristic peaks of phosphorous ions arising from the DEHPA solvent and iron were identified (Figure 3).

Figure 3. EDX spectrum of Fe-XAD8-DEHPA sample.

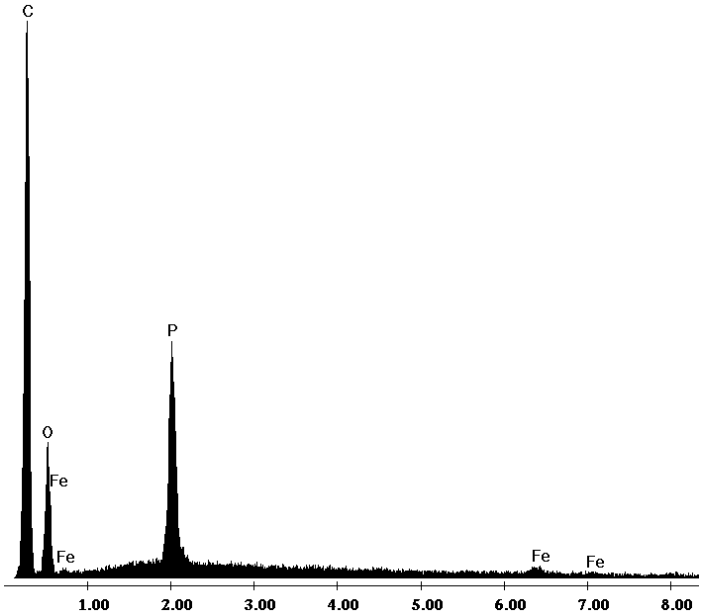

2.2. Sorption Equilibrium Tests

2.2.1. Study of the Kinetics of Adsorption

In order to determine the time when the equilibrium between the arsenate and the impregnated resin is reached kinetic studies were performed. The effect of contact time on the equilibrium adsorption capacity of Fe-XAD8-DEHPA during the removal process of As(V) from aqueous solution at room temperature is presented in Figure 4. According to this data, saturation was reached after 24 h contact time. At an initial 100 ppb As(V) concentration value, the equilibrium adsorption capacity was determined to be ~13 μg As(V)/g of impregnated resin.

Figure 4. Effect of contact time on the As(V) adsorption capacity of Fe-XAD8-DEHPA pH = 9 ± 0.1; T = 298 ± 1 K; C_0 = 100 μg/L; m = 0.1 ± 0.0001 g; V = 25 ± 0.1 mL.

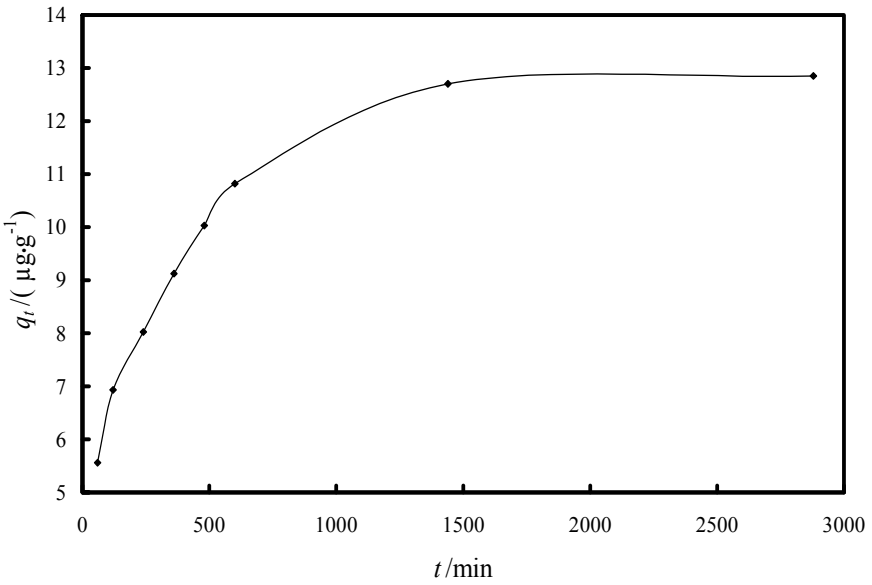

In order to investigate the arsenic adsorption mechanism onto the Fe-XAD8-DEHPA resin, three kinetic models, namely (i) pseudo-first-order equation of Lagergren based on solid capacity; (ii) pseudo-second-order reaction model of Ho and Mckay based on the solid phase sorption; and (iii) intra-particle diffusion model were tested. Descriptions of the integral form of the models are given in the following. The pseudo-first-order kinetic model is defined by the Equation [14,36]:

$$\ln(q_e - q_t) = \ln q_t - k_1 \cdot t \quad (1)$$

where q_e and q_t are the amount of the As(V) adsorbed onto the Fe-XAD8-DEHPA (μg/g) at equilibrium and after time t, respectively. t is the contact time (min), k_1 is the specific sorption rate constant (min^{-1}). The values of the adsorption rate constant (k_1) were determined from the ln(q_e − q_t) in terms of t (Figure 5).

Figure 5. Linear model of the pseudo-first-order reaction kinetics of As(V) adsorption onto Fe-XAD8-DEHPA resin.

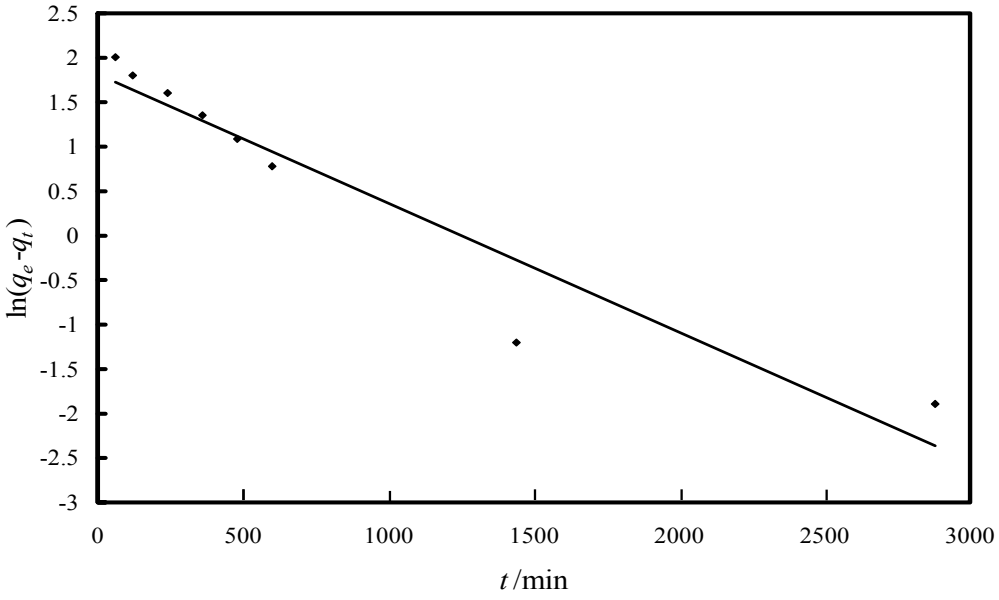

The linear form of the pseudo-second order model is defined by [2,37]:

$$\frac{t}{q_t} = \frac{1}{k_2 \cdot q_e^2} + \frac{t}{q_e} \quad (2)$$

where q_e and q_t are the amount of the As(V) adsorbed onto the studied material ($\mu g \cdot g^{-1}$) at equilibrium and at time t, respectively. t is the contact time (min), k_2 is the pseudo-second-order adsorption rate constant ($g \cdot \mu g^{-1} \cdot min^{-1}$). The value q_e and k_2 are determined from the slope and intercept of ($t \cdot q_t^{-1}$) *versus* t (Figure 6). In Equation (2), the expression $k_2 \cdot q_e^2$ in the intercept term describes the initial sorption rate $h/(\mu g \cdot (g \cdot min)^{-1})$ as $t \rightarrow 0$.

Figure 6. Linear model of the pseudo-second-order reaction kinetics of As(V) adsorption onto Fe-XAD8-DEHPA resin.

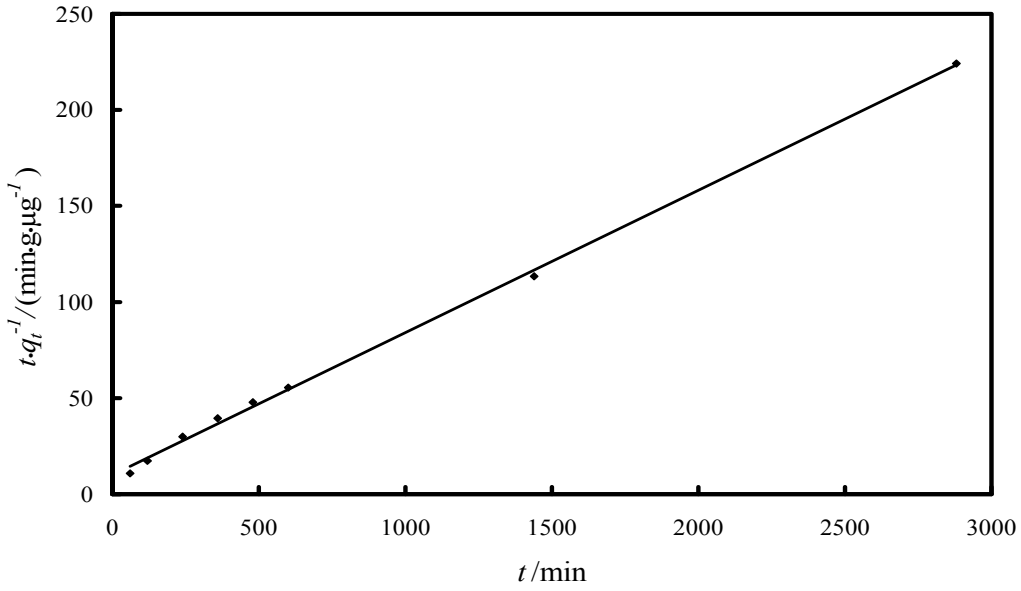

Intra-particle diffusion is an important phenomenon for sorption processes in porous materials. The adsorption of As(V) ions onto the Fe-XAD8-DEHPA may be controlled via external film diffusion at earlier stages and later by the particle diffusion. The possibility of intra-particle diffusion resistance was identified by using the following Weber-Morris intra-particle diffusion model [6,7,9]:

$$q_t = k_{dif} \cdot t^{1/2} + C \quad (3)$$

where k_{dif} is the intra-particle diffusion rate constant ($\mu g \cdot g^{-1} \cdot min^{-1/2}$) and C is the intercept. The values of q_t versus $t^{1/2}$ and the rate constant k_{dif} are directly evaluated from the slope of the regression line (Figure 7).

Figure 7. The Weber-Morris plot for intra-particle diffusion of the As(V) adsorption kinetic data on Fe-XAD8-DEHPA resin.

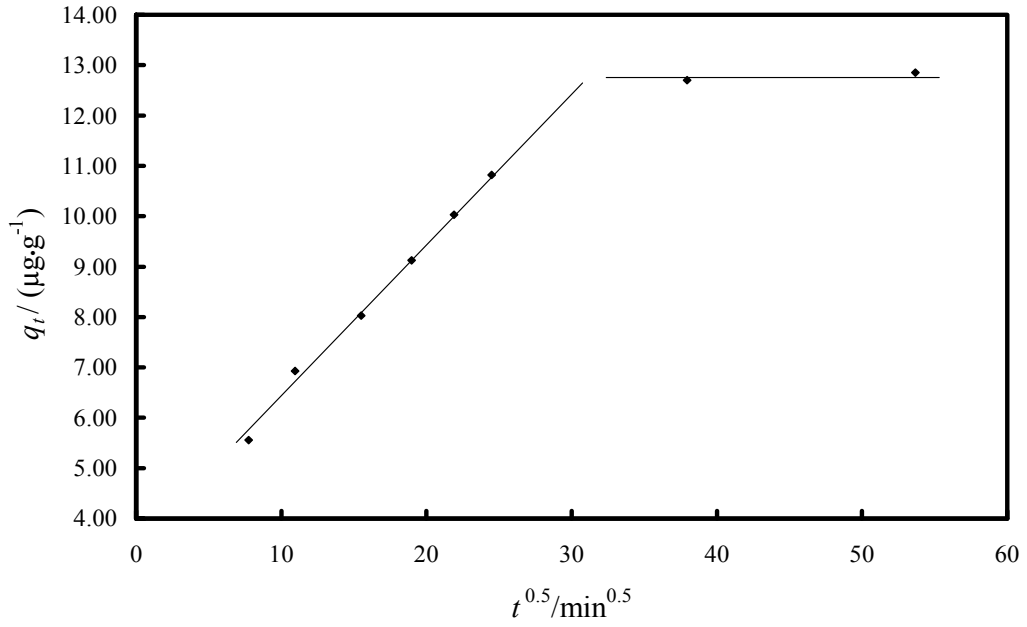

The application of the different kinetic models unveiled some interesting features regarding the mechanism and rate-controlling step in the overall sorption process. The values of the constants, together with the regression coefficients (R^2) obtained in all cases are summarized in Table 1.

A poor regression of the pseudo-first-order equation infers that this model does not adequately describe the present adsorption process. Further, there is a great difference between the q_e values obtained experimentally and the values obtained directly from the kinetic plot (Figure 5). At the same time, the correlation coefficient for the linear plot of the pseudo-second-order kinetic plot is excellent, greater than 0.99. The q_e values experimentally obtained shows excellent agreement with the value calculated from the kinetic plot. This shows that the kinetic of As(V) removal by Fe-XAD8-DEHPA can be well described by a pseudo-second-order expression.

Table 1. Kinetic parameters for As(V) adsorption onto Fe-XAD8-DEHPA resin.

Model/Parameter	Value
Pseudo-first-order model	
k_1/min^{-1}	0.0014
R^2	0.9158
q_e (experimental)/(μg·g^{-1})	13
q_e (kinetic plot)/(μg·g^{-1})	6.13
Pseudo-second-order model	
k_2/(g·μg^{-1}·min^{-1})	5.45×10^{-4}
R^2	0.9957
q_e (experimental)/(μg·g^{-1})	13
q_e (kinetic plot)/(μg·g^{-1})	13.5
Intra-particle diffusion model	
k_{dif}/(μg·g^{-1}·min$^{-1/2}$)	0.3049

In order to obtain some information regarding which is the rate-limiting step (boundary layer diffusion or intra-particle (pore) diffusion of solute towards the solid surface) of the arsenic adsorption process onto Fe-XAD8-DEHPA resin, the Weber-Morris intraparticle diffusion model was studied. The straight line which passes through origin obtained from the plot of q_t against square root of time shows that the rate limiting step is the intraparticle diffusion [38,39]. The deviation of the plot from the line indicates the rate-limiting step should be boundary layer (film) diffusion controlled. The plot of q_t *versus* $t^{0.5}$ in Figure 7 shows that the dependence is not linear for the duration of entire reaction. The line does not pass through the origin, and thus, intra particle diffusion cannot be the rate-limiting step in the sorption process. The plot shows two straight sections, suggesting two different types of sorption mechanisms at the beginning and at the end of the process. The first linear section indicates initial rapid uptake due to film diffusion and consequent external surface coverage by the sorbate. The second linear section suggests the transportation of sorbate inside the sorbent particles [38,39]. This suggests that the As(V) removal by Fe-XAD8-DEHPA is a complex process.

2.2.2. Study of the Adsorption Isotherm

The adsorption isotherm of As(V) is presented in Figure 8. At high equilibrium concentrations, the adsorption capacity approaches a constant value. This value represents the experimentally determined maximum adsorption capacity of As(V) onto Fe-XAD8-DEHPA ($q_{m\,exp} > 20.2$ μg·g^{-1}).

Langmuir and Freundlich isotherm studies were conducted in order to investigate the maximum adsorption capacity of Fe-XAD8-DEHPA resin towards As(V) [40]. The relation between the amounts of adsorbate adsorbed by the adsorbent can be expressed by the linearized Langmuir adsorption isotherm as:

$$\frac{C_e}{q_e} = \frac{1}{K_L \cdot q_m} + \frac{C_e}{q_m} \tag{4}$$

and the Freundlich isotherm as:

$$\ln q_e = \ln K_F + \frac{1}{n} \cdot \ln C_e \quad (5)$$

where q_e is the amount of adsorbate adsorbed per unit of the adsorbent ($\mu g \cdot g^{-1}$), K_L the adsorption constant related to the enthalpy of adsorption ($L \cdot \mu g^{-1}$), C_e the equilibrium concentration of As(V) ($\mu g \cdot L^{-1}$), q_m the maximum adsorption capacity ($\mu g \cdot g^{-1}$), and n and K_F are the constants depending upon the nature of the adsorbate and adsorbent where n represents the adsorption intensity and K_F represents the adsorption capacity ($\mu g \cdot g^{-1}$). A linear Langmuir isotherm was drawn by plotting $C_e \cdot q_e^{-1}$ *versus* C_e (Figure 9), while Freundlich isotherm for the adsorption was drawn by plotting $\ln q_e$ *versus* $\ln C_e$ (Figure 10). The calculated parameters, as well as the correlation coefficients (R^2) for As(V) removal through adsorption onto Fe-XAD8-DEHPA are presented in Table 2.

Figure 8. Adsorption isotherm of As(V) ions onto Fe-XAD8-DEHPA resins; T = 298 ± 1 K; pH = 9 ± 0.1; C_0 = range:10 to 300 $\mu g \cdot L^{-1}$; m = 0.1 ± 0.0001 g; V = 25 ± 0.1 mL; t = 24 h.

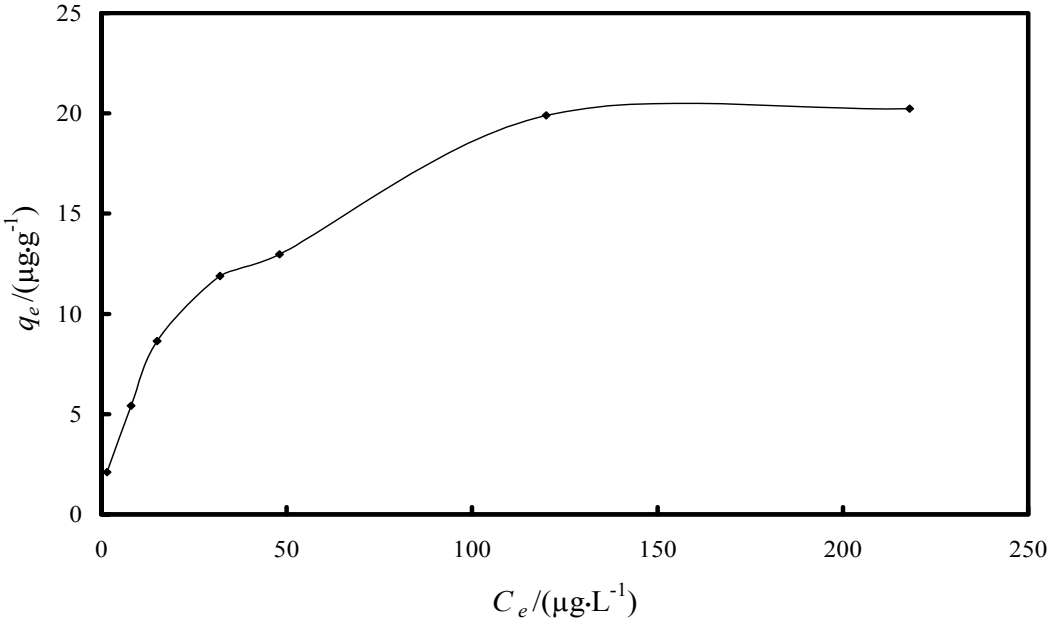

Figure 9. Langmuir isotherm model for As(V) adsorption onto Fe-XAD8-DEHPA resin.

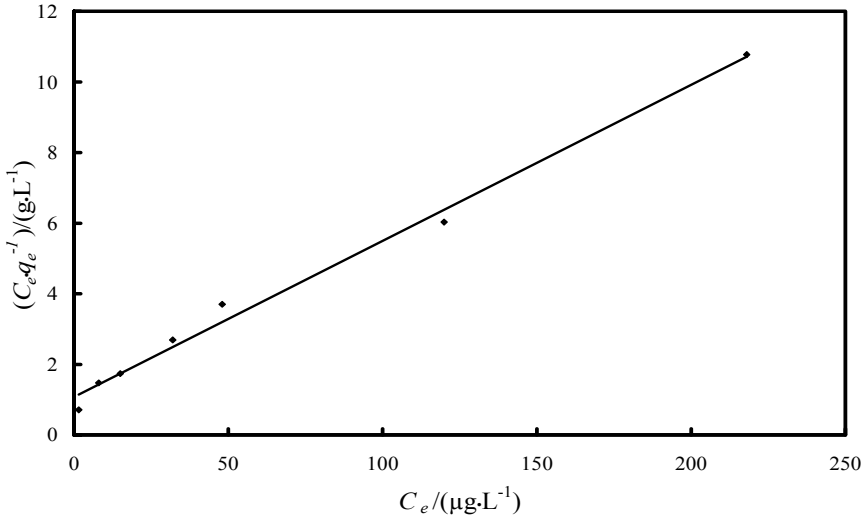

Figure 10. Freundlich isotherm model for As(V) adsorption onto Fe-XAD8-DEHPA resin.

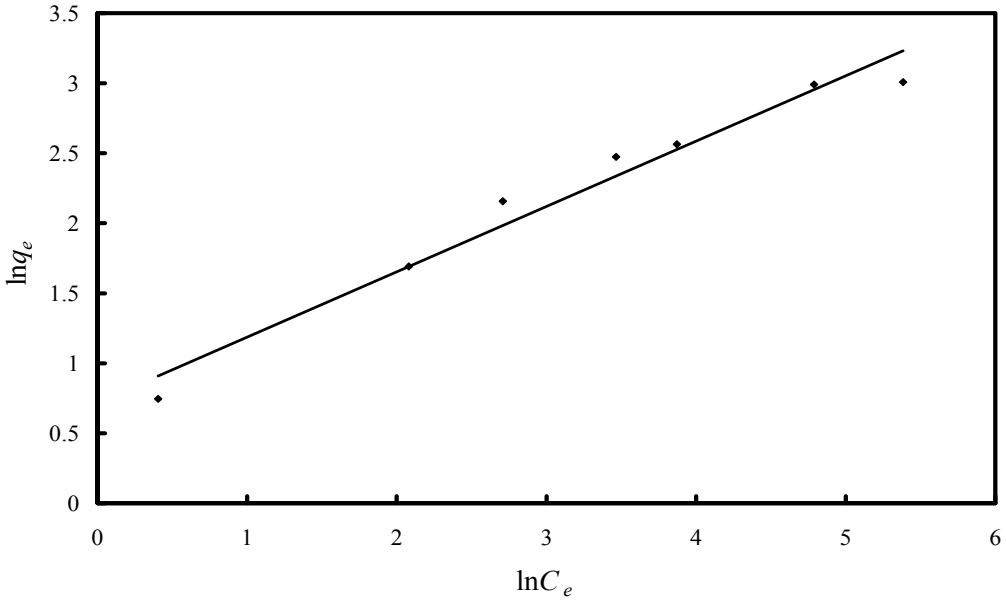

Table 2. Parameters of Freundlich, Langmuir and D-R isotherms for As(V) adsorption onto Fe-XAD8-DEHPA resin.

Isotherm/Parameter	Value
Langmuir isotherm	
K_L/(L·μg^{-1})	0.041
q_m/(μg·g^{-1})	22.6
R^2	0.9918
Freundlich isotherm	
K_F/(μg·g^{-1})	2.055
1/n	0.4664
R^2	0.9667
D-R isotherm	
k/(mol^2·kJ^{-2})	0.0096
q_m/(μg·g^{-1})	24.16
R^2	0.9921

The Freundlich plot has a lower correlation coefficient than the Langmuir plot. This suggests that the use of the Freundlich isotherm is limited. The Langmuir model effectively describes the equilibrium sorption data (Figure 9); the linear plot has a good correlation coefficient (>0.99) and the maximum adsorption capacity is close to that determined experimentally. The isotherm describes the sorption process for the entire studied concentration range. The maximum adsorption capacity, developed by the studied adsorbent in the removal process of arsenic from water, was compared with other adsorption capacities developed by other materials loaded with iron ions presented in literature (Table 3).

Table 3. Maximum adsorption capacities develop by various adsorbent loaded with iron ions in the removal process of arsenic from water.

Adsorbent	q_m, µg·g^{-1}	References
Fe-XAD8-DEHPA	22.6	Present work
Fe-XAD7-DEHPA	17.6	[18]
Fe-IR-120(Na)-DEHPA	21.8	[41]
Alginate bead (doped and coated with iron ions	14	[42]
Iron oxide coated sand	8	[43]
Iron oxide coated sand-2	18	[44]

It can be notice that the present adsorbent developed a higher efficiency in the removal process of As(V) from aqueous solutions compared with other iron loaded materials present in the literature. The studied adsorbent can be used with success for arsenic removal from waters containing trace concentrations, the most often situation for drinking waters.

However, neither Langmuir nor Freundlich isotherms provide information about the adsorption mechanism. In order to assess the type of adsorption process, the Dubinin-Radushkevich (D-R) isotherm was also employed [45]. This can be expressed as:

$$\ln q_e = \ln q_m - k \cdot \varepsilon^2 \tag{6}$$

where ε (Polanyi potential) is given as:

$$\varepsilon = R \cdot T \cdot \ln\left(1 + \frac{1}{C_e}\right) \tag{7}$$

In the above expression, q_e is the amount of As(V) adsorbed (mg·g^{-1}) at equilibrium per unit weight of adsorbent, q_m the maximum adsorption capacity (mg·g^{-1}), C_e the equilibrium concentration of As(V) in the solution (ppm), k the constant related to adsorption energy (mol^2·kJ^{-2}), R the universal gas constant (kJ·mol^{-1}·K^{-1}) and T is the temperature (K). The D-R isotherm was drawn by plotting lnq_e against ε^2 (Figure 11). q_m and k where calculated from the slop and intercept of the graph and the obtained values are presented in Table 2.

Figure 11. D-R isotherm model for As(V) adsorption onto Fe-XAD8-DEHPA resin.

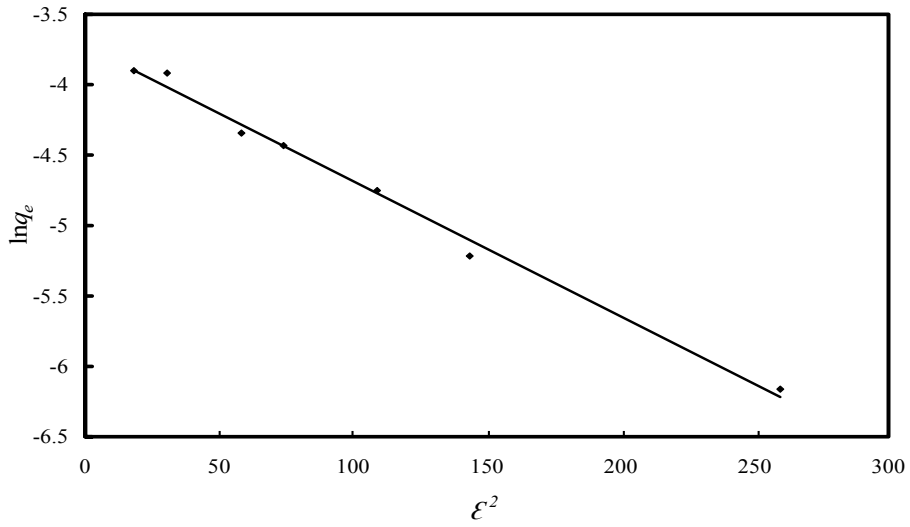

The D-R plot has a good correlation coefficient (>0.99). The monomolecular adsorption capacity q_m for Fe-XAD8-DEHPA in the removal process of As(V) from aqueous solutions is 24.16 μg·g^{-1}; a value which is very close to that determined experimentally. The mean free energy of adsorption (E), defined as free energy change when one mole of ion is transferred from infinity in solution to the surface of the solid, was calculated from the k value using the following formula [22,45]:

$$E = \frac{1}{\sqrt{2k}} \tag{8}$$

The magnitude of E is a indicator which shows if the adsorption is physical in nature ($E \leq 8$ kJ·mol^{-1}) or chemical (E is in the range of 8–16 kJ·mol^{-1}) [22,40]. The value of E found in this study was 7.2 kJ·mol^{-1}, suggesting a physical adsorption (due to weak van der Waals forces).

In order to predict the adsorption efficiency of the adsorption process and to assess if the process is favourable or unfavourable for the Langmuir type adsorption, the isotherm shape can be classified by a term R_L, a dimensionless constant separation factor, which is defined by the following equation:

$$R_L = \frac{1}{1 + K_L \cdot C_0} \tag{9}$$

where C_0 is the initial concentration of As(V) (ppb) and K_L is the Langmuir isotherm constant. The value of R_L indicates the shape of the isotherm to be unfavourable, $R_L > 1$; linear, $R_L = 1$; favourable $0 < R_L < 1$; and irreversible, $R_L = 0$ [5–7,12,36]. In our case R_L values were found to be between 0 and 1 for all the concentration of As(V) ions showing that the adsorption is favourable. Furthermore, the standard Gibbs free energy changes ($\Delta G°$) for the adsorption process can be calculated by using the following equation:

$$\ln\left(\frac{1}{K_L}\right) = \frac{\Delta G^0}{RT} \tag{10}$$

where K_L is the Langmuir isotherm constant (L·mg^{-1}), R the universal gas constant (8.314 J·mol^{-1}·K^{-1}), and T is the absolute temperature (K). The calculated $\Delta G°$ value is −9.2 kJ·mol^{-1}. The negative $\Delta G°$ value indicates that the adsorption is spontaneous.

2.3. Fixed-Bed Column Study

The efficiency of the treatment technique depends on the concentration and species of arsenic as well as on the presence of other constituents in the water. A fixed bed column study was conducted with real arsenic bearing ground water. The real arsenic-bearing water sample had the composition: NO^{3-}: 20 mg·L^{-1}; NO^{2-}: 0.5 mg·L^{-1}; P_2O_5: 5 mg·L^{-1}; SO_4^{2-}:10.2 mg·L^{-1}; NH_4^+: 6.4 mg·L^{-1}; Fe^{n+}: 1.8 mg·L^{-1}; Mn^{2+}: 0.6 mg·L^{-1}; Na^+: 120 mg·L^{-1}; K^+: 1.75 mg·L^{-1}; Ca^{2+}: 30 mg·L^{-1}; Mg^{2+}: 18 mg·L^{-1}; As^{n+}: 80 μg·L^{-1}.

The breakthrough curve is shown in Figure 12. The breakthrough time obtained was 6 h and corresponds to $C/C_0 = 0.0375$ (when 3 L of arsenic-bearing water were treated), while the exhaust time, that corresponds to $C/C_0 = 0.5$ was found to be at 14.6 h (when 7.3 L arsenic-bearing water were treated). The fixed bed column was designed by the logit method [45,46]. The logit equation can be written as:

$$\ln\left[\frac{C}{C_0 - C}\right] = -\frac{KNX}{v} + KC_0 t \tag{11}$$

where C is the solute concentration at any time t, C_0 the initial solute concentration (80 ppb), v the approach velocity (~7.6 cm/h), X the bed depth (5 cm), K the adsorption rate constant ($L\cdot(\mu g\cdot h)^{-1}$), and N is the adsorption capacity coefficient ($\mu g\cdot L^{-1}$). Plot of $\ln[C\cdot(C_0 - C)]$ versus t is shown in Figure 13. The value of adsorption rate coefficient (K) and adsorption capacity coefficient (N) was obtained as $7.41/(L\cdot(mg\cdot h)^{-1})$ and $10.09/(mg\cdot L^{-1})$. These values could be used to design the adsorption column.

Figure 12. Breakthrough curve for arsenic using Fe-XAD8-DEHPA.

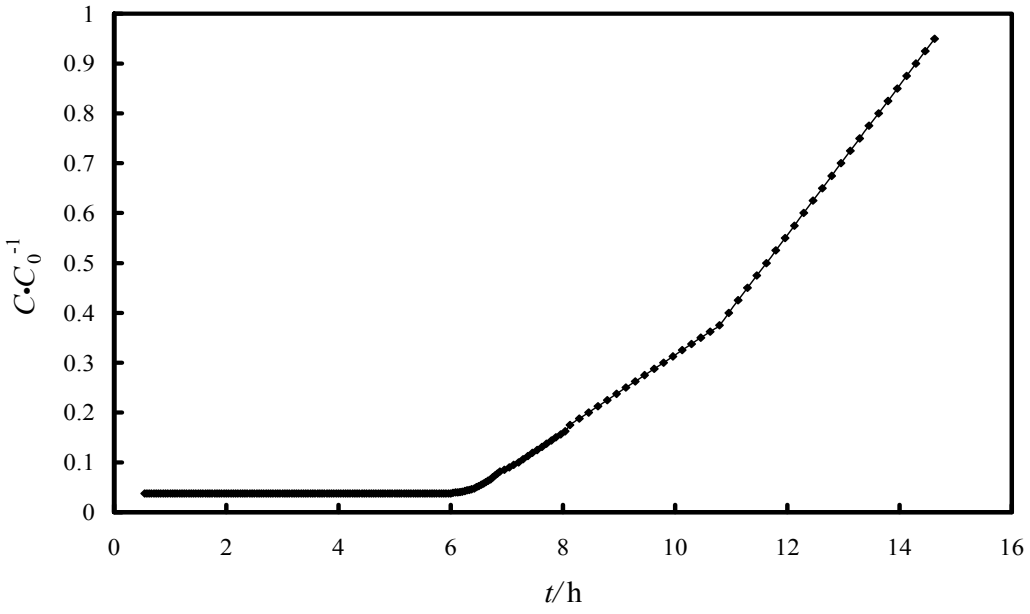

Figure 13. Linearized form of logit model.

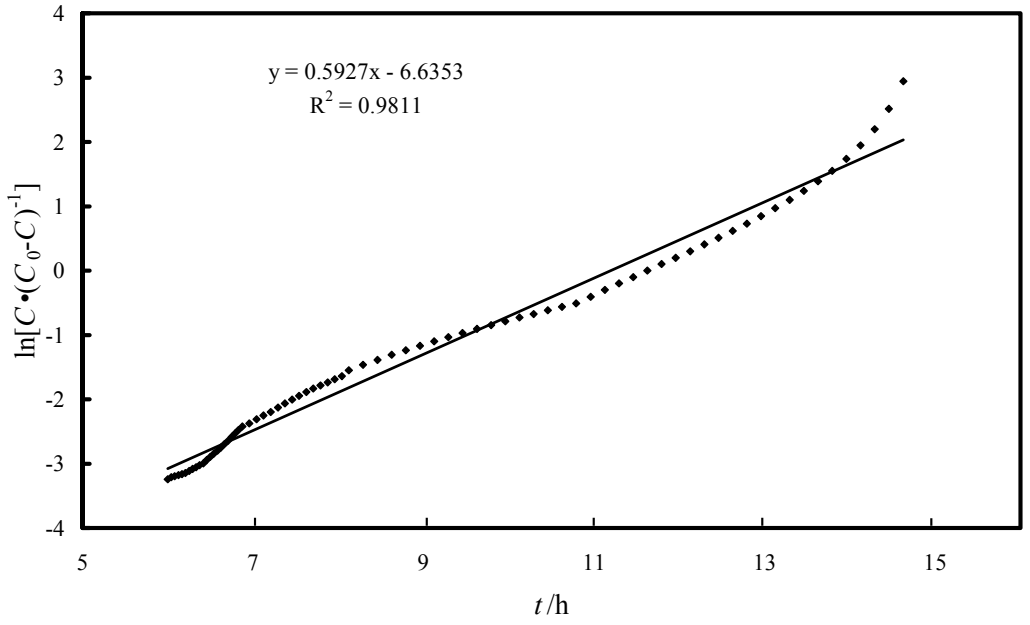

2.4. Quality Parameters of the Effluent Water

The quality parameters of the effluent water after column adsorption were also determined. It was observed that beside arsenic, the studied adsorbent could also remove iron and manganese ions from the sample (residual concentrations fell under the AAS limits of detection of 0.01 $mg \cdot L^{-1}$ for iron and manganese and 0.01 $\mu g \cdot L^{-1}$ for arsenic). These results are in agreement with other studies where it was observed that the arsenic was quantitatively removed together with iron and manganese ions [47]. The pH of the effluent water remained almost the same as in the influent water suggesting that no post treatment is necessary. All these indicate that the Fe-XAD8-DEHPA resin could be used as an efficient and practical adsorbent for arsenic removal from underground waters.

2.5. Desorption Study

From the standpoints of cost-effectiveness and environmental friendliness; it is highly desirable that the sorbent to be amenable to efficient regeneration and re-use. We found that the regeneration capacity of exhausted Fe-XAD8-DEHPA increased with the increasing concentration of the used regenerant (HCl or NaOH). The adsorbent could be efficiently regenerated by using a 5% HCl solution, but in this case Fe ions loaded onto XAD8-DEHPA resin leached out together with the arsenic ions. Consequently the regenerated resin should in such cases be reloaded with Fe(III) ions before re-use, which somewhat increases the cost of the adsorption process. For this reason, we consider the 5% NaCl solution to be the better regenerant, with the use of which the desorption performance is still 92%.

Even if some authors mentioned that the use of ion-exchange for arsenic removal present a better Environmental Sustainability Assessment compared with the adsorption process [48], the research from this paper showed that the use of Fe-XAD8-DEHPA as adsorbent material in the As(V) removal process presents good efficiency both in batch and fixed-bed column tests, and especially in the treatment process of real underground drinking water, without the applying any extra pre-treatment processes. The adsorbent material can be regenerated and efficiently reused in the adsorption process in this way decreasing the treatment costs. All these results underline the sustainability of arsenic removal through adsorption.

3. Experimental Section

3.1. Adsorbent Preparation

The Amberlite XAD8 resin (Rohm and Haas Co., Philadelphia, PA, U.S.A.) was impregnated with di(2-ethylhexyl) phosphoric acid (DEHPA) via the dry method. This macro reticular polymeric adsorbent is dimensionally and chemically quite stable and quite insoluble. The impregnation procedure was described elsewhere [18,22]. Scheme 1 shows the possible mechanism of impregnation.

The resulted phosphorylated resin was further loaded with Fe(III) ions. The hydroxyl iron ions after coordination in the aqueous medium with the neutral waters molecules are loaded onto the impregnated resin according to the reaction mechanism described in Scheme 2.

Scheme 1. The mechanism of XAD8 impregnation with DEHPA.

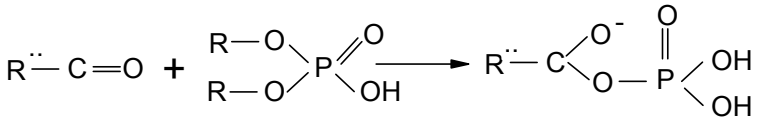

Scheme 2. Loading mechanism of Fe(III) ions onto XAD8-DEHPA resin.

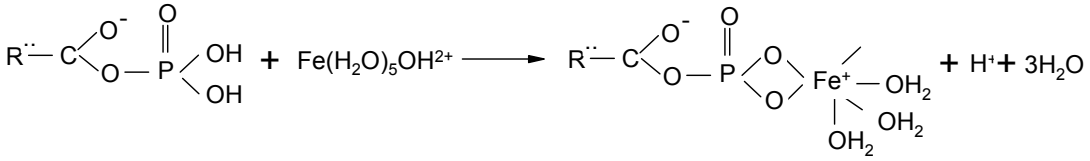

In order to determine the maximum quantity of Fe(III) ions that can be loaded onto the impregnated resin, the influence of the Fe(III) ions initial concentration onto the Fe(III) uptake was investigated. To this end 0.1 g of resin was suspended in 25 mL of Fe(III) ions solutions ($Fe(NO_3)_3$ Merck Standard solution) each having a different Fe(III) concentrations in the range from 10 to 200 $mg \cdot L^{-1}$). The suspensions were let to stand in contact for 24 h in order to reach the equilibrium. After this contact time the samples were filtrated and the concentration of iron in the clear solutions was determined using a Varian SpectrAA 280 type atomic absorption spectrometer (Varian Australia Pty Ltd., Mulgrave, VIC, Australia) equipped with an air-acetylene flame atomizer. The optimum concentration of the Fe(III) ions solution for the XAD8-DEHPA resin loading was found to be 100 $mg \cdot L^{-1}$. A higher quantity of XAD8-DEHPA impregnated resin was equilibrated with a 100 $mg \cdot L^{-1}$ Fe(III) ions solution in the S:L ratio S:L = 0.1:25 for 24 h. Fe loaded XAD8-DEHPA resin was separated by vacuum filtration, washed with distilled water until pH was neutral and dried at 323 K. The obtained Fe-XAD8-DEHPA was submitted to FTIR spectroscopy and EDX analysis in order to establish if the impregnation with DEHPA and the iron loading occurred. The FTIR spectra of KBr-pelletized samples were recorded using a (Prestige-21) FTIR spectrophotometer (Shimadzu Europa GmbH, Duisburg, Germany) in the range of 4000–400 cm^{-1} with 2 cm^{-1} resolution and 40 scans were performed. The EDX study was performed using an Inspect S50 scanning electron microscope (FEI, Hillsboro, OR, USA).

3.2. Batch Experiments for Arsenic Removal

Due to the fact that in aqueous solution at pH value of 9 ± 0.1 the anionic species of As(V) [$H_2AsO_4^-$ or $HAsO_4^{2-}$] are the predominant ones [6,9,11], all the experiments were carried out at this pH value. The pH of the solutions was adjusted to this value using a 1 M NaOH solution, thereby keeping the volume variation of the solution to a value as low as possible. The pH was controlled with MultiMeter MM41 (Crison, Barcelona, Spain) fitted with a glass electrode calibrated by using various buffer solutions. Prior to the equilibrium sorption experiments, a stock solution of arsenic in 0.5 M HNO_3 was prepared using an appropriate amount of H_3AsO_4 (Merck, Darmstadt, Germany). Other solutions of As(V) ions were prepared from the stock solution by appropriate dilution. The arsenate adsorption onto the Fe(III) loaded XAD8-DEHPA resin is mainly attributable to the adsorption of monovalent arsenate anions $H_2AsO_4^-$. The adsorption of monovalent arsenate may take place by releasing hydroxyl anions or neutral water molecules from the coordination sphere of the Fe(III) ions

loaded onto the XAD8-DEHPA resin (Scheme 3), similar to the mechanism proposed for other iron or zirconium-based adsorbents [28,31,32,35–46,49–51].

Scheme 3. The mechanism of arsenate adsorption onto Fe-XAD8-DEHPA resin.

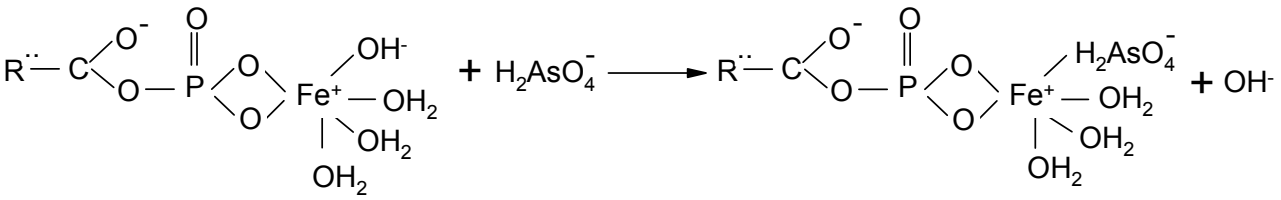

In the first experiment the effect of contact time was studied. The arsenic adsorption performance of the Fe-XAD8-DEHPA the experiments was assessed using 0.1 g of the adsorbent and 25 mL of a 100 $\mu g \cdot L^{-1}$ As(V) solution. The samples were kept in contact for different times (range: 1–24 h) at the room temperature 298 K. After the contact time, the suspensions were filtered and the residual arsenic concentration in the filtrates was determined by hydride generation atomic absorption spectrometry, using a Varian SpectrAA 110 flame atomic absorption spectrometer equipped with a Varian VGA 77 hydride generation system. Similar equilibrium experiments were performed to study the influence of the initial As(V) concentration (10, 30, 50, 80, 100, 200 and 300 $\mu g \cdot L^{-1}$). In each experiment, 0.1 g of studied material was suspended in 25 mL of As(V) solution of different concentration (range: 10–300 $\mu g \cdot L^{-1}$) for 24 h at the room temperature. After the contact time the filtrate was collected and subjected to arsenic analysis.

The adsorption capacity of the impregnated resin expressed as the metal uptake, $q/\mu g \cdot g^{-1}$, can be obtained using the next mass balance expression [36,45,51]:

$$q_t = \frac{(C_0 - C_t) \cdot V}{m} \tag{12}$$

where C_0 and C_t are the concentrations of As(V) ions ($\mu g \cdot L^{-1}$) in the solution initially ($t = 0$) and after a time t (min), respectively, V is the volume of the solution and m is the mass of adsorbent. The experimental results are given as an average of five sets of data obtained under identical working conditions.

3.3. Fixed-Bed Column Study for Arsenic Removal

The arsenic adsorption in dynamic regime was made on a fixed-bed column packed with Fe-XAD8-DEHPA resin. The installation was composed from: a glass column with an i.d. of 2 cm and 30 cm length, where the impregnated resin layer was of 5 cm, a vessel which contain the arsenic-containing water from where it was pumped with the help of a peristaltic pump in the column in the down-flow mode with a volumetric flow rate of 8.33 $mL \cdot min^{-1}$ (0.796 $m^3 \cdot m^{-2} \cdot h^{-1}$). At the bottom of the column the samples were collected at certain time intervals and were analyzed for their arsenic concentrations.

3.4. Desorption Studies

Desorption of arsenic from the exhausted Fe-XAD8-DEHPA resin was carried out using 1 g of exhausted adsorbent, 25 mL of HCl solution and NaCl solutions of various concentrations (1%, 3%,

and 5%) by magnetic agitation for 2 h at the room temperatures. After the contact time the filtrate was collected for arsenic analysis.

All chemicals employed in the experiments were A.R. grade and used without further purification. Distilled water was used throughout.

4. Conclusions

In the present study we have shown that Fe-XAD8-DEHPA adsorbent can be efficiently used for the removal of arsenic from natural underground waters. The adsorption mechanism appears to follows a pseudo-second-order kinetics. The presence of intraparticle diffusion showed that adsorption process is complex and involves multiple mechanisms. The adsorption was also evaluated according to the Langmuir, Freundlich and D-R isotherm models, obtaining a maximum adsorption capacity from the Langmuir isotherm of 22.6 μg As(V)/g of Fe-XAD8-DEHPA resin. The values obtained from the fixed-bed column test could be used to design an adsorption column. In addition, on the column study was demonstrated that a residual concentration of arsenic lower than the maximum limit allowed by the World Health Organization of 10 μg/L can be reached. Compared with other iron loaded adsorbent material mentioned in the literature the proposed one developed a highest adsorption capacity, it can be used with success for arsenic removal from waters containing trace concentrations, the most often situation for drinking waters.

Acknowledgments

This work was partially supported by the strategic grant POSDRU/89/1.5/S/57649, Project ID 57649 (PERFORM-ERA), co-financed by the European Social Fund—Investing in People, within the Sectoral Operational Programme Human Resources Development 2007–2013.

Author Contributions

C.M.D. initiated and supervised the POSDRU project, this publication being part of this project. C.M.D. and P.N. conceived and designed the impregnation process and wrote the paper. P.N. analyzed and interpreted the characterization of the obtained adsorbent material. A.N. and M.C. performed the adsorption experiments, arsenic analyses and wrote the paper. L.L. fitted and interpreted the experimental data and wrote and edited the manuscript. All authors read and approved the final manuscript.

Conflicts of Interest

The authors declare no conflicts of interest.

References

1. Cotruvo, J.; Fawell, J.K.; Giddings, M.; Jackson, P.; Magara, Y.; Festo Ngowy, A.V.; Ohanian, E. *Arsenic in Drinking Water*; World Health Organization: Geneva, Switzerland, 2011.
2. Ramesh, A.; Hasegawa, H.; Maki, T.; Ueda, K. Adsorption of inorganic and organic arsenic from aqueous solutions by polymeric Al/Fe modified montmorillonite. *Sep. Purif. Technol*. **2007**, *56*, 90–100.

3. Guo, H.; Stuben, D.; Berner, Z. Arsenic removal from water using natural iron mineral-quartz sand columns. *Sci. Total Environ*. **2007**, *377*, 142–151.
4. Kundu, S.; Gupta, A.K. Adsorptive removal of As(III) from aqueous solution using iron oxide coated cement (IOCC): Evaluation of kinetic, equilibrium and thermodynamic models. *Sep. Purif. Technol.* **2006**, *51*, 165–172.
5. Borah, D.; Satokawa, S.; Kato, S.; Kojima, T. Surface-modified carbon black for As(V) removal. *J. Colloid Interface Sci.* **2008**, *319*, 53–62.
6. Borah, D.; Satokawa, S.; Kato, S.; Kojima, T. Sorption of As(V) from aqueous solution using acid modified carbon black. *J. Hazard. Mater.* **2009**, *162*, 1269–1277.
7. Negrea, A.; Lupa, L.; Ciopec, M.; Lazau, R.; Muntean, C.; Negrea, P. Adsorption of As(III) ions onto iron-containing waste sludge. *Adsorpt. Sci. Technol.* **2010**, *28*, 467–484.
8. Goswami, R.; Deb, P.; Thakur, R.; Sarma, K.P.; Bsumalick, A. Removal of As(III) from aqueous solution using functionalized ultrafine iron oxide nanoparticles. *Sep. Sci. Technol*. **2011**, *46*, 1017–1022.
9. Gupta, K.; Ghosh, U.C. Arsenic removal using hydrous nanostructure iron(III)-titanium(IV) binary mixed oxide from aqueous solution. *J. Hazard. Mater.* **2009**, *161*, 884–892.
10. Hlavay, J.; Polyak, K. Determination of surface properties of iron hydroxide coated alumina adsorbent prepared from drinking water. *J. Colloid Interface Sci.* **2005**, *284*, 71–77.
11. Banerjee, K.; Amy, G.L.; Prevost, M.; Nour, S.; Jekel, M.; Gallagher, P.M.; Blumenschein, C.D. Kinetic and thermodynamic aspects of adsorption of arsenic onto granular ferric hydroxide (GFH). *Water Res.* **2008**, *42*, 3371–3378.
12. Oke, I.A.; Olarinoye N.O.; Adewusi, S.R.A. Adsorption kinetics for arsenic removal from aqueous solutions by untreated powdered eggshell. *Adsorption* **2008**, *14*, 73–83.
13. Juang, R.S. Preparation, properties and sorption behaviour of Impregnated resins containing acidic organophosphorus extractants. *Proc. Natl. Sci. Counc. ROC* **1999**, *23*, 353–364.
14. Shao, W.; Li, X.; Cao, Q.; Luo, F.; Li, J.; Du, Y. Adsorption of arsenate and arsenite anions from aqueous medium by using metal(III)-loaded Amberlite resins. *Hydrometallurgy* **2008**, *91*, 138–143.
15. Zhu, X.; Jyo, A. Removal of arsenic(V) by zirconium(IV)-loaded phosphoric acid chelating resin. *Sep. Sci. Technol.* **2001**, *36*, 3175–3189.
16. Saha, B.; Gill, R.J.; Bailey, D.G.; Kabay, N.; Arda, M. Sorption of Cr(VI) from aqueous solution by Amberlite XAD-7 resin impregnated with ALiquat 336. *React. Funct. Polym.* **2004**, *60*, 223–244.
17. Belkhouche, N.E.; Didi, M.A. Extraction of Bi(III) from nitrate medium by D2EHPA impregnated onto Amberlite XAD-1180. *Hydrometallurgy* **2010**, *103*, 60–67.
18. Negrea, A.; Ciopec, M.; Lupa, L.; Davidescu, C.M.; Popa, A.; Ilia, G.; Negrea, P. Removal of As(V) by Fe(III) loaded XAD7 impregnated resin containing di(2-ethylhexyl) phosphoric acid (DEHPA): Equilibrium, Kinetic and Thermodynamic modelling studies. *J. Chem. Eng. Data* **2011**, *56*, 3830–3838.
19. Ciopec, M.; Negrea, A.; Davidescu, C.M.; Negrea, P.; Muntean, C.; Popa, A. Use of Di-(2-Ethylhexyl)-Phosphoric Acid (DEHPA) Impregnated XAD-8 Copolymer Resin for the Separation of Metal Ions from Water. *Chem. Bull.* **2010**, *55*, 127–131.

20. Suzuki, T.M.; Bomani, J.O.; Matsunga, H.; Yokoyama, T. Preparation of porous resin loaded with crystalline hydrous zirconium oxide and its application to the removal of arsenic. *React. Funct. Polym.* **2000**, *43*, 165–172.
21. Haron, M.J.; Shiah, L.L.; Wan Yunus, W.M.Z. Sorption of arsenic *V(by titanium oxide loaded poly(hydroxamic acid) resin. *Malays. J. Anal. Sci.* **2006**, *10*, 261–268.
22. Benamor, M.; Bouariche, Z.; Belaid, T.; Draa, M.T. Kinetic studies on cadmium ions by Amberlite XAD7 impregnated resin containing di(2-ethylhexyl) phosphoric acid as extractant. *Sep. Purif. Technol*. **2008**, *59*, 74–84.
23. Mendoza, R.N.; Medina, I.S.; Vera, A.; Rodriguez, M.A. Study of the sorption of Cr(III) with XAD-2 resin impregnated with di-(2,4,4-trimethylpentyl)phosphinic acid (Cyanex 272). *Solvent Extr. Ion Exch.* **2000**, *18*, 319–343.
24. Muraviev, D.; Ghantous, L.; Valiente, M. Stabilization of solvent impregnated resin capacities by different techniques. *React. Funct. Polym.* **1998**, *38*, 259–268.
25. Mukherjee, A.; Sengupta, M.K.; Hossain, M.A.; Ahamed, S.; Das, B.; Nayak, B.; Lodh, D.; Rahman, M.M.; Chakraborti, D. Arsenic contamination in groundwater: A global perspective with emphasis on the Asian scenario. *J. Health Popul. Nutr*. **2006**, *24*, 142–163.
26. Negrea, A.; Muntean, C.; Ciopec, M.; Lupa, L.; Negrea, P. Removal of arsenic from underground water to obtain drinking water. *Chem. Bull.* **2009**, *54*, 82–84.
27. Awual, M.R.; Shenashen, M.A.; Yaita, T.; Shiwaku, H.; Jyo, A. Efficient arsenic(V) removal from water by ligand exchange fibrous adsorbent. *Water Res.* **2012**, *46*, 5541–5550.
28. Awual, M.R.; El-Safty, S.A.; Jyo, A. Removal of trace arsenic (V) and phosphate from water by a highly selective ligand exchange adsorbent. *J. Environ. Sci.* **2011**, *23*, 1947–1954.
29. Awual M.R.; Urata, S.; Jyo, A.; Tamada, M.; Katakai, A. Arsenate removal from water by a weak-base anion exchange fibrous adsorbent. *Water Res*. **2008**, *42*, 689–696.
30. Awual, M.R.; Hossain, A.; Shenashen, M.A.; Yaita, T.; Suzuki, S.; Jyo, A. Evaluating of arsenic(V) removal from water by weak-base anion exchange adsorbent. *Environ. Sci. Pollut. Res*. **2013**, *20*, 421–430.
31. Awual, M.R.; Jyo, A. Rapid column-mode removal of arsenate from water by crosslinked poly(allylamine) resin. *Water Res*. **2009**, *43*, 1229–1236.
32. Chanda, M.; O'Driscoll, K.F.; Rempel, G.L. Ligand exchange sorption of arsenate and arsenite anions by chelating resins in ferric ion form: II. Iminodiacetic chelating resin chelex 100. *React. Polym*. **1988**, *8*, 85–95.
33. Greenleaf, J.E.; Lin, J.C.; Sengupta, A.K. Two novel applications of ion exchange fibers: Arsenic removal and chemical-free softening of hard water. *Environ. Prog*. **2006**, *25*, 300–311.
34. German, M.; Seingheng, H.; SenGupta, A.K. Mitigating arsenic crisis in the developing world: Role of robust, reusable and selective hybrid anion exchange (HAIX). *Sci. Total Environ*. **2014**, *488–489*, 547–553.
35. Etmannski, T.R.; Darton, R.C. A methodology for the sustainability assessment of arsenic mitigation technology for drinking water. *Sci. Total Environ*. **2014**, *488*, 509–515.
36. Streat, M.; Hellgardt, K.; Newton, N.L.R. Hydrous ferric oxide as an adsorbent in water treatment: Part 2. Adsorption studies. *Process Saf. Environ*. **2008**, *86*, 11–20.

37. An, B.; Steinwinder, T.R.; Zhao, D. Selective removal of arsenate from drinking water using a polymeric ligand exchanger. *Water Res*. **2005**, *39*, 4993–5004.
38. Chen, Y.N.; Chai, L.Y.; Shu, Y.D. Study of arsenic (V) adsorption on bone char from aqueous solution. *J. Hazard. Mater.* **2008**, *160*, 168–172.
39. Weber, W.J.; Moris, J.C. Kinetics of adsorption on carbon from solution. *J. Sanit. Eng. Div. Am. Soc. Civ. Eng*. **1963**, *89*, 31–60.
40. Mendoza-Barron, J.; Jacobo-Azuara, A.; Levya-Ramos, R.; Berber-Mendoza, S.; Guerrero-Coronado, R.M.; Fuentes-Rubio, L.; Martinez-Rosales, J.M. Adsorption of arsenic (V) from a water solution onto a surfactant-modified zeolite. *Adsorption* **2011**, *17*, 489–496.
41. Ciopec, M.; Negrea, A.; Lupa, L.; Davidescu, C.; Negrea, P.; Sfarloaga, P. Performance evaluation of the Fe-IR-120(Na)-DEHPA impregnated resin in the removal process of As(V) from aqueous solution. *J. Mater. Sci. Eng. B* **2011**, *1*, 421–432.
42. Zouboulis, A.J.; Kalsoyiannis, I.A. Arsenic removal using iron oxide, loaded aliginate beads. *Ind. Eng. Chem. Res.* **2002**, *41*, 6149–6155.
43. Thirunavukkarasu, O.S.; Viraraghavan, T.; Subramanian, K.S.; Tanjore, S. Organic arsenic removal from drinking water. *Urban Water* **2002**, *4*, 415–421.
44. Viraghavan, T.; Thirunavukkarasu, O.S.; Subramanian, K.S. Removal of arsenic in drkingin water by iron oxide coated sand and ferrihydrite—batch studies. *Water Qual. Res. J. Can.* **2001**, *36*, 55–70.
45. Maji, S.K.; Pal, A.; Pal, T. Arsenic removal from real-life ground water by adsorption on laterite soil. *J. Hazard. Mater.* **2008**, *151*, 811–820.
46. Adak, A.; Bandyopadhyay, M.; Pal, A. Removal of anionic surfactant form wastewater by alumina: A case study. *Colloid Surf. A: Physicochem. Eng. Asp*. **2005**, *254*, 165–171.
47. Noubactep, C.; Care, S.; Blatkeu, B.D.; Nanseu-Njiki, C.P. Enhancing the sustainability of household Fe^0/sand filters by using bimetallics and MnO_2. *CLEAN Soil Air Water* **2012**, *40*, 100–109.
48. Dominguez-Ramos, A.; Chavan, K.; Garcia, V.; Jimeno, G.; Albo, J.; Marathe, K.V.; Yadav, G.D.; Irabien, A. Arsenic removal from natural waters by adsorption or ion exchange: An environmental sustainability assessement. *Ind. Eng. Chem. Res.* **2014**, doi:10.1021/ie4044345.
49. Mohan, D.; Pittman, C.U. Arsenic removal from water/wastewater using adsorbents—A critical review. *J. Hazard. Mater.* **2007**, *142*, 1–53.
50. Rau, I.; Gonzalo, A.; Valiente, M. Arsenic (V) adsorption by immobilized iron mediation. Modeling of the adsorption process and influence of interfering anions. *React. Funct. Polym*. **2003**, *54*, 85–94.
51. Ohe, K.; Tagai, Y.; Nakamura, S.; Oshima, T.; Baba, Y. Adsorption behaviour of arsenic(III) and arsenic(V) using magnetite. *J. Chem. Eng. Jpn.* **2005**, *38*, 671–676.

Sample Availability: Samples of the compounds Fe-XAD8-DEHPA are available from the authors.

Open Chem., 2015; 13: 105–112

Research Article

Open Access

Adina Negrea, Mihaela Ciopec, Petru Negrea, Lavinia Lupa#, Adriana Popa*, Corneliu M. Davidescu, Gheorghe Ilia

Separation of As^{V} from aqueous solutions using chelating polymers containing Fe^{III} -loaded phosphorus groups

Abstract: As^{V} ions were removed by batch equilibrium with Fe^{III}-loaded chelating polymers containing aminophosphinic or aminophosphonic groups. It was effectively removed As^{V} from a synthetic wastewater as well as from a real drinking water containing 40 μg As per liter. Sorption is best described by pseudo-second order kinetics and a Langmuir isotherm

Keywords: Arsenic removal, chelating polymers, aminophosphinic groups, aminophosphonic groups

DOI: 10.1515/chem-2015-0025
received February 03, 2014; accepted May 2, 2014.

1 Introduction

Arsenic-contaminated drinking water is a major environmental problem. The primary source of dissolved arsenic in ground water is oxidative weathering and geochemical reactions; uncontrolled industrial waste discharge is also a problem. Arsenic has been associated with cancerous and non-cancerous health effects [1-7]. Its toxicity strongly depends on the oxidation state. The distributions of the principal aqueous forms of inorganic arsenic (arsenate – As^{V} and arsenite - As^{III}) are influenced by pH and redox conditions [5,7,8]. At pH 6 - 9 As^{III} predominates; at pH above 9 the more toxic As^{V} (arsenic acid oxyanions: $H_2AsO_4^-$ and $HAsO_4^{2-}$) predominates [3,7,9-11]. The World Health Organization (WHO) limit in drinking water is 10 μg L^{-1} [4,8-10,12]. This stringent standard will require many utilities to upgrade their present system or consider new treatment options. Ion exchange is currently an EPA-identified best available technology (BAT) for As^{V} removal [13].

The use of chelating polymers for trace element preconcentration and separation is reasonably well understood and progress is mainly in improving resin specificity and application techniques. Chelating polymers comprise two components, (a) inert solid support and (b) chelating ligand. The attachment of functional groups to the polymer makes it capable of forming metal chelate rings [14-16]. The atoms capable of forming chelate rings include oxygen, nitrogen, phosphorus and sulfur. Ligand incorporation can be either by adsorption (impregnation) on the solid support or by chemical anchoring [17]. The polymer and chelating group structures and their interactions determine the applications.

Insoluble crosslinked polystyrene resins are preferred as support. If the functional group is selective for a target it can be isolated by simple filtration [18]. Polymers with immobilized phosphorus acid ligands are important due to their selectivity [19]. Dual mechanism bifunctional polymers (DMBPs) represent a new class of chelating ion exchange resins [20].

The polymers were loaded with Fe^{III} due to its high affinity for arsenic [1,4,5,7,10,12,21-23]. The As^{V} adsorption of Fe^{III}-loaded chelating polymers containing aminophosphinic or aminophosphonic groups was examined.

***Corresponding author: Adriana Popa:** Institute of Chemistry Timisoara of Romanian Academy, Romanian Academy, RO-300223 Timisoara, Romania, E-mail: apopa_ro@yahoo.com
#Corresponding author: Lavinia Lupa: "Politehnica" University, Faculty of Industrial Chemistry and Environmental Engineering, RO-300006 Timisoara, Romania, E-mail: lavinia.lupa@chim.upt.ro
Adina Negrea, Mihaela Ciopec, Petru Negrea, Corneliu M. Davidescu: "Politehnica" University, Faculty of Industrial Chemistry and Environmental Engineering, RO-300006 Timisoara, Romania
Gheorghe Ilia: Institute of Chemistry Timisoara of Romanian Academy, Romanian Academy, RO-300223 Timisoara, Romania

2 Experimental procedure

2.1 Materials

Styrene-1% divinylbenzene copolymer grafted with amine groups (Fluka, 2 mmol amine /g polymer, N = 2.8%), phenylphosphinic acid (Fluka, techn. 97%), phosphorous acid (Aldrich, 99%), benzaldehyde (Merck, *p.a.*), propionaldehyde (Merck, *p.a.*), methanol, acetone and diethyl ether (Chimreactiv, *p.a*), $(Fe(NO_3)_3$ in 0.5 M HNO_3 (Merck Standard Solution), H_3AsO_4 in 0.5 M HNO_3 (Merck Standard Solutions) were used.

The stock arsenic solution was prepared by diluting H_3AsO_4 in 0.5 M HNO_3 (Merck Standard Solutions). Other As^V solutions were prepared by dilution of the stock solution. All other chemicals were of analytical reagent grade and used as received. Distilled water was used in all experiments.

2.2 Instruments

The polymeric resins were characterized using a Shimadzu Prestige-21 FTIR spectrophotometer from 4000–400 cm^{-1}, (KBr pellets). Thermal properties were characterized by thermogravimetric analysis (TGA) and differential thermal analysis (DTA), performed on a Mettler 851-LF1100 TGA/SDTA from 25 to 900°C at 10°C min^{-1} under nitrogen. Phosphorus was determined by a modified Schoniger method [24]. Energy dispersive X-ray analysis (EDX) was performed using an Inspect S scanning electron microscope, which also provided images. The pH was measured by a CRISON MultiMeter MM41 with a calibrated glass electrode. Iron concentrations were determined using a Varian SpectrAA 280 Fast Sequential Atomic Absorption Spectrometer with an air-acetylene flame at λ = 248.3 nm. Arsenic was determined using a Varian SpectrAA 110 atomic absorption spectrometer with a Varian VGA 77 hydride generation system. For batch experiments an MTA (Kutesz, Hungary) mechanical shaker bath was used.

2.3 Preparation of aminophosphinic acid (AP1, AP2) and aminophosphonic acid (AP3, AP4) grafted on styrene divinylbenzene copolymer

6 g of styrene-1% divinylbenzene copolymer grafted with amine groups were mixed with benzaldehyde (or propionaldehyde), phenylphosphinic acid (or phosphorous acid) and 50 mL tetrahydrofuran and stirred for 24 h at 55°C. The molar ratio of amine : benzaldehyde (or propionaldehyde) : phenylphosphinic acid (or phosphorous acid) was 1 : 1 : 1.5. The polymer beads were separated by filtration, washed with methanol, acetone and diethyl ether. Washing was repeated three times using 20 mL of each solvent. The products were dried at 50°C for 24 hours.

2.4 Preparation of chelating polymers loaded with Fe^{III} ions

The polymers with aminophosphinic (AP1, AP2) and aminophosphonic (AP3, AP4) acid groups were loaded with Fe^{III}. To determine the maximum iron loading, 0.1 g of each polymer was placed in 25 mL of Fe^{III} solution (10-200 mg L^{-1}) for 24 h. The pH was adjusted to ~3 to avoid Fe^{III} precipitation. The solutions were filtered and the residual iron concentrations determined by AA. The dependence of the Fe^{III} adsorption on the initial solution Fe^{III} concentration was established.

2.5 Experimental separation methods

Adsorption experiments were performed with aminophosphinic (AP1, AP2) and aminophosphonic (AP3, AP4) acid containing polymers loaded with Fe^{III} at pH 9.00. Solution pH was adjusted with 1 M NaOH. The effects of initial arsenic concentration and contact time were studied. 0.1 g of adsorbent were placed in 25 mL of As^V solution (10-300 μg L^{-1}) for 48 h at 25 ± 1°C. The solutions were filtered and arsenic concentrations were determined. To examine the effect of contact time, 0.1 g of each adsorbent in 25 mL of 100 μg L^{-1} As^V solutions stood for 1, 2, 4, 6, 8, 10, 14, 24 and 48 h. The solutions were filtered and arsenic concentrations determined.

2.6 As^V adsorption of from a real drinking water

The real drinking water sample had the composition: NO_3^-: 22 mg L^{-1}; NO_2^-: 0.3 mg L^{-1}; P_2O_5: 46.7 mg·L^{-1}; SO_4^{2-}: 11.1 mg L^{-1}; NH_4^+: 6.6 mg L^{-1}; Fe^{n+}: 2 mg L^{-1}; Mn^{2+}: 0.51 mg L^{-1}; Na^+: 118 mg L^{-1}; K^+: 1.67 mg L^{-1}; Ca^{2+}: 30.8 mg L^{-1}; Mg^{2+}: 18.2 mg L^{-1}; As^{n+}: 40 μg L^{-1} and pH= 6.64.

0.1 g of adsorbent was placed in 25 mL of drinking water for 24 hours. Ion concentrations were analyzed before and after adsorption to examine the effects of foreign ions on arsenic adsorption. Fe^{n+}, Mn^{2+}, Na^+, K^+, Ca^{2+}, and Mg^{2+}

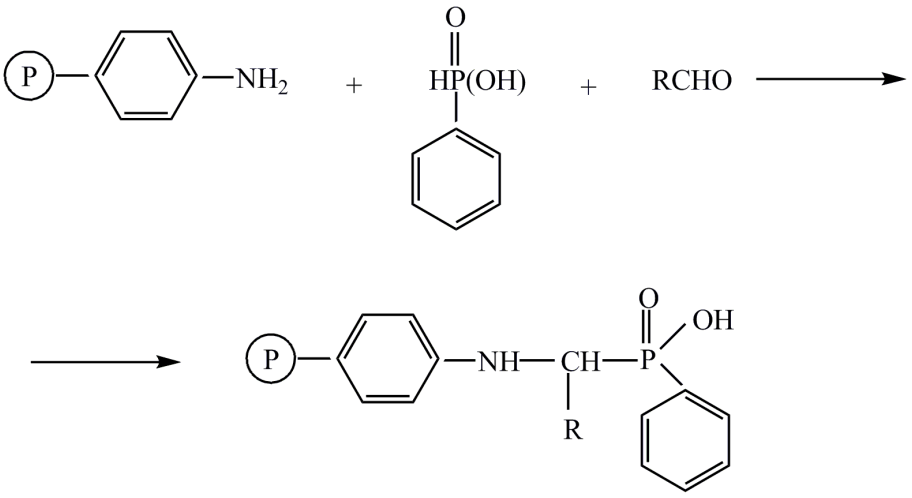

Scheme 1: Preparation of the aminophosphinic acid grafted on styrene-1% divinylbenzene copolymer: R= CH_3CH_2- (AP1); C_6H_5- (AP2).

were determined by AA. Nitrite, nitrate, phosphate and ammonium ions were determined using a Cary 50 VARIAN UV-VIS spectrophotometer. Sulfate was determined with barium chloride using a WTW Turb 555 IR turbidmeter. The pH was measured using a Denver pH meter.

2.7 Sorption performance

Sorption is quantified in terms of metal uptake, q_e (μg g^{-1}). The material balance can be expressed by [3,6,7,9,24,25]:

$$q = \frac{(C_0 - Ce)\,V}{m} \quad (1)$$

where: C_0 - initial solution arsenic concentration, μg L^{-1}; C_e - equilibrium solution arsenic concentration, μg L^{-1}; V - solution volume, L; m - amount of the adsorbent, g.

Freundlich and Langmuir isotherms were used to model the adsorption [2-7,9,22,24-26]. The linear form of the Freundlich isotherm can be written:

$$\ln q_e = \ln K_F + \frac{1}{n}\ln C_e \quad (2)$$

and the Langmuir isotherm as:

$$\frac{C_e}{q_e} = \frac{1}{K_L q_m} + \frac{C_e}{q_m}, \quad (3)$$

K_F and 1/n are constants characteristic of the adsorption; q_m is a measure of monolayer adsorption capacity [mg g^{-1}]; K_L is a constant related to the free energy of adsorption.

Pseudo-first order [3-7,9,23,26], pseudo-second order [3-7,9,23,26] and intra-particle diffusion [3,4,9,27] models were used to determine the adsorption kinetics.

3 Results and discussion

3.1 Characterization of polymers with aminophosphinic or aminophosphonic groups

Aminophosphonic acids and their derivatives belong to an important group of organophosphorus compounds [28,29]. Preparations of aminophosphinic acid groups and aminophosphonic acid groups grafted on styrene–divinylbenzene copolymer (Schemes 1 and 2) have been reported [30,31].

The characteristics of chelating polymers with aminophosphinic (AP1, AP2) and aminophosphonic (AP3, AP4) acid groups are given in Table 1.

FTIR spectra are in Fig. 1. The intense bands between 2950-2800 cm^{-1} are CH_3 and CH_2 stretching vibrations; $\rho(CH_2)_n$ – 750 cm^{-1}; the bands around 980 cm^{-1}, 1035 cm^{-1} and 1380 cm^{-1} are attributed to the P-OH, P-O-alkyl and P=O vibrations. The band at 535 cm^{-1} is attributed to the group ν(Fe-O) + ν(C-C) [32,33].

Fig. 2 shows a SEM micrograph of aminophosphinic acid grafted polymeric resin. The particles ranged from 30 to 60 μm.

TGA thermograms are in Fig. 3. The copolymer with aminophosphonic acid (AP3, AP4) showed higher thermal stability than the plain copolymer with amino groups (support), showing that the aminophosphonic acid group modified the thermal decomposition pathways. The total weight loss for the plain copolymer was 94% and for the copolymer with aminophosphonic acid (AP3, AP4) 86% and 85%.

Table 1: Characteristics of the styrene-1% divinylbenzene copolymer functionalized with aminophosphinic acid groups (AP1, AP2) and aminophosphonic acid groups (AP3, AP4).

Code	Phosphorus content (wt. %)	Residual amine concentration (mmol amine per g copolymer)	Ligand concentration (mmol aminophosphinic or aminophosphonic acid per g copolymer)	Modification yield (%)
AP1	4.20	0.14	1.31	90.50
AP2	3.20	0.41	1.04	71.43
AP3	3.84	0.30	1.23	76.20
AP4	4.61	0.06	1.40	95.25

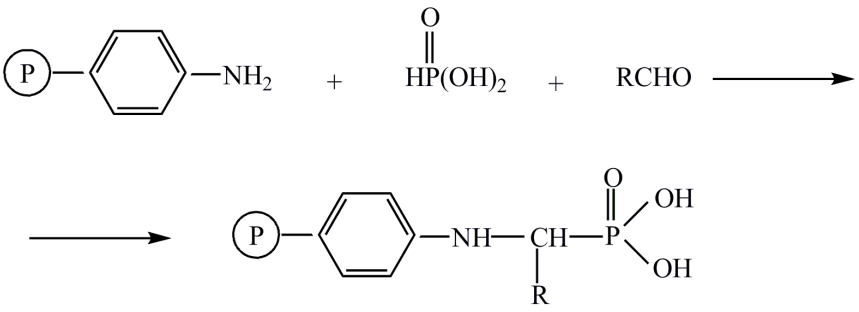

Scheme 2: Preparation of the aminophosphonic acid grafted on styrene-1% divinylbenzene copolymer: R= CH_3CH_2- (AP3); C_6H_5- (AP4).

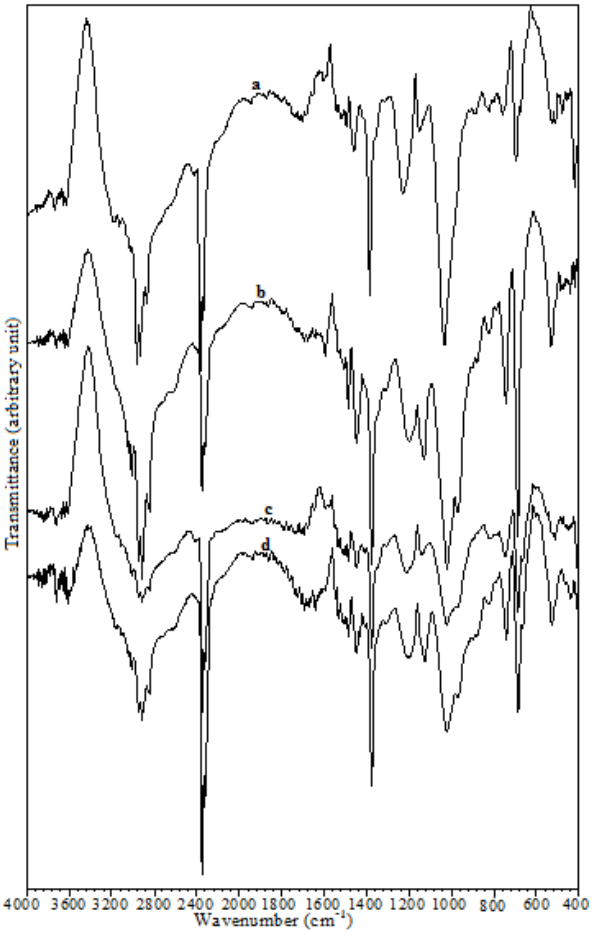

Figure 1: IR spectra of the Fe^{III}-loaded polymers; a- AP1; b- AP2; c- AP3; d- AP4.

3.2 Establishment of the optimum Fe^{III} loading

To determine the maximum iron loading the Fe^{III} uptake was plotted against the initial iron concentration (Fig. 4).

Fe^{III} uptake increased with initial iron concentration up to a limiting value. For polymer grafted with aminophosphonic acid (AP3 and AP4) the maximum was loaded at 50 mg Fe^{III} L^{-1}, for polymer grafted with aminophosphinic acid (AP1 and AP2) the maximum occurred at 80 mg L^{-1}. These concentrations were used for subsequent experiments. Fe^{III} uptake by aminophosphinic acid grafted polymer was higher than that of aminophosphonic acid grafted polymer.

3.3 Effect of initial arsenic concentration and sorption modelling

The adsorption isotherms are presented in Fig. 5. The equilibrium uptake increases with As^V concentration. The heterogeneous distribution of binding sites predicts that all sites are not equally effective. The sites with higher As^V affinity contribute more to sorption.

The equilibrium data have been compared with Freundlich and Langmuir isotherms over the entire concentration range. The Freundlich plots (Fig. 6) have very low regression coefficients suggesting limited validity of the Freundlich isotherm. The constants

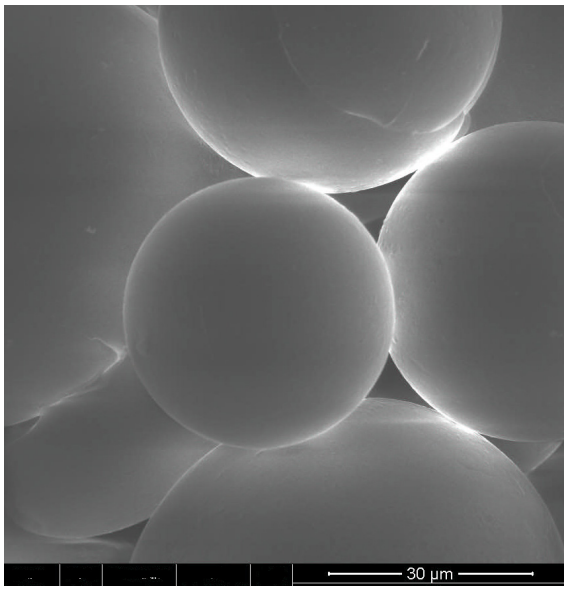

Figure 2: SEM Image of AP1 polymeric resin.

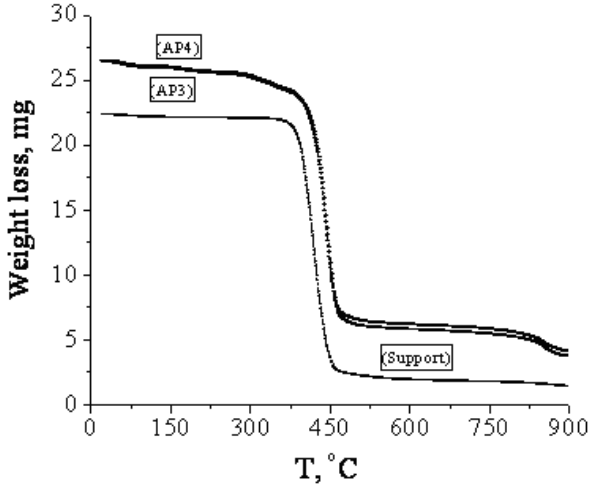

Figure 3: TGA thermograms for the support and aminophosphonic acid (AP3, AP4).

K_F and 1/n computed from the plot are presented in Table 2. K_F can be defined as an adsorption coefficient which gives the quantity of adsorbed metal for unit equilibrium concentration. The slope 1/n is a measure of surface heterogeneity. For 1/n = 1, the partition between the two phases is independent of concentration. The situation 1/n < 1 is the most common and corresponds to a normal L-type Langmuir isotherm, while 1/n > 1 indicates cooperative adsorption involving strong interactions between adsorbate molecules. The observed 1/n < 1 implies favorable As^V adsorption.

The Langmuir model parameters estimated from the slope and intercept of the linear plot (Fig. 7) are given in Table 2. This model better describes the sorption data

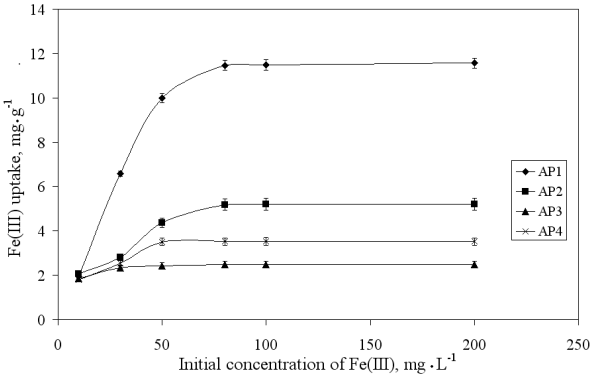

Figure 4: Effect of initial Fe^{III} concentration on metal uptake by the polymeric adsorbents, C_0=10-200 mg L^{-1}, m=0.1 g, V=0.025 L, t=24 h, T=25 ± 1°C; pH=3.

with correlation coefficients closer to 1. The isotherm follows the sorption over the entire concentration range for all four materials, and the maximum sorption capacities are very close to those experimentally obtained. The dimensionless separation factor (R_L) describes the essential characteristics of a Langmuir isotherm. It measures the adsorbent capacity (Eq. 4). Its value decreases with increasing K_L and initial concentration.

$$R_L = \frac{1}{1 + K_L \cdot C_0} \tag{4}$$

R_L relates to the equilibrium isotherm as follows: unfavourable, R_L >1; linear, R_L = 1; favourable 0<R_L<1; and irreversible, R_L=0 [2-4,34-36]. The values for the entire concentration range lie between 0 and 1 in all cases, demonstrating favourable sorption.

AP1 and AP2 resins, which contain more Fe^{III} than the AP3 and AP4 resins, are more effective in As^V removal, in agreement with the results in section 3.2.

3.4 Effect of contact time and sorption dynamics

The effect of contact time on As^V sorption is shown in Fig. 8. Adsorption by all adsorbents increased with time up to 10 h, then remained constant.

Application of the different kinetic models revealed some interesting features of the mechanism and rate-controlling step. First, the Lagergren pseudo-first order kinetic model was applied (Fig. 9). The plots show low correlation coefficients and the equilibrium metal uptakes (q_e) deviated much from the experimental value. This model does not describe the sorption kinetics well.

Table 2: Parameters of Freundlich and Langmuir isotherms for As^V adsorption.

Material	$q_{m,exp}$, μg g^{-1}	Freundlich isotherm			Langmuir isotherm		
		K_F, μg g^{-1}	1/n	R^2	K_L, L μg^{-1}	$q_{m,calc}$, μg g^{-1}	R^2
AP1	10.5	3.271	0.2538	0.8453	0.3096	10.6	0.9998
AP2	10	2.508	0.2907	0.9182	0.1405	10.4	0.9986
AP3	6.3	1.582	0.2762	0.8892	0.0872	6.6	0.9955
AP4	5	1.262	0.2707	0.9041	0.0735	5.3	0.9952

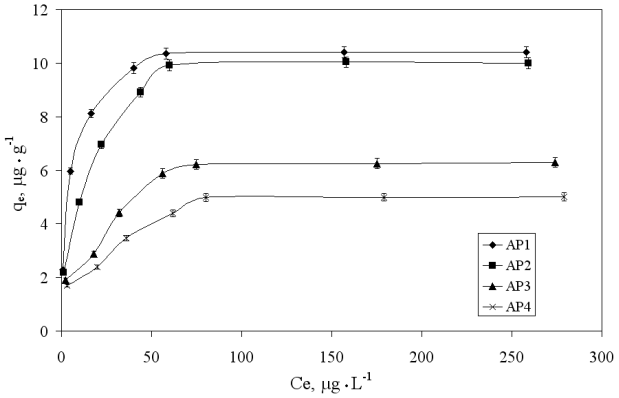

Figure 5: Adsorption isotherms of As^V onto the polymeric adsorbents. C_0=10-300 μg L^{-1}, m=0.1 g, V=0.025 L, t=24 h, T=25 ± 1°C; pH=9.

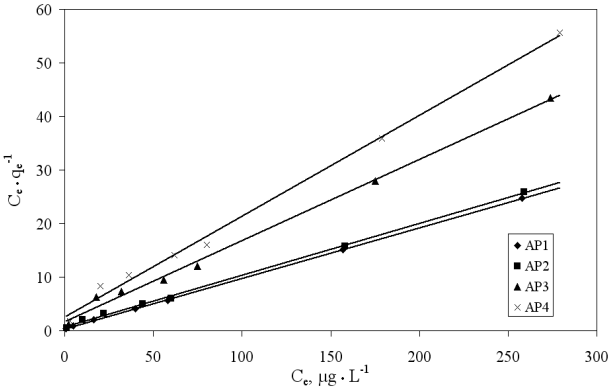

Figure 7: Langmuir plot for As^V adsorption onto polymeric adsorbents.

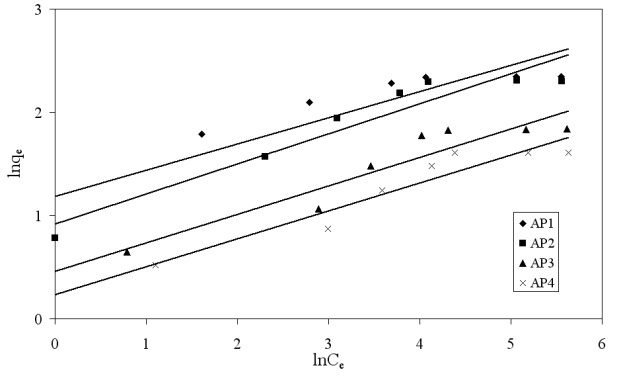

Figure 6: Freundlich plot for As^V adsorption onto polymeric adsorbents.

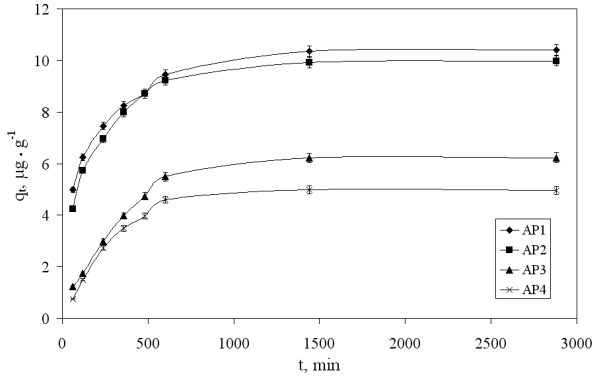

Figure 8: Effect of contact time on adsorption capacity.C_0 = 100 μg L^{-1}; m=0.1 g; V=0.025 L; pH = 9.

It was then applied the pseudo-second order model. The plots of t/q_t against t (Fig. 10) showed better linearity with correlation coefficients higher than 0.99. The equilibrium sorption capacity (q_e) and the rate constant (k_2) from the slope and intercept are reported in Table 3. The predicted equilibrium adsorption capacities were close to the experimental values. This model describes the As^V adsorption kinetics adequately.

Sorption by porous sorbents takes place by three consecutive mass transport steps: (1) film diffusion - the sorbate is transported from solution to the active part of the sorbent external surface; (2) intraparticle diffusion - sorbate is transported through the sorbent pores; and (3) sorption - adherence of the sorbate to the sorbent. The slowest (rate limiting) step is either boundary layer diffusion or intraparticle diffusion. A plot of q_t versus the square root of time was used to identify the slowest step [3,4,7,9,27]. If the plot is a straight line through the origin intra-particle diffusion is rate-limiting. A nonlinear plot shows that boundary layer diffusion is rate-limiting. In Fig. 11 the plots do not pass through the origin and contain two linear sections instead of one. Intra particle diffusion is excluded as the rate limiting step for all the adsorbents. Therefore the adsorption of

Table 3: Kinetic parameters for As^V sorption.

Model/parameters	AP1	AP2	AP3	AP4
$q_{e,\,exp}$, μg g^{-1}	10.5	10	6.3	5
Pseudo-first order model				
$q_{e,\,calc}$, μg g^{-1}	3.83	4.05	3.65	2.44
k_1, min^{-1}	0.0015	0.002	0.0016	0.002
R^2	0.8845	0.9343	0.8338	0.6976
Pseudo-second order model				
$q_{e,\,calc}$, μg g^{-1}	1.002×10^{-3}	1.03×10^{-3}	5.5×10^{-4}	7.5×10^{-4}
k_2, $min^{-1}(\mu g\ g^{-1})^{-1}$	10.8	10.4	6.9	5.5
R^2	0.9996	0.9996	0.9941	0.9907
Intraparticle diffusion model				
k_{id}, μg (g $min^{-0.5})^{-1}$	0.2556	0.2918	0.2595	0.2295

Table 4: Drinking water composition after adsorption.

Composition	Adsorbents			
	AP1	AP2	AP3	AP4
NO_3^-, mg L^{-1}	21.3	20.9	22	22
NO_2^-, mg L^{-1}	0.1	0.1	0.1	0.1
P_2O_5, mg L^{-1}	46.3	46.4	46.7	46.5
SO_4^{2-}, mg L^{-1}	11	11	11	11
NH_4^+, mg L^{-1}	6.5	6.6	6.4	6.5
Fe^{n+}, mg L^{-1}	BDL*	BDL*	BDL*	BDL*
Mn^{2+}, mg L^{-1}	0.5	0.49	0.5	0.5
Na^+, mg L^{-1}	118	118	118	118
K^+, mg L^{-1}	1.67	1.66	1.66	1.67
Ca^{2+}, mg L^{-1}	18.9	19.2	20.8	21.3
Mg^{2+}, mg L^{-1}	11.3	10.9	13.2	13.1
As^{5+}, μg L^{-1}	BDL*	BDL*	3.5	5
pH	7.1	6.6	6.5	7

*BDL – below detection limit

As^V occurs by two processes. At the beginning of the process As^V is rapidly uptaken though film diffusion, and at the end it is transported inside the adsorbent particle. [3,4,7,9,27].

3.5 Adsorption of As^V from a real drinking water

The real drinking water sample had the composition: NO_3^-: 22 mg L^{-1}; NO_2^-: 0.3 mg L^{-1}; P_2O_5: 46.7 mg L^{-1}; SO_4^{2-}: 11.1 mg L^{-1}; NH_4^+: 6.6 mg L^{-1}; Fe^{n+}: 2 mg L^{-1}; Mn^{2+}: 0.51 mg L^{-1}; Na^+: 118 mg L^{-1}; K^+: 1.67 mg L^{-1}; Ca^{2+}: 30.8 mg L^{-1}; Mg^{2+}: 18.2 mg L^{-1}; As^{n+}: 40 μg L^{-1} and pH= 6. Its composition after adsorption by the resins is in Table 4.

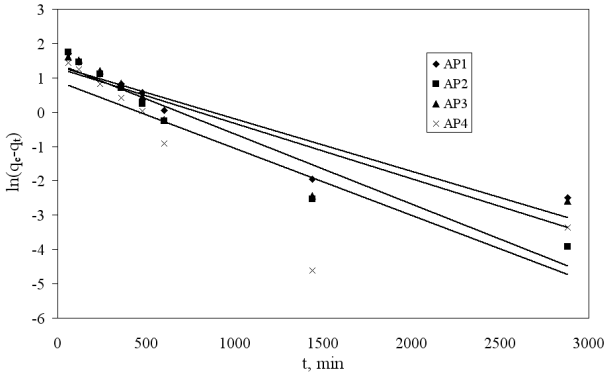

Figure 9: Pseudo-first order kinetic plot for As^V adsorption.

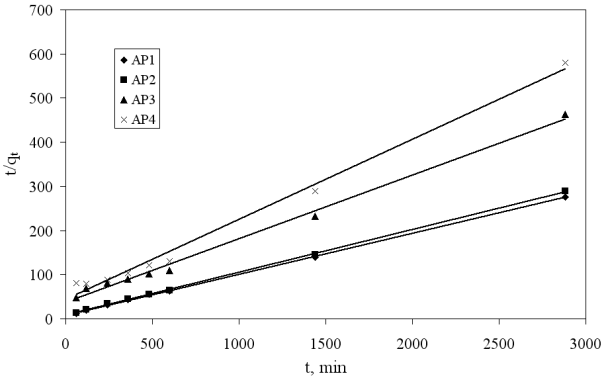

Figure 10: Pseudo-second order kinetic plot for As^V adsorption.

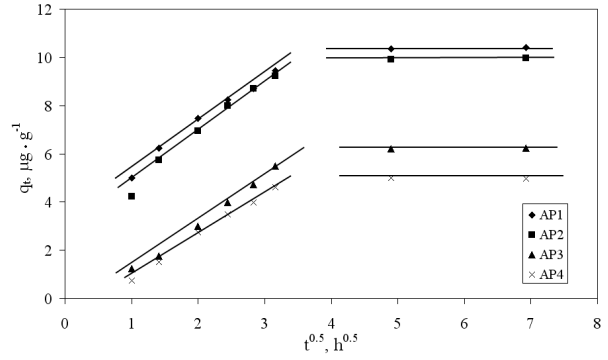

Figure 11: Weber-Morris plots for intra-particle diffusion.

As^V adsorption takes place with complete iron adsorption because arsenic has a high affinity for iron ions. The amounts of calcium and magnesium decrease although these ions do not influence arsenic adsorption. Arsenic content after adsorption is lower than the WHO limit of 10 μg L^{-1}. These resins effectively remove arsenic from drinking water.

4 Conclusions

As^{V} sorption by aminophosphinic and aminophosphonic acids grafted on styrene-1% divinylbenzene copolymer loaded with Fe^{III} was evaluated. Aminophosphinic acid grafted polymer is more efficient than aminophosphonic acid grafting in removing As^{V} from aqueous solutions. More Fe^{III} can be loaded onto aminophosphinic acid, giving a higher adsorption capacity.

As^{V} adsorption was better described by the Langmuir model and follows pseudo-second order kinetics. The adsorption process is complex and involves multiple steps.

All four resins were very efficient in removing arsenic from a real drinking water containing 40 μg L^{-1}. The residual arsenic was less than the WHO limit of 10 μg L^{-1}.

Acknowledgement: This work was partially supported by strategic grant POSDRU/89/1.5/S/57649, Project ID 57649 (PERFORM-ERA), co-financed by the European Social Fund – Investing in People, within the Human Resources Development Operational Program 2007-2013.

The authors are grateful for functionalized polymers provided by partial financial support from Program 2, Project 2.4 from the Romanian Academy Timisoara Institute of Chemistry.

References

[1] Kundu S., Gupta A.K., Sep. Purif. Technol., 2006, 51, 165
[2] Borah D., Satokawa S., Kato S., Kojima T., J. Colloid Interface Sci., 2008, 319, 53
[3] Borah D., Satokawa S., Kato S., Kojima T., J. Hazard. Mater., 2009, 162, 1269
[4] Negrea A., Lupa L., Ciopec M., Lazau R., Muntean C., Negrea P., Adsorpt. Sci. Technol. 2010, 28, 467
[5] Ahmad R.A., Awwad A.M., J. Chem. Eng. Data, 2010, 55, 3170
[6] An B., Steinwinder T.R., Zhao D., Water Research, 2005, 39, 4993
[7] Negrea A., Ciopec M., Lupa L., Davidescu C.M., Popa A., Ilia G., Negrea P., J. Chem. Eng. Data, 2011, 56, 3830
[8] Maji S.K., Pal A., Pal T., J. Hazard. Mater., 2008, 151, 811
[9] Gupta K., Basu T., Ghosh U.C., J. Chem. Eng. Data, 2009, 54, 2222
[10] Banerjee K., Amy G.L., Prevost M., Nour S., Jekel M., Gallagher P.M., Blumenschein C.D., Water Research, 2008, 42, 3371
[11] Hlavay J., Polyak K., J. Colloid Interface Sci., 2005, 284, 71
[12] Partey F., Norman D., Ndur S., Nartey R.J., Colloid Interface Sci., 2008, 321, 493
[13] EPA, Arsenic removal from drinking water by ion exchange and activated alumina plants, EPA/600/R-00/088, Office of Research and Development, Washington, DC, 04.07.2011, www.epa.gov
[14] Buruian L.I., Avram E., Popa A., Stoica I., Ioan S., J. Appl. Polym. Sci., 2013, 129(4), 1752
[15] Kantipuly C., Katragadda S., Chow A., Gesser H.D., Talanta, 1990, 37, 491
[16] Kirci S., Gulfen M., Aydin A.O., Separ. Sci. Technol., 2009, 44, 1869.
[17] Pilsniak M., Trochimczuk A.W., Apostoluk W., Separ. Sci. Technol., 2009, 44, 1099
[18] Yavuz E., Tekin E.T., Kandaz M., Senkal B.F., Separ. Sci. Technol., 2010, 45, 687
[19] Smolik M., Jakobik-Kolon A., Poranski M., Hydrometallurgy, 2009, 95, 350
[20] Beauvais R.A., Alexandratos S.D., React. Funct. Polym., 1998, 36, 113
[21] Jeong Y., Fan M., Singh S., Chuang C.L., Saha B., van Leeuwen J.H., Chem. Eng. Process., 2007, 46, 1030
[22] Mondal P., Majumder C.B., Mohanty B., J. Hazard. Mater., 2008, 150, 695
[23] Chanda M., O`Driscoll K.F., Rempel G.L., React. Polym., 1988, 8, 85
[24] Popa A., Muntean S.G., Paska O.M., Iliescu S., Ilia G., Zhang Z., Polym. Bull., 2011, 66, 419
[25] Ohe K., Tagai Y., Nakamura S., Oshima T., Baba Y., J. Chem. Eng. Jpn., 2005, 38, 671.
[26] Shao W., Li X., Cao Q., Luo F., Li J., Du Y., Hydrometallurgy, 2008, 91, 138
[27] Chen Y.N., Chai L.Y., Shu Y.D., J. Hazard. Mater., 2008, 160, 168
[28] Wang B., Miao Z.W., Wang J., Chen R.Y., Zhang X.D., Amino Acids, 2008, 35, 463
[29] Kozyra K., Klimek-Ochab M., Brzezińska-Rodak M., Żymańczyk-Duda E., Cent. Eur. J. Chem, 2013, 11(9), 1542
[30] Davidescu C.M., Ciopec M., Negrea A., Popa A., Lupa L., Dragan E.S., Ardelean R., Ilia G., Iliescu S., Polym. Bull., 2013, 70, 277
[31] Ciopec M., Davidescu C.M., Negrea A., Lupa L., Popa A., Muntean C., Ardelean R., Ilia G., Polym. Eng. Sci. 2013, 53(5), 1117
[32] Balaban T., Banciu M., Pogany I.I., Applications of physical methods in organic chemistry, Scientific and Encyclopedic Publishing, Bucharest, 1983
[33] Milodi H., Tayeb A., Boos A., Mehyou Z., Goetz-Grandmont G., Benguedach A., Arab. J. Chem., DOI 10.1016/j.arabjc.2013.06.023
[34] Chabani M., Amrane A., Bensmaili A., Desalination, 2007, 206, 560
[35] Hosseini-Bandegharaei A., Hosseini M.S., Sarw-Ghadi M., Zowghi S., Hosseini E., Hosseini-Bandegharaei H., Chem. Eng. J., 2010, 160, 190
[36] Saha B., Gill R.J., Bailey D.G., Kabay N., Arda M., React. Funct. Polym., 2004, 60, 223